Calculating Corrections in F-Theory from Refined BPS Invariants and Backreacted Geometries

Dissertation

zur
Erlangung des Doktorgrades (Dr. rer. nat.)
der
Mathematisch-Naturwissenschaftlichen Fakultät
der
Rheinischen Friedrich-Wilhelms-Universität Bonn

vorgelegt von

Maximilian Poretschkin

aus Bonn

Bonn 2014

Dieser Forschungsbericht wurde als Dissertation von der Mathematisch-Naturwissenschaftlichen Fakultät der Universität Bonn angenommen und ist auf dem Hochschulschriftenserver der ULB Bonn *http://hss.ulb.uni-bonn.de/diss_online* elektronisch publiziert.

1. Gutachter:	Professor Dr. Albrecht Klemm
2. Gutachter:	Privatdozent Dr. Stefan Förste

Tag der Promotion:	22.08.2014
Erscheinungsjahr:	2015

Abstract

This thesis presents various corrections to F-theory compactifications which rely on the computation of refined Bogomol'nyi-Prasad-Sommerfield (BPS) invariants and the analysis of backreacted geometries.

Detailed information about rigid supersymmetric theories in five dimensions is contained in an index counting refined BPS invariants. These BPS states fall into representations of $\mathrm{SU}(2)_L \times \mathrm{SU}(2)_R$, the little group in five dimensions, which has an induced action on the cohomology of the moduli space of stable pairs.

In the first part of this thesis, we present the computation of refined BPS state multiplicities associated to M-theory compactifications on local Calabi-Yau manifolds whose base is given by a del Pezzo or half K3 surface. For geometries with a toric realization we use an algorithm which is based on the Weierstrass normal form of the mirror geometry. In addition we use the refined holomorphic anomaly equation and the gap condition at the conifold locus in the moduli space in order to perform the direct integration and to fix the holomorphic ambiguity. In a second approach, we use the refined Göttsche formula and the refined modular anomaly equation that govern the (refined) genus expansion of the free energy of the half K3 surface. By this procedure, we compute the refined BPS invariants of the half K3 from which the results of the remaining del Pezzo surfaces are obtained by flop transitions and blow-downs. These calculations also make use of the high symmetry of the del Pezzo surfaces whose homology lattice contains the root lattice of exceptional Lie algebras. In cases where both approaches are applicable, we successfully check the compatibility of these two methods.

In the second part of this thesis, we apply the results obtained from the calculation of the refined invariants of the del Pezzo respectively the half K3 surfaces to count non-perturbative objects in F-theory. The first application is given by BPS states of the E-String which are counted in the dual F-theory compactification. Using the refined BPS invariants we can count these states and explain their space-time spin content. In addition, we explain that they fall into representations of E_8 which can be explicitly determined. The second application is given by a proposal how to count $[p, q]$-strings within F-theory which is based on the D3 probe-brane picture and the dual Seiberg-Witten description.

As a third contribution to F-theory which is independent of the results obtained in the first part, we consider the backreaction of G_4-flux onto the geometry of a local model of a Calabi-Yau fourfold geometry. This induces a non-trivial warp-factor and modifies the Kaluza-Klein reduction ansatz. Taking this into account we demonstrate how corrections to the 7-brane gauge coupling function can be computed within F-theory.

Danksagungen

Der größte Dank gebührt meinem Doktorvater Professor Albrecht Klemm für die Möglichkeit meine Doktorarbeit auf diesem spannenden Forschungsfeld anzufertigen. Durch seine fortwährende Unterstützung, Motivation und Begeisterung für die Forschung hat er mich bis an die Grenzen moderner Stringtheorie geführt. Stets konnte ich auf seinen unglaublichen Wissensschatz zurückgreifen, den er gerne und geduldig zugänglich gemacht hat.

Ich danke Privatdozent Dr. Stefan Förste für die Übernahme des Korreferates und seine Unterstützung während meiner Promotionszeit. Ebenfalls danke ich Professor Hans Peter Nilles für allgemeine Unterstützung. Professor Klaus Desch und Professor Claus Kiefer danke ich für die Übernahme der BCGS Mentorate.

Meine Promotion hat erheblich durch die hervorragende Zusammenarbeit mit meinen Kolloborationspartnern profitiert. Ich danke Professor Minxin Huang, Dr. Thomas Grimm, Dr. Denis Klevers und Thorsten Schimannek für spannende und erkenntnisreiche Diskussionen, dass sie ihre Einsichten mit mir geteilt haben, aber auch für Motivation und konstruktive Kritik.

Den Mitgliedern der Arbeitsgruppe Dr. Hans Jockers, Thaisa Guio, Jie Gu, Jonas Reuter, Marc Schiereck, Hung-Yu Yeh, Andreas Gerhardus und Thorsten Schimannek danke ich für das gute Arbeitsklima und die allgemeine Hilfsbereitschaft. In diesen Dank sind die ehemaligen Mitglieder Professor Jan Manschot, Dr. Murad Alim, Dr. Thomas Grimm, Dr. Tae-Won Ha, Dr. Babak Haghighat, Dr. Denis Klevers, Dr. Daniel Lopes, Dr. Masoud Soroush, Dr. Marco Rauch, Dr. Thomas Wotschke, Navaneeth Gaddam und Jose Miguel Zapata Rolon selbstverständlich eingeschlossen. Insbesondere danke ich meinen Freunden Denis Klevers und Thomas Wotschke für die gemeinsame Zeit im Büro und darüber hinaus, für viele interessante und anregende Diskussionen über Physik und andere Dinge und die Tatsache, dass ich immer auf sie zählen konnte.

Weiterhin sei Dr. Denis Klevers, Dr. Hans Jockers, Dr. Thomas Wotschke, Andreas Gerhardus und Thorsten Schimannek für das Korrekturlesen meiner Arbeit und viele wertvolle Hinweise gedankt.

Der Deutsche Telekom Stiftung danke ich für die Förderung meiner Promotion. Die Stipendiatentreffen und Workshops haben die Zeit meiner Promotion sehr bereichert. Insbesondere danke ich Dr. Torsten Minkwitz für die engagierte Wahrnehmung seines Mentorates, viele interessante Einsichten in die Welt der Wirtschaft und die Möglichkeit während eines Praktikums alle Abteilungen seines Bereiches IT-Architektur kennen zu lernen. Frau Christiane Frense-Heck danke ich für die gute und unbürokratische Betreuung.

Der Studienstiftung des deutschen Volkes danke ich für die ideelle Förderung meiner Promotion. Besonders danke ich meinem Vertrauensdozenten Professor Wolfram Kinzig für die Begleitung seit Beginn meines Studiums und während meiner Promotion. Sommerakademien, Seminare sowie die Treffen der Vertrauensdozentengruppe haben mein Studium und meine Promotion zu einer außergewöhnlichen Zeit werden lassen, an die ich stets gerne zurückdenken werde.

Ich danke der Graduiertenschule BCGS für eine finanzielle Teilunterstützung.

Schliesslich danke ich meinen Freunden Hendrik und Philipp Pomp sowie Timo Richarz für die gemeinsame Zeit während und ausserhalb des Studiums. Meinen Eltern Monika Wust-Poretschkin und Dr. Alexander Poretschkin, sowie meinen Brüdern Constantin und Klaus-Ferdinand danke ich für ihre allzeitige Unterstützung und Liebe.

Contents

1. Introduction

This thesis makes two contributions to modern string theory research. In the first part, we compute refined Bogomol'nyi-Prasad-Sommerfield (BPS) invariants of local Calabi-Yau manifolds. In the second part, we discuss corrections and non-perturbative phenomena in F-theory which are partly based on the results obtained in the first part.

To embed this thesis into a broader scientific context, we start with an overview of the current state of fundamental physics that provides a consistent and very successful picture of our universe. We point out that despite the huge success of our description of nature we are in need of new physics that is able to explain open questions from particle physics and cosmology. This new physics should also allow to approach conceptual questions that arise in the underlying framework which is provided by quantum field theory and general relativity.

String theory is a natural candidate for a theory that unifies the concepts of particle physics and cosmology and provides furthermore a consistent, perturbative formulation of quantum gravity. Moreover, it implies the concept of (a partial) geometrization of physics, which states that physical questions can be translated into geometrical ones. Besides contributing to the field of theoretical physics, the idea of geometrization has also led to a fruitful exchange with mathematics and caused many important developments on both sides. We therefore continue by outlining some key properties of string theory and shed more light on these concepts. Finally, we end the introduction by explaining how the results from the present thesis fit into this discussion.

The modern physical description of nature

By today we have a very profound understanding of fundamental physics. On large scales, our universe is described by the standard model of cosmology, while the sub-atomic world of particles is governed by the standard model of particle physics. Both have been enormously successful in explaining known phenomena, making predictions and passing various tests. In the following we briefly review the main features of these two theories.

The Standard Model of Cosmology

Modern cosmology has started with Einstein's theory of general relativity which reinterpretes gravity as the curvature of space-time. This theory successfully explains phenomena like the precision of mercury and predicts e.g. gravitational lensing and gravitational time dilation, which both have been confirmed.

Even more importantly, Einstein's theory can be used to describe the dynamics of the whole universe. The Friedman-Lemaître-Robertson-Walker solutions give rise to the standard model of cosmology which is in addition based on the cosmological principle stating that our universe is on large scales isotropic and homogeneous. This theory depends in addition crucially on various parameters such as Ω_m, Ω_r and Ω_Λ which describe the density of matter, radiation and vacuum energy. The standard model describes an expanding universe that has started with a big bang and successfully explains/predicts e.g. the observed

Hubble expansion, the cosmic microwave background (CMB) and a helium density of 25% within gas clouds with few metal. During the last years, cosmology has become a high precision science and many of these parameters have been measured with great accuracy, e.g. the data of the Planck mission [3] fix the above parameters as $\Omega_\Lambda = 0.686 \pm 0.02$ and $\Omega_m = 0.314 \pm 0.020$ and almost vanishing Ω_r which corresponds to an (almost) flat universe which is dark energy dominated[1].

The standard model of cosmology is extended by the inflation mechanism, which is based on the idea of a much higher vacuum energy in early times of the universe, and predicts an exponential expansion during this epoch. This is a favorable explanation for the horizon problem which addresses the questions why the CMB is homogeneous even on small scales and also provides an answer how the observed flatness of our universe can be explained without fine-tuning.

The Standard Model of Particle Physics

Our current understanding of particle physics is governed by a gauge theory with gauge group $\mathrm{SU}(3)_C \times (\mathrm{SU}(2)_L \times \mathrm{U}(1)_Y)$. The first factor describes the strong force being mediated by the massless gluons, whereas the second factor is spontaneously broken to $\mathrm{U}(1)_{\mathrm{EM}}$ by the Higgs mechanism. This results in three massive gauge bosons $W^\pm$ and Z^0 that mediate the weak force while the remaining massless photon is the carrier of the electromagnetic interaction. In addition, the fundamental constituents of matter are organized within three families of quarks and leptons which receive their masses through Yukawa couplings with the Higgs boson. Just like cosmology, modern particle physics is a high precision science offering setups for very stringent tests for the standard model like the B_s decay into two muons to state one recent example [4]. The discovery of the Higgs boson two years ago [5, 6] and the subsequent confirmation of its desired properties, leading finally to the Nobel Prize 2013, is the cope stone of the confirmation of the particle content of the standard model.

Frameworks of Modern Physics

The achievement of both theories is also based on two very successful frameworks which are however very different in nature. This reflects the diverse validity ranges of the two standard models. General relativity unifies Newton's theory of gravity with Einstein's theory of special relativity by considering gravity as the curvature of space-time due to the presence of matter and energy. Quantum field theory on the other hand unifies Einstein's theory of special relativity with quantum theory and successfully describes the creation and annihilation of particles and their interactions within space-time. Stated differently, while general relativity is able to describe the dynamics of space-time, it does not have to say much about the nature of the objects that cause this dynamics and vice versa, quantum field theory describes the dynamics of these objects but in the background of space and time.

Open Questions and the Demand for New Physics

Although the standard model of particle physics has been tested to a very high accuracy, it also produces new open questions that ask for physics beyond the standard model. One is the hierarchy problem which adresses the question why the electroweak breaking scale is so

[1] This conclusion has already been drawn before Planck, we just display the precision.

much lower than the cut-off scale Λ_{cut} of quantum field theory which could be as large as the Planck scale M_P. The electroweak scale is fixed by the standard model Higgs vacuum expectation value which receives quadratic quantum corrections in Λ_{cut}. A promising solution is provided by supersymmetry being a new symmetry between bosons and fermions such that the new particles cure the quadratic divergence. It was found in recent years that neutrinos have a small mass which is not incorporated by the standard model. One way to achieve this is the see-saw mechanism that includes right-handed neutrinos with large Majorana masses and Yukawa couplings to the left-handed neutrinos. This can be implemented within grand unified theories (GUTs) which unify the microscopic forces by embedding the standard model gauge group into one of the Lie groups SU(5), SO(10) or E_6. In combination with supersymmetry, this also leads to gauge coupling unification. Another obstacle is provided by the gauge couplings and mass parameters of the standard model. Besides the fact that it is un-satisfying to have 19 parameters which need to be determined by experiment, many of them are found to be extremely small. In order to avoid fine-tuning it would be desirable to have a symmetry explaining the smallness. Apart from that, it would also be interesting to have a mechanism that explains why there are three families of particles and why they come precisely in the representations which are observed[2] or why this physics takes place in four space-time dimensions[3].

Also the cosmological point of view contains open questions, most notably that of the nature of dark matter and dark energy. It is known from e.g. the measurement of rotational curves of galaxies that only a small part of the matter is of baryonic nature, which only contributes 0.04 to the overall Ω. Even more importantly, the nature of dark energy is completely unknown. In addition, the physics that is responsible for the generation of matter/antimatter asymmetry after the big bang or describes the microscopic processes of inflation is unknown.

While the problems of particle physics might be answered by an extension of the standard model of particle physics on its own, the questions raised within cosmology already point towards an answer within a unified description of both theories. Apart from that also the frameworks, general relativity and quantum field theory are both struggling with conceptual questions.

From a more abstract point of view, already the fact that general relativity is a classical theory leads to a clash. In fact, any classical interaction allows in principle to determine the position and velocity of a particle with arbitrary precision, which violates Heisenberg's uncertainty principle. Another theoretical argument is provided by the proper description of black holes. First of all - although hidden behind the event horizon -, the differential-geometric description of space-time breaks down at the singularity. In addition, it was found by Bekenstein and Hawking that black holes obey the laws of thermodynamics if one assigns to them an entropy which is proportional to their event horizon. However, in general relativity a black hole is only characterized by mass, charge and angular momentum and no microscopic explanation can be given. A third problem is given by the information paradox: How can unitarity within quantum mechanics be maintained if a well-defined state enters the black hole, but the latter only radiates thermally?

Quantum field theory on the other hand uses the concept of perturbation theory which calculates physical quantities typically in a power-series of a coupling constant. A famous experimentally confirmed result of this principle is the magnetic moment of the electron.

[2]There is a partial answer from anomaly cancellation to this question.
[3]This question could equally well be addressed to cosmology.

However, this series is in general only meaningful, if the coupling constant is small which makes quantum chromodynamics so difficult to solve. Apart from that, it was already pointed out by Dyson [7] that the perturbation series has not to converge at all. Finally, if one tries to apply the concepts of quantum field theory to gravity, one finds that the resulting theory is not renormalizable.

All this provides convincing evidence that we are in need of an extension of the physics known by today. These physics should include the features of particle physics and cosmology and in particular include a theory of quantum gravity.

String Theory and its Key Properties

String theory [8, 9] is a promising candidate to solve some of the problems discussed above or to at least improve the situation. The key idea is that the smallest building stones of nature are not given by particles but by a one-dimensional object, the string, whose oscillations are identified with matter and forces, including gravity. In addition, its length l_s introduces a new fundamental scale. This leads to a Copernican revolution: Physics is not governed by quantum fields within space-time but by quantum fields on the world-sheet swept out by the propagation of the string through space-time. In addition, all couplings and dynamics of the physical fields should in principle be determined by the minimal embedding of the world-sheet into space-time which implies that l_s becomes the only scale of the system! In particular, the value of the string coupling constant g_s which describes the probability that a string splits into two strings is determined dynamically.

Implications of the Finite String Length

The finite length l_s of the string has important consequences: In contrast to a world-line, the concept of a world-sheet does not allow to single out one particular interaction point. Instead the interaction is reflected by the non-local geometry of the world-sheet. This cures UV-divergences arising from nearby interaction points. In particular, as its spectrum naturally contains gravitons, string theory thus provides a consistent, perturbative formulation of quantum gravity.

Secondly, extended objects probe space-time very differently. In contrast to the field theory limit, where one gets a tower of massless states when performing a Kaluza-Klein compactification on a circle in the limit of large radius, one obtains in the stringy case a massless tower also in the limit of vanishing radius which comes from light winding modes. This shows that (closed) string theory is only able to probe space-time up to length scales of l_s.

In the limit $l_s \to 0$, which corresponds to the supergravity limit, one obtains back the equations of motion for gravity and gauge theories while string theory corrects these at finite l_s.

The Web of String Theories

The field theory on the world-sheet is in fact conformal and the preservation of Weyl invariance upon quantization restricts space-time to be ten-dimensional. Moreover consistency of the theory at one loop in perturbation theory, or equivalently the cancellation of tachyons, predicts on the one hand side space-time supersymmetry but also gives rise to five different ways to formulate this theory known as Type IIA, Type IIB, Heterotic $E_8 \times E_8$, Heterotic SO(32) and Type I theory.

All string theories are connected through a web of dualities. These dualities can roughly be divided into two classes, S- and T-dualities which are related to the expansion in g_s and l_s respectively. S-duality exchanges a weakly coupled theory with a strongly coupled one and T-duality exchanges a theory at large scales with a theory at small scales. These can be used to map non-perturbative physics onto perturbative descriptions that are easier to deal with. It should be pointed out that T-duality can be proven while S-duality can only be tested by considering non-perturbative objects which are by supersymmetry protected against decay even in the strong coupling regime.

A consistent unification of all five string theories and their dualities might be provided by M-theory, which is a conjectured eleven-dimensional theory whose low-energy effective action is given by eleven-dimensional supergravity and which reproduces in certain limits all five known string theories.

Compactifications and the Geometrization of Physics

As stated above, a consistent formulation of string theory requires a ten-dimensional spacetime. As this is clearly in contrast with daily life experience, six dimensions have to be compactified on small spaces with diameter below the today experimentally accessible length scales[4]. It is desirable to preserve some of the ten-dimensional supersymmetry in this process, as this gives on the one hand side some control over the resulting four-dimensional theory and is phenomenologically favored on the other hand, as discussed previously. The string theory equations of motion and preservation of supersymmetry demand that these compactification geometries have to be complex three-dimensional Calabi-Yau manifolds X. These are three-dimensional Kähler manifolds with vanishing first Chern class. As a next step, one performs a Kaluza-Klein reduction on X and integrates out massive higher Kaluza-Klein modes to obtain the four-dimensional Wilsonian effective action.

In contrast to the original idea by Kaluza and Klein to obtain gauge theories from gravity and the geometry in a higher-dimensional space, the situation at hand is different. The higher-dimensional string theories already incorporate besides gravity also higher form fields and gauge fields. This is reflected in the fact that a consistent background for compactifications requires besides a Calabi-Yau manifold X also additional data such as flat G-bundles in the Heterotic case or brane/orientifold configurations in a Type II set-up and in general fluxes which constitute non-trivial background field configurations. These additional structures may take one away from the Calabi-Yau condition and lead to more complicated compactification geometries.

F-Theory

Instead of the compactification of string theory on three-dimensional Calabi-Yau manifolds, one can also consider the compactification of F-theory [11] on Calabi-Yau fourfolds. F-theory is a twelve-dimensional theory[5] which is a non-perturbative formulation of Type IIB string theory. The latter possesses an SL(2,$\mathbb{Z}$) symmetry which acts in particular on the string coupling constant and exchanges the theory at weak coupling with another Type IIB realization at strong coupling. More precisely, one combines the string coupling constant g_s with another field of the theory, the so-called C_0 field as $\tau = C_0 + \frac{i}{g_s}$ and interprets this

[4] There are exceptions like e.g. Randall-Sundrum scenarios. See also [10] for a review of possible scenarios.

[5] In constrast to string and M-theory, there is no twelve-dimensional supergravity action which could serve as the low-energy effective action of F-theory.

as the complex structure modulus of an auxiliary torus and the SL(2,$\mathbb{Z}$) symmetry as the group of large diffeomorphisms of this torus. Moreover, if one fibers the auxiliary torus over space-time and thus allows a different value of τ over each point (in a smooth way), one obtains a non-perturbative description of Type IIB string theory. This allows insights into the dynamics of strongly coupled objects within Type IIB string theory which could not be obtained from the weak coupling description. In addition, 7-branes that are a source of gauge theories within Type IIB are interpreted as degenerations of the auxiliary torus in F-theory which allows to study the properties of these gauge theories geometrically.

Wrapping up, despite its stringent formulation in ten dimensions, string theory looses its predictability in lower dimensions. By today, there is no mechanism known that would single out one particular or at least a manageable subset of these possible string theory vacua. One is therefore led to perform a change of paradigm and address the question how certain physical properties can be geometrically addressed respectively engineered. There are two directions one can proceed into. One can investigate how certain properties within cosmology or particle physics can be obtained, e.g. how to build models that explain inflation or a standard-model like gauge theory with three families of particles. This is the arena of string cosmology and string phenomenology respectively. In an optimistic scenario one would expect that these insights together with an improved understanding of the theoretical framework of string theory will finally lead to constraints that a so severe that they allow for new predictions. The second, of course not completely unrelated question one can ask within this geometrization program is how certain conceptual properties within the underlying theoretical framework like e.g. black hole entropies can be adressed. In the following we focus on the second question and discuss topological string theory which has provided deep insights into these issues during recent years.

Topological String Theory

Within the last years, it has been shown that a certain sub-sector of the full string theory, the topological string theory, is enormously useful in investigating the conceptual consequences of the geometrization procedure. Topological string theory [12, 13] arises by performing a so-called topological twist in the world-sheet conformal field theory, which redefines the spins of the fields. By this, the theory becomes a topological field theory. As a consequence, it does not have a space-time interpretation anymore, but only probes the compact geometry. Although the theory for itself is therefore unphysical it computes a part of the physical amplitudes of string theory and has many important physical and mathematical applications.

Mirror Symmetry

There are two ways to perform the above mentioned twist, resulting in the A- and the B-model. On the world-sheet, these differ only by a sign, but from a space-time point of view this implies that the A-model on a certain Calabi-Yau manifold X is physically equivalent [14, 15] to the B-model on a different Calabi-Yau manifold Y, called the mirror of X. An important insight is to not consider single theories but instead complete families of theories parameterized by so-called moduli. The A-model is parameterized by the complexified Kähler moduli of the Calabi-Yau manifold, while the B-model is sensitive to the complex structure moduli. The assignment of the mirror manifold works via a map

which exchanges the complex structure moduli space of one family of Calabi-Yau manifolds with the quantum-corrected Kähler moduli space of another family of Calabi-Yau manifolds, the so-called mirror map. Thus mirror symmetry builds a bridge between complex and symplectic geometry.

This has led to the mathematical conjecture of homological mirror symmetry [16], stating that the Fukaya category on a Calabi-Yau manifold modeling A-branes by Lagrangian submanifolds and open strings by Floer cohomology is equivalent to the derived category of coherent sheaves where open strings are modeled by Ext-groups.

Counting Curves and BPS States via Enumerative Geometry

It turns out that one is for physical and mathematical reasons often interested to count curves inside a Calabi-Yau manifold. Here we refer to complex curves, i.e. Riemann surfaces. These are basically given by a sphere with g handles attached to it. From the mathematics perspective this is the arena of enumerative geometry and such countings provide invariants of the geometries under consideration.

In physics one obtains a particle in space-time, once one wraps a two-dimensional extended object, a brane, around a curve. Moreover under certain conditions, the holomorphicity of the wrapped curve implies that the resulting particle is a Bogomol'nyi-Prasad-Sommerfield (BPS) state. This constitutes a super-symmetric state that is protected against decay[6] if one enters the strongly coupled regime of string theory and therefore provides valuable information.

Topological string theory is able to count these curves as follows. The respective twists for the A- and B-model imply that the semi-classical approximations to the path integrals become exact. It turns out that the B-model localizes on constant maps while the A-model localizes on holomorphic maps from the world-sheet into space-time. Roughly speaking this implies that the B-model is easy to compute, whereas the A-model is harder to compute. The latter encodes however the desired information about the curves one wants to count. Let us sketch how this works. String theory is defined as a perturbation series, which is organized by the genera (number of handles). At genus g, the amplitude of the topological A-model takes roughly the form

$$F^g(t) = \sum_\beta N^g_\beta Q^\beta \,.$$

F^g is called the free energy and N^g_β count in a certain sense how many maps from a genus g curve into the class $\beta \in H_2(X, \mathbb{Z})$ exist. They are called genus g Gromov-Witten invariants [13, 18]. Physically, the Q^β correspond to instantons that correct the perturbative evaluation of the amplitude.

Applications of Topological String Theory

Geometrical Engineering

One application of topological string theory is given by the idea of geometric engineering[7], i.e. to the construction of a field theory whose field content and dynamics is completely con-

[6] This statement only holds true if the remaining moduli are fixed. Otherwise there are phenomena like wall-crossing that can lead to a decay of these states and only an appropriate index is invariant.

[7] See e.g. [17] for a review and references therein.

trolled by the geometry. A prominent example is the engineering of Seiberg-Witten theory on non-compact, three-dimensional Calabi-Yau manifolds. Seiberg-Witten theory [19] determines the effective four-dimensional theory of gauge theories with $\mathcal{N} = 2$ supersymmetry at all values of the gauge coupling function. It builds up on the strong non-renormalization theorems for $\mathcal{N} = 2$ supersymmetry and interprets the vacuum expectation values of the Cartan generators as the periods of a meromorphic one-form on an auxiliary Riemann surface. This Riemann surface can be used as a basis for a non-compact Calabi-Yau manifold which upon compactifying topological theory on it gives rise to the four-dimensional gauge theory. In this way a whole dictionary between gauge theory and geometry can be established. For example, the actions of $\mathcal{N} = 2$ supersymmetric, four-dimensional theories are completely determined by a function that depends on the superfields and is called the prepotential. This is just given by the genus zero free energy of the topological string and can be exactly computed using mirror symmetry.

The geometric solution of $\mathcal{N} = 2$ theories also incorporates an appropriate description of non-perturbative objects like magnetic monopoles and dyons and shows how the infinite instanton contributions can be meaningfully re-summed. In addition, questions like confinement in $\mathcal{N} = 2$ supersymmetric versions of quantum chromodynamics can be addressed and solved within this framework. It is even possible to go one step further and to geometrically describe gauge theories without a known Lagrangian description [20].

Black Hole Micro-state Counting

As already mentioned above, it is important to understand the microscopic origin of black holes. In the case of five-dimensional, extremal black-holes within $\mathcal{N} = 2$ supergravity such an understanding was achieved by Strominger and Vafa [21]. Such black holes are characterized by their angular momentum J and the charge Q that stand in a certain relation and their entropy can be calculated within supergravity as

$$S_0 = 2\pi\sqrt{Q^3 - J^2}\,.$$

The crucial idea is to engineer these black holes geometrically by BPS particles. These arise in M-theory compactifications on a Calabi-Yau manifold X by wrapping M2-branes around curves C in X. More precisely for any curve C there is a dual two-form ω_C that can be used to (Kaluza-Klein) reduce the M-theory form-field C_3 on it which gives rise to a U(1)-field under which these black holes are charged. In addition, one can also geometrically identify the angular momentum, but this is less intuitive. It comes from a Lefshetz action on the moduli space of these curves [22–24]. Fortunately, these curves can be counted by the topological string! In fact, it is possible to compute a generating function $\Omega(Q, J)$ for the degeneracies of BPS states with charge Q and one finds that

$$S(Q, J) = \log(\Omega(Q, J))$$

reproduces the macroscopic result in the limit of large charge and angular momentum.

A similar result exists in four dimensions, where the Ooguri-Strominger-Vafa conjecture [25] relates the black-hole partition function to that of the topological string as

$$Z_{BH} = |Z_{top}|^2, \qquad Z_{top} = \exp\left(\sum_g F_g(t) g_s^{2g-2}\right)\,.$$

Embedding the Thesis into the Context

This thesis contributes a new application of topological string theory to count objects namely E- and $[p,q]$-strings that appear in F-theory. For these purposes we use a modified version of the topological string, the refined topological string [26], which governs the first main part of this thesis. In the second part we discuss besides the counting of E- and $[p,q]$-strings also a second contribution to F-theory which is independent of topological string theory, namely the computation of the D7-brane gauge coupling function within F-theory which relies on the analysis of backreacted geometries.

Enumerative Geometry of Refined Topological Strings

As discussed previously, five-dimensional BPS-particles arise by wrapping M2-branes around curves in three-dimensional Calabi-Yau manifolds. Moreover, their spins are encoded in the geometry and can be displayed by the topological string [22–24]. The true spin content of a five-dimensional massive particle is given by two SU(2) spins, i.e. the little group is SO(4) = SU(2) × SU(2). We are interested in the numbers $N^{\beta}_{j_L,j_R}$ of particles coming from an M2-brane wrapping the class $\beta \in H_2(X,\mathbb{Z})$ and have spin (j_L, j_R). These are called refined BPS states and are counted by the refined topological string, whereas the usual topological string only counts the index

$$n^{\beta}_{j_L} = \sum_{j_R} (-1)^{2j_R} (2j_R+1) N^{\beta}_{j_L,j_R} \,.$$

Let us emphasize that the generating function $\Omega(Q,J)$ in the above discussion only depends on $n^{\beta}_{j_L}$.

The refined topological string contains therefore considerably more information than the unrefined string. However due to technical[8] reasons this counting is only possible on toric Calabi-Yau manifolds. From a mathematical perspective, refined BPS invariants constitute new enumerative invariants of toric Calabi-Yau manifolds, named refined stable pair invariants and have only recently been defined [27, 28].

In this thesis we compute the refined stable pair invariants for local Calabi-Yau manifolds which are constructed as anti-canonical bundles over del Pezzo and half K3 surfaces. These computations are technically involved and rely on the use of mirror symmetry, the refined holomorphic anomaly equations [29, 30] and modularity properties[9] [31–34]. It is however crucial to stress that it is the physical insight coming e.g. from Seiberg-Witten theory and topological string theory which allows to perform these calculations. Apart from that the above geometries have a beautiful inner structure, as their homology is governed by exceptional groups [35]. In the following we explain how the results can be used to count non-perturbative objects in F-theory.

E-strings and Phase Transitions in F-Theory Vacua

F-theory theory compactifications on Calabi-Yau manifolds play an important role in the web of string theory vacua. Such vacua are parameterized by the moduli spaces of the Calabi-Yau manifolds. Most notably it is possible to connect different families of vacua

[8] By this we do not mean computational reasons. In fact the theory requires an additional U(1) symmetry which is only present on toric Calabi-Yau manifolds.

[9] This is a selection among those contributions that are of particular importance for us.

by phase transitions [36, 37]. This happens if some subspace in the geometry shrinks to zero size and some other subspace grows. Technically, this corresponds to a bi-rational transformation within the geometry. At the point of the phase transition itself, one expects new physics to enter. The reason is as discussed earlier, higher-dimensional objects within string theory, so-called branes can wrap these shrinking subspaces and appear as point-particles within space-time. In addition, their masses are determined by the volumes of the wrapped subspaces and thus they become light when the latter shrink. A different description of such a process is given by the Heterotic string where a so-called E-String [31, 32, 38–40] becomes tensionless which governs the physics of small E_8 instantons [32, 39, 41, 42]. It is extremely interesting to study the new physics that happens at such transitions, as (so far) no Lagrangian description for the new massless states exists [36]. The latter is caused by the fact that at the same time magnetically and electrically charged states become massless. However using the refined topological string we are able to count these states and to predict their space-time spins as well as their gauge theory quantum numbers!

$[p, q]$-Strings in F-Theory

Type IIB string theory contains besides the fundamental string also another, non-perturbative, one-dimensional object, the D1-brane. This can form a bound state with the fundamental string which is referred to as a $[p, q]$-string. These constitute the microscopic ingredients for gauge enhancements on strongly coupled 7-brane stacks [43–46]. As previously discussed, these get part of the geometry in F-theory. However, not much is known about a microscopic formulation of F-theory, i.e. in particular what are the microscopic ingredients for gauge enhancements in F-theory. Using the results obtained from the stable pair invariants of the half K3 surface we make a proposal how these states can be identified as refined BPS states within F-theory and suitably counted.

Gauge Coupling Function from Backreacted Geometry

Finally, the second part of this thesis also discusses a contribution to F-theory that does not resort on the calculations which are performed in the first part. Besides the question of identifying non-perturbative objects in F-theory, it is important to discuss how the results known from type IIB string theory compactifications can be re-produced from an F-theory perspective and extended away from the small coupling limit. In particular, we investigate how the D7-brane gauge coupling function can be recomputed within F-theory. As D7-branes get part of the geometry, all these data, including stringy corrections in l_s must be encoded in the geometry and the G_4-flux. We answer this question using the M-/F-theory duality by constructing a local model of the neighborhood of a D7-brane stack consisting of periodic Kaluza-Klein monopole solutions in M-theory. This is in turn used to show that the desired corrections obtain an interpretation in terms of back-reaction of G_4-flux onto the geometry and modifications of the Kaluza-Klein reduction ansatz.

Besides its conceptual relevance, the results obtained in this part are also of phenomenological relevance. G_4-flux plays an important role in the understanding of moduli stabilization [47, 48], the generation of a chiral spectrum [49–55] and is essential to cancel D3-brane tadpoles [47, 48] and a complete analysis asks for the inclusion of its backreaction. In addition, the understanding of corrections to the gauge coupling function is crucial for the investigation of gauge coupling unification in F-theory, e.g. [56–58].

Outline

This thesis is divided into two parts. The first part is concerned with the computation of refined BPS state multiplicities. It consists of the chapters 2 to 6. The second part discusses applications to F-theory and includes chapter 7, 8 and 9. The conclusion is presented in chapter 10.

In chapter 2 we introduce topological string theory starting with superconformal field theories and discuss the geometric realization in terms of nonlinear Sigma models. The A- and the B-model are introduced and mirror symmetry is discussed. We proceed to topological string theory and discuss the space-time interpretation of the free energy of the A-model and Gopakumar Vafa invariants. At the end we introduce refinement and its mathematical formulation in terms of refined stable pair invariants.

In chapter 3 we discuss the formalism of direct integration and its extension to the refined case. In particular, we discuss the refined holomorphic anomaly equations. Afterwards we present an algorithm that relies on the Weierstrass normal form of an elliptic curve and allows to perform the direct integration procedure very efficiently for geometries with a genus one mirror curve.

Chapter 4 deals with geometric background material. We discuss the geometry of del Pezzo surfaces and the half K3 and present the tools needed to construct toric Calabi-Yau mirror pairs.

We use the methods of the introductory chapters to compute the refined BPS invariants of toric del Pezzo surface which include toric del Pezzo and almost del Pezzo surfaces, as well as massless higher del Pezzo surfaces in chapter 5. We also discuss a toric example with has a genus two mirror curve. Most of the results of this chaper have appeared in [1].

Afterwards the computation of the refined BPS invariants of the half K3 surface is discussed in chapter 6 which is based on [1]. The main ingredients here are the refined Göttsche formula and the refined modular anomaly equations. We discuss the massless and massive half K3 separately and comment on the boundary conditions that are needed to fix the modular ambiguity of the refined modular anomaly equations.

The second part of this thesis starts with a brief review of F-theory in chapter 7 including the discussion as the strong coupling limit of Type IIB and its dualities with M-theory and the Heterotic string.

Afterwards we demonstrate how the results of the first part can be used to count non-perturbative objects in F-theory which are given by E-Strings and $[p, q]$-flux in chapter 8. Both subjects are briefly reviewed before we comment on the progress which has appeared in [1].

In chapter 9 the computation of the 7-brane gauge coupling function within F-theory is presented which relies on the analysis of a backreacted geometry. This chapter is based on the results in [2].

Finally, the conclusions are presented in chapter 10.

The appendix A contains some calculations and results that are too long to be presented in the main text and are referred to when needed.

This thesis is based on the following two publications of the author:

- M. -X. Huang, A. Klemm and M. Poretschkin, "Refined stable pair invariants for E-, M- and $[p, q]$-strings," [arXiv:1308.0619 [hep-th]].
  Published in *Journal of High Energy Physics*, **1311** (2013) 112.
- T. W. Grimm, D. Klevers and M. Poretschkin, "Fluxes and Warping for Gauge Couplings in F-theory," [arXiv:1202.0285 [hep-th]].
  Published in *Journal of High Energy Physics*, **1301** (2013) 023.

Part I.

Refined BPS State Counting

2. The Refined Topological String

In this chapter we discuss the necessary background material from refined topological string theory. We start with a review of superconformal field theories and their deformation rings in section 2.1 and explain how one constructs topological field theories by the topological twist. Afterwards, we proceed to the nonlinear Sigma model realization of superconformal field theories in section 2.2 and discuss the A- and the B-model. In particular, we discuss their moduli spaces and identify the deformation ring, which is the basis for the discussion of mirror symmetry in section 2.3 where we also review the coupling of the A- and B-model to gravity to obtain topological string theory. In addition, we consider the holomorphic anomaly equations. In the last section 2.4, we review the notion of Gopakumar Vafa invariants and show how the free energy of the A-model can also be computed by integrating out BPS particles in a self-dual gravi-photon background field. This serves as preparation for the discussion of refinement and refined BPS invariants which follows next. Finally, we end the chapter by briefly discussing the mathematical formulation of refined BPS invariants which is constituted by the notion of refined stable pair invariants.

2.1. Twisting superconformal field theories

In this section we discuss the basic features of superconformal field theories as these are the foundation for a discussion of mirror symmetry. As our goal for this section is to construct topological field theories, these get introduced first.

2.1.1. Topological field theories

A topological field theory of Witten or cohomological type is defined by the following properties. It has a scalar Grassmann symmetry operator $\mathcal{Q}$, also referred to as BRST operator, that obeys

$$\mathcal{Q}^2 = 0, \tag{2.1.1}$$

such that the action as well as the energy-momentum tensor are $\mathcal{Q}$-exact

$$S = \{\mathcal{Q}, V\}, \qquad T_{\mu\nu} = \{\mathcal{Q}, G_{\mu\nu}\}. \tag{2.1.2}$$

The first condition (2.1.1) implies that the observables of the topological theory are given by the $\mathcal{Q}$-cohomology of the theory as the observables have to be $\mathcal{Q}$-invariant operators while correlation functions containing $\mathcal{Q}$-exact operators vanish which implies that the latter decouple from the theory. The second condition (2.1.2) implies that the correlation functions do not depend on the background metric, as the variation with respect to the metric results in the insertion of an energy-momentum operator into the correlation function. Finally it implies that the semi-classical evaluation of the path integral becomes exact. See e.g. [179] for details.

2.1.2. $\mathcal{N} = (2,2)$ superconformal field theories

The $\mathcal{N} = 2$ superconformal algebra is generated by the energy momentum tensor $T(z)$, two anti-commuting super-currents $G^{\pm}(z)$ and a U(1) current $J(z)$

$$T(z) = \sum_{n\in\mathbb{Z}} L_n z^{-n-2}, \qquad G^{\pm}(z) = \sum_{n\in\mathbb{Z}} G^{\pm}_{n\pm a} z^{-(n\pm a)-3/2}, \qquad J(z) = \sum_{n\in\mathbb{Z}} J_n z^{-n-1}\,. \tag{2.1.3}$$

Here a takes into account the possible boundary conditions being 0 for the Ramond sector and $\frac{1}{2}$ in the NS sector. The fields (2.1.3) are subject to the following OPEs

$$\begin{aligned}
T(z)T(w) &\sim \frac{c/2}{(z-w)^4} + \frac{2T(w)}{(z-w)^2} + \frac{\partial_w T(w)}{z-w}\,,\\
T(z)G^{\pm}(w) &\sim \frac{3/2}{(z-w)^2} G^{\pm}(w) + \frac{\partial_w G^{\pm}(w)}{z-w}\,,\\
T(z)J(w) &\sim \frac{J(w)}{(z-w)^2} + \frac{\partial_w J(w)}{(z-w)}\,,\\
G^{\pm}(z)G^{\mp}(w) &\sim \frac{2c/3}{(z-w)^3} \pm \frac{2J(w)}{(z-w)^2} + \frac{2T(w) \pm \partial_w J(w)}{(z-w)}\,,\\
J(z)G^{\pm}(w) &\sim \pm\frac{G^{\pm}(w)}{(z-w)}\,,\\
J(z)J(w) &\sim \frac{c/3}{(z-w)^2}\,.
\end{aligned} \tag{2.1.4}$$

An $\mathcal{N} = (2,2)$ superconformal theory is obtained by adding an anti-holomorphic copy of these fields which have trivial OPEs with the holomorphic sector. See e.g. [124] for more background material.

2.1.3. The chiral ring

A highest weight state is given by

$$L_n\,|\phi\rangle = 0, \quad G^{\pm}_r\,|\phi\rangle = 0, \quad J_m\,|\phi\rangle = 0, \quad n,r,m > 0 \tag{2.1.5}$$

and labeled by the zero modes

$$L_0\,|\phi\rangle = h_\phi\,|\phi\rangle\,, \quad J_0\,|\phi\rangle = q_\phi\,|\phi\rangle\,. \tag{2.1.6}$$

A primary field ϕ creates a highest weight state $|\phi\rangle = \phi\,|0\rangle$ and is called chiral primary field if

$$G^{+}_{-\frac{1}{2}}\,|\phi\rangle = 0 \tag{2.1.7}$$

and anti-chiral primary field it is annihilated by $G^{-}_{-\frac{1}{2}}$. From the OPE one can deduce that

$$h_\phi = (-)\frac{q_\phi}{2} \tag{2.1.8}$$

for an (anti-) chiral primary field. In addition, the OPE of (anti-)chiral operators is again an (anti-)chiral operator (this statement is understood to hold in correlation functions) such

that one gets a ring structure

$$\phi_i \phi_j = C_{ij}^k \phi_k \,. \tag{2.1.9}$$

Taking also the anti-holomorphic sector into account, one obtains four choices for these rings called (c,c), (c,a), (a,c), (a,a). As the last two choices are related by complex conjugation to the first two, there are only two physical rings which are referred to as chiral (c,c) and anti-chiral ring (a,c).

2.1.4. Deformations

(Anti-)chiral operators are also important to study deformations of the conformal field theory. These are caused by marginal operators that have conformal weights[1] $h = \bar{h} = 1$. In the following we only consider the chiral ring, as the anti-chiral ring works analogously. Choose a basis ϕ_i in the space $\mathcal{H}^{(1,1)}$ of chiral operators of charge[2] $(1,1)$. One then constructs marginal operators as follows[3]

$$\phi_i^{(2)}(w,\bar{w}) = \oint dz G^-(z) \oint d\bar{z} \bar{G}^-(\bar{z}) \phi_i(w,\bar{w}) \tag{2.1.10}$$

$$\bar{\phi}_{\bar{\imath}}^{(2)}(w,\bar{w}) = \oint dz G^+(z) \oint d\bar{z} \bar{G}^+(\bar{z}) \bar{\phi}_{\bar{\imath}}(w,\bar{w}) \tag{2.1.11}$$

The reason for this construction is that the chiral operators have weights $(h,\bar{h}) = (\frac{1}{2},\frac{1}{2})$, which gets corrected by this construction. The deformation space constructed by these operators is called the moduli space $\mathcal{M}$. Choosing coordinates $t^i, \bar{t}^{\bar{\imath}}$, these parameterize the deformations of the action as

$$\delta S = t^i \int_{\Sigma_g} \phi_i^{(2)} + \bar{t}^{\bar{\imath}} \int_{\Sigma_g} \bar{\phi}_{\bar{\imath}}^{(2)} \tag{2.1.12}$$

In the next section, we investigate how the space of vacua varies over this moduli space.

2.1.5. The vacuum bundle

In the following we consider a vector-bundle V over the moduli space $\mathcal{M}$ whose fiber consists of the ground-states of the theory and which is called the vacuum bundle[4]. While the bundle V does not change, there are certain ways of splitting the vacuum bundle into sub-spaces and in fact this splitting varies. For the following discussion it is assumed that the central charge c is nine, which is the case we will be finally interested in. In this case, due to anomaly cancellation [191], one has to demand that the charges of operators inserted into a sphere correlation function sums up to three.

We consider[5] the sub-ring of the chiral ring which is created by the $(1,1)$ operators and choose a basis denoted by $(\phi_0, \phi_i, (\phi_D)_i, (\phi_D)_0)$, $i = 1,\ldots,n$ whose elements have charges $(0,0),(1,1),(2,2),(3,3)$ respectively. Here ϕ_0 is just the identity operator. In addition, there is the topological metric

$$\eta_{ij} = \langle \phi_i (\phi_D)_j \rangle \tag{2.1.13}$$

[1] We are restricting ourselves to spinless operators.
[2] The fields $\bar{\phi}^{\bar{\imath}}$ in the (a,a) ring have charges $(-1,-1)$.
[3] See e.g. [180, 213] for more details.
[4] Our presentation of the vacuum bundle and its identification in the A- and the B-model is partly based on [180].
[5] See e.g. [61, 64] for details of this construction.

and the three-point function is defined by

$$C_{ijk} = \langle \phi_i \phi_j \phi_k \rangle = C_{jk}^m \eta_{im}. \tag{2.1.14}$$

Denoting $\phi^i = \eta^{ij}(\phi_D)_j$ and choosing a section for the unique ground state as $|e_0\rangle$ one can display the representation of the chiral ring as [180]

$$\phi_i \begin{pmatrix} |e_0\rangle \\ |e_j\rangle \\ |e^j\rangle \\ |e^0\rangle \end{pmatrix} = \underbrace{\begin{pmatrix} 0 & \delta_i^k & 0 & 0 \\ 0 & 0 & C_{ijk} & 0 \\ 0 & 0 & 0 & \delta_i^j \\ 0 & 0 & 0 & 0 \end{pmatrix}}_{:=C_i} \begin{pmatrix} |e_0\rangle \\ |e_k\rangle \\ |e^k\rangle \\ |e^0\rangle \end{pmatrix}, \tag{2.1.15}$$

where $|e_j\rangle = \phi_j |e_0\rangle$, $\left|e^j\right\rangle = \phi^j |e_0\rangle$, $\left|e^0\right\rangle = \phi^0 |e_0\rangle$ and induces a splitting of the bundle V as

$$V = \mathcal{H}^{(0,0)} \oplus \mathcal{H}^{(1,1)} \oplus \mathcal{H}^{(2,2)} \oplus \mathcal{H}^{(3,3)}. \tag{2.1.16}$$

Here $\mathcal{H}^{(i,i)}$ denotes the subspace created by the charge (i,i) operators[6] . The insertion of ϕ_i can also be understood as taking a derivative ∂_{t^i}. In this way the bundle can be endowed with a connection $\nabla = \partial_{t_i} - C_i$ which is flat

$$[\nabla_i, \nabla_j] = 0 \tag{2.1.17}$$

and is called the Gauss-Manin connection. In fact, there is a second way basis for the vacuum bundle which also gives rise to a flat connection. For these purposes, one introduces the CPT operator Θ on the world-sheet and considers the metric

$$g_{a\bar{b}} = \left\langle e_a \middle| \Theta e^b \right\rangle \tag{2.1.18}$$

which gives rise to the new basis

$$|e_{\bar{\imath}}\rangle = g_{k\bar{\imath}} \left|e^k\right\rangle, \qquad |e_{\bar{0}}\rangle = g_{0\bar{0}} \left|e^0\right\rangle. \tag{2.1.19}$$

The action of the chiral ring reads in the new basis[7]

$$\begin{aligned} \phi_i \begin{pmatrix} |e_0\rangle \\ |e_j\rangle \\ |e_{\bar{\jmath}}\rangle \\ |e_{\bar{0}}\rangle \end{pmatrix} &= \underbrace{\begin{pmatrix} 0 & \delta_i^k & 0 & 0 \\ 0 & 0 & C_{ijk} g^{k\bar{k}} & 0 \\ 0 & 0 & 0 & g^{0\bar{0}} g_{i\bar{\jmath}} \\ 0 & 0 & 0 & 0 \end{pmatrix}}_{:=C_i} \begin{pmatrix} |e_0\rangle \\ |e_k\rangle \\ |e_{\bar{k}}\rangle \\ |e_{\bar{0}}\rangle \end{pmatrix} \\ \phi_{\bar{\imath}} \begin{pmatrix} |e_0\rangle \\ |e_j\rangle \\ |e_{\bar{\jmath}}\rangle \\ |e_{\bar{0}}\rangle \end{pmatrix} &= \underbrace{\begin{pmatrix} 0 & 0 & 0 & 0 \\ g^{\bar{0}0} g_{\bar{\imath}j} & 0 & 0 & 0 \\ 0 & C_{\bar{\imath}\bar{\jmath}\bar{k}} g^{\bar{k}k} & 0 & 0 \\ 0 & 0 & \delta_{\bar{\imath}}^{\bar{k}} & 0 \end{pmatrix}}_{:=C_{\bar{\imath}}} \begin{pmatrix} |e_0\rangle \\ |e_k\rangle \\ |e_{\bar{k}}\rangle \\ |e_{\bar{0}}\rangle \end{pmatrix} \end{aligned} \tag{2.1.20}$$

[6] To be more precise, such an operator gives rise to another vacuum state via the analog of the Hodge decomposition.

[7] By abuse of notation, we also denote the following transformation by C_i although it differs from (2.1.15).

One can thus decompose V as

$$V = \mathcal{L} \oplus \mathcal{L} \otimes T\mathcal{M} \oplus \overline{\mathcal{L} \otimes T\mathcal{M}} \oplus \bar{\mathcal{L}}. \tag{2.1.21}$$

Here $\mathcal{L}$ denotes the line bundle generated by the preferred ground-state $|e_0\rangle$ from which the other ground states can be generated by acting with chiral operators of weight $(1,1)$. However, these were identified with deformations and can in turn be identified with a section of $\mathcal{L} \otimes T\mathcal{M}$. One can introduce a connection on the bundle spanned by the new basis which is given as

$$(A_i)^b_a = g^{b\bar{c}} \partial_i g_{a\bar{c}}. \tag{2.1.22}$$

It is easily checked that this quantity transforms under gauge transformations indeed as a connection. This connection induces a covariant derivative

$$D_i |e_a\rangle = \partial_i |e_a\rangle - (A_i)^b_a |e_b\rangle \ . \tag{2.1.23}$$

The commutators of the covariant derivative with respect to this connection are called tt^* equations and read as follows

$$\begin{aligned} [D_i, \bar{D}_{\bar{\jmath}}] &= -[C_i, \bar{C}_{\bar{\jmath}}] \\ [D_i, D_j] = [\bar{D}_{\bar{\imath}}, \bar{D}_{\bar{\jmath}}] &= [D_i, \bar{C}_{\bar{\jmath}}] = [\bar{D}_{\bar{\imath}}, C_j] = 0\,, \\ D_i C_j = D_j C_i\,, &\qquad \bar{D}_{\bar{\imath}} \bar{C}_{\bar{\jmath}} = \bar{D}_{\bar{\jmath}} \bar{C}_{\bar{\imath}}\,. \end{aligned} \tag{2.1.24}$$

The derivation of these equations is rather involved and based on explicit path integral integral computations. We refer to the original literature [60] or reviews [61, 64] for details. These can be used to define a flat connection given by

$$\nabla_i = D_i + \alpha C_i, \qquad \bar{\nabla}_{\bar{\jmath}} = \bar{D}_{\bar{\jmath}} + \alpha^{-1} \bar{C}_{\bar{\jmath}}\,. \tag{2.1.25}$$

(2.1.25) is also a realization of the Gauss - Manin connection. This splitting of the vacuum bundle will be important for the discussion of the holomorphic anomaly in section 2.3.2. The tt^* metric can furthermore be used to endow $\mathcal{M}$ with a Kähler metric by setting

$$G_{i\bar{\jmath}} = \frac{g_{i\bar{\jmath}}}{g_{0\bar{0}}} \tag{2.1.26}$$

Here the Kähler potential is given as $g_{0\bar{0}} = e^{-K}$ and the equality $G_{i\bar{\jmath}} = \partial_{t_i} \partial_{t_{\bar{\jmath}}} K$ is a consequence of the tt^* equations (2.1.24), see e.g. [61] for a derivation of this fact.

2.1.6. The topological twist

In this section we will introduce the topological twist [13] that transforms an $\mathcal{N} = (2,2)$ SCFT into a topological field theory. This algebra possesses two isomorphisms, also called twists that are given as

$$\begin{aligned} A: &\quad T(z) \longrightarrow T(z) + \frac{1}{2}\partial J(z), \qquad \bar{T}(\bar{z}) \longrightarrow \bar{T}(\bar{z}) - \frac{1}{2}\bar{\partial}\bar{J}(\bar{z}) \\ B: &\quad T(z) \longrightarrow T(z) - \frac{1}{2}\partial J(z), \qquad \bar{T}(\bar{z}) \longrightarrow \bar{T}(\bar{z}) - \frac{1}{2}\bar{\partial}\bar{J}(\bar{z}) \end{aligned} \tag{2.1.27}$$

There are two more twists, but these are related to these two by complex conjugation. For the moment we concentrate on the holomorphic part of the A-twist and analyze its implications. We do not work out all the new OPEs but remark that

$$\begin{aligned} T(z)T(w) &\sim \frac{2T(w)}{(z-w)^2} + \frac{\partial_w T(w)}{z-w}\,, \\ T(z)J(w) &\sim -\frac{c}{3}\frac{1}{(z-w)^3} + \frac{J(w)}{(z-w)^2} + \frac{\partial J(w)}{(z-w)}\,. \end{aligned} \tag{2.1.28}$$

Here the first OPE implies that no ghosts are necessary in order to quantize the system, while the second OPE displays that the twisted current acquires an anomaly. Another effect of the twisting is that the conformal charge of G^+ becomes one, which can be used to define a BRST operator

$$\mathcal{Q} = \oint G^+\,. \tag{2.1.29}$$

Also, the energy-momentum tensor T becomes exact

$$\tilde{T} = \frac{1}{2}\{\mathcal{Q}, G^-\}, \tag{2.1.30}$$

which implies that the theory gets topological by the twist.

The discussion of an-holomorphic sector and of the B-twist works analogously. Altogether the twisting leads to two sets of BRST operators[8]

$$\begin{aligned} (a,c): &\quad \mathcal{Q}_A = G_0^- + \bar{G}_0^+ \\ (c,c): &\quad \mathcal{Q}_B = G_0^+ + \bar{G}_0^+ \end{aligned} \tag{2.1.31}$$

that annihilate the anti-chiral respectively the anti-chiral ring.

In fact, the two twists are related by the re-definition $J \mapsto -J$ and from the conformal point of view there is no difference between them. A crucial difference between them will arise, once one considers the realization by non-linear Sigma-models. This is the subject of the next section.

2.2. Nonlinear Sigma model realization

One important realization of SCF theories is given by a non-linear Sigma-model (see e.g. [61, 64, 180, 186] for further reference), i.e. a supersymmetric embedding of a Riemann surface Σ_g of genus g into a Calabi-Yau threefold[9] X

$$x^i : \Sigma_g \longrightarrow X\,. \tag{2.2.1}$$

In particular, it will be used in the following to geometrically realize the A- and the B-model. The full field content of the theory reads as follows, note that we also display the effect of twisting

[8] The twisting changes the conformal weight, which results in a shift within the mode expansion.
[9] We restrict in general our discussion to threefolds.

	Section before twisting	Section (A) twist	Section (B) twist
x	$\Gamma(\Sigma_g, X)$	$\Gamma(\Sigma_g, X)$	$\Gamma(\Sigma_g, X)$
ψ	$\Gamma(\Sigma_g, x^*(TX^{(1,0)}) \otimes K^{\frac{1}{2}})$	$\Gamma(\Sigma_g, x^*(TX^{(1,0)}))$	$\Gamma(\Sigma_g, x^*(TX^{(1,0)}) \otimes K)$
$\bar{\psi}$	$\Gamma(\Sigma_g, x^*(TX^{(1,0)}) \otimes \bar{K}^{\frac{1}{2}})$	$\Gamma(\Sigma_g, x^*(TX^{(1,0)}) \otimes \bar{K})$	$\Gamma(\Sigma_g, x^*(TX^{(1,0)}) \otimes \bar{K})$
χ	$\Gamma(\Sigma_g, x^*(TX^{(0,1)}) \otimes K^{\frac{1}{2}})$	$x^*(TX^{(0,1)} \otimes K)$	$\Gamma(\Sigma_g, x^*(TX^{(0,1)}))$
$\bar{\chi}$	$\Gamma(\Sigma_g, x^*(TX^{(0,1)}) \otimes \bar{K}^{\frac{1}{2}})$	$\Gamma(\Sigma_g, x^*(TX^{(0,1)}))$	$\Gamma(\Sigma_g, x^*(TX^{(0,1)})$

$TX = TX^{(1,0)} \oplus TX^{(0,1)}$ denotes the complexified tangent bundle of X and K denotes the canonical bundle of Σ_g. The dynamics of the un-twisted fields are governed by the following action

$$\begin{aligned} S &= \int_{\Sigma_g} d^2z \Big(\sqrt{\eta} g_{i\bar{\jmath}} \eta^{\mu\nu} \partial_\mu x^i \partial_\nu x^{\bar{\jmath}} + \sqrt{\eta} B_{i\bar{\jmath}} \eta^{\mu\nu} \partial_\mu x^i \partial_\nu x^{\bar{\jmath}} \\ &\quad - i g_{i\bar{\jmath}} \bar{\chi}^{\bar{\jmath}} D_{\bar{z}} \bar{\psi}^i - i g_{i\bar{\jmath}} \chi^{\bar{\jmath}} D_z \psi^i - \frac{1}{2} R_{i\bar{\jmath}k\bar{l}} \psi^i \bar{\psi}^k \bar{\chi}^{\bar{\jmath}} \chi^{\bar{l}} \Big) \end{aligned} \tag{2.2.2}$$

Here $\eta_{\mu\nu}$ denotes the world-sheet metric on Σ_g, in contrast to the space-time metric $g_{i\bar{\jmath}}$. The covariant derivative acting on the fermionic fields reads as follows, with Γ^i_{kl} denoting the Christoffel symbols

$$\begin{aligned} D_z \psi^i &= \partial_z \psi^i - \frac{i}{2} \omega_z \bar{\psi}^i + \Gamma^i_{kl} \partial_z x^k \psi^l \,, \\ D_{\bar{z}} \bar{\psi}^i &= \partial_{\bar{z}} \bar{\psi}^i + \frac{i}{2} \omega_{\bar{z}} \bar{\psi}^i + \Gamma^i_{kl} \partial_{\bar{z}} x^k \bar{\psi}^i \,. \end{aligned} \tag{2.2.3}$$

The operators of the superconformal algebra are realized as follows

$$\begin{aligned} \mathcal{J} &= g_{i\bar{\jmath}} (\psi^i \bar{\chi}^{\bar{\jmath}} + \bar{\psi}^i \chi^{\bar{\jmath}}) \,, \\ \mathcal{G}^+ &= g_{i\bar{\jmath}} (\psi^i \partial_z x^{\bar{\jmath}} + \bar{\psi}^i \partial_{\bar{z}} x^{\bar{\jmath}}) \,, \\ \mathcal{G}^- &= g_{i\bar{\jmath}} (\chi^{\bar{\jmath}} \partial_z x^i + \bar{\chi}^{\bar{\jmath}} \partial_{\bar{z}} x^i) \,, \\ \mathcal{T} &= g_{i\bar{\jmath}} (\partial_z x^i \partial_{\bar{z}} x^{\bar{\jmath}} + i \chi^{\bar{\jmath}} \partial_z \psi^i + i \bar{\chi}^{\bar{\jmath}} \partial_{\bar{z}} \bar{\psi}^i) \,. \end{aligned} \tag{2.2.4}$$

The curly quantities denote the sum of right- and left-moving part, e.g. $\mathcal{J} = J + \bar{J}$. Before we discuss the A- and the B-model in detail, we briefly comment on the distinguished role of Calabi-Yau threefolds.

2.2.1. The special role of Calabi-Yau threefolds

This section explains the special role of Calabi-Yau threefolds among the possible target spaces [61]. In fact $\mathcal{N} = (1,1)$-supersymmetric models can be formulated on any Riemannian manifold, the extension to $\mathcal{N} = (2,2)$ supersymmetry requires the manifold to be Kähler, which allows for left- and right-running U(1) R-symmetries. These can be linearly combined to vector $\mathrm{U}(1)_V$ and axial $\mathrm{U}(1)_A$ currents. The topological twist can be shown to be equivalent to a coupling of the form

$$\int_{\Sigma_g} \hat{J} \omega_S, \tag{2.2.5}$$

where ω_S denotes the spin connection and $\hat{J}$ is the respective linear combination of U(1) currents. The A-model couples to the vector current and can therefore be defined on any

Kähler manifold. The B-model gets couples to the $\mathrm{U}(1)_A$ current which acquires an anomaly

$$-\frac{c}{3}\int_{\Sigma_g} x^*(c_1(TM)). \tag{2.2.6}$$

The cancellation of this anomaly is equivalent to demanding that X is a Calabi-Yau manifold. However, in the following discussion it is assumed that both, the A- and the B-model are defined on Calabi-Yau manifolds. To point out the distinguished role of three complex dimensions, one has to anticipate some results from topological string theory, see also 2.3.2.

Firstly, for $d = 3$ the anomalous coefficient in (2.1.28) becomes -3, which reflects the fact, that one can establish an isomorphism between the bosonic and the topological field theory. This will be important for the construction of the topological string in section 2.3.2. Secondly, the virtual dimension of the moduli space $\bar{\mathcal{M}}_g(X,\beta)$ of stable maps from a Riemann surface of genus g has dimension [61]

$$\text{vir dim}\bar{\mathcal{M}}_g(X,\beta) = \int_\beta c_1(X) + \dim(X-3)(1-g) \tag{2.2.7}$$

which becomes zero in the case of threefolds but negative for higher dimensions, if $g \geq 1$. Roughly speaking, this implies that topological string theory is uninteresting on these spaces.

2.2.2. The moduli space of Calabi-Yau threefolds

As the understanding of the moduli space of Calabi-Yau manifolds [184] is crucial for the discussion of A- and B-model, it is briefly analyzed in the following. Consider an infinitesimal variation $g_{\mu\nu} + \delta g_{\mu\nu}$ of a Ricci-flat metric on a Calabi-Yau manifold X. Demanding that the Ricci-flatness is preserved

$$R_{\mu\nu}(g) = 0, \qquad R_{\mu\nu}(g+\delta g) = 0 \tag{2.2.8}$$

one is lead in the gauge $\nabla^\nu g_{\mu\nu} = 0$ to the so-called Lichnerowicz equation

$$\nabla^\lambda \nabla_\lambda \delta g_{\mu\nu} + 2R_{\mu\ \nu}^{\ \kappa\ \tau}\delta g_{\kappa\tau} = 0\,. \tag{2.2.9}$$

Using the splitting of the indices μ,ν into holomorphic and anti-holomorphic indices $m,\bar{n}$, one can analyze $\delta g_{m\bar{n}}$ and δg_{mn} separately. It turns out that (2.2.9) demands that $\delta g_{m\bar{n}}$ is harmonic with respect to Δ_d, while $\delta g^m = g^{m\bar{k}}\delta_{\bar{k}\bar{n}}d\bar{z}^{\bar{n}}$ is $\Delta_{\bar{\partial}}$ harmonic. These are therefore associated with elements of $H^{(1,1)}(X,\mathbb{C})$ and $H^{(0,1)}(X,T^{(1,0)}X)$ respectively. The latter is due to the globally non-vanishing holomorphic three-form isomorphic to $H^{(2,1)}(X,\mathbb{C})$.

As the first type of deformation preserves the index structure it is identified with deformations of the Kähler form, which can accordingly be expanded within a basis ω^k of $H^{(1,1)}(X,\mathbb{C})$ as

$$\omega = \sum_k t_k\omega^k\,. \tag{2.2.10}$$

Here t_k denote the real Kähler parameter. Note that not any deformation is allowed but only those which do not violate the positivity condition, i.e.

$$\int_C \omega \geq 0, \quad \int_S \omega\wedge\omega \geq 0, \quad \int_X \omega\wedge\omega\wedge\omega \geq 0\,. \tag{2.2.11}$$

for all curves C and surfaces S which leads to the notion of the Kähler cone. Later on, it turns out to be useful to consider the complexified Kähler form $J = \omega + iB$, where B denotes the Kalb-Ramond field.

The second type of variations changes the index structure of the metric. One therefore needs an anti-holomorphic coordinate transformation[10] to restore the original type. These deformations are accordingly associated with complex structure deformations.

2.2.3. The A-model

In this case the twist is given by

$$\tilde{T} = T + \frac{1}{2}\partial J, \qquad \bar{\tilde{T}} = \bar{T} - \frac{1}{2}\bar{\partial}\bar{\jmath} \tag{2.2.12}$$

The BRST-operator

$$\mathcal{Q}_A = \oint G^- dz + \oint \bar{G}^+ d\bar{z} \tag{2.2.13}$$

acts as follows on the fields

$$\begin{aligned} \delta_A x^i = \epsilon\psi^i, \quad \delta_A\psi^i = 0, \quad \delta_A\bar{\psi}^{\bar{\imath}} &= 2i\epsilon\bar{\partial}x^i + \epsilon\Gamma^i_{jk}\bar{\psi}^{\bar{\jmath}}\psi^k, \\ \delta_A x^{\bar{\imath}} = \epsilon\bar{\chi}^{\bar{\imath}}, \quad \delta_A\bar{\chi}^{\bar{\imath}} = 0, \quad \delta_A\chi^{\bar{\imath}} &= -2i\epsilon\partial x^{\bar{\imath}} + \epsilon\Gamma^{\bar{\imath}}_{\bar{\jmath}\bar{k}}\bar{\chi}^{\bar{\jmath}}\chi^{\bar{k}}. \end{aligned} \tag{2.2.14}$$

Here, Γ^i_{jk} denote the Christoffel symbols with respect to the space-time metric and we have set[11] $\epsilon_+ = \bar{\epsilon}_-$ and made use of the notation

$$\delta_A f = [\mathcal{Q}_A, f]_\pm \,. \tag{2.2.15}$$

The vanishing of the fermionic variations implies that the BRST-invariant configurations are given by holomorphic maps. The A-twisted action of the non-linear sigma model action is given by[12]

$$S = it\delta_A\left(\int_{\Sigma_g} d^2z V\right) + t\int_{\Sigma_g} d^2z\, x^* J, \qquad V = g_{i\bar{\jmath}}\left(\chi^{\bar{\jmath}}\partial_{\bar{z}}x^i + \partial_z x^{\bar{\jmath}}\bar{\psi}^{\bar{\imath}}\right) . \tag{2.2.16}$$

with J denoting the complexified Kähler form. This form of the action can be used to show that the A-model is invariant under deformations of the complex structure up to BRST trivial terms. See e.g. [186]. The BRST closed operators of the topological field theory take the form

$$\omega_{i_1\ldots i_p\bar{\jmath}_1\ldots\bar{\jmath}_q}\psi^{i_1}\ldots\psi^{i_p}\bar{\chi}^{\bar{\jmath}_1}\ldots\bar{\chi}^{\bar{\jmath}_q} \,. \tag{2.2.17}$$

The identification ($u, \bar{u}$ being local coordinates)

$$\psi^i \mapsto du^i, \qquad \bar{\chi}^{\bar{\jmath}} \mapsto d\bar{u}^{\bar{\jmath}}, \qquad \mathcal{Q}_A \mapsto d = \partial + \bar{\partial} \tag{2.2.18}$$

implies that the A-model calculates the de Rham cohomology of the target space. The deformations of the A-model are given by the (1,1)-elements of the anti-chiral ring that

[10] It is non-trivial that the infinitesimal transformation can be integrated to a finite one. See e.g. [185].

[11] This swallows some cohomological information. See [61] for the full transformations.

[12] Here t denotes a parameter that takes the role of $\hbar$ in QFT and is not to be confused with a Kähler modulus.

take the form

$$\omega_{i\bar{j}}\psi^i\bar{\chi}^{\bar{j}} \tag{2.2.19}$$

and are identified with Kähler deformations[13] using (2.2.18).

2.2.4. A-model realization of the vacuum bundle

The realization of the vacuum bundle within the A-model relies on the notion of quantum cohomology [187, 188], see also [61, 186]. The basic idea is to deform the classical intersection numbers by world-sheet instantons. This happens as follows. The charge conservation and anomaly cancellation constrain the correlation function on a sphere to take the following form

$$C_{ijk} = \langle \phi_i(0)\phi_j(1)\phi_k(\infty)\rangle \tag{2.2.20}$$

where in addition the SL(2,$\mathbb{Z}$) invariance has been used. (2.2.20) is also called Yukawa coupling as it gives rise to this quantity in e.g. certain Heterotic compactifications. The operators ϕ_i are elements of $H^{(1,1)}(X,\mathbb{C})$ and we denote their dual divisors by D_i. As the path integral localizes on the holomorphic maps this path integral can in a first step reduced to the moduli space of maps

$$C_{ijk} = \sum_{\beta\in H_2(X,\mathbb{Z})} Q^\beta \int_{\mathcal{M}_{0,3}(X,\beta)} \mathrm{ev}_0^*(\omega_1)\wedge \mathrm{ev}_1^*(\omega_2)\wedge \mathrm{ev}_\infty^*(\omega_3)\,. \tag{2.2.21}$$

The notation is as follows. $\mathcal{M}_{0,3}(X,\beta)$ denotes the moduli space of stable[14] maps of genus zero with three punctures. $\mathrm{ev}_i : \mathcal{M}_{0,3}(X,\beta) \longrightarrow X$ is the evaluation map. In addition choose dual bases e_i and e^j of $H^{1,1}(X)$ and $H_2(X)$ respectively such that the Kähler form reads $J = t^i e_i$ and any class $\beta = d_i e^i$. The Kähler parameters are explicitly given as

$$t^i = \int_{e^i} J = \int_{e^i} \omega + iB\,. \tag{2.2.22}$$

Also $Q_k = e^{-2\pi i t^k}$ and we denote in the following $\prod_{i=1}^{h^{(1,1)}} Q_i^{d_i} = Q^\beta$. The three-point function can accordingly we evaluated as

$$C_{ijk} = D_i \cap D_j \cap D_k + \sum_{0\neq\beta\in H_2(X,\mathbb{Z})} N_\beta^0 d_i d_j d_k Q^\beta. \tag{2.2.23}$$

Here N_β^0 are the values of the integrals over the moduli spaces $\mathcal{M}_{0,3}(X,\beta)$ and are called Gromov-Witten invariants at genus zero. The map with $d_i = 0$ is special and corresponds to the map which sends the punctured sphere onto a point in X. It reproduces the classical intersections that get corrected by world-sheet instantons. This evaluation takes place around a point in the moduli space, where the volume of the corresponding curves is large and the instanton sum has a sensible meaning. This is called the large radius point.

The three-point function can also be expressed as the third derivative of the prepotential

[13] To obtain complexified deformations one has to add the hermitian conjugate which vanishes in $\mathcal{Q}_A$ BRST-cohomology.

[14] A map from a pointed nodal curve Σ into X is called stable if any contracted component of genus zero has at least three special points and any of genus one at least one in order to cancel the isometries.

which is also called the free energy at genus zero.

$$F^0(t) = \frac{1}{3!}\int J\wedge J\wedge J + \sum_{0\neq\beta\in H_2(X,\mathbb{Z})} N^0_\beta Q^\beta, \qquad C_{ijk} = \partial_{t_i}\partial_{t_j}\partial_{t_k}F^0\,. \tag{2.2.24}$$

The vacuum bundle discussed in section 2.1.5 is realized in the A-model via the sequence [180]

$$H^0(X,\mathbb{C}) \xrightarrow{\nabla_A} H^2(X,\mathbb{C}) \xrightarrow{\nabla_A} H^4(X,\mathbb{C}) \xrightarrow{\nabla_A} H^6(X,\mathbb{C}). \tag{2.2.25}$$

To define the connection ∇_A one picks a generator η_0 of $H^0(X,\mathbb{C})$ and a basis η_i of $H^2(X,\mathbb{C})$. In addition one chooses bases χ_i and χ_0 of $H^4(X,\mathbb{C})$ and $H^6(X,\mathbb{C})$ that are dual to the first two with respect to the symplectic pairing. The connection reads

$$\nabla_A\eta_0 = \sum_{i=1}^n \eta_i\otimes\frac{dQ_i}{Q_i}, \quad \nabla_A\eta_k = \sum_{i,j=1}^n C_{ijk}\chi_j\otimes\frac{dQ_i}{Q_i}, \quad \nabla_A\chi_j = \chi_0\frac{dQ_j}{Q_j}, \quad \nabla_A\chi_0 = 0\,. \tag{2.2.26}$$

2.2.5. The B-model

The BRST operator of the B-model [61, 186] is given as follows

$$\mathcal{Q}_B = \oint G^+dz + \oint \bar{G}^+d\bar{z} \tag{2.2.27}$$

and in order to display its action on the fields it is useful to introduce the combinations

$$\eta^{\bar{\imath}} = (\chi^{\bar{\imath}} + \bar{\chi}^{\bar{\imath}}), \quad \theta_j = g_{\bar{\imath}j}(\bar{\chi}^{\bar{\imath}} - \chi^{\bar{\imath}}). \tag{2.2.28}$$

The BRST transformations on the operators read as follows

$$\delta_B x^i = 0, \quad \delta_B x^{\bar{\imath}} = \bar{\epsilon}\eta^{\bar{\imath}}, \quad \delta_B\psi^i = i\bar{\epsilon}\partial x^i, \quad \delta_B\bar{\psi}^i = -i\bar{\epsilon}\bar{\partial}x^i, \quad \delta_B\eta^{\bar{\imath}} = 0, \quad \delta_B\theta_i = 0. \tag{2.2.29}$$

In contrast to the A-model this implies that the B-model path integral localizes on constant maps into the target space, which is one source of its easier computability. After twisting the action takes the following form

$$\begin{aligned} S = it\int\{Q_B, V\} + tW, \qquad V &= g_{i\bar{\jmath}}(\psi^i\partial_{\bar{z}}x^{\bar{\jmath}} + \bar{\psi}^i\partial_z x^{\bar{\jmath}}), \\ W &= \int_{\Sigma_g}\big(-\theta_i D\psi^i - \frac{i}{2}R_{i\bar{\imath}j\bar{\jmath}}\psi^i\wedge\psi^j\eta^{\bar{\imath}}\theta_k g^{\bar{\jmath}k}\big)\,. \end{aligned} \tag{2.2.30}$$

One can show that the B-model is BRST cohomologically invariant under Kähler deformations. The physical operators of the B-model take the form

$$\omega(x)^{i_1\ldots i_p}_{\bar{\jmath}_1\ldots\bar{\jmath}_q}\eta^{\bar{\jmath}_1}\ldots\eta^{\bar{\jmath}_q}\theta_{i_1}\ldots\theta_{i_p} \tag{2.2.31}$$

and after identifying

$$\eta^{\bar{\imath}}\mapsto d\bar{z}^{\bar{\imath}}, \quad \theta_i\mapsto\partial_{z^i}, \quad \mathcal{Q}_B\mapsto\bar{\partial} \tag{2.2.32}$$

one notices that the topological operators are just given by the elements of the twisted cohomology group $H^{(0,q)}(\wedge^p TX^{(1,0)})$ which can be identified with $H^{(3-p,q)}(X,\mathbb{C})$ by making

use of the globally non-vanishing three-form Ω. The deformations of the B-model are given by operators of the form

$$\phi^a = (b^a)^j_{\bar{i}} \eta^{\bar{i}} \theta_j \tag{2.2.33}$$

where b^a constitute a basis of $H^{(0,1)}(X, T^{(1,0)}X)$.

2.2.6. Hodge filtration and Picard-Fuchs equations

The moduli space of the B-model is given by the complex structure moduli space of the target space. The bundle corresponding to the deformation sub-ring is therefore given as $H^3(X, \mathbb{C})$. Once a complex structure is chosen, there is a natural splitting [61, 180]

$$H^3(X, \mathbb{C}) = \bigoplus_{p+q=3} H^{p,q}(X)\,. \tag{2.2.34}$$

Unfortunately, this splitting does not vary holomorphically as one moves in the complex structure moduli space. Instead one is led to consider the so-called Hodge filtration, which does vary holomorphically

$$H^3 = F^0 \supset F^1 \supset F^2 \supset F^3, \qquad F^p = \bigoplus_{a \geq p} H^{a,3-a}(X) \subset H^3 \tag{2.2.35}$$

from which the split (2.2.34) can be re-discovered as

$$H^{p,q}(X) = F^p(X) \cap \overline{F^q(X)}\,. \tag{2.2.36}$$

In addition the filtration (2.2.35) is equipped with a flat connection, named the Gauss-Manin connection, that enjoys the so-called Griffiths transversality condition $\nabla F^p \subset F^{p-1}$. This property can be used to construct a basis of $H^3(X, \mathbb{C})$ that reads

$$\begin{aligned} \vec{\Omega} = \{\Omega_\beta\} = (\Omega^{(3,0)}, \Omega_i^{(2,1)}, \Omega^{i\,(1,2)}, \Omega^{(0,3)}), \\ i = 1, \ldots, h^{(2,1)}, \quad \beta = 0, \ldots h^3(X). \end{aligned} \tag{2.2.37}$$

The Gauss-Manin connection takes up to exact terms the form

$$\nabla_i \vec{\Omega}(z) = (\partial_i - \mathcal{A}_i)\vec{\Omega}(z) = 0 \tag{2.2.38}$$

which implies that it annihilates the periods

$$\Pi^\alpha_\beta(z) = \int_{\gamma^\alpha} \Omega_\beta(z), \qquad \gamma^\alpha \in H_3(X), \qquad \alpha, \beta = 0, \ldots h^3(X)\,. \tag{2.2.39}$$

Here γ^α denotes a basis of $H_3(X)$. Also, the Griffiths transversality condition implies that it is meaningful to define

$$C_{ijk} = \int_X \Omega \wedge \nabla_i \nabla_j \nabla_k \Omega\,. \tag{2.2.40}$$

Denote by $\{z^k\}$ a set of coordinates on the complex structure moduli. One notices that

$$\begin{aligned} \frac{\partial\Omega}{\partial z^k} &\in H^{(3,0)} \oplus H^{(2,1)}\,, \\ \frac{\partial^2\Omega}{\partial z^k \partial z^l} &\in H^{(3,0)} \oplus H^{(2,1)} \oplus H^{(1,2)}\,, \\ \frac{\partial^3\Omega}{\partial z^k \partial z^l \partial z^k} &\in H^{(3,0)} \oplus H^{(2,1)} \oplus H^{(1,2)} \oplus H^{(0,3)}\,. \end{aligned} \tag{2.2.41}$$

This implies that there is a set of forth order differential equations $\mathcal{L}_\alpha$, such that

$$\mathcal{L}_\alpha \Pi^\alpha = 0. \tag{2.2.42}$$

The Picard-Fuchs equations can be seen as one manifestation of the flatness of the Gauss-Manin connection. As the moduli space is not simply connected, corresponding to the fact that singular and orbifold loci are cut out, the periods can have non-trivial monodromy although the connection is flat. The monodromy group Γ is generated by transport around loops $\gamma^i \in H^1(\mathcal{M})$ and is a subgroup of $\mathrm{Sp}(h^3(X), \mathbb{Z})$, see [61] for more details.

B-model realization of the vacuum bundle

Next, we construct suitable coordinates for the complex structure moduli space. We start by picking a symplectic bases for $H_3(X, \mathbb{Z})$ [61, 176, 180]

$$A_k \cap B^l = \delta_k^l, \qquad A_i \cap A_j = 0, \qquad B^i \cap B^j = 0 \tag{2.2.43}$$

and a Poincaré dual one of $H^3(X, \mathbb{Z})$ such that

$$\int_X \alpha_k \wedge \beta^l = \int_{A_l} \alpha_k = -\int_{B_k} \beta^l = \delta_k^l\,. \tag{2.2.44}$$

The allows accordingly for an expansion of Ω as

$$\Omega(z) = X^k(z)\alpha_k + \mathcal{F}_k(z)\beta^k, \qquad X^k = \int_{A_k} \Omega, \quad \mathcal{F}_k = \int_{B^k} \Omega \tag{2.2.45}$$

and one writes $\Pi^t = (X^i,\ \mathcal{F}_i)$. The Riemann bilinear identity implies that

$$\partial_{X^i}\mathcal{F}_j = \partial_{X^j}\mathcal{F}_i \tag{2.2.46}$$

which implies in turn the existence of the so-called prepotential which satisfies

$$\mathcal{F} = \frac{1}{2} X^i \mathcal{F}_i, \qquad \partial_{X^i}\mathcal{F} = \mathcal{F}_i. \tag{2.2.47}$$

The complex structure moduli space locally coincides with $H^{2,1}(X, \mathbb{C})$ which has dimension $\frac{1}{2}h^3 - 1$. One can show that the X^k are homogeneous coordinates for the complex structure moduli space and inhomogeneous coordinates are provided by

$$t^a = X^a / X^0\,. \tag{2.2.48}$$

The latter are also called flat or special coordinates. The normalized three-form $v_0 = \Omega(t)/X^0$ has the following expansion [180]

$$v_0 = \alpha_0 + t^a \alpha_a + \beta^b F_b(t) + (2F^0(t) - t^c F_c(t))\beta^0 \tag{2.2.49}$$

with

$$F^0(t) = (X_0)^{-2}\mathcal{F}, \qquad F_a(t) = \frac{\partial F^0(t)}{\partial t^a}. \tag{2.2.50}$$

One also defines

$$\begin{aligned} v_a &= \alpha_a + \beta^b F_{ab}(t) + (F_a(t) - t^b F_{ab}(t))\beta^0\,, \\ v_D^a &= \beta^a - t^a\beta^0\,, \\ v^0 &= -\beta^0\,. \end{aligned} \tag{2.2.51}$$

In addition, the three-point function takes in these coordinates the form

$$C_{abc} = \partial_a\partial_b\partial_c F_0(t) = \int_X v_0 \wedge \partial_a\partial_b\partial_c v_0\,. \tag{2.2.52}$$

This form makes also contact with the field theory definition of the three-point function as the derivative with respect to t^a corresponds to the insertion of a marginal operator. Indeed, it is known that the three-point function takes the form [61]

$$\langle\phi_1\phi_2\phi_3\rangle = \int_X (\phi_1)^{i_1}_{\bar{j}_1}(\phi_2)^{i_2}_{\bar{j}_2}(\phi_3)^{i_3}_{\bar{j}_3}\Omega_{i_1i_2i_3}d\bar{z}^{\bar{j}_1}\wedge d\bar{z}^{\bar{j}_2}\wedge d\bar{z}^{\bar{j}_3}\wedge\Omega. \tag{2.2.53}$$

In these quantities the action of the derivative $\partial_a = \frac{\partial}{\partial t^a}$ can finally be expressed as [180]

$$\partial_a \begin{pmatrix} v_0 \\ v_b \\ v_D^b \\ v^0 \end{pmatrix} = \begin{pmatrix} 0 & \delta_a^c & 0 & 0 \\ 0 & 0 & C_{abc} & 0 \\ 0 & 0 & 0 & \delta_a^b \\ 0 & 0 & 0 & 0 \end{pmatrix} \begin{pmatrix} v_0 \\ v_c \\ v_D^c \\ v^0 \end{pmatrix}. \tag{2.2.54}$$

This defines the Gauss-Manin connection (2.2.38) in special coordinates and is the B-model realization of the chiral ring structure (2.1.15).

There is also a B-model realization of second the decomposition (2.1.20) of the vacuum bundle that leads to the tt^*-equations. This can be constructed as follows. To obtain the corresponding Kähler potential, one identifies the projectively unique three-form Ω (in a certain complex structure) as the section of a line bundle $\mathcal{L}$ over the complex structure moduli space and introduces the Kähler potential K as

$$g_{0\bar{0}} = e^{-K} = -i\int \Omega\wedge\overline{\Omega} \tag{2.2.55}$$

Here the Kähler potential is manifestly invariant under $\mathrm{Sp}(h^3,\mathbb{Z})$ and can be expressed in terms of the periods as

$$K = -\log\Big(\Pi^\dagger\Sigma\Pi\Big), \qquad \Sigma = \begin{pmatrix} 0 & \mathbf{1} \\ -\mathbf{1} & 0 \end{pmatrix}. \tag{2.2.56}$$

Π denotes the period vector defined in (2.2.45). One also define bases of $H^{(2,1)}$ and $H^{(1,2)}$ respectively as

$$\chi_i = D_i\Omega = (\partial_i + K_i)\Omega, \qquad \bar{\chi}_{\bar{\imath}} = D_{\bar{\imath}}\overline{\Omega} = (\partial_{\bar{\imath}} + K_{\bar{\imath}})\overline{\Omega}, \tag{2.2.57}$$

and finds a Kähler metric

$$g_{i\bar{\jmath}} = i\int_X \chi_i \wedge \bar{\chi}_{\bar{\jmath}} = e^{-K}G_{i\bar{\jmath}} = e^{-K}\partial_i\partial_{\bar{\jmath}}K. \tag{2.2.58}$$

$G_{i\bar{\jmath}}$ is called the Weyl-Petersen metric. In these coordinates the Gauss-Manin connection is expressed as

$$D_i\begin{pmatrix}\Omega\\ \chi_j\\ \bar{\chi}_{\bar{\jmath}}\\ \overline{\Omega}\end{pmatrix} = \begin{pmatrix}0 & \delta_i^k & 0 & 0\\ 0 & 0 & iC_{ijk}e^K G^{k\bar{k}} & 0\\ 0 & 0 & 0 & G_{i\bar{\jmath}}\\ 0 & 0 & 0 & 0\end{pmatrix}\begin{pmatrix}\Omega\\ \chi_k\\ \bar{\chi}_{\bar{k}}\\ \overline{\Omega}\end{pmatrix}. \tag{2.2.59}$$

This is completely analogous to (2.1.20).

2.3. Mirror symmetry and topological string theory

We recall that the two twists (2.1.27) differ from a CFT perspective just by a map $J \mapsto -J$, which exchanges chiral and anti-chiral ring. Furthermore we have shown, that the (1,1)-elements of the chiral and anti-chiral ring are realized by the cohomology groups $H^{(1,1)}(X,\mathbb{C})$ respectively $H^{(2,1)}(X,\mathbb{C})$. This leads to the far reaching conjecture that for any Calabi-Yau manifold X there is another Calabi-Yau manifold Y, such that the A-model on X is equivalent to the B-model on Y and vice versa. In particular this implies that

$$h^{(1,1)}(X,\mathbb{C}) = h^{(2,1)}(Y,\mathbb{C}), \qquad h^{(1,1)}(Y,\mathbb{C}) = h^{(2,1)}(X,\mathbb{C})\,. \tag{2.3.1}$$

It is a crucial question how the Kähler moduli of X are identified with the complex structure moduli of Y. This is answered by the identification of the deformation bundle in the A- and the B-bundle respectively and their comparison to the abstract CFT. This leads to the following identification. Denote the period vector in the A-model by

$$\Pi_A(t) = (1, t_A^i, \partial_i F_A^0, 2F_A^0 - t_A^i\partial_i F_A^0) \tag{2.3.2}$$

Here F_A denotes the prepotential of the A-model side, i.e. the free energy at genus zero. t^i are the Kähler moduli as defined in (2.2.22). This gets identified with the period vector

$$\Pi_B(t) = (1, t_B^i, \partial_i F_B^0, 2F_B^0 - t_B^i\partial_i F_B^0) \tag{2.3.3}$$

on the B-model side. Here the t_B^i are the special coordinates defined by (2.2.48).

The large radius point on the A-model side gets under the mirror map identified with the point of maximal unipotent monodromy[15]. At this point, the solutions to the Picard-Fuchs

[15] It is a corollary of the mirror conjecture that such a point exists in the moduli space of any Calabi-Yau manifold. [192]

equations take the following structure [199]

$$\Pi(z) = \begin{pmatrix} X^0 \\ \vdots \\ X^{h^{2,1}} \\ \mathcal{F}_0 \\ \vdots \\ \mathcal{F}_{h^{2,1}} \end{pmatrix} = \begin{pmatrix} \int_{A_0} \Omega \\ \vdots \\ \int_{A_{h^{2,1}}} \Omega \\ \int_{B^0} \Omega \\ \vdots \\ \int_{B^{h^{2,1}}} \Omega \end{pmatrix} = \begin{pmatrix} \omega_0 \\ \vdots \\ \omega_{h^{2,1}} \\ \omega_{2h^{2,1}+2} + \sum_{i=1}^{2h^{2,1}} c_i^0 \omega_i \\ \sum_{i=0}^{2h^{2,1}-1} c_i^1 \omega_i \\ \vdots \end{pmatrix} \tag{2.3.4}$$

Here, ω_0 denotes a holomorphic power series, ω_i, $1 \leq i \leq h^{2,1}$ denote single logarithmic solutions, ω_i, $h^{2,1}+1 \leq i \leq 2h^{2,1}+1$ are double logarithmic solutions and finally, $\omega_{2h^{2,1}+2}$ is the projectively unique triple logarithmic solution. We refer to [61, 181, 199] for further expositions.

2.3.1. Topological string theory and mirror symmetry at higher genus

So far with have been dealing with topological field theories and the only world-sheet geometry was a sphere[16]. There exits a generalization of the prepotential to arbitrary genus g called the free energy $F^g(t)$ of genus g. These are organized as

$$F(t) = \sum_{n=0}^{\infty} g_s^{2g-2} F^g, \qquad Z(t) = \exp(F(t)) \tag{2.3.5}$$

and $Z(t)$ is called the partition function. In particular, mirror symmetry states that

$$F_A^g(t_A) = (X^0)^{2g-2} F_B^g(z(t)). \tag{2.3.6}$$

The definition of the higher genus free energies demands to go beyond field theory and to consider topological string theory. This is the subject of the next section, where we start on the B-model side.

2.3.2. Coupling the B-model to topological gravity

We consider a correlation function[17]

$$\langle \prod_a \mathcal{O}_{\phi_a} \rangle \tag{2.3.7}$$

for operators $\mathcal{O}_{\phi_a}$ which are related to cohomology elements of $H^{p,q}(X, \mathbb{C})$. The anomalous $\mathrm{U}(1)_A$ current demands that [212]

$$\sum_a p_a = \sum_a q_a = d(1-g). \tag{2.3.8}$$

which implies that a-priori only the sphere and the torus give rise to non-trivial correlation functions. This can be traced back to the fact that one is integrating over a fixed metric.

[16] One can also consider the torus as a world-sheet within field theory. See below.
[17] See [61, 186, 212] for further reference.

Coupling the theory to two-dimensional gravity allows also for non-trivial higher genus correlation functions. Note that so far we have been strictly speaking dealing with topological field theories. By this step we pass over to what is called topological string theory. To proceed one notices by inspecting the OPEs (2.1.28) that one can establish an isomorphism [186, 212] to the bosonic string

$$(G^+, J, T, G^-) \longmapsto (Q, J_{ghost}, T, b) \tag{2.3.9}$$

which allows to carry over the methods of coupling the bosonic string to gravity to the topological string. By the usual Fadeev-Popov procedure one reduces the path integral to an integral over the moduli space $\mathcal{M}_g$ times an integral over the "matter and ghost" system. The moduli space of Riemann surfaces is parametrized by the Beltrami differentials $\mu \in H^{(1,0)}(\Sigma_g, T^{(0,1)}\Sigma_g)$ and has real dimension $6g-6$ for $g \geq 2$.

The construction of the measure can be interpreted as follows. In analogy to the bosonic string where one has to insert $6g-6$ anti-ghosts in order to soak up the zero modes, one has here to insert this number of G^- operators to cancel the anomaly of the axial anomaly.

One defines a top form on the moduli space $\mathcal{M}_g$ of Riemann surfaces of genus g by

$$\omega_g = \bigwedge_{i=1}^{3g-3} dm_i \wedge d\bar{m}_i \left\langle \prod_{i=1}^{3g-3} |G^-(\mu_i)|^2 \right\rangle, \qquad G^-(\mu_i) = \int_{\Sigma_g} G^-_{zz}(\mu_i)^z_{\bar{z}} dz \wedge d\bar{z}. \tag{2.3.10}$$

In analogy to the bosonic string the free energies at genus g are then defined as

$$F^g = \int_{\mathcal{M}_g} \omega_g \tag{2.3.11}$$

which transform as sections of $\mathcal{L}^{2-2g}$, where $\mathcal{L}$ denotes the line bundle specified by the choice of holomorphic three-form Ω as its section.

The holomorphic anomaly equations

It is certainly difficult to perform the integrals (2.3.11) directly. Fortunately the free energies string obey a recursive relation, the so-called holomorphic anomaly equations that read as follows

$$\bar{\partial}_{\bar{\imath}} F^g = \frac{1}{2} \bar{C}_{\bar{\imath}\bar{\jmath}\bar{k}} e^{2K} G^{j\bar{\jmath}} G^{k\bar{k}} \big(D_j D_k \mathcal{F}^{g-1} + \sum_{r=1}^{g-1} D_j \mathcal{F}^r D_k \mathcal{F}^{g-r} \big) . \tag{2.3.12}$$

Here K denotes the Kähler potential defined in (2.2.56) and D_i denotes the covariant derivative[18] (2.2.57). The holomorphic anomaly reflects the fact that the Hodge decomposition does not vary holomorphically over the moduli space which leads to the consequence that the anti-holomorphic deformations, corresponding to the (a,a)-ring do not completely decouple. In the following we do not repeat the whole derivation of the holomorphic anomaly equations which is quite complicated. Instead we just point out the idea and refer to the original literature [86] for details or nice reviews [61, 199]. In usual QFT, an anomaly arises whenever a classical symmetry does not leave the path integral measure invariant. Something similar happens here. We consider again the perturbation of the action by marginal

[18] Note that this may acquire additional contributions from the Christoffel symbols of the Weyl-Peterson metric (2.2.58).

operators

$$S = \int_{\Sigma_g} d^2z\mathcal{L}_0 + \sum_i t^i \int_{\Sigma_g} d^2z\phi_i + \sum_{\bar{\imath}} \bar{t}^{\bar{\imath}} \int_{\Sigma_g} d^2z\bar{\phi}_{\bar{\imath}}\,. \tag{2.3.13}$$

The derivative with respect[19] to $\bar{t}^{\bar{\imath}}$ leads to the insertion of an (a,a) operator $\bar{\phi}_{\bar{\imath}}$ (in the B-model). This can be shown to be BRST exact

$$\bar{\phi}_{\bar{\imath}} = -\frac{1}{2} dz d\bar{z}\{G^+ + \bar{G}^+, [G^+ - \bar{G}^+, \bar{\phi}_{\bar{\imath}}]\} \tag{2.3.14}$$

and upon taking commutators would - naively thought - annihilate the expression when one finally hits the vacuum. However this argument gets destroyed by the insertion of the additional G^- operators from the measure. Instead these commutators lead to the insertion of additional energy momentum tensors. These can be traded for derivatives with respect to the moduli m^a of the Riemann surface Σ_g exploiting the well-known relation

$$\int_{\Sigma_g} d^2z\sqrt{\eta}\delta\eta^{ab}T_{ab} = \int_{\Sigma_g} d^2z\mu_{\bar{z}}^{(a)z}\delta m^a T_{zz} + \bar{\mu}_z^{a\bar{z}}\delta\bar{m}^a\bar{T}_{\bar{z}}\,. \tag{2.3.15}$$

Re-expressing everything being said so far in formulae we obtain

$$\begin{aligned}
\frac{\partial}{\partial\bar{t}^i}F^g &= \frac{\partial}{\partial\bar{t}^i}\int_{\mathcal{M}_g}\omega_g \\
&= \int_{\mathcal{M}_g}[dm]\sum_{b,\bar{b}=1}^{3g-3}\Big\langle\int\bar{\phi}_{\bar{\imath}}\int 2\mu_b T\int 2\bar{\mu}_{\bar{b}}\bar{T}\prod_{a\neq b}\int\mu_a G^-\prod_{\bar{a}\neq\bar{b}}\int\bar{\mu}_{\bar{a}}\bar{G}^-\Big\rangle_{\Sigma_g} \\
&= \int_{\mathcal{M}_g}[dm]\sum_{b,\bar{b}=1}^{3g-3}4\frac{\partial^2}{\partial m_b\partial\bar{m}_{\bar{b}}}\Big\langle\int\bar{\phi}_{\bar{\imath}}\prod_{a\neq b}\int\mu_a G^-\prod_{\bar{a}\neq\bar{b}}\int\bar{\mu}_{\bar{a}}\bar{G}^-\Big\rangle_{\Sigma_g}\,.
\end{aligned} \tag{2.3.16}$$

The last integral would vanish if the boundary of the moduli space of Riemann surfaces had no boundaries. In fact it does have, which displays the possible degenerations of Riemann surfaces. Either a handle pinches off which decreases the genus by one and is reflected by the first term in (2.3.12), while the second term in (2.3.12) corresponds to a split into two lower genus Riemann surfaces, compare also figure (2.1). The free energy at genus one obeys its own anomaly equation which reads

$$\partial_i\bar{\partial}_{\bar{\jmath}}F^1 = \frac{1}{2}C_{ikl}\bar{C}_{\bar{\jmath}}^{kl} - \Big(\frac{\chi}{24} - 1\Big)G_{i\bar{\jmath}}, \qquad \bar{C}_{\bar{\jmath}}^{kl} = e^{2K}G^{k\bar{k}}G^{l\bar{l}}\bar{C}_{\bar{\jmath}\bar{k}\bar{l}}\,. \tag{2.3.17}$$

Here χ denotes the Euler characteristic of the Calabi Yau manifold.

2.3.3. Coupling the A-model to topological gravity

Coupling the topological A-model to topological gravity works analogously to the discussion of the B-model. As for the prepotential, one obtains for the higher genus amplitudes a

[19] This only holds for the distinguished coordinates $\bar{t}^{\bar{\imath}}$. For general coordinates one has to take the covariant derivative.

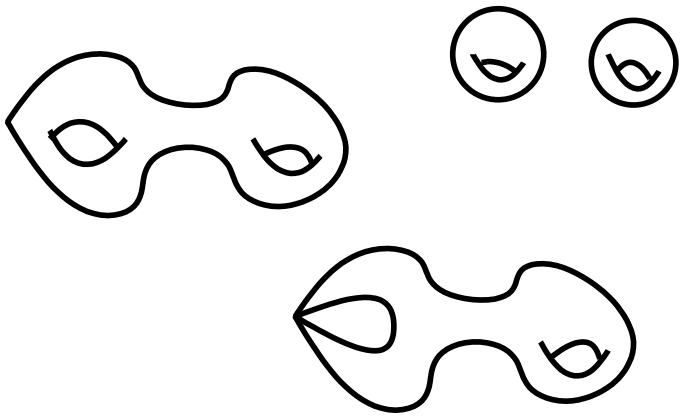

Figure 2.1.: Two boundary components (on the right) of the moduli space of Riemann surface of genus two.

classical contribution and a series of word-sheet instanton corrections.

$$\begin{aligned} F_1(t) &= -\frac{1}{24}\int J\wedge c_2(X) + \sum_\beta N^1_\beta Q^\beta\,, \\ F_{g\geq 2}(t) &= (-1)^g\frac{\chi(X)}{2}\int_{\bar{\mathcal{M}}_g}\lambda^3_{g-1} + \sum_\beta N^g_\beta Q^\beta\,. \end{aligned} \tag{2.3.18}$$

Here λ_{g-1} is the gth Chern class of the Hodge bundle[20] and the corresponding integral is found [70] to be

$$\int_{\bar{\mathcal{M}}_g}\lambda^3_{g-1} = \frac{|B_{2g}||B_{2g-2}|}{2g(2g-2)(2g-2)!}\,. \tag{2.3.19}$$

B_{2g} denote the Bernoulli numbers and the numbers N^g_β are called higher genus Gromov-Witten invariants. They can be computed similarly to the discussion as the integrals over certain moduli spaces. There is a well developed machinery to carry out these integrals for toric Calabi-Yau manifolds. We refer to the literature for a discussion [61, 64, 79]. Instead we continue by discussing how the topological string computes certain type IIA amplitudes.

2.4. Space-time perspective and refinement

Apart from providing valuable insights into mirror symmetry, the topological string computes a part of the amplitudes of the physical Type IIA string. A general scattering amplitude of the physical string takes the form [189, 190]

$$A \simeq \frac{\langle(\text{space-time operators})\rangle}{(\det \text{Im}\tau)^{\frac{d}{2}}}\cdot\langle(\sigma\text{-model of the internal theory})\rangle\,. \tag{2.4.1}$$

In case the space-time part of the integral cancels the factor coming from the period matrix τ of the world-sheet, the remaining expression is completely determined by the zero-mode

[20] Over $\mathcal{M}_g$ one has a vector bundle whose fibers consist of the holomorphic sections of the line bundle K_{Σ_g} over $\mathcal{M}_g$. This is called the Hodge bundle.

part of the internal d-dimensional sigma-model. In fact, this happens for higher derivative terms in the four-dimensional effective action of the physical Type II string. These take the following form

$$\int d^4x d^4\theta \mathcal{W}^{2g} F^g(t_i) = \int d^4 F^g(t_i) R_+ \mathcal{F}_+^{2g-2} + \dots \tag{2.4.2}$$

Here, $\mathcal{W}$ denotes the Weyl multiplet and R_+ and $\mathcal{F}_+$ denote the self-dual parts of the curvature respectively the graviphoton field and F^g denotes the free energy that was introduced in (2.3.5). There is also second perspective on these amplitudes coming from integrating out certain BPS particles which leads to the notion of Gopakumar Vafa invariants. In the following we sketch this point of view in some more detail.

2.4.1. The Gopakumar Vafa invariants

Such BPS particles arise in type IIA compactifications from D2-D0 bound states wrapping a holomorphic curve $\mathcal{C}$ in the class $\beta \in H^2(X, \mathbb{Z})$ of the Calabi-Yau manifold X [22, 23]. In fact, it is easier to discuss the problem in the equivalent M-theory setup obtained by decompactifying the fifth dimension. This limit is possible, as the amplitudes under consideration correspond to the computation of corrections to the vector multiplet moduli space from which the dilaton decouples. In the following we therefore consider a compactification of M-theory on $X \times S^1$. A general BPS state transforming under the little groups $\mathrm{SO}(4) = \mathrm{SU}(2)_L \times \mathrm{SU}(2)_R$ is represented by a field content of the form

$$[(\frac{1}{2}, 0) \oplus 2(0,0)] \otimes \sum_{j_1, j_2} N_{j_1,j_2}(j_1, j_2), \qquad N_{j_1,j_2} \in \mathbb{Z}. \tag{2.4.3}$$

As was shown in [22, 23], the first factor in (2.4.3) is absorbed by the insertion of the factor R_+^2 in (2.4.2) such that the integral can be reduced to a Schwinger loop calculation.

The mass of such a BPS particle consists of the volume of the wrapped curve in the class $\beta \in H_2(X, \mathbb{Z})$ as well as momentum along the additional circle

$$m = \frac{1}{g_s} \int_\beta J + 2\pi i n, \quad n \in \mathbb{Z} \tag{2.4.4}$$

where g_s denotes the string coupling constant and J the complexified Kähler form. By integrating out a particle of mass m and charge e in the background field strength $\mathcal{F}$ one obtains a contribution to the free energy F as

$$F = \int_\epsilon^\infty \frac{ds}{s} \frac{\mathrm{Tr}(-1)^{F_f} e^{-sm^2} e^{-2se\sigma_L \cdot \mathcal{F}}}{(2 \sin \frac{se\mathcal{F}}{2})^2}\,. \tag{2.4.5}$$

Here F_f denotes the fermion number and σ_L is the Cartan element of $\mathrm{SU}(2)_L$. To evaluate this expression, we introduce the numbers $N^\beta_{j_L, j_R}$ which count the numbers of M2-branes wrapping a curve in the homology class β and give rise to particles with the spin content (j_L, j_R) in five dimensions. We postpone the discussion of the geometric origin of the spin content to the next section. As the field strength of the graviphoton field is self-dual it only couples to the left spin which implies that is useful to introduce the weighted, right-spin averaged numbers

$$n^\beta_{j_L} = \sum_{j_R} (-1)^{2j_R} (2j_R + 1) N^\beta_{(j_L, j_R)}\,. \tag{2.4.6}$$

As a next step, we perform a change of spin basis

$$\sum_{r=0}^{\infty} n_r^\beta I_r = \sum_{j_L} n_{j_L}^\beta [j_L], \qquad I_r = [(1/2)+2(0)]^{\otimes r}. \tag{2.4.7}$$

The new numbers n_r^β are called Gopakumar-Vafa invariants and provide another set of geometric invariants of the Calabi-Yau manifold X, see also the discussion in section (2.4.3). Also note that I_r is just the SU(2) spin content of the Lefshetz decomposition of a torus T^r which will get an interpretation in the next section. Any particle in the representation I_r coming from the class β contributes to (2.4.5) as

$$\sum_n \int \frac{ds}{s} e^{-s(t\cdot\beta+2\pi i n)} \left(2\sin\left(\frac{sg_s}{2}\right)\right)^{2r-2}. \tag{2.4.8}$$

Here we have already summed over all n - accounting for all possible momenta along the circle - and taken the trace which can be easily evaluated for the representation I_r. (2.4.8) can be re-summed to

$$\sum_{m\geq 0} \frac{1}{m} e^{-mt\cdot\beta} \left(2\sin\left(\frac{sg_s}{2}\right)\right)^{2r-2}. \tag{2.4.9}$$

Taking into account the classical terms as well as contributions from unwrapped D2-branes, the final form of the free energy is given by

$$\begin{aligned} F(t,g_s) \;=\; & \frac{1}{g_s^2}\big(\frac{1}{6}C_{ijk}t^it^jt^k + P_2(t)\big) - \frac{1}{24}c_2(X)t_i + \text{const} \\ & + \sum_{g>1} \frac{-\chi B_g B_{g-1}}{4g(2g-2)(2g-2)!} g_s^{2g-2} + \sum_{g=0}^{\infty}\sum_{\beta}\sum_{d=1}^{\infty} \frac{1}{d} n_\beta^g \Big(2\sin\big(\frac{dg_s}{2}\big)\Big)^{2g-2} Q^{d\beta}, \end{aligned} \tag{2.4.10}$$

$c_2(X)$ is the second Chern class of X and $P_2(t_i)$ is a ambiguous term (see [64] for a comment on this). In addition, we have made again use of the notation $Q^\beta = e^{-t\cdot\beta}$. It is satisfying to see that this computation gives back precisely the term that comes from the evaluation of the Hodge integral (2.3.19).

The Gopakumar-Vafa invariants are integers[21] and give furthermore insight in the enumerative meaning of the Gromov-Witten invariants which are in general rational numbers. The latter receive corrections from multi-covering [86, 193] and bubbling contributions. The first correction comes about as follows. Given a holomorphic map $x : \mathbb{P}^1 \longrightarrow X$ in the class β one can compose this with a degree d cover of $\mathbb{P}^1$ to obtain a contribution to the class $d\beta$. In order to properly count primitive maps one has to subtract the contributions coming from multi-covering curves of lower degree. If one expands the last contribution of (2.4.10) in g one finds

$$F_g(t) = \sum_\beta \Big(\frac{|B_{2g}|n_0^\beta}{2g(2g-2)!} + \frac{2(-1)^g n_2^\beta}{(2g-2)!} \pm \cdots - \frac{g-2}{12} n_{g-1}^\beta + n_g^\beta\Big) \mathrm{Li}_{3-2g}(Q^\beta) \tag{2.4.11}$$

which gives a precise description of the multi-cover contributions.

The second effect, the bubbling, comes from gluing a very small Riemann surface of genus

[21] This follows from the definition (2.4.6) and the fact that the diagonal elements of the transformation matrix (2.4.7) are given by 1.

h into another one of genus g one obtains a map from a Riemann surface of genus $g+h$ which implies that primitive maps at genus g also contribute in this way to higher genus maps [212].

2.4.2. The geometrical origin of the spin content

In this section we explain the geometric origin of the five-dimensional spin content [23]. There are eight scalars arising from the world-volume theory of the M2 brane. Four of them describe the displacement within space-time and another four the deformations within the Calabi-Yau manifold. From the IIA perspective there are seven scalars and the U(1) field strength which dualizes in three dimensions to another scalar. The moduli space of deformations $\hat{\mathcal{M}}$ is given by deformations of Σ_g within X and the choice of a flat U(1) connection on Σ_g. Therefore one has a fiber map with a section

$$\hat{\mathcal{M}} \longrightarrow \mathcal{M}, \qquad \iota : \mathcal{M} \hookrightarrow \hat{\mathcal{M}}\,. \tag{2.4.12}$$

whose fiber is given by $Jac(\Sigma) \cong T^{2g}$. $\hat{\mathcal{M}}$ is Kähler and enjoys a Lefshetz action that splits[22] into two separate Lefshetz actions on the fiber $(\mathrm{SU}(2)_L)$ and on the base $(\mathrm{SU}(2)_R)$. These get identified with the spin quantum numbers of the BPS particles in five dimensions [23], see [61] for a pedagogical derivation. In particular the representation I_g from (2.4.7) is identified with the spin content of the Lefshetz decomposition of the Jacobian. The Euler characteristics of the two moduli spaces, $\mathcal{M}$, $\hat{\mathcal{M}}$ are encoded in the Gopakumar Vafa invariants as

$$n_0^\beta = (-1)^{\dim_{\mathbb{C}} \hat{\mathcal{M}}} \chi(\hat{\mathcal{M}}), \qquad n_g^\beta = (-1)^{\dim_{\mathbb{C}} \mathcal{M}} \chi(\mathcal{M})\,. \tag{2.4.13}$$

In easy cases, the definition (2.4.12) can be used to directly compute the numbers $N^\beta_{j_L,j_R}$.
Example. Consider the canonical class of $F_0 = \mathbb{P}^1 \times \mathbb{P}^1$ which is given by $2b+2f$, where b, f denote the class of the base and fiber respectively. This is a torus given by a bi-quadratic curve (A.1.16) in $\mathbb{P}^1 \times \mathbb{P}^1$. The moduli space of this curve together with its Jacobian is given by a $\mathbb{P}^7$ bundle over $\mathbb{P}^1 \times \mathbb{P}^1$. Choosing a connection a torus corresponds by T-duality to picking a point p on the dual torus. Mark this point in $\mathbb{P}^1 \times \mathbb{P}^1$. This moduli space of bi-quadratic curves passing through this point p is given by $\mathbb{P}^7$. Let us first calculate the diagonal Lefshetz decomposition[23] of $\mathbb{P}^1 \times \mathbb{P}^1 \times \mathbb{P}^7$ which gives

$$\left(\frac{1}{2}\right) \otimes \left(\frac{1}{2}\right) \otimes \left(\frac{7}{2}\right) = \left(\frac{9}{2}\right) \oplus 2\left(\frac{7}{2}\right) \oplus \left(\frac{5}{2}\right) \tag{2.4.14}$$

The Lefshetz decomposition of the fiber, being a torus, gives $I_1 = \left(\frac{1}{2}\right) \oplus 2(0)$. We also know that the decomposition has to contain a summand with the highest left spin, i.e $\left(\frac{1}{2}\right)$ and that taking the diagonal has to give a back the decomposition (2.4.14). This information suffices to conclude that (j_L, j_R)-decomposition[24] is given by

$$\left(\frac{1}{2}, 4\right) \oplus \left(0, \frac{7}{2}\right) \oplus \left(0, \frac{5}{2}\right). \tag{2.4.15}$$

Using these numbers one can compute the Gopakumar Vafa invariants via (2.4.6) and

[22] The Kähler class k can be split as $k_L = (k - \pi^*(\iota^*(k)))$ and $k_R = \iota^*(k)$.
[23] The Lefshetz decomposition of $\mathbb{P}^n$ is $\left(\frac{n}{2}\right)$.
[24] In fact this is precisely the decomposition that we find by the refined topological string computation listed in table (5.4).

(2.4.7). In fact it is often easier to calculate the free energies on the mirror side, to transfer this result accordingly to the A-model side and to extract the Gopakumar-Vafa invariants from the expansion (2.4.10). Besides that there are important techniques like the topological vertex [79] , or the B-model version of the Eynard-Orantin formalism [123] which we do not go into in this thesis.

2.4.3. Refinement of the free energy

In the last section, Gopakumar Vafa invariants were introduced which arose from integrating out BPS particles in a self-dual graviphoton background field by a Schwinger-Loop calculation. Instead one can drop the self-duality condition

$$\mathcal{F} = g_s dx_1 \wedge dx_2 + g_s dx_3 \wedge dx_4 \tag{2.4.16}$$

and consider a general background field strength that is parameterized by

$$\mathcal{F} = \epsilon_1 dx_1 \wedge dx_2 - \epsilon_2 dx_3 \wedge dx_4 \,. \tag{2.4.17}$$

In this case one expects to see also the right spin content. In fact, the generalized Schwinger loop calculation yields [108]

$$F(\epsilon_1,\epsilon_2,t) = \sum_{\substack{j_L,j_R=0\\k=1}}^{\infty} (-1)^{2(j_L+j_R)} \frac{N^{\beta}_{j_L,j_R}}{k} \frac{\sum_{m_L=-j_L}^{j_L} q_L^{km_L}}{2\sinh\left(\frac{k\epsilon_1}{2}\right)} \frac{\sum_{m_R=-j_R}^{j_R} q_R^{km_R}}{2\sinh\left(\frac{k\epsilon_2}{2}\right)} Q^{k\beta} \tag{2.4.18}$$

which is called the refined free energy. Here we have defined $\epsilon_{L/R} = \epsilon_1 \mp \epsilon_2$ and $q_{L/R} = e^{\epsilon_{L/R}}$. The numbers $N^{\beta}_{j_L,j_R}$ are called refined BPS invariants[25]. This leads accordingly to a decomposition of the free energy as

$$F(\epsilon_1,\epsilon_2,t) = \sum_{n,g=0}^{+\infty} (\epsilon_1+\epsilon_2)^{2n} (\epsilon_1\epsilon_2)^{g-1} F^{(n,g)}(t) \,. \tag{2.4.19}$$

Note that the limit $g_s = \epsilon_1 = -\epsilon_2$ gives back the usual expansion (2.3.5). In addition, the refined topological string partition function takes the form [108]

$$Z = \prod_{\beta\in H_2(X,\mathbb{Z})} \prod_{j_{L/R}} \prod_{m_{L/R}=-j_{L/R}}^{j_{L/R}} \prod_{m_1,m_2=1}^{\infty} \left(1 - q_L^{m_L} q_R^{m_R} e^{\epsilon_1(m_1-\frac{1}{2})} e^{\epsilon_2(m_2-\frac{1}{2})} Q^{\beta}\right)^{(-1)^{2(j_L+j_R)} N^{\beta}_{j_L,j_R}} . \tag{2.4.20}$$

An important question is whether the refined BPS invariants are also enumerative invariants. To answer this question, we step back to the Gopakumar Vafa invariants. These are counted by the following five-dimensional index

$$I(\alpha,\beta) = \mathrm{Tr}_{\mathrm{BPS}} (-1)^{2j_L+2j_R} \exp(-\alpha J_3^L - \beta H) \tag{2.4.21}$$

[25] So far, this is just a name.

where H denotes the Hamiltonian and the trace is taken over the whole Hilbert space. This index reproduces the topological string partition [23] function[26]. One can show that only the short BPS multiplets which are annihilated by the supercharge transforming as $2(0,\frac{1}{2})$ effectively contribute to the above trace. While the numbers $N^{\beta}_{j_L,j_R}$ can change under complex structure deformations, the BPS multiplets that are created or destroyed in this process always have to pair up in long multiplets that do not contribute to the above index. This shows that the Gopakumar Vafa invariants are in fact invariant under complex structure deformations [23]. See [24, 29] for examples where $N^{\beta}_{j_L,j_R}$ change under complex structure deformations. One can ask under which circumstances it might be possible to define an index that computes the refined BPS numbers $N^{\beta}_{j_L,j_R}$. In fact, if there is an additional $\mathrm{U}(1)_{\mathcal{R}}$ symmetry one can use the generator $J^3_{\mathcal{R}}$ to define the following index[27] counting refined BPS invariants

$$Z_{BPS}(\epsilon_1,\epsilon_2) = \mathrm{Tr}(-1)^{2(j_L+j_R)} \exp -\big((\epsilon_1-\epsilon_2)J^3_L+(\epsilon_1+\epsilon_2)J^3_R+(\epsilon_1+\epsilon_2)J^3_{\mathcal{R}}+\beta H\big)\,. \quad (2.4.22)$$

This index was developed in [26] in the study of supersymmetric five-dimensional gauge theories. Fixing $(\epsilon_1+\epsilon_2)(J^3_R+J^3_{\mathcal{R}}) = J'^3_R$ corresponds to the following twist in the five-dimensional theory. Its symmetry group is given as $\mathrm{SU}(2)_L \times \mathrm{SU}(2)_R \times \mathrm{SU}(2)_{\mathcal{R}}$, where the first two factors correspond to the little group and the last one refers to the $\mathcal{R}$-symmetry. If one chooses instead the Lorentz group $\mathrm{SU}(2)_L \times \mathrm{SU}(2)_{R'}$ where the last factor is the diagonal in $\mathrm{SU}(2)_R \times \mathrm{SU}(2)_{\mathcal{R}}$ the eight super-charges transform as a self-dual two-from $Q^+_{\mu\nu}$, a vector G_μ and scalar Q. Then one considers the equivariant cohomology of the BRST operator

$$\tilde{Q} = Q + E_a \Omega^{\alpha\nu}_{\mu} x^{\mu} Q_{\nu} \quad (2.4.23)$$

where $E_a \in \mathfrak{so}(4)$ and $\Omega^{\alpha\nu}_{\mu} x^{\mu}\partial_{\nu}$ is the generator for a rotation. $\tilde{Q}$ becomes an equivariant differential on the moduli space of framed instantons that are counted by the Nekrasov partition function [26].

If the theory has more symmetries, like e.g. flavor symmetries, one can use different U(1) generators $\tilde{J}_{\mathcal{R}}$ to perform the twisting $(\epsilon_1+\epsilon_2)(J^3_R+\tilde{J}^3_{\mathcal{R}}) = J'^3_R$. Typically such a twist can result in a shift of mass parameters of the five-dimensional fields, such as $m_i \mapsto m_i + q_i\epsilon_R$, where q_i denotes the charge under the generator $\tilde{J}_{\mathcal{R}}$ [129].

A geometry that realizes the two twists is referred to as Ω-background. It can be constructed as follows [129] . Consider a four-dimensional $\mathcal{N}=2$ theory that can be lifted to a six-dimensional $\mathcal{N}=1$ theory, whose dimensional reduction gives back the four-dimensional theory. As a next step one compactifies the six-dimensional theory on a $\mathbb{R}^4$ over a torus T^2 such that there are non-trivial holonomies of a flat $\mathrm{SU}(2) \times \mathrm{SU}(2)$ connection that read explicitly

$$\big(e^{\frac{ir}{2}\mathrm{Re}(\epsilon_1+\epsilon_2)\sigma_3}, e^{\frac{ir}{2}\mathrm{Re}(\epsilon_1-\epsilon_2)\sigma_3}\big) \quad \text{and} \quad \big(e^{\frac{ir}{2}\mathrm{Im}(\epsilon_1+\epsilon_2)\sigma_3}, e^{\frac{ir}{2}\mathrm{Im}(\epsilon_1-\epsilon_2)\sigma_3}\big). \quad (2.4.24)$$

Next one embeds the first SU(2) factor of the connection into the six-dimensional $\mathcal{R}$ symmetry group and finally one takes the limit $r \longrightarrow 0$ to obtain the twisted four-dimensional theory. In fact the above procedure works also for an arbitrary four-manifold that has U(1) $\times$ U(1) symmetry[28]. Another often used geometric realization [214], see also [78], of the

[26] To be more precise its holomorphic part. See 3.2.2 and 3.2.3 for details.
[27] See also the appendix of [197], for a nice discussion.
[28] It was conjectured in [129] that also a U(1) invariant conformal structure suffices.

twisting is a compactification of M-theory on the following space

$$X \times S^1 \times TN, \tag{2.4.25}$$

where X denotes again a toric Calabi-Yau manifold. These allow for an additional U(1) symmetry which realizes the isometry of the second S^1. The four-dimensional space is given by a Taub-Nut space[29] TN, coordinized by z_1, z_2, that is twisted along the S^1 as

$$z_1 \mapsto e^{i\epsilon_1} z_1, \qquad z_2 \mapsto e^{i\epsilon_2} z_2\,. \tag{2.4.26}$$

The additional U(1) symmetry on toric Calabi-Yau manifolds reflects the fact that these do not have complex structure deformations which reconciles with the starting point of the discussion. We close the discussion by mentioning that (2.4.26) only preserves supersymmetry in the case that X is compact if $\epsilon_1 + \epsilon_2 = 0$ which corresponds to the unrefined case.

2.4.4. Refined stable pair invariants

Finally, in the last section of this chapter, we review the basic mathematical background material in order to define refined BPS invariants which is based on the notion of stable pairs.

A stable pair [71–73] on a smooth threefold X consists of a sheaf $\mathcal{F}$ on X and a section s such that

- $\mathcal{F}$ is pure of dimension 1
- s generates $\mathcal{F}$ outside a finite set of points

A stable pair is a D6-D2-D0 bound state[30] and can be written as a complex

$$0 \longrightarrow \mathcal{J}_C \longrightarrow \mathcal{O}_X \xrightarrow{s} \mathcal{F} \longrightarrow Q \longrightarrow 0\,. \tag{2.4.27}$$

Here C is the curve supporting the D2 brane with $\mathcal{J}_C$ its annihilation ideal. $\mathcal{Q}$ denotes the cokernel that encodes the D0 brane charge and $\mathcal{O}_X$ denotes the structure sheaf. We denote by $P_n(X,\beta)$ the moduli space of stable pairs with $\mathrm{ch}_2\mathcal{F} = \beta, \chi(\mathcal{F}) = n$. The fact that X is Calabi Yau implies that $P_n(X,\beta)$ supports a symmetric obstruction theory[31], which follows from Serre duality and the triviality of the canonical class [85]. Due to the symmetric obstruction theory the virtual dimension of $P_n(X,\beta)$ becomes zero and in addition one has a virtual class of degree zero $[P_n(X,\beta)]^{vir}$ which can be integrated

$$P_{n,\beta} = \int_{[P_n(X,\beta)]^{vir}} 1 \overset{\text{smooth}}{=} (-1)^{\dim(P_n(X,\beta)} \chi(P_n(X,\beta))\,. \tag{2.4.28}$$

Here the last equality holds only in the smooth case. These are counted by the Pandharipande-Thomas partition function

$$Z_{PT} = \sum_{n,\beta} P_{n,\beta} q^n Q^\beta\,. \tag{2.4.29}$$

[29] This includes in particular the case $\mathbb{R}^4$ if the charge equals one.
[30] The D6 brane gets transparent from (2.4.25) as a Taub-Nut space is the M-theory lift of a D6-brane.
[31] I.e. the obstructions are dual to their deformations.

We recall the partition function for the Gromov-Witten invariants

$$Z_{GW} = \exp\left(F_{GW}(\lambda, Q)\right), \qquad F_{GW} = \sum_{\beta\neq 0}\sum_{g} N_{\beta}^{g} g_s^{2g-2} Q^{\beta}\,. \tag{2.4.30}$$

It is conjectured that after the variable transformation $q = -e^{ig_s}$ it holds that $Z_{PT} = Z_{GW}$. This has been proven in the toric case [73]. The basic idea to compute the Pandharipande Thomas invariants for toric Calabi-Yau manifolds is to note that the moduli space $P_n(X,\beta)$ inherits the torus action of the Calabi-Yau manifold which can be used to localize the integral (2.4.28) to T-fixed stable pairs. For such a T-fixed stable pair the ideal $\mathcal{J}_C$ is monomial and by this property in one-to-one correspondence with three-dimensional partitions. The computation is therefore reduced to a combinatorial box-counting problem [71], see also [27] for a good review.

Via an extension of the classical Bialynicki-Birula decomposition to the virtual case it is possible to refine the obstruction theory [27]. This requires a $\mathbb{C}^*$-action on $P_n(X,\beta)$ with finitely many fixed points. Denoting by t the coordinate of $\mathbb{C}^*$, one can consider the cells

$$U_p^+ = \left\{x \in P_n(X,\beta) | \lim_{t\to 0} t\cdot x = p\right\}, \qquad U_p^- = \left\{x \in P_n(X,\beta) | \lim_{t\to \infty} t\cdot x = p\right\} \tag{2.4.31}$$

for each fixed point p of dimensions d_p^+ and d_p^- respectively. Picking a generic enough $\mathbb{C}^*$-action, such that its fixed points coincide with those of the torus action one defines the virtual motive

$$[P_n(X,\beta)]^{vir} = \sum_{p\in P_n(X,\beta)^{\mathbb{C}^*}} \left(-\mathbb{L}^{-1/2}\right)^{d_p^+ - d_p^-}. \tag{2.4.32}$$

where $\mathbb{L}$ denotes the absolute motive of $\mathbb{C}$. From this expression one extracts the refined BPS numbers as follows. First one notices that the SU(2) characters

$$[j_R]_{\mathbb{L}} := \mathbb{L}^{-j_R} + ... + \mathbb{L}^{j_R} \tag{2.4.33}$$

form a basis of the Laurent polynomials[32] in $\mathbb{L}^{1/2}$. Accordingly we can rewrite (2.4.32) in terms of (2.4.33) and extract the refined BPS numbers from the expansion

$$[P_{1-p_a}(X,\beta)]^{vir} = \sum_{j_R} (-1)^{2j_R} N^{\beta}_{p_a/2,j_R}\,[j_R]\,. \tag{2.4.34}$$

These are counted by the refined Pandharipande Thomas partition function

$$Z_{PT}^{r} = \prod_{\beta,j_L,j_R}\prod_{m_{L/R}=-j_{L/R}}^{j_{L/R}}\prod_{m=1}^{\infty}\prod_{j=0}^{m-1}\left(1-\mathbb{L}^{-m/2+1/2+j-m_R}(-q)^{m-2m_L}Q^{\beta}\right)^{(-1)^{2(J_L+J_R)}N^{\beta}_{j_L,j_R}} \tag{2.4.35}$$

which coincides with (2.4.20) after the identification

$$q_L^{1/2} \longmapsto -q^{-1}, \quad q_R \longmapsto \mathbb{L}^{-1}, \quad e^{-\epsilon_1} \longmapsto \mathbb{L}^{-1/2}(-q), \quad e^{-\epsilon_2} \longmapsto \mathbb{L}^{1/2}(-q)\,. \tag{2.4.36}$$

[32] Here the multiplication is given by the decomposition into irreducible representations.

3. Direct Integration of the Refined Holomorphic Anomaly Equations

The aim of this chapter is to explain how the refined BPS invariants can be computed using mirror symmetry and the direct integration approach on the B-model side. As discussed in the last chapter, the notion of refined BPS invariants is only meaningful on non-compact Calabi-Yau manifolds. We start the discussion with a brief review how the unrefined holomorphic anomaly equations can be integrated using special geometry relations in section 3.1. Afterwards, we continue with the introduction of two important limits given by the local and the holomorphic limit in section 3.2. The latter is contrasted with the expansion of the string theory partition function in terms of modular forms in the wave-function picture. After these preliminaries we proceed to the discussion of the direct integration of refined holomorphic anomaly equations in section 3.3. We discuss their local B-model interpretation and comment on the definition of the corresponding refined free energies. As a next step, we comment on the gap condition which allows to fix the holomorphic ambiguity. Finally, the last section 3.4 presents a very efficient algorithm that allows to perform the direct integration which applies to geometries that have an elliptic mirror curve and which is based on the Weierstrass normal form of the latter.

3.1. Integration of the unrefined holomorphic anomaly equations

The starting point for the integration of the holomorphic anomaly equations (2.3.12) is the so-called special geometry relation which can be derived from the tt^*-equations (2.1.24)

$$\bar{\partial}_{\bar{\imath}}\Gamma^k_{ij} = \delta^k_i G_{j\bar{\imath}} + \delta^k_j G_{i\bar{\imath}} - C_{ijl}\bar{C}^{kl}_{\bar{\imath}} \,. \tag{3.1.1}$$

From which one may deduce [172, 173] relations for the propagators S^{ij}, S^i, S, transforming as sections of $\mathcal{L}^{-2}\otimes \mathrm{Sym}^2 T^*\mathcal{M}$, $\mathcal{L}^{-2}\otimes T^*\mathcal{M}$ and $\mathcal{L}^{-2}$ respectively, which are central objects in the integration procedure of the holomorphic anomaly equations.

$$\begin{aligned}
D_i S^{jk} &= \delta^j_i S^k + \delta^k_i S^j - C_{imn}S^{mj}S^{nk} + h^{jk}_i \,, \\
D_i S^j &= 2\delta^j_i S - C_{imn}S^m S^{nj} + h^{jk}_i K_k + h^j_i \,, \\
D_i S &= -\frac{1}{2}C_{imn}S^m S^n + \frac{1}{2}h^{mn}_i K_m K_n + h^j_i K_j + h_i \,, \\
D_i K_j &= -K_i K_j - C_{ijk}S^k + C_{ijk}S^{kl}K_l + h_{ij} \,.
\end{aligned} \tag{3.1.2}$$

Here, the covariant derivative[1] and K_i are again given by (2.2.57) and h_i, h_i^j, h_i^{jk} and h_{ij} denote holomorphic functions. These equations are solved by

$$\begin{aligned} S^{ij} &= (C_k^{-1})^{jl}\big((\delta_k^i\partial_l + \delta_l^i\partial_k)K + \Gamma_{kl}^i + f_{kl}^i\big)\,, \\ S^i &= (C_k^{-1})^{il}\big((\partial_k K\partial_l K - \partial_k\partial_l K + f_{kl}^j\partial_j K)f_{kl}\big)\,, \\ S &= \frac{1}{h^{1,1}}\big((h^{1,1}+1)S^i - D_j S^{ij} - S^{ij}S^{kl}C_{jkl}\big)\partial_i(K + \log(|f|)/2) \\ &\quad + \frac{1}{2h^{1,1}}(D_i S^i + S^i S^{jk}C_{ijk})\,. \end{aligned} \tag{3.1.3}$$

f, f_{ij}, f_{ij}^k denote holomorphic functions, K is the Kähler potential and Γ_{ij}^k denotes the Christoffel symbol of the Weyl-Peterson metric defined in (2.2.58). These solutions can be used to construct the free energies at higher genus as follows. First of all one notices that the holomorphic anomaly equation for F^1 (2.3.17) can be integrated as [86]

$$\partial_i F^1 = \frac{1}{2}C_{ijk}S^{jk} - \big(\frac{\chi}{24} - 1\big)K_i + A_i, \qquad A_i = \partial_i\big(\tilde{a}_j \log\Delta_j + \tilde{b}_j \log z_j\big)\,. \tag{3.1.4}$$

Δ_j denote irreducible components of the conifold locus[2]. In the last expression $\tilde{a}_i, \tilde{b}_j$ are un-known numbers that need to be determined from suitable boundary conditions (compare also the discussion in section 3.3.2). This implies that the derivative of F^1 is expressible in terms of the propagators and the derivative of the Kähler potential. χ denotes the Euler number of the compact Calabi-Yau geometry. Next, one observes that any anti-holomorphic dependence of the free energies must be inherited from the propagators and the Kähler potential as the Yukawa coupling is a holomorphic quantity. Using the relations

$$\partial_{\bar{\imath}} S^{ij} = \bar{C}_{\bar{\imath}}^{ij}, \qquad \partial_{\bar{\imath}} S^j = G_{i\bar{\imath}}S^{ij}, \qquad \partial_{\bar{\imath}} S = G_{i\bar{\imath}}S^i\,, \tag{3.1.5}$$

it is therefore possible to rewrite the anti-holomorphic dependence of F^g using (3.1.2) as

$$\bar{\partial}_{\bar{\imath}} F^g = \bar{C}_{\bar{\imath}}^{jk}\frac{\partial F^g}{\partial S^{jk}} + G_{i\bar{\imath}}\Big(\frac{F^g}{\partial K_i} + S^i\frac{\partial F^g}{\partial S} + S^{ij}\frac{\partial F^g}{\partial S^j}\Big)\,. \tag{3.1.6}$$

Note that the indices of the Yukawa coupling need to be raised with the metric $g_{i\bar{\jmath}}$ instead the Weyl-Peterson metric itself. This implies that the holomorphic anomaly equations (2.3.12) can be re-expressed under the assumption of the independence of $G_{i\bar{\imath}}$ and $\bar{C}_{\bar{\imath}}^{jk}$ as

$$\frac{\partial F^g}{\partial S^{ij}} = \frac{1}{2}D_i D_j F^{g-1} + \frac{1}{2}\sum_{r=1}^{g-1} D_i F^{g-r} D_j F^r. \tag{3.1.7}$$

See also [176, 199] for further expositions.

3.2. The local and the holomorphic limit

In this section we discuss two important limits which are important for our setups. The holomorphic limit where all anti-holomorphic dependence is dropped and the local limit

[1] If the covariant derivative acts on objects that also transform as a section of $T^*\mathcal{M}$ it obtains a contribution from the Christoffel symbol of the Weyl Peterson metric, too.

[2] The conifold is the locus in the moduli space where a cycle shrinks to zero size.

which reduces the formalism to computations on local Calabi-Yau manifolds.

3.2.1. The local limit

The non-compact limit of a Calabi-Yau corresponds physically to decoupling gravity in type II compactifications[3]. This means that one passes from special geometry of $\mathcal{N} = 2$ supergravity which is realized in the moduli space of Calabi-Yau manifolds to rigid $\mathcal{N} = 2$ geometry which is realized in the moduli space of Riemann surfaces[4].

In this case one proceeds as in section 2.2.6. One chooses a symplectic basis[5] and computes the periods of the meromorphic one-form that arise from the holomorphic three-form by integrating out the non-compact directions[6].

$$t^i = \int_{a^i} \lambda, \qquad F_i = \int_{b_i} \lambda \tag{3.2.1}$$

Also in this case there exists a prepotential F, such that $F_i = \frac{\partial F}{\partial t^i}$. This encodes in particular the period matrix of the Riemann surface as

$$\tau_{ij} = \frac{\partial^2 F}{\partial t^i \partial t^j}. \tag{3.2.2}$$

One important difference to the case of compact Calabi-Yau manifolds is given by the fact that the t^i are already the flat coordinates. In fact, when analyzing the Picard Fuchs system one sees that the analytic period (2.3.4) is given by a constant, see also 4.3.2, and therefore the homogeneous coordinates coincide with the inhomogeneous ones. The Kähler potential reads in the local case

$$K = \frac{i}{2}(t^i \bar{F}_i - \bar{t}^{\bar{i}} F_i) \; = \mathrm{Im}\tau_{ij}. \tag{3.2.3}$$

See e.g. [104] or [194] for a nice discussion and derivation. This Kähler potential implies the metric

$$G_{i\bar{j}} = \partial_i \partial_{\bar{j}} K = \frac{1}{2i}(\tau_{ij} - \bar{\tau}_{\bar{i}\bar{j}})\,. \tag{3.2.4}$$

In contrast to the case of compact Calabi-Yau manifolds there may also be additional parameters m^α on which the surface depends, which are no real moduli. These correspond to non-normalizable directions in the moduli space that arise from periods of the meromorphic one-form λ that have no compact dual within the surface. Stated differently, they are encircling points where λ has non-vanishing residua. They are also called mass parameters as they correspond to the masses in the geometrically engineered Seiberg-Witten theory[7].

[3] Roughly speaking because the four-dimensional Newton constant is proportional to the volume of the Calabi-Yau.

[4] See e.g. [195] for details.

[5] The Riemann surfaces that appear as mirrors of non-compact Calabi-Yau are naturally non-compact and therefore a symplectic basis need not to exist, but one has instead $a_i \cap b^j = n_i^j \in \mathbb{Z}$. For purposes of cleaner notation the following discussion applies however to the symplectic case and is easily modified.

[6] We refer to section 4.3.2 for the derivation of the meromorphic one-form that is induced from the holomorphic three-form in the case of toric Calabi-Yau manifolds. See also [66].

[7] Actually, this is not quite true. Only those parameters that correspond to blow-ups within the geometry correspond to masses in four-dimensional Seiberg-Witten theory. Recall that the easiest way to geometrically engineer Seiberg-Witten theory is by compactifying type II on a Hirzebruch surface [66]. F_0 already has such an isomonodromic parameter, but this gets frozen in the geometrical engineering resulting in pure SU(2) Seiberg-Witten theory. See also the discussion in 5.4.

In complete analogy to the latter, they also are also invariant under monodromy transformations, but may appear in the monodromy transformations of real moduli, i.e. one has [33]

$$\begin{aligned} \tilde{F}_i &= A_i^j F_j + B_{ij} t^j + E_{i\alpha} m^\alpha \,, \\ \tilde{t}^i &= C^{ij} F_j + D^i_j t^j + F^i_\alpha m^\alpha \,, \qquad \begin{pmatrix} A & B \\ C & D \end{pmatrix} \in \mathrm{Sp}(2\tilde{g}, \mathbb{Z}), \quad E_{i\alpha}, F^i_\alpha \in \mathbb{Z}. \\ \tilde{m}^\alpha &= m^\alpha \,. \end{aligned} \tag{3.2.5}$$

Note that the genus of the mirror curve is denoted by $\tilde{g}$ and not to be confused with the world-sheet genus denoted by g. Therefore yet another characterization for these parameters is as isomonodromic deformations. See also [33, 104] for further explanations.

3.2.2. The holomorphic limit

The holomorphic limit denotes an expansion around the point $\bar{t} \longrightarrow \infty$ making all quantities purely holomorphic. As the prepotential and the Yukawa couplings are holomorphic in any case, all the anti-holomorphic dependence comes from the Kähler potential and the expressions derived from it, i.e. the topological metric[8] $G_{i\bar{\jmath}}$ and the Christoffel symbols Γ^k_{ij}. These drastically simplify in this limit as follows [86]

$$K \longrightarrow -\log(\omega_0), \qquad G_{i\bar{\jmath}} = \frac{\partial T_i}{\partial z_j} \qquad \Gamma^k_{ij} = G^{k\bar{l}} \partial_i G_{j\bar{l}}. \tag{3.2.6}$$

Note in particular that the holomorphic limit of the Kähler potential vanishes in the case of a local Calabi-Yau manifolds. Consequently many expressions simplify in the limit.

3.2.3. Holomorphicity versus modularity

This subsection is devoted to a discussion of the interpretation of the topological string partition function as a wave function. It was shown in [171] that the topological string partition function is interpreted as a state $|Z\rangle$ in the Hilbert space obtained by quantizing $H^3(M, \mathbb{Z})$ where g_s plays the role of $\hbar$. After picking a basis α this state gives rise to a wave-function $Z(\alpha) = \langle \alpha | Z \rangle$. There are two important choices of such a basis. First of all one can pick a symplectic basis A^I, B_J in order to parametrize the complex structure moduli space

$$x^I = \int_{A^I} \omega, \qquad p_J = \int_{B_J} \omega, \qquad \omega \in H^3(X, \mathbb{C}) \,. \tag{3.2.7}$$

This results in a wave function $Z(x)$ and is called the real polarization. There is second important basis which relies on choosing a background complex structure Ω to define a Hodge decomposition of $H^3(M, \mathbb{C})$ that decomposes ω according to

$$\omega = \varphi \Omega + z^i D_i \Omega + \bar{z}^i \bar{D}_i \bar{\Omega} + \bar{\varphi} \bar{\Omega} \tag{3.2.8}$$

which results in a wave-function $Z(\varphi, z^i)$. This is called the holomorphic polarization. As was shown in [171], the second basis is physically the natural one.

[8] Here we refer to the Weyl Peterson metric transformed to the complex structure coordinates z_i. In many expressions, the Weyl Peterson metric enters as $\log(|G_{i\bar{\jmath}}|)$ and in the holomorphic limit only the Jacobian $\frac{\partial t_i}{\partial z_j}$ survives.

Instead of deriving the holomorphic anomaly equations from the wave-function picture directly as in [171], one can investigate [33] how this can be directly used in order to constrain the form of the free energies. In particular one can ask how the action of the monodromy group $\Gamma \subset \mathrm{Sp}(2n,\mathbb{Z})$ constrains the form of the free energies. Here the two bases are particularly useful. In the holomorphic polarization the wave function becomes dependent on the monodromies as the symplectic basis changes under these transformations. On the other hand, in the holomorphic polarization, the wave function is not allowed to transform under Γ as it is physical. This has the following consequences

1. In the holomorphic polarization the free energies are almost modular forms (i.e. modular invariant but not holomorphic) having an expansion

$$\hat{F}^g = F_0^g + h((\mathrm{Im}\tau)^{-1}) \tag{3.2.9}$$

with $h((\mathrm{Im}\tau)^{-1})$ is a polynomial without constant part and τ denotes the period matrix[9].

2. In the real polarization the free energies are quasi modular forms (i.e. holomorphic but not modular invariant) F^g and in fact $F^g \equiv F_0^g$ in (3.2.9).

3. The propagator can be shown to be a modular form of weight two

$$\hat{E}^{IJ}(\tau,\bar{\tau}) = E^{IJ}(\tau) + \left((\mathrm{Im}\tau)^{-1}\right)^{IJ} \tag{3.2.10}$$

transforming as

$$\begin{aligned} \hat{E}^{IJ}(\tau,\bar{\tau}) &\mapsto (C\tau+D)^I_K (C\tau+D)^J_L \hat{E}^{KL}(\tilde{\tau},\bar{\tilde{\tau}}) \qquad \begin{pmatrix} A & B \\ C & D \end{pmatrix} \in \mathrm{Sp}(2\tilde{g},\mathbb{Z})\,, \\ \tau &\mapsto \tilde{\tau} = (A\tau+B)(C\tau+D)^{-1}\,. \end{aligned} \tag{3.2.11}$$

Here E takes values in $\mathbb{C}^{\tilde{g}\times\tilde{g}}$. In fact, any free energy $\hat{F}^g$ in holomorphic polarization can be written as a polynomial in $\hat{E}^{IJ}(\tau,\bar{\tau})$ where the coefficients are given by modular forms. Finally, the holomorphic anomaly equations can be re-derived by considering the coordinate transformation from the holomorphic to the real polarization. For the theory of almost and quasi modular forms we refer to [109].

3.3. Direct integration of the refined topological string

So far we have discussed how the special geometry relations can be used to integrate the unrefined holomorphic anomaly equations. In addition, it was explained how to calculate the prepotential $F^{(0,0)}$, which does not get refined. In the following we discuss the refined holomorphic anomaly equations that allow analogously to the unrefined ones to recursively determine the refined free energies. They need besides $F^{(0,0)}$ and $F^{(0,1)}$ also the refined free energy $F^{(1,0)}$ as an input datum.

[9] We restrict here to non-compact Calabi-Yau manifolds, as the period matrix of a compact matrix has signature $(h^{2,1},1)$ See also [33].

3.3.1. The refined holomorphic anomaly equations

Refined holomorphic equations have been proposed in [29, 30]

$$\bar{\partial}_{\bar{i}} F^{(n,g)} = \frac{1}{2}\bar{C}_{\bar{i}}^{jk}\big(D_j D_k F^{(n,g-1)} + \sum_{m,h}{}' D_j F^{(m,h)} D_k F^{(n-m,g-h)}\big)\,, \quad n+g>1\,. \tag{3.3.1}$$

Here the covariant derivatives are as in (2.3.12) and and the prime denotes omission of $(m,h) = (0,0)$ and (n,g) in the sum. These equations have some similarity to the holomorphic anomaly equations for a genus g amplitude where n fields have in addition been inserted [86]

$$F^{(n,g)}(t) = \int_{\bar{\mathcal{M}}_g} \langle \mathcal{O}^n \prod_{k=1}^{3g-3} \beta^k \bar{\beta}^k \rangle_g dm \wedge d\bar{m}. \tag{3.3.2}$$

Here the operator $\mathcal{O}$ should take the form of an integral over a descendant from a 0-form field $\phi^{(0)}$, $\mathcal{O} = \int_{\Sigma_g} \phi^{(2)}$. In fact it was argued in [30] that a candidate for the field ϕ is provided by the dilaton as its contact terms with marginal fields vanish in the limit of a local Calabi Yau manifold. Repeating the same arguments as for the derivation of the unrefined holomorphic anomaly equations, one has in addition to distribute the n insertion points among the degenerate world sheet topologies, which gives rise to the second sum in (3.3.1). As so far a world-sheet description of the refined topological string is missing, it is difficult to derive these equations rigorously away from the local limit[10]. However, there is a rigorous way to compute refined free energies which is given by the refined holomorphic vertex [107, 108]. In all cases where a comparison is possible, the results coincide. It is however important to stress that the refined holomorphic anomaly equations have a much wider range of applicability as the underlying geometry is not required to engineer a gauge theory. Besides that these equations have also been checked with the Eynard-Orantin formalism and Seiberg-Witten theories [29, 30]. So far these proposals have passed all tests which are highly non-trivial, as the extracted refined BPS numbers are required to be integers. See also [112, 113] for a slightly different approach to a refinement of the holomorphic anomaly equations.

3.3.2. The refined free energies at genus one and the propagator

Here we discuss how the free energies are computed in the local and holomorphic limit where many expressions considerably simplify.

The holomorphic equation at genus one (2.3.17) integrates in the local and holomorphic limit to

$$F^{(0,1)} = \frac{1}{2}\log\Big(\det G^{-1}_{i\bar{j}}|f_1|^2\Big)\,. \tag{3.3.3}$$

Here f_1 is a holomorphic ambiguity which is given as

$$f_1 = \Delta^a \prod_j z_j^{b_j}. \tag{3.3.4}$$

The apriori unknown constants a, b_j can be either fixed from embedding the geometry into

[10] As it has been discussed, refined BPS invariants are only well defined in the local limit.

a compact model and calculating

$$\lim_{z_i\to 0} F^{(0,1)} = -\frac{1}{24}\sum_{i=1}^{h^{2,1}} t_i \int_X c_2 J_i \tag{3.3.5}$$

or by matching - which is in practice easier - with a few known BPS numbers. In addition, there is the universal behaviour of the exponent $a = -\frac{1}{12}$ at conifold loci[11] Δ [196]. Note that the covariant derivative also drastically simplifies as the Kähler potential vanishes in the holomorphic and local limit and the line bundle $\mathcal{L}$ becomes trivial. The covariant derivative is accordingly given as

$$D_i = \partial_i - \Gamma_i \,. \tag{3.3.6}$$

This also implies a great simplification of the propagators (3.1.2). Indeed, the only surviving object is S^{ij} which is accordingly determined from

$$\begin{aligned} D_i S^{kl} &= -C_{imn} S^{km} S^{lm} + f_i^{kl} \,, \\ \Gamma_{ij}^k &= -C_{ijl} S^{kl} + \tilde{f}_i^{kl} \,, \\ \partial_i F_1 &= \frac{1}{2} C_{ijk} S^{jk} + A_i \,. \end{aligned} \tag{3.3.7}$$

These equations can be solved from the following ansätze

$$\begin{aligned} f_i^{kl} &= \frac{h(z_i)}{\prod_i z_i^{m_i} \Delta^p} \,, \\ A_i &= \partial_i\big(\tilde{a}_j \log \Delta_j + \tilde{b}_j \log z_j\big) \,. \end{aligned} \tag{3.3.8}$$

The first formula applies to both, f_i^{kl} and $\tilde{f}_i^{kl}$. $h(z_i)$ is a polynomial and m_i and p denote exponents which need to be determined from the equations (3.3.7).

We turn our attention to the refined free energy $F^{(1,0)}$. More generally, it was conjectured in [30], that the refined free energy at genus 0, $F^{(n+1,0)}$ takes the form

$$F^{(n+1,0)} = \langle \phi^{(0)}(0)\phi^{(0)}(1)\phi^{(0)}(\infty)\mathcal{O}^n \rangle_{g=0} \tag{3.3.9}$$

which implies in particular that $F^{(1,0)}$ is holomorphic, as the boundary of the moduli space of stable rational curves with n punctures is caused by coincident punctures. The most general ansatz for $F^{(1,0)}$ reads correspondingly

$$F^{(1,0)} = \frac{1}{24} \log(\Delta^a \prod_i z_i^{b_i}) \,. \tag{3.3.10}$$

To determine the constants a, b_i one requires regularity at infinity and needs information about the vanishing of a few low degree BPS numbers.

3.3.3. The behavior at the conifold and the gap condition

The behavior of the topological amplitudes at the conifold locus is of particular interest as it allows to fix the holomorphic ambiguity, i.e. the integration constant that needs to be

[11] The conifold is the locus in the moduli space where a cycle shrinks to zero size.

fixed upon integrating[12] (3.3.1). This takes in general the form

$$f^{(n,g)}(u,\underline{m}) = \frac{p(z_i)}{z_i^{d_i}\Delta^{2(g+n)-2}} \tag{3.3.11}$$

where the degree of the unknown polynomial p is such that f is regular at infinity. In fact the leading behavior of $F(\epsilon_1,\epsilon_2,t)$ at the nodes of the mirror-curve can be determined by explicitly performing the Schwinger-Loop integral under the assumption that that a single hypermultiplet with mass $m = t_c$ becomes massless at the node. Let us denote by t_c the vanishing coordinate at the node under investigation, then the leading behavior reads [29]

$$\begin{aligned} F(s,g_s,t_c) &= \int_0^\infty \frac{ds}{s}\frac{\exp(-st_c)}{4\sinh(s\epsilon_1/2)\sinh(s\epsilon_2/2)} + \mathcal{O}(t_c^0) \\ &= \big[-\frac{1}{12}+\frac{1}{24}(\epsilon_1+\epsilon_2)^2(\epsilon_1\epsilon_2)^{-1}\big]\log(t_c) \\ &\quad + \frac{1}{\epsilon_1\epsilon_2}\sum_{g=0}^{\infty}\frac{(2g-3)!}{t_c^{2g-2}}\sum_{m=0}^{g}\hat{B}_{2g}\hat{B}_{2g-2m}\epsilon_1^{2g-2m}\epsilon_2^{2m}+\dots \\ &= \big[-\frac{1}{12}+\frac{1}{24}sg_s^{-2}\big]\log(t_c) + \big[-\frac{1}{240}g_s^2+\frac{7}{1440}s-\frac{7}{5760}s^2g_s^{-2}\big]\frac{1}{t_c^2} \\ &\quad + \big[\frac{1}{1008}g_s^4-\frac{41}{20160}sg_s^2+\frac{31}{26880}s^2-\frac{31}{161280}s^3g_s^{-2}\big]\frac{1}{t_c^4}+\mathcal{O}(t^0) \\ &\quad + \text{contributions to } 2(g+n)-2>4\,, \end{aligned} \tag{3.3.12}$$

where[13] $g_s^2 = (\epsilon_1\epsilon_2)$ and $s = (\epsilon_1+\epsilon_2)^2$.

In order to perform computations at the conifold locus one needs good coordinates, which are in general given by choosing one coordinate being normal to the conifold locus and the rest tangential and solving the Picard Fuchs equations in these coordinates . In case that not all discriminant components have normal crossing one has to resolve the conifold locus by suitable blow-ups [174, 175]. The normal coordinate corresponds to the period t_c that vanishes at this locus and has to be compared to the Schwinger-Loop calculation.

In general, if t_c does also depend on further tangential directions one finds that the vanishing of the sub-leading singularities yields an over-determined system, which turns out to be solvable. It was argued in [111] that, since the only type of degeneration of a Riemann surface in complex co-dimension one is the nodal degeneration, the gap structure (3.3.12) holds universally true regardless of the particular conifold point[14] nor the direction from which it is approached. On the other hand (3.3.12) provides only information to solve for all except for one unknown of the ambiguity. The last one can be fixed by matching with (2.4.10).

3.4. Elliptic curve mirrors and closed modular expressions

One main concern of this thesis are Calabi-Yau manifolds defined as the anti-canonical bundle over toric (almost) del Pezzo surfaces S, i.e. the total space of $\mathcal{O}(-K_S)\to S$. As

[12] See also [102] for higher genus local mirror symmetry in the unrefined case.

[13] Here $\hat{B}_m = \big(\frac{1}{2^{m-1}}-1\big)\frac{B_m}{m!}$ and the Bernoulli numbers B_m are defined by $t/(e^t-1) = \sum_{m=0}^{\infty} B_m \frac{t^m}{m!}$.

[14] Except from intersections of the conifold locus with the large radius regime. In addition, to be more precise, this argument was given for the un-refined case.

will be discussed in section 4, their mirror geometries are given by a genus one curve $\mathcal{C}$ with punctures and a meromorphic differential λ, with the property that $\partial_u \lambda$ is the holomorphic differential of $\mathcal{C}$. For our applications it is sufficient that this is true up to exact terms.

Any family of elliptic curves can be brought into Weierstrass form

$$y^2 = 4x^3 - g_2(u, \underline{m})x - g_3(u, \underline{m}) \ . \tag{3.4.1}$$

In the following we present a powerful algorithm [30] which allows us to perform the direct integration procedure completely in terms of the Weierstrass normal form of the elliptic curve. Our formalism distinguishes $u \in \mathcal{M} = \mathbb{P}^1 \setminus \{p_1, \ldots, p_r\}$ as the complex modulus of the family of curves, defining the monodromy of $\mathcal{C}$, from the "mass" parameters $\underline{m} = \{m_1, \ldots, m_{n_f}\}$ which do not transform under monodromies, as discussed in 3.2.1.

3.4.1. Computing the period and prepotential from the elliptic curve

With the formalism developed in [30] one can calculate the prepotential $F^{(0,0)}(t, \underline{m})$ using its relation

$$\frac{\partial^2}{\partial^2 t} F^{(0,0)}(t, \underline{m}) = -\frac{c_0}{2\pi i} \tau(t, \underline{m}) \tag{3.4.2}$$

to the τ-function of the elliptic curve. Here the constant c_0 reflects the fact that the mirror-curve is potentially non-compact what might prevent the finding of a canonically normalized symplectic basis of the homology violating the relation $t_D = \partial_t F^{(0,0)}$. This implies the following form of the Yukawa coupling

$$C_{ttt} = \frac{\partial^3 F^{(0,0)}}{\partial t^3} = -\frac{2\pi i}{c_0} \frac{d\tau}{dt}. \tag{3.4.3}$$

Here the relation between the local flat coordinate t at a cusp point in $\mathcal{M}$, the fundamental region of SL(2,$\mathbb{Z}$), and $(u, \underline{m})$ is obtained by integrating [215]

$$\frac{dt}{du} = \sqrt{\frac{E_6(\tau) g_2(u, \underline{m})}{E_4(\tau) g_3(u, \underline{m})}} \tag{3.4.4}$$

with vanishing constant of integration. The g_i are not invariants of the curve, but can be re-scaled as

$$g_i \to \lambda^i(u, \underline{m}) g_i, \tag{3.4.5}$$

which changes (3.4.4). One can fix this ambiguity so that $\frac{dt}{du} = \frac{1}{2\pi i} \int_\mu \frac{dx}{y}$ for the vanishing cycle μ. In praxis this is done by matching the leading behavior of the integral. E_4 and E_6 are the Eisenstein series. We obtain τ as a function of $(t, \underline{m})$ by inverting the $j(\tau)$-function

$$j = 1728 \frac{g_2^3(t, \underline{m})}{\Delta(t, \underline{m})} = \frac{E_4^2(\tau)}{E_4^3(\tau) - E_6^2(\tau)} = \frac{1}{q} + 744 + 192688 q + \ldots \ . \tag{3.4.6}$$

Here $\Delta = g_2^3(t, \underline{m}) - 27 g_3^2(t, \underline{m})$ denotes the discriminant and $q = \exp(2\pi i \tau)$. With this information (3.4.2) determines $F^{(0,0)}(t, \underline{m})$ up to classical terms, which can be recovered from properties of constant genus zero maps. The prepotential also determines the metric

(3.2.4) on the moduli space as [30]

$$G_{t,\bar{t}} = \frac{4\pi}{c_0}\,\mathrm{Im}\tau\ . \tag{3.4.7}$$

3.4.2. Determining the higher genus sector

As discussed in section 3.3.2, the unrefined free energy at genus one $F^{(0,1)}(t,\underline{m})$ takes in general the form (3.3.3) which simplifies in this case to

$$F^{(0,1)} = -\frac{1}{2}\log\left(G_{u\bar{u}}|\Delta u^{a_0}\prod_i m_i^{a_i}|^{\frac{1}{3}}\right), \tag{3.4.8}$$

where the integration constants a_0, a_i are fixed as in (3.3.2) by constant genus one maps. It is convenient for the integration formalism to rewrite the holomorphic part of the metric $G_{u\bar{u}}$ in terms of Eisenstein series

$$F^{(0,1)}_{hol} = -\frac{1}{12}\log\left(\frac{E_6}{g_3}\Delta u^{2a_0}\prod_i m_i^{2a_i}\right)\ . \tag{3.4.9}$$

The function $F^{(1,0)}(t,\underline{m})$ is holomorphic, compare also to 3.3.2 and its form follows from its behavior at $\Delta = 0$ as

$$F^{(1,0)} = \frac{1}{24}\log(\Delta u^{b_0}\prod_i m_i^{b_i})\ . \tag{3.4.10}$$

To determine the constants b_0, b_i one requires regularity at infinity and needs information about the vanishing of a few low degree BPS numbers.

The higher $F^{(n,g)}$ with $n+g>1$ have the general form [30]

$$F^{(n,g)} = \frac{1}{\Delta^{2(g+n)-2}(u,\underline{m})}\sum_{k=0}^{3g+2n-3} X^k p_k^{(n,g)}(u,m). \tag{3.4.11}$$

Here the non-holomorphic generator $\hat{X}$ is given by

$$\hat{X} = \frac{g_3(u,\underline{m})}{g_2(u,\underline{m})}\frac{\hat{E}_2(\tau)E_4(\tau)}{E_6(\tau)}\,. \tag{3.4.12}$$

With $\hat{E}_2$ we denote the non-holomorphic second Eisenstein series

$$\hat{E}_2(\tau,\bar{\tau}) = E_2(\tau) - \frac{3}{\pi\mathrm{Im}(\tau)}\,. \tag{3.4.13}$$

We note that we choose λ in (3.4.5) so that

$$\frac{E_6^2}{E_4^3} = 27\frac{g_3^2}{g_2^3}\ . \tag{3.4.14}$$

The proof of (3.4.11) proceeds by using (3.4.14) and (3.4.4) and the Ramanujan identities

$$\begin{array}{ll} \frac{\mathrm{d}}{\mathrm{d}\tau}E_2 & = \frac{1}{12}(E_2^2 - E_4) \ , \\ \frac{\mathrm{d}}{\mathrm{d}\tau}E_4 & = \frac{1}{3}(E_2E_4 - E_6) \ , \\ \frac{\mathrm{d}}{\mathrm{d}\tau}E_6 & = \frac{1}{2}(E_2E_6 - E_4^2) \ , \end{array} \tag{3.4.15}$$

to derive

$$\begin{array}{ll} \frac{\mathrm{d}}{\mathrm{d}t}X & = \frac{1}{\Delta}\frac{\mathrm{d}u}{\mathrm{d}t}(AX^2 + BX + C) \ , \\ \frac{\mathrm{d}^2u}{\mathrm{d}^2t} & = \frac{1}{\Delta}\frac{\mathrm{d}u}{\mathrm{d}t}(AX + \frac{B}{2}) \ , \end{array} \tag{3.4.16}$$

with

$$A = \frac{9}{4}(2g_2\partial_u g_3 - 3g_3\partial_u g_2), \qquad B = \frac{1}{2}(g_2^2\partial_u g_2 - 18g_3\partial_u g_3), \qquad C = \frac{g_2 A}{3^3} \ . \tag{3.4.17}$$

For any family of curves (3.4.1) this gives a description of the ring of quasi-modular forms in which the holomorphic anomaly equation (3.3.1) can be integrated. It is convenient to rewrite the refined holomorphic anomaly equations in terms of the generator X. One first notices that whole anti-holomorphicity of the free energy is inherited from $\hat{E}_2$ which allows to re-express

$$\frac{d}{d\bar{\tau}} = \frac{3i}{2\pi\tau_2^2}\frac{d}{d\hat{E}_2} \tag{3.4.18}$$

and accordingly the anti-holomorphic derivative of the free energies may be written as

$$2\partial_{\bar{a}}F^{(n,g)}(C_{\bar{t}}^{tt})^{-1} = 24\frac{dF^{(n,g)}}{d\hat{E}_2} \ . \tag{3.4.19}$$

The ring of almost quasi-modular forms is represented as $\mathbb{C}[\hat{E}_2, E_4, E_6]$. The holomorphic limit $\bar{\tau} \longrightarrow \infty$ which implies $\frac{1}{\tau_2} \longrightarrow 0$ establishes an isomorphism onto the ring of quasi modular forms $\mathbb{C}[E_2, E_4, E_6]$. In this limit also the covariant derivative D_t gets identified with the usual derivative. The refined holomorphic anomaly equations may therefore be re-expressed as

$$\begin{aligned} 24\frac{\partial F^{(n,g)}}{\partial X} \quad = \quad & \frac{g_2(u)}{g_3(u)}\frac{E_6}{E_4}\Big[\left(\frac{du}{dt}\right)^2\frac{\partial^2 F^{(n,g-1)}}{\partial u^2} + \frac{d^2u}{dt^2}\frac{\partial F^{(n,g-1)}}{\partial u} \\ & + \left(\frac{du}{dt}\right)^2 {\sum_{m,h}}' \frac{\partial F^{(m,h)}}{\partial u}\frac{\partial F^{(n-m,g-h)}}{\partial u}\Big] \ . \end{aligned} \tag{3.4.20}$$

As discussed in [30] one can deduce inductively that the r.h.s. of (3.4.20) is a polynomial of X of maximal degree $2(g+n)-3$ and a rational function in $(u, \underline{m})$ with denominator $\Delta^{2(g+n)-2}(u, \underline{m})$. Equation (3.4.20) can also be used to integrate the holomorphic anomaly efficiently up to the polynomial $p_k^{(n,g)}(u, \underline{m})$, which is undetermined after the integration. This ambiguity is fixed by comparing to the refined Schwinger Loop calculation (3.3.12) as described previously.

3.4.3. Fixing the holomorphic ambiguity

In order to perform calculations one needs good coordinates at the conifold locus. These are obtained by choosing the normal coordinate, i.e. the right coordinate is given by the

discriminant

$$u_{\text{con}} = \Delta\,. \tag{3.4.21}$$

This establishes in particular a map form the large radius coordinates to the conifold coordinates. The discriminant Δ is in general a polynomial in the large radius coordinate u_{lr} and the mass parameters m_i giving only closed expressions for the conifold variables if its degree is equal or less than four[15]. However, as the m_i are valid in the whole moduli space, one can always obtain u_{lr} as a power series in the m_i and u_{con}.

Analogously to the discussion for the large radius, one obtains the vanishing period t_c at the conifold again from (3.4.4) evaluated in u_{con} which reads

$$t_c = C_0 u_{\text{con}} + \mathcal{O}(u_{\text{con}}^2, m_i), \qquad C_0 \in \mathbb{C}. \tag{3.4.22}$$

The un-determined constant C_0 is also fixed by matching with the expansion (3.3.12).

[15] In practice two.

4. Geometry of del Pezzo Surfaces and Toric Mirror Symmetry

In this chapter we discuss some geometrical background material. We start with a brief review of the geometry of del Pezzo surfaces and the half K3 and their algebraic realizations in section 4.1. Afterwards we turn to the Batyrev construction of toric mirror pairs in section 4.2. As the main concern of the present thesis are non-compact Calabi-Yau geometries, we present two ways towards non-compact mirror symmetry in section 4.3. These are given by either embedding the local geometry into a compact one by constructing an elliptic fibration over it or a direct toric construction. Finally, in the last section 4.4 we present a method to efficiently compute the mirror curves of all two-dimensional toric Fano varieties.

4.1. The geometry of del Pezzo and half K3 surface

By definition of a rational surface $h_{2,0} = h_{1,0}(S) = 0$, hence the arithmetic genus $\chi_0 = \sum_i h_{i,0} = 1$. The Hirzebruch-Riemann-Roch theorem gives for the arithmetic genus and the signature $\sigma = b_2^+ - b_2^-$

$$\begin{aligned} 1 = \chi_0(S, \mathcal{O}_S) &= \int_S \mathrm{ch}(\mathcal{O}_S)\mathrm{td}(S) = \int_S \mathrm{td}(S) = \frac{1}{12}\int_S c_1^2(S) + c_2(S)\,, \\ \sigma &= \frac{1}{3}\int_S p_1(S) = \frac{1}{3}\int_S c_1^2 - 2c_2\,, \end{aligned} \tag{4.1.1}$$

respectively. Blowing up increases the Euler number $\chi(S)$ and the second Betti number $b_2(S)$ by 1. From $\chi(\mathbb{P}^2) = 3$ and the first equation of (4.1.1) follows $k = \int_{\mathcal{B}_n} c_1^2 = 9 - n$, a quantity often called the degree of the del Pezzo surface. Further from $b_2(\mathbb{P}^2) = 1$ and $\sigma(\mathcal{B}_n) = 1 - n$ it follows that the middle cohomology lattice

$$\Lambda = H_2(\mathcal{B}_n, \mathbb{Z}) \tag{4.1.2}$$

has signature $(1, n)$. Let h denote the hyperplane class in $\mathbb{P}^2$ and e_i the exceptional divisors associated to the i'th blow-up, then the intersection pairing "$\cdot$" is defined by the non-vanishing intersections $h^2 = -e_i^2 = 1$. The anti-canonical class is

$$K = c_1(\mathcal{B}_n) = 3h - \sum_{i=1}^{n} e_i, \tag{4.1.3}$$

so that again $k = K_{\mathcal{B}_n}^2 = 9 - n$, i.e. the positivity of $K_{\mathcal{B}_n}$ restricts the number of blow-ups to $n < 9$. Let us denote by $\Lambda' \subset \Lambda$ the sub-lattice orthogonal to $c_1(\mathcal{B}_n)$

$$\Lambda' = \{x \in \Lambda | x \cdot K = 0\}\ . \tag{4.1.4}$$

The intersection form "$\cdot$" is negative on Λ' and since all coefficients in K are odd it has even intersections. The determinant is equal to the degree $9-n$, so for $n=8$, Λ' is the unique even self-dual lattice of rank 8, the E_8 lattice and for $n=9$ it becomes the $\hat{\mathrm{E}}_8$ lattice. Similar one can see that for $n=2,\ldots,8$ the lattice Λ' corresponds to the root (or co-root lattice) of the exceptional Lie algebras as follows

$$\left|\begin{array}{c|cccccccc|c|}\text{degree}=9-n & 9 & 8 & 7 & 6 & 5 & 4 & 3 & 2 & 1 & 0 \\ G & - & - & A_1 & A_1\times A_2 & A_4 & \mathrm{D}_5 & \mathrm{E}_6 & \mathrm{E}_7 & \mathrm{E}_8 & \hat{\mathrm{E}}_8 \end{array}\right| . \tag{4.1.5}$$

The simple roots are given by $\alpha = e_1 - e_2$ for $n=2$ and for the case $n \geq 3$ as

$$\alpha_i = e_i - e_{i+1}, \quad i=1,\ldots n-1, \qquad \alpha_n = h - e_1 - e_2 - e_3. \tag{4.1.6}$$

It is also convenient to introduce the weight lattice

$$\Lambda'' := \Lambda/(K\mathbb{Z}), \tag{4.1.7}$$

so that the pairing on Λ yields a perfect pairing

$$\Lambda'' \otimes \Lambda' \to \mathbb{Z} \ . \tag{4.1.8}$$

Further the center of E_n is given by

$$\mathbb{Z}_{9-n} \sim \Lambda''/\Lambda' \ . \tag{4.1.9}$$

In addition, $\mathbb{P}^1 \times \mathbb{P}^1$ is a del Pezzo surface with $\Lambda_2 = \Gamma^{1,1}$ the hyperbolic lattice. For us it is natural to include examples in which $c_1(B_2)$ is only semi-positive, which we call almost Fano varieties. These are numerically effective, but not Fano, as it is discussed e.g. in section 15.4 of [64] for the Hirzebruch surface F_2. This is notion also used in [74]. Another important generalization is to the half K3, also denoted by $\frac{1}{2}K3 := \mathcal{B}_9$ that has the lattice

$$\Lambda\left(\frac{1}{2}K3\right) = \Gamma^{1,1} \times \mathrm{E}_8 \ . \tag{4.1.10}$$

To each del Pezzo surface $\mathcal{B}_n$ one can associate an elliptic pencil

$$\{aC_1 + bC_2\} \in \mathbb{P}^2 \times \mathbb{P}^1 \tag{4.1.11}$$

of sections C_1, C_2 of the canonical sheaf of $\mathbb{P}^2$ with $9-n$ base points. The base point free pencil for $\mathcal{B}_9$ defines a rational elliptic surface fibered over $\mathbb{P}^1$, which is isomorphic to $\mathcal{B}_9$ as can be seen by projection to the first factor. Hence the $\frac{1}{2}K3$ is a rational elliptic surface. If all base points of the elliptic pencil are blown up these (-1)-curves e_i become sections of the elliptic surface and the corresponding Mordell-Weyl group is a free abelian group of rank 8 [97][1]

$$MW = \mathbb{Z}_8 \times \mathrm{Weyl}(\mathrm{E}_8) \tag{4.1.12}$$

while the torsion part is the Weyl group of E_8 [98]. Indeed, the Weyl group of E_n acts already on the cohomology of $\mathcal{B}_n$ [98] and beside becoming the Mordell-Weyl group of the rational elliptic surface in the last blow-up, it is also extended to the affine Weyl group of

[1] Rank eleven Mordell-Weyl groups have also been constructed by Néron [96].

$\hat{\mathrm{E}}_8$ on the full cohomology of the $\frac{1}{2}K3$ [35].

In families of del Pezzo surfaces the action of the Weyl group can be generated explicitly by deforming S to a singular surface so that the vanishing cycle corresponds to a simple root α. By the Picard-Lefshetz monodromy theorem the monodromy in the moduli space around the point where the cycle $\alpha \in H_2(S,\mathbb{Z})$ vanishes, generates a Weyl reflection[2] on the hyperplane defined by $\alpha = 0$, i.e. on any cycle $\beta \in H_2(S,\mathbb{Z})$ with non-trivial intersection with α the monodromy action is $S_\alpha(\beta) = \beta - (\beta \cdot \alpha)\alpha$. For the $\frac{1}{2}K3$ the intersection of the irreducible components of the singular fibers are given by Kodairas classification with affine intersection form and the corresponding monodromies generate $\hat{\mathrm{E}}_8$.

In order to explicitly specify the action of the Weyl group $\hat{\mathrm{E}}_8$ on the moduli parameters, denote the "volumes[3]" of exceptional $\mathbb{P}^1$'s by m_i and the modulus of the elliptic fiber emerging in the ninth blow-up by τ. Then the Weyl group is generated by the reflexions

$$\begin{aligned} m_i &\longleftrightarrow m_j, && \text{for any pair } (i,j), \\ m_i &\longleftrightarrow -m_j, && \text{for any pair } (i,j), \\ m_i &\longrightarrow m_i - \tfrac{1}{4}\textstyle\sum_{j=1}^{8} m_j, \end{aligned} \tag{4.1.13}$$

which defines the Weyl group of E_8. For the affine $\hat{\mathrm{E}}_8$ there is an additional infinite shift symmetry

$$\begin{aligned} m_i &\longrightarrow m_i + 2\pi\alpha_i \\ m_i &\longrightarrow m_i + 2\pi\alpha_i\tau\,. \end{aligned} \tag{4.1.14}$$

Here $\vec{\alpha} = (\alpha_1, \ldots, \alpha_8)$ is an element of the root lattice of E_8. Recall that the latter is defined as the sub-lattice of $\mathbb{R}^8$ whose elements have either all integer or half-integer entries, such that the sum of all entries adds up to an even integer. In addition, there is an SL(2,$\mathbb{Z}$) symmetry acting on the fiber modulus

$$\begin{aligned} \tau &\longrightarrow \tau + 1\,, \\ \tau &\longrightarrow -\tfrac{1}{\tau}, \qquad \vec{m} \longrightarrow \tfrac{\vec{m}}{\tau}\,, \end{aligned} \tag{4.1.15}$$

making the affine characters Jacobi forms with τ being their modular parameter and $\vec{m}$ a tuple of elliptic parameters. The ring of these forms relevant for the direct integration approach of our refined holomorphic anomaly equation (6.2.11) is summarized in appendix A.3.1.

4.1.1. Algebraic realizations

The D_5, E_6, E_7 and E_8 del Pezzo surfaces can be represented by the zero locus of two quadrics in $\mathbb{P}^4$, the cubic in $\mathbb{P}^3$, the quartic in $\mathbb{P}^3(1,1,1,4)$ and the sixtic in $\mathbb{P}^3(1,1,2,3)$. By use of the adjunction formula the Euler number can be calculated to be $8, 9, 10$ and 11 while $c_1(S) = (\sum w_i - \sum d_k)h = h$. Here w_i denote the weights, d_i are degree(s) of the defining polynomial constraints and h is the hyperplane class of the ambient space. Generic anti-canonical models for higher degree del Pezzo surfaces cannot be realized as hypersurfaces

[2] For ADE singularities these inner automorphisms generate the Weyl group. Singularities corresponding to non-simply laced Lie algebras are obtained by a suitable outer automorphism action acts on the classes in the Hirzebruch-Jung sphere configuration, e.g. by monodromy in a family, see [121] for review. In this thesis we only consider simply laced singularities.

[3] The e_i do not lie in the Kähler cone and the "volumes" can formally be negative for flopped $\mathbb{P}^1$'s.

or complete intersections. E.g. the degree six $A_1 \times A_2$ del Pezzo is a determinantal variety in $\mathbb{P}^6$ and the degree five A_4 del Pezzo is given by five linear quadrics in $\mathbb{P}^5$ [69].

Finding these algebraic realizations is closely related to the problem of constructing ample families of elliptic curves $\mathcal{E}$ with d rational points Q_i, $i = 1, \ldots, d$, i.e. such that $\mathcal{E}$ is embeddable in some (weighted) projective space $\mathbb{P}^n(\underline{w})$.The construction of the ample families of elliptic curves proceeds as follows. Assume the embedding exists, consider the bundle $\mathcal{L} = \mathcal{O}(\sum_i^d Q_i)$ over $\mathcal{E}$ and match $m\mathcal{L} = K_{\mathbb{P}^n(\underline{w})}$ so that a trivial canonical class is obtained. The ideal of the relations of the sections in $m\mathcal{L}$, which has according to the Riemann-Roch theorem $\delta = h^0(m\mathcal{L}) = \deg(m\mathcal{L})$ sections, defines the desired embedding of $\mathcal{E}$ into $\mathbb{P}^n(\underline{w})$. To be explicit call x_k, $k = 1, \ldots, d$ the sections of the degree w_k line bundles L_k of $\mathbb{P}^n(\underline{w})$. We can assume that x_{k_i} vanishes at Q_i (in general $d \leq n+1$ with the strict inequality for weighted projective space), so that $\deg(m\mathcal{L}) = m\sum_i w_{k_i}$.

Let us discuss two concrete example given by the case of an elliptic curve with two and four sections. We consider first the line bundle associated to two sections $\mathcal{L} = \mathcal{O}(P+Q)$. According to Riemann-Roch we expect to find $2n$ sections of $H^0(n\mathcal{L})$. Call the sections of $H^0(\mathcal{L})$ v, w. They give rise to three sections v^2, w^2, vw so that we get an additional section x. Iterating this procedure one finds

$$\begin{array}{rc} H^0(\mathcal{L}) & v, w \\ H^0(2\mathcal{L}) & v^2, w^2, vw, x \\ H^0(3\mathcal{L}) & v^3, w^3, v^2w, vw^2, vx, wx \\ H^0(4\mathcal{L}) & v^4, w^4, v^3w, v^2w^2, vw^3, v^2x, w^2x, vwx, x^2 \end{array} \tag{4.1.16}$$

For $n = 4$ we find nine sections - note that these precisely coincide with the monomials of polyhedron 13 - although only eight are expected. Therefore one concludes that there has to be a relation which gives a homogeneous quadric in $\mathbb{P}^{(1,1,2)}$

$$a_0v^4 + a_1w^4 + a_2v^3wv^2 + a_3w^2 + a_4vw^3 + a_5v^2x + a_6w^2x + a_7vwx + a_8x^2 = 0\,. \tag{4.1.17}$$

Let us also quickly discuss the case of four sections for which the line bundle reads $\mathcal{L} = \mathcal{O}(P+Q+R+T)$. and call the four sections r, s, t, u. Accordingly $H^0(2\mathcal{L})$ has eight sections, but we know actually ten $r^2, s^2, t^2, u^2, rs, rt, ru, st, su, tu$, implying two relations between them. Therefore we conclude that the elliptic curve is given by two quadratics in $\mathbb{P}^3$. These can be brought into Weierstrass normal form as described in [118].

It is easy to see that the case $d = 1$ requires weights $w = (1, 2, 3)$ and one gets $m = 6$, $\delta = 6$ and the seven sections of $6\mathcal{L}$ are represented by the monomials of polyhedron 10 of figure 1 made explicit in figure 4. $d = 3$ requires $m = 3$, $3\mathcal{L} = K_{\mathbb{P}^2}$ has degree $\delta = 9$, leading to one relation among the ten sections, the monomials of degree three in x_1, x_2, x_3, i.e. the monomials of polyhedron 15 and the embedding is the cubic in $\mathbb{P}^2$. For $d = 5$, $m = 2$ and $\delta = 10$ one gets five linear independent quadrics in $\mathbb{P}^4$ and $d = 6$ has $m = 2$ $\delta = 12$ i.e. nine conditions in $\mathbb{P}^5$.

The anti-canonical divisor defines for all Fano varieties of dimension d a Calabi-Yau manifold X_c of dimension $d-1$, while as discussed $\mathcal{O}(-K_B) \to B$ defines a non-compact Calabi-Yau of dimension $d+1$. In the del Pezzo case the anti-canonical bundle in S is of course an elliptic curve $\mathcal{E}$. If we use the above model for the algebraic realization it allows d rational points. The anti-canonical model determines the local mirror geometry of $\mathcal{O}(-K_S) \to S$.

4.2. The Batyrev construction

In this section we review Batyrev's construction [84] of families of mirror symmetric Calabi-Yau manifolds using toric geometry that is based on the notion of a reflexive pair of polyhedra.

4.2.1. Toric Fano varieties and non-compact Calabi-Yau spaces

The d-dimensional toric[4] Fano varieties are most easily classified by d-dimensional reflexive polyhedra. Toric almost del Pezzo surfaces are given by reflexive polyhedra in two dimensions, which are depicted in figure 1, where also the reflexive pairs (Δ_2, Δ_2^*) are indicated. The anti-canonical class is only semi-positive if there is a point on one edge of the toric diagram, otherwise positive and ample. In particular the polyhedra 1,2,3,5,7 correspond to toric del Pezzo surfaces, by the construction explained below.

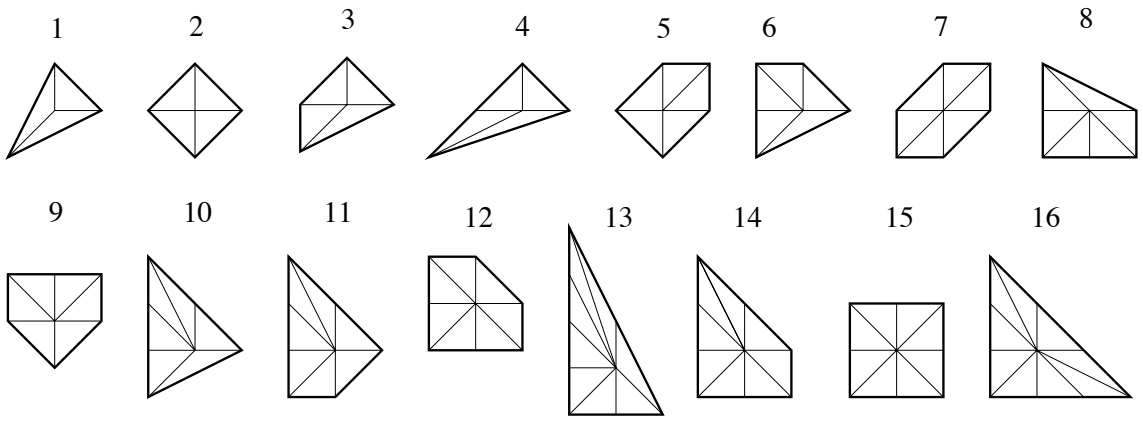

Figure 4.1.: These are the 16 reflexive polyhedra in two dimensions, which build 11 dual pairs (Δ_2, Δ_2^*). Polyhedron k is dual to polyhedron $17-k$ for $k = 1, \ldots, 6$. The polyhedra $k = 7, \ldots, 10$ are self-dual. The points are labeled counter-clockwise with the one right to the origin with label 1. The origin has label 0.

Let Γ be a lattice and denote by $\Gamma_{\mathbb{R}} = \mathbb{R} \otimes \Gamma$. The dual objects are denoted by Γ^* and $\Gamma^*_{\mathbb{R}}$ and

$$\langle , \rangle : \Gamma \times \Gamma^* \longrightarrow \mathbb{Z} \tag{4.2.1}$$

denotes the pairing. A d-dimensional lattice polyhedron Δ_d is given as the convex hull of points $\mathcal{N} = \{\nu^{(i)} \in \Gamma\}$, such that $0 \in \mathcal{N}$ and span $\mathcal{N} = \Gamma_{\mathbb{R}}$. The dual polyhedron Δ_d^* is defined by

$$\Delta_d^* = \{y \in \Gamma^*_{\mathbb{R}} | \, \langle y, x \rangle \geq -1, \, \forall x \in \Delta_d\} \, . \tag{4.2.2}$$

A pair of polyhedra (Δ_d, Δ_d^*) is called reflexive, if both are lattice polyhedra.

4.2.2. Constructing toric ambient spaces

Given a pair of lattice polyhedra, one associates to them a family of mirror symmetric Calabi-Yau manifolds as follows. A triangulation of Δ_d defines a toric fan Σ_{Δ_d}. Any point

[4] We refer to [99, 115] for a general background in toric geometry.

in Δ_d defines a one-dimensional cone of Σ_{Δ_d} which gets identified with a divisor D_i. Also choose for each such ray a coordinate Y_i whose vanishing defines D_i. Next one finds a basis[5] l_i of relations among all integer points of $l(\Delta_d)$. The toric (ambient) space $\mathbb{P}_{\Delta_d}$ is now defined by

$$\mathbb{P}_{\Delta_d} = \frac{\mathbb{C}^{|\Sigma(1)|} \backslash Z_{\Delta_d}}{\mathrm{Hom}(A_{d-1}(\mathbb{P}_\Delta), \mathbb{C}^*)} \,. \tag{4.2.3}$$

Here $A_{d-1}(\mathbb{P}_\Delta)$ denotes the Chow group of $\mathbb{P}_\Delta$ and the homomorphism group is given by

$$\mathrm{Hom}(A_{d-1}(\mathbb{P}_\Delta), \mathbb{C}^*) = (\mathbb{C}^*)^{rk A_{d-1}(\mathbb{P}_\Delta)} \times A_{d-1}(\mathbb{P}_{\Delta_d})_{\mathrm{tors}} \,. \tag{4.2.4}$$

The last factor denotes the torsion part, that arises e.g. from A_k-singularities within $\mathbb{P}_{\Delta_d}$. The action of this group on the coordinates reads as

$$Y_i \mapsto Y_i (\mu^{(k)})^{l_i^k} \,. \tag{4.2.5}$$

The Stanley-Reisner ideal Z depends on a triangulation of Δ_d and consists of all loci of intersections of divisors $D_{i_1} \cap \cdots \cap D_{i_k}$ for which the corresponding points ν_{i_j} are not on a common triangle.

The same construction of a toric ambient space also applies to the dual polyhedron.

4.2.3. Constructing mirror families of Calabi-Yau manifolds

Given a toric ambient space constructed as discussed in the previous section, one can construct a compact Calabi-Yau as a section of the anti-canonical bundle. This can be constructed as follows [93]

$$\Omega = \mathcal{O}_{X_{\Delta_d^*}}(D_{\Delta_d^*}), \qquad D_{\Delta_d^*} = D_1 + \ldots D_n \,, \tag{4.2.6}$$

where D_i are the divisors corresponding to the coordinates Y_i and its global sections are given by

$$H^0(X_{\Delta^*}, \mathcal{O}_{X_{\Delta_d^*}}(D_{\Delta_d^*})) = \bigoplus_{\nu^{*(i)} \in \Delta^*} \mathbb{C} \prod_{\nu^{(k)}} Y_k^{\langle \nu^{*(i)}, \nu^{(k)} \rangle + 1} \,. \tag{4.2.7}$$

Using the adjunction formula one can construct a family of Calabi-Yau manifolds as follows

$$W_\Delta = \sum_{i=0}^{l(\Delta)-1} a_i X_i = \sum_{\nu^{(i)} \in \Delta} a_i \prod_{\nu^{*(k)}} Y_k^{\langle \nu^{(i)}, \nu^{*(k)} \rangle + 1} = 0 \,. \tag{4.2.8}$$

The coefficients a_i redundantly parametrize the complex structure moduli of X. Points inside co-dimension one faces of Δ can be excluded from the summation, as the corresponding monomials can be removed by the automorphism group of $\mathbb{P}_{\Delta^*}$. Analogously the mirror manifold X^* can be defined as a hypersurface

$$W_{\Delta^*} = \sum_{i=0}^{l(\Delta^*)-1} a_i Y_i = \sum_{\nu^{*(i)} \in \Delta^*} a_i^* \prod_{\nu^{(k)}} X_k^{<\nu^{*(i)}, \nu^{(k)}\rangle + 1} = 0 \,. \tag{4.2.9}$$

[5] To be more precise, one has to choose a basis of the Mori cone which is the cone of all effective curves. See e.g. [182] for computational details.

4.3. Non-compact mirror symmetry

Instead of constructing Calabi-Yau manifolds as hypersurfaces in toric ambient spaces, one can also construct Calabi-Yau manifolds directly as toric spaces. The condition for a toric variety to be Calabi-Yau is equivalent to requiring that all generators lie in one common hyperplane. This already shows that toric Calabi-Yau manifolds cannot be compact as compactness requires the fan to cover the whole lattice.

An important class of non-compact Calabi-Yau manifolds is given by the anti-canonical bundles $\mathcal{O}(-K_{\mathbb{P}_{\Delta_d}})$ over toric varieties $\mathbb{P}_{\Delta_d}$ associated to polyhedrons Δ_d. The former ones are torically constructed by embedding Δ_d in a $(d+1)$-dimensional lattice by sending $\nu^{(i)} \mapsto \bar{\nu}^{(i)} = (1, \nu^{(i)})$ and considering the convex hull of the points $\bar{\nu}^{(i)}$.

Note however that it is not necessary that Δ_d is a reflexive polyhedron. In fact any maximally triangulated convex polyhedron can be embedded as above in a $(d+1)$-dimensional lattice and gives rise to a non-compact Calabi-Yau manifold. Eventually one has to crepantly resolve the resulting Calabi-Yau manifold which happens when the points $\bar{\nu}^{(i)}$ do not span the full lattice. Note that the corresponding diagrams of these Calabi-Yau manifolds may have an arbitrary number of inner points, which is physically interesting as this geometrically engineers higher rank gauge groups.

There are two ways to define the mirror of a non-compact Calabi-Yau. The first one globally embeds the local geometry into a compact Calabi-Yau space. In this case the Batyrev construction is applicable. Practically this means that one constructs an elliptic fibration over the local geometry whose fiber is decoupled to recover the local geometry. The second way is to directly construct a non-compact mirror geometry which is given by a conic $\mathbb{C}^2$ bundle over a punctured Riemann surface [183]. This Riemann surface, also referred to as the mirror curve, is obtained as a section of the elliptic fibration in the first construction [66, 101]. We summarize both approaches in the following subsections.

4.3.1. Local mirror symmetry as a limit of compact mirror symmetry

As the main focus of this thesis lies on threefold computations and moreover the virtual dimension of the moduli space of stable pairs is only zero in dimension three (compare also the discussion in section 2.2.1 and (2.2.7)) we restrict the discussion to the embedding of $\mathbb{P}_{\Delta_2^{B*}}$ into compact Calabi-Yau threefolds. This corresponds to the embedding of a two-dimensional polyhedron Δ_2^{B*} into a four-dimensional reflexive polyhedron Δ_4^*. This gives rise to the following pair of reflexive polyhedra $(\Delta_4^*,\ \Delta_4)$, which are constituted by the convex hull of the points

$$\left|\begin{array}{cc|cc} \multicolumn{2}{c|}{\nu_i^* \in \Delta_4^*} & \multicolumn{2}{c}{\nu_j \in \Delta_4} \\ & \nu_i^{F*} & & \nu_j^F \\ \Delta_2^{B*} & \vdots & s_{ij}\Delta_2^B & \vdots \\ & \nu_i^{F*} & & \nu_j^F \\ 0\dots 0 & & 0\dots 0 & \\ \vdots & \Delta_2^{*F} & \vdots & \Delta_2^F \\ 0\dots 0 & & 0\dots 0 & \end{array}\right| . \tag{4.3.1}$$

Here one considers all points $\nu_j^{F*} \in \Delta_F^*$ and defines

$$s_{ij} = \langle \nu_i^F, \nu_j^{F*} \rangle + 1 \in \mathbb{N} . \tag{4.3.2}$$

Also we have rescaled $\Delta_2^B \longrightarrow s_{ij}\Delta_2^B$ in (4.3.1) which implies in general that the polyhedron $s_{ij}\Delta_2^B$ contains more points than Δ_2^B. In general, one obtains a fibration of toric spaces $X_\Sigma \longrightarrow X_{\Sigma'}$ associated to two fans Σ and Σ' if there is a map $\Sigma \longrightarrow \Sigma'$, such that any face $\sigma \subset \Sigma$ gets mapped into a face $\sigma' \subset \Sigma'$. Let us discuss how this applies to our construction. In the following we restrict ourselves to Δ and rename $s_{ij}\Delta_B$ to Δ_B. First of all one has an exact sequence

$$0 \longrightarrow \Gamma_F \longrightarrow \Gamma \longrightarrow \Gamma_B \longrightarrow 0 \tag{4.3.3}$$

where Γ_F and Γ_B refer to the sub-lattices associated to Δ_2^F and Δ_2^B. Note that Δ_2^B is the image of a projection of Δ_4 along the fiber direction. This establishes a fibration

$$\mathbb{P}_{\Delta_4} \longrightarrow \mathbb{P}_{\Delta_2^B} \tag{4.3.4}$$

whose generic fibers are $\mathbb{P}_{\Delta_2^F}$. Accordingly, the hypersurface $W_{\Delta_4^*} = 0$ becomes an elliptic fibration whose generic fiber is defined by a section of the anti-canonical bundle in $\mathbb{P}_{\Delta_2^F}$. The non-compact model is obtained by scaling the volume of the elliptic fiber to infinity [101].

4.3.2. Local mirror symmetry without a compact embedding

Here we describe the second approach to compute the local mirror symmetry [101, 183]. The starting point is the basis of relations l_i of the diagram described above, which correspond to the generators of the Mori cone, i.e. the dual of the Kähler cone. The vectors Q_i^α can be used to construct the invariant coordinates

$$z_\alpha = (-1)^{Q_0^\alpha} \prod_{i=1}^{k+3} x_i^{Q_i^\alpha} \,. \tag{4.3.5}$$

In general the mirror geometry is given by

$$w^+ w^- = H = \sum_{i=1}^{k+3} x_i. \tag{4.3.6}$$

Using the relations (4.3.5) one can eliminate the variables x_i and obtains a conic bundle over $\mathbb{C}^* \times \mathbb{C}^*$ which is given as

$$F = w^+ w^- - H(x, y, z_\alpha) = 0, \qquad x = e^u, \quad y = e^v. \tag{4.3.7}$$

The fiber degenerates over the locus $H = 0$ which defines a non-compact Riemann surface (with punctures). It is important to discuss this geometry in some more detail. First of all one notices that the holomorphic three-form gets inherited from $\mathbb{C}^4$ as

$$\Omega = \frac{dw^+ \wedge dx \wedge dy}{xy\ \partial F/\partial w^-} \,. \tag{4.3.8}$$

The homology of this local Calabi-Yau manifold can be thought of as follows[6]. Compact cycles correspond to compact cycles in the Riemann surface which get filled up to a surface D that carries an S^1-fibration over it which degenerates at the boundary, so that one altogether

[6] See also [198, 200] for a nice discussion.

obtains an S^3. Non-compact cycles take the topology of a three-ball. Using Cauchy's theorem one first integrates out the fiber and reduces the integral to period integrals of a meromorphic one-form [66] over the Riemann surface.

$$\int_{A/B}\Omega=\int_{A/B}\frac{dw^+\wedge dx\wedge dy}{w^+xy}=2\pi i\int_D d\left(\log(y)dx\right)=2\pi i\int_{a/b}\lambda,\qquad \lambda=\frac{\log(y)dx}{x}\,. \tag{4.3.9}$$

Here we have denoted the symplectic basis[7] of the middle homology of the Calabi-Yau by A/B and that of the Riemann surface by a/b.

For toric varieties the Picard Fuchs equations can be explicitly evaluated by making use of the Dwork-Griffiths reduction method and expressed in terms of the charge vectors Q_i^α as [101]

$$D_\alpha=\prod_{Q_i^\alpha>0}\partial_{x_i}^{Q_i^\alpha}-\prod_{Q_i^\alpha<0}\partial_{x_i}^{-Q_i^\alpha}\,. \tag{4.3.10}$$

These differential equations are also referred to as the GKZ system and can be solved using the Frobenius method. First one calculates the so-called fundamental period [101]

$$\omega_0(z_i,\rho_i)=\sum_{n^\alpha}\frac{1}{\prod_i\Gamma(Q_i^\alpha(n^\alpha+\rho^\alpha)+1)}((-1)^{Q_0^\alpha}z^\alpha)^{n^\alpha} \tag{4.3.11}$$

from which all other solutions may be calculated. One finds explicitly one constant solution

$$t^0=\omega(z_i,0)=1 \tag{4.3.12}$$

and a number of simple logarithmic solutions

$$t^i=\frac{1}{2\pi i}\frac{\partial}{\partial\rho^i}\omega_0\big|_{\rho_i=0}\,. \tag{4.3.13}$$

These solutions give rise to the so-called mirror map at large radius. In particular one finds

$$z_i=e^{2\pi i t^i}+\mathcal{O}(t_i) \tag{4.3.14}$$

which implies that the limit $z_i\longrightarrow 0$ corresponds to a large volume of the i^{th} generator of the Mori cone. Finally, combinations of higher derivatives

$$t^{\alpha_{i_1},\ldots\alpha_{i_n}}=\frac{1}{(2\pi i)^n}\frac{\partial}{\partial\rho^{\alpha_{i_1}}}\cdots\frac{\partial}{\partial\rho^{\alpha_{i_n}}}\omega_0\big|_{\rho_i=0} \tag{4.3.15}$$

make up the remaining solutions to the Picard-Fuchs equations. Note that the actual number of double-logarithmic solutions is in the case of local Calabi-Yau threefolds given by the genus of the mirror curve.

4.4. Constructing the mirror curves of two-dimensional toric Fano varieties

In this section we construct the mirror curves of the anti-canonical bundles of the two-dimensional Fano varieties following the procedure in 4.3.1. We take the tenth polyhedron

[7] Assuming that it exists.

$\Delta(10)$ as Δ_2^{*F} i.e. $\Delta_2^{*F} = \text{conv}\{(1,0),\,(-1,2),\,(-1,-1)\}$ and for $\nu_3^{F*} = (-1,-2)$. Since Δ_2^{*F} is self-dual, $\Delta_2^F = \text{conv}\{(1,0),\,(-1,2),\,(-1,-1)\}$ and $\nu_j^F = (-1,-2)$, so $s_{ij} = 6$. The mirror of the del Pezzo in the base must occur as a specialization of the constraint (4.2.9). Due to the form of Δ we can always find a triangulation that leads to an elliptic fibration, not necessarily a smooth and flat one. However for the discussion of the complex deformations of the mirror geometry, this is good enough. Denoting the coordinates associated to $(0,0,-1,-1)$, $(0,0,2,-1)$ and $(0,0,-1,1)$ by y, x and z, W_{Δ^*} is realized in the Tate form

$$W_{\Delta^*} = y^2 + h_1(\underline{X}'_B)xyz + h_3(\underline{X}'_B)yz^3 - (x^3 + h_2(\underline{X}'_B)x^2z^2 + h_6(\underline{X}'_B)z^6)\,. \tag{4.4.1}$$

In the mirror geometry the restriction is given by $y = x = 0$ implying $z \neq 0$ because of the form of the Stanley-Reisner ideal and hence the constraint

$$W_{\Delta^*} = z^6 h^6_{\Delta^*_B}(\underline{X}'_B) = 0 \tag{4.4.2}$$

implies $h^6_{\Delta^*_B}(\underline{X}'_B) = 0$. Further note the possibility of rescaling z which leads to the afore mentioned $\mathbb{C}^*$-identification $X'_{iB} \sim \mu X'_{Bi}$ with $\mu \in \mathbb{C}^*$. Secondly the scaling (4.3.2) is only due to the global embedding and the corresponding refinement of the lattice of Δ' w.r.t to Δ can be undone in the local case by an êtale map

$$\phi_{s_{ij}} : (X'_0, \ldots : X'_{l(\Delta_B)}) \mapsto (X_0^{s_{ij}} : \ldots : X^{s_{ij}}_{l(\Delta_B)})\,. \tag{4.4.3}$$

Hence the mirror geometry to $\mathcal{O}(-K_{\mathbb{P}_{\Delta^*}}) \to K_{\mathbb{P}^*_\Delta})$ is simply given as the Newton polynomial

$$H(\underline{X}) = h^6_{\Delta^*_B}(\underline{X}_B) = 0 \tag{4.4.4}$$

of Δ_2^{*B} itself.

We define therefore the coordinates of Newton polynomials of Δ^{*B} for the biggest three polyhedra in which all other polyhedra are embeddable. These numbers of polyhedra are 16 yielding the most general cubic in $\mathbb{P}^2$, 13 for the most general quartic in $(\mathbb{P}(1,1,2)$ and 15 for the most general bi-quadratic in $\mathbb{P}^1 \times \mathbb{P}^1$. The Newton polynom is defined by (4.2.9) letting $\nu^{*(i)}$ run over Δ_2^{B*} and $\nu^{*(i)}$ over the corners of the dual polyhedron Δ_2^B and the coordinate ring is subject to (4.4.3). This yields the coordinates as indicated in figure 4.2.

Using the remaining scaling of the above projective spaces we can write

$$H(X, Y, \underline{a^*}) = h^6_{\Delta^*_B}(X, Y, \underline{a^*}) \tag{4.4.5}$$

as an inhomogeneous equation. Note that there as many independent a_i^* as there are relations between the points on Δ^{*B}. So in two dimensions we can gauge away three a_i^*. The formalism does not depend on the existence of a global embedding and in particular Δ^{*B} must not be reflexive. However for reflexive polyhedra the corresponding elliptic curves can be readily brought into Weierstrass form using simple transformation algorithms such as Nagell's algorithm, which is very useful for further calculations and will be summarized in Appendix A.1. Moreover the Mori cones and triangulations have been calculated. These data will be used to relate the parameters a_i^* in the Newton polynomials to the Kähler parameters. The upshot is that the compact part, i.e. the elliptic curve, of the mirror to the local del Pezzo geometry is the anti-canonical class in the del Pezzo surface defined by the Newton polynomial of Δ_B^* which fixes a choice of the automorphism group.

It follows from the above and the general discussion in sections 3.2.1 and 4.3.2 and that

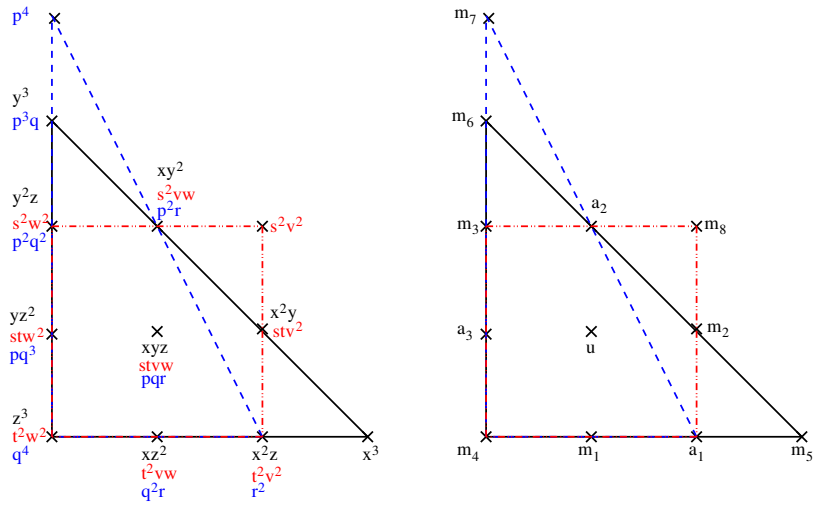

Figure 4.2.: All 16 reflexive polyhedra can be embedded into this diagram.

the mirror curves to toric del Pezzo surfaces have one complex structure parameter called u and $l(\Delta) - 4$ mass parameters called m_i, corresponding to the canonical class of del Pezzo and the e_i-curves respectively. If more then three points are blown up, the del Pezzo surfaces have in addition to the Kähler structure moduli, complex structure moduli and the toric description by the reflexive polyhedra with $l(\Delta) - 4 > 3$ holds only at a special fixed value of the complex structure. This is not a problem for the goal to describe the full Kähler structure moduli space of the del Pezzo surface by the elliptic curve as long as $h_{1,1}(S) \leq 7$ (the bound comes simply from polyhedron 16 which has the maximal $l(\Delta) = 10$), because Kähler and complex structure moduli decouple in $N = 2$ theories. Above $h_{1,1}(S) > 7$ i.e. for the E_8 and E_7 del Pezzo we find torically no mirror in which all masses can be turned on.

5. Refined BPS Invariants of Toric Calabi-Yau Geometries

In this chapter we apply the methods of chapters 3 and 4 to compute the refined BPS invariants of toric Calabi-Yau manifolds using the direct integration procedure. We start with the massless D_5, E_6, E_7 and E_8 del Pezzo surfaces in section 5.1. These results are checked by using standard B-model techniques in section 5.2. Then we proceed to toric del Pezzo surfaces in section 5.3 and toric almost del Pezzo surfaces, i.e. geometries with blow-ups at non-generic points in 5.4 which also includes a mass deformation of the E_8 surface. This discussion follows closely [1]. We end this chapter by presenting a geometry that has a genus two mirror curve in 5.5.

As discussed in section 3.4, our formalism for geometries with a genus one mirror curve distinguishes $u \in \mathcal{M} = \mathbb{P}^1 \setminus \{p_1, \ldots, p_r\}$ as the complex modulus of the family of curves, defining the monodromy of $\mathcal{C}$, from the "mass" parameters $\underline{m} = \{m_1, \ldots, m_{n_f}\}$, whose number ranges between $0 \leq n_f \leq 6$ for the toric (almost) del Pezzo surfaces and between $0 \leq n_f \leq 8$ for the general del Pezzo surfaces.

These masses enjoy various interpretations in the different physical context. They are masses of matter in various representations in Seiberg-Witten theories with one Coulomb parameter, they are interpreted as non-renormalizable deformations of $[p, q]$ 5-brane webs [75], as Wilson lines in the E-string picture, as bundle moduli of the dual heterotic string in the F-theory geometrization [74] or as positions of $[p, q]$ 7-branes in the brane probe picture, compare also the discussion in chapter 8. They are related to Kähler parameters of the del Pezzo surface, which are obtained for the generic del Pezzo surfaces by linear transformations in the homology lattice from the volume af the hyperplane class in $\mathbb{P}^2$ and the volumes of the exceptional divisors. Indeed for the Seiberg-Witten limit we have spelled out the connection between mass and Kähler parameters in the examples (5.3.19), (5.3.32), (5.3.37), (5.4.6) and (5.4.12). Besides that we discuss the matching between mass parameters and Kähler parameters explicitly for the example $\mathcal{B}_3$ in appendix A.2

For the almost del Pezzo surfaces, see definition after (4.1.9), the m_i can be related by rational transformations to the Kähler parameters. Examples for these rational transformation occur first for the Hirzebruch surface F_2 in (5.3.34) and (5.3.36) [1]. These transformations are necessary, because the exceptional divisors are not in the Kähler cone. In all applications there are additional "flavor" symmetries acting on the mass parameters, which makes it natural to group them in characters of the Weyl group.

5.1. The massless D_5, E_6, E_7 and E_8 del Pezzo surfaces

In this section we discuss the massless higher del Pezzo surfaces. In this one parameter family one sums over all classes Λ' of the del Pezzo surface, by setting the corresponding Kähler classes to $t_i \to 0$, i.e. $q_i = e^{t_i} = 1$. Since the Weyl group of the corresponding Lie

[1] For other geometries they can be found in (5.4.3, 5.4.5), (5.4.14, 5.4.15) and (5.4.18, 5.4.21).

algebra acts on Λ' we expect to find the states organized in the dimensions of the Weyl orbits. Physically the specialization corresponds to setting the mass parameters in the five-dimensional theory to zero. We will denote $\beta \in H_2(M,\mathbb{Z})$ simply by the positive integer d, the degree of the holomorphic maps.

5.1.1. The E_8 del Pezzo surface

According to the discussion in section 4.4, the massless E_8 can be obtained from the polyhedron 10 with all mass parameters on the edges set to zero. This is simply done by setting in (A.1.1) (see table) all parameters to zero except $m_2 = m_4 = m_6 = 1$ while keeping $\tilde{u}$. The right large complex structure variable $u = \frac{1}{\tilde{u}^{\frac{1}{6}}}$ is found based on the analysis of the Mori cone given in (5.4.19). Then we get after a rescaling $g_i \to \lambda^i g_i$ with $\lambda = 18u^{7/3}$

$$g_2 = 27u^4, \qquad g_3 = -27u^6(1-864u)\,. \tag{5.1.1}$$

so that near $u = 0$, we get $\frac{dt}{du} = \frac{1}{u} + 60 + 13860u + 4084080u^2 + \mathcal{O}(u^3)$. The j-function

$$j = \frac{1}{1728u(1-432u)}\,. \tag{5.1.2}$$

identifies this as the special family whose monodromy group is classic and has already been discussed in [114]. As a consistency check we can also take the curve (A.2.1) and turn off all the Wilson lines by setting the $\chi_i(0)$ to the values of the dimensions of the weight modules. Let us define the Dynkin diagram of the affine E_8 as

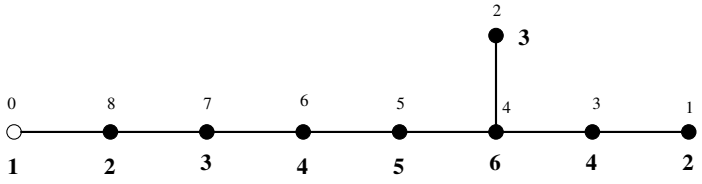

where we denote by the bold numbers the Coxeter labels. The smaller numbers give simply an ordering of the basis of Cartan generators and the basis for the weights. Let us denote by w_i the weight of the classical Lie algebra with a 1 at the ith entry and w_0 the trivial weight. We record the dimensions of the corresponding weight modules

$$\begin{array}{llll} \chi_1(0) & = 3875, & \chi_2(0) = 147250, & \chi_3(0) = 6696000, \quad \chi_4(0) = 6899079264, \\ \chi_5(0) & = 146325270, & \chi_6(0) = 2450240, & \chi_7(0) = 30380, \quad \chi_8(0) = 248\,. \end{array} \tag{5.1.3}$$

Specializing (A.2.1) gives indeed the same family as can be seen by comparing the j-functions.

For the BPS states $N^d_{j_L,J_R}$ at $d = 1$ one gets:

$2j_L \backslash 2j_R$	0	1
0	248	
1		1

$d = 1$

It is obvious that the adjoint representation 248 of E_8 appears as the spin $N^1_{0,0}$, which decomposes into two Weyl orbits with the weights $w_1 + 8w_0$. I. e. we are counting exactly the BPS numbers of the $[p, q]$-string configurations, which are relevant for the gauge theory enhancement in F-theory, see also the discussion in section 8.2. Note that the contributions of different Weyl orbits come in general from curves with different genus. In this way also the higher spin invariants fall systematically into Weyl orbits of weights of E_8. E.g. $3876 = 1 + 3875$, where the latter decomposes in the Weyl orbits of $w_1 + 7w_8 + 35w_0$. The multiplicities of the Weyl Orbits are encoded in the solution of the $\frac{1}{2}K3$ model by the formula (6.4.3), where we report the dimension of some lower E_8 Weyl orbits in equation (6.3.3).

$2j_L \backslash 2j_R$	0	1	2	3
0		3876		
1			248	
2				1

$d = 2$

At $d = 3$ we see the decompositions into representations $4124 = 1 + 248 + 3875$, $34504 = 1 + 248 + 30380$, $34504 = 1 + 248 + 30380$, $151374 = 1 + 248 + 3875 + 147250$ and $30628 = 248 + 30380$ while for higher degree the geometric multiplicities of the Weyl orbits become

$2j_L \backslash 2j_R$	0	1	2	3	4	5	6
0	30628		151374		248		
1		4124		34504		1	
2	1		248		4124		
3				1		248	
4							1

$d = 3$

bigger with the lower spins farer away from the maximal spin, still it obvious how the states decompose into Weyl orbits, e.g. $7726504 = 2 + 9 \times 248 + 6 \times 3875 + 6 \times 147250 + 669600$.

$2j_L \backslash 2j_R$	0	1	2	3	4	5	6	7	8	9	10
0		3480992		7726504		212879		248			
1	185878		1209127		3632614		38876		1		
2		38876		251755		1030753		4373			
3	248		4373		39125		217003		249		
4		1		249		4373		35000		1	
5					1		249		4125		
6								1		248	
7											1

$d = 4$

5.1.2. The E_7 del Pezzo surface

The massless E_7 del Pezzo corresponds to the polyhedron 13 with all parameters on the edges set to zero. Again this is simply done by specializing the Weierstrass form (A.1.15) to

$$a_1 = 1, \quad m_4 = 1, \quad m_5 = 1, \quad u = \frac{1}{(-\tilde{u})^{\frac{1}{4}}}, \tag{5.1.4}$$

while setting all other parameters to zero. Again the inverse quartic root identification of $u = \frac{1}{(-\tilde{u})^{\frac{1}{4}}}$ can be predicted from the Mori cone vector $l = (-4, 1, 1, 2)$. It could be also

obtained by firstly requiring at large radius $t(u) \sim \log(u)$ and at the conifold $t_D(u) \sim \Delta$. This also fixes the -1 in (5.1.4), in fact that $t(u) = \log(u) - 12u + 210u^2 + \mathcal{O}(u^3)$ and secondly knowing that genus zero curves exist at $d = 1$.

Relative to (5.1.4) we have to scale the g_2 and g_3 by $\lambda = 18iu^{\frac{2}{5}}$ yielding[2]

$$g_2^b = 27u^4(1 - 192u), \quad g_3^b = 27u^6(1 + 576u) \tag{5.1.5}$$

and the j-function as

$$j_b = \frac{(192u - 1)^3}{1728u(64u + 1)^2} \ . \tag{5.1.6}$$

It is well-known that massless theories can be formulated on isogeneous curves [89]. These curves are not distinguished by their Picard-Fuchs equation, neither for the holomorphic nor the meromorphic differential, but they are distinguished by a choice of a relative factor $\kappa \in \mathbb{N}_+$ in the normalization of the a- and the b-cycles. As pointed out in [89] this exchanges the two cusp points – corresponding to the large radius and conifold points – of the curves, but is not a symmetry of the $N = 2$ theory neither of the topological string. In the context of the del Pezzo surfaces the existence of isogeneous curves has been discussed in [111]. It finds a natural interpretation in terms of the center of E_n given in (4.1.9) as follows. Since the Picard-Fuchs equations depend only on the linear relations among the points in the polyhedra, the polyhedron 4 with one mass at the edge of the corner set to zero will lead to the same Picard-Fuchs operator. Now with the Weierstrass form obtained by embedding polyhedron 4 into polyhedron[3] 13 by setting all coefficients to zero except

$$a_1 = 1, \quad a_2 = 1, \quad m_5 = 1, \quad u = \frac{1}{(\tilde{u})^{\frac{1}{4}}} \, , \tag{5.1.7}$$

we can precisely understand the relation between the two geometries. With $\lambda = 18u^{\frac{2}{5}}$ we get now

$$g_2^s = 27u^4(48u + 1), \quad g_3^s = 27u^6(72u + 1) \tag{5.1.8}$$

and the j-function as

$$j_s = \frac{(48u + 1)^3}{1728u^2(64u + 1)} \tag{5.1.9}$$

so that the $\mathbb{Z}_2$ transformations

$$\mathbb{Z}_2 : u \mapsto -\frac{1}{64} - u, \quad \mathbb{Z}_2 : j_b \leftrightarrow j_s, \quad \mathbb{Z}_2 : \tau_s \leftrightarrow 2\tau_b \tag{5.1.10}$$

exchanges as in [89] the conifold with the large radius point and identifies $j_b \leftrightarrow j_s$ and rescales the $U(1)$-coupling. However to get integral charges for the matter representations, or equivalently integral Kähler classes, one has to choose the curve corresponding to the big polyhedron.

Note that the last relation in (5.1.10) can be already seen from the fact that $\Delta = 1 + 64u$ appears quadratically in the denominator of j_b. The story is analogous for the E_6 group with the big polyhedron being polyhedron 15 and the small polyhedron being polyhedron 1. So we conclude that the volumes of polyhedra P_b and P_s the are related to the center of

[2] The labels b and s refer as big and small to the size of the polyhedra used to define the geometries.

[3] Of course this family can be also realized as special cubic by embedding polyhedron 4 into polyhedron 15. That does not change the analysis.

the groups, or the volumes of the fundamental cell in the lattices Λ' and Λ'' as

$$\frac{\mathrm{Vol}(P_b)}{\mathrm{Vol}(P_s)} = \frac{\mathrm{Vol}(\Lambda'')}{\mathrm{Vol}(\Lambda')} \tag{5.1.11}$$

and the existence of the self-dual polyhedron 10 is a consequence of the self-duality of the E_8 lattice. We further notice that the j-function of the massless E_7 curve of A.2.1

$$j^{es}_{E7} = \frac{(u_{es}-36)^3}{(1728(u_{es}-52)} \tag{5.1.12}$$

is not very naturally related to $j_b(u_b)$ or $j_s(u_s)$

$$u_{es} = -12 - \frac{1}{u_s}, \quad u_{es} = \frac{52-768u_b}{1+64u_b}\ . \tag{5.1.13}$$

Let us agree on the Dynkin diagram of E_7 in the following conventions

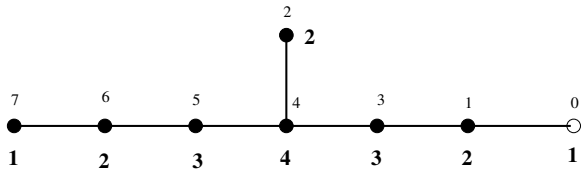

$$\begin{aligned}&\chi_1(0)=133, \quad \chi_2(0)=912, \quad \chi_3(0)=8645, \quad \chi_4(0)=365750, \quad \chi_5(0)=27664,\\ &\chi_6(0)=1539, \quad \chi_7(0)=56\ .\end{aligned} \tag{5.1.14}$$

From either the big or the small polyhedron we get the following refined BPS invariants. Again there are the Weyl orbits for curves in different genera which combine in simple representations of E_7.

$2j_L \backslash 2j_R$	0
0	56

d=1

$2j_L \backslash 2j_R$	0	1	2
0		133	
1			1

d=2

$2j_L \backslash 2j_R$	0	1	2	3
0	56		912	
1				56

d=3

We note that there is a periodicity with the degree mod 2 in the contributions of the BPS states with highest spins. In even degree we always find for the highest spin the trivial and the adjoint representation 133 in the Weyl orbits $w_1 + 7w_0$ of E_7, while in odd degrees we find the 56 representation in a single Weyl orbit. This is a consequence of the nontrivial center of E_7 (4.1.9), which is reflected on the square root of the line bundle $\mathcal{Q}$ for the E_7 case.

At $d = 3$ the 912, w_2+6w_7 representation appears and again we find the behavior that the higher degree stable pair invariants decompose in a simple fashion into representations and hence Weyl orbits. The systematic can again be understood form the solution of the $\frac{1}{2}K3$ and formula (6.4.3). The relevant dimensions of the Weyl orbits for the $E_5 = D_5, \ldots, E_7$ groups are summarized in table 6.1.

E.g. at $d = 4$: $8778 = 8645 + 133$, with 8645 decomposes as $w_3 + 5w_6 + 22w_1 + 77w_0$ and

$1673 = 1539 + 133 + 1$ with $1539 = w_6 + 6w_1 + 27w_0$.

$2j_L \backslash 2j_R$	0	1	2	3	4	5	6
0		1673		8778		1	
1			134		1673		
2				1		133	
3							1

$d = 4$

At degree $d = 4$ we have the following decomposition $1024 = 912 + 2 \times 56$, $7504 = 4 \times 1539 + 912 + 2 \times 133 + 3 \times 56 + 2$, $8472 = 5 \times 1539 + 5 \times 133 + 2 \times 56$, $36080 = 27664 + 5 \times 1539 + 5 \times 133 + 56$ and $93688 = 3 \times 27664 + 8645 + 1539 + 3 \times 133 + 2 \times 56 + 1$.

$2j_L \backslash 2j_R$	0	1	2	3	4	5	6	7	8
0	6592		36080		93688		968		
1		968		8472		36080		56	
2			56		1024		7504		
3						56		968	
4									56

$d = 5$

$2j_L \backslash 2j_R$	0	1	2	3	4	5	6	7	8	9	10	11	12
0		225912		650050		1062065		54419		133			
1	10451		73839		289109		650184		13588		1		
2		1807		13855		75512		234691		1807			
3	1		134		1808		13855		61924		134		
4				1		134		1808		12048		1	
5							1		134		1674		
6										1		133	
7													1

$d = 6$

5.1.3. The E_6 del Pezzo surface

As we mentioned before, we specialize the polyhedron 15 to the massless case by setting all coefficients in (A.1.9) to zero except of

$$m_4 = 1, \quad m_5 = 1, \quad m_6 = 1, \quad u = \frac{1}{\tilde{u}^{1/3}} \,. \tag{5.1.15}$$

With $\lambda = 18u^{\frac{8}{3}}$ we get

$$g_2 = 27u^4(1 - 216u), \quad g_3 = 27u^6(1 + 540u - 5832u^2) \,, \tag{5.1.16}$$

hence the j-function of the $\Gamma_0(3)$ curve.

$$j_b = -\frac{(1 - 216u)^3}{1728u(1 + 27u)^3} \,. \tag{5.1.17}$$

Similar the isogeneous $\Gamma(3)$ curve is obtained by considering the small polyhedron 1 by setting $a_2 = 1$, $m_2 = 1$, $m_4 = 1$ and $u = \frac{1}{\tilde{u}^{1/3}}$, which yields with the same scaling λ, $g_2 = 27u^4(24u + 1)$ and $g_3 = 27u^6\left(216u^2 + 36u + 1\right)$ so

$$j_s = -\frac{(1 + 24u)^3}{1728u^3(1 + 27u)} \tag{5.1.18}$$

and the relating data between the isogeneous curves are

$$\mathbb{Z}_2 : u \mapsto -\frac{1}{27} - u, \quad \mathbb{Z}_2 : j_b \leftrightarrow j_s, \quad \mathbb{Z}_2 : \tau_s \leftrightarrow 3\tau_b \,. \tag{5.1.19}$$

Note that the massless E_6 curve of A.2.1

$$j^{es}_{E6} = \frac{(u_{es}-18)^3(u_{es}+6)}{1728(u_{es}-21)} \tag{5.1.20}$$

is again not completely naturally related to $j_{b/s}(u_{b/s})$

$$u_{es} = -6 - \frac{1}{u_s}, \quad u_{es} = \frac{21-162u_b}{1+2bu_b} \,. \tag{5.1.21}$$

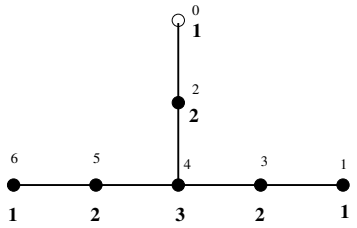

We record the characters according to the above basis of weights

$$\chi_1(0) = 27, \quad \chi_2(0) = 78, \quad \chi_3(0) = 351, \quad \chi_4(0) = 2925, \quad \chi_5(0) = 351, \quad \chi_6(0) = 27 \,. \tag{5.1.22}$$

The low degree spin invariants fall in these representations.

$2j_L \backslash 2j_R$	0
0	27

d=1

$2j_L \backslash 2j_R$	0	1
0		27

d=2

$2j_L \backslash 2j_R$	0	1	2	3
0	1		78	
1				1

d=3

$2j_L \backslash 2j_R$	0	1	2	3	4
0		27		351	
1					27

d=4

Note that the periodicity in which the adjoint representation appears is now the degree d modulo 3 as expected from the center of E_6.

The first splitting representation that appears is the $378 = 351 + 27$ where 351 splits in the Weyl orbits $w_3 + 5w_6$ and further $1755 = 5 \times 351$, see (6.4.3) and table 6.1.

$2j_L \backslash 2j_R$	0	1	2	3	4	5	6
0	27		378		1755		
1				27		378	
2							27

$d = 5$

$2j_L \backslash 2j_R$	0	1	2	3	4	5	6	7	8	9
0		730		3732		8984		78		
1			79		808		3732		1	
2				1		79		730		
3							1		78	
4										1

$d = 6$

$2j_L \backslash 2j_R$	0	1	2	3	4	5	6	7	8	9	10	11
0	2133		10584		30240		47439		2133			
1		378		2889		12717		30240		405		
2			27		405		2889		10584		27	
3						27		405		2484		
4									27		378	
5												27

$d = 7$

5.1.4. The D_5 del Pezzo surface

Finally we discuss the case of the D_5 surface which can be obtained from the polyhedra 2 (small) and 15 (big). We consider again the massless limit by the following choice of coefficients and redefinition of u

$$\begin{aligned} a_1 = i, \quad m_3 = i, \quad m_4 = i, \quad m_8 = i, \quad u = \tilde{u}^{-\frac{1}{2}} \quad \text{(big)} \\ a_2 = i, \quad a_3 = i, \quad m_1 = i, \quad m_2 = i, \quad u = \tilde{u}^{-\frac{1}{2}} \quad \text{(small)}. \end{aligned} \tag{5.1.23}$$

All the other mass parameters vanish. Accordingly, one obtains the respective Weierstrass normal forms

$$\begin{aligned} g_2 &= 27u^4\left(256u^2+16u+1\right), \\ g_3 &= -27u^6\left(4096u^3+384u^2-24u-1\right), \quad \text{big polyhedron,} \end{aligned} \tag{5.1.24}$$

$$\begin{aligned} g_2 &= 27\left(\frac{1}{u^2}+\frac{16}{u}+16\right)u^6, \\ g_3 &= 27\left(\frac{1}{u^3}+\frac{24}{u^2}+\frac{120}{u}-64\right)u^9, \quad \text{small polyhedron.} \end{aligned} \tag{5.1.25}$$

In both cases we have performed a rescaling with

$$\lambda = 18u^3 \tag{5.1.26}$$

in order to arrive at the respective expressions for g_2 and g_3. Finally the j-functions are given as

$$j_b = \frac{\left(256u^2+16u+1\right)^3}{1728u^2(16u+1)^2}, \qquad j_s = \frac{\left(16u^2+16u+1\right)^3}{1728u^4(16u+1)}. \tag{5.1.27}$$

In contrast to the previous cases (E_6, E_7, E_8) we observe a different behavior concerning the exchange of the conifold locus and the large radius point

$$\mathbb{Z}_2 : u \mapsto -u - \frac{1}{16}, \quad \mathbb{Z}_2 : j_b \leftrightarrow j_b, \quad j_s \leftrightarrow j_s' = -\frac{\left(256u^2 - 224u + 1\right)^3}{1728u(16u+1)^4}, \quad \mathbb{Z}_2 : \tau_s \leftrightarrow 4\tau_s'. \tag{5.1.28}$$

Instead the j-functions of the two polyhedra are related by the map

$$u_b \mapsto -\frac{16u - (8u+1)\sqrt{16u+1}+1}{32(16u+1)}. \tag{5.1.29}$$

We end the discussion by comparing the curves to the massless D_5 curve given by Sakai and Eguchi. This is given by again setting the characters to the dimensions of the fundamental representations in (A.2.8). The Weierstrass data of this curve are given by

$$g_2 = \frac{1}{12}(u+4)^2\left(u^2 - 8u - 32\right), \qquad g_3 = \frac{1}{216}(u+4)^3\left(u^3 - 12u^2 - 24u + 224\right), \tag{5.1.30}$$

and the j-function reads

$$j^{es}_{\mathrm{D}_5} = \frac{\left(32u_{es}^2 + 8u_{es} - 1\right)^3}{1728u_{es}^4\left(48u_{es}^2 + 8u_{es} - 1\right)}. \tag{5.1.31}$$

In contrast to the previous cases, this curve is not connected to any of the two previous curves by a bi-rational coordinate transformation.

The Dynkin diagram of $\hat{\mathrm{D}}_5$

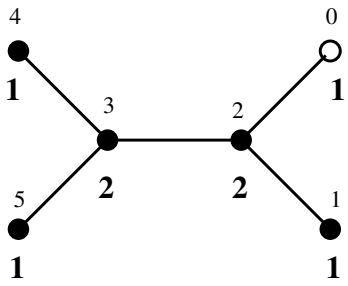

leads to the following dimensions of the weight modules

$$\chi_1(0) = 10, \quad \chi_2(0) = 45, \quad \chi_3(0) = 120, \quad \chi_4(0) = 16, \quad \chi_5(0) = 16\ . \tag{5.1.32}$$

We see the periodicity with respect to the degree is now modulo four and the adjoint representation of $D5$ appears for the first time at $d = 4$. The representation 45 falls in the Weyl orbits $w_2 + 5w_0$. The Weyl orbit of w_2 is 40-dimensional and gets contributions only from genus zero curves, while the w_i get contributions from a genus two curve, whose leading contribution is at spin $[1/2, 2]$.

$2j_L \backslash 2j_R$	0
0	16

d=1

$2j_L \backslash 2j_R$	0	1
0		10

d=2

$2j_L \backslash 2j_R$	0	1	2
0			16

d=3

$2j_L \backslash 2j_R$	0	1	2	3	4
0		1		45	
1					1

d=4

$2j_L \backslash 2j_R$	0	1	2	3	4	5
0			16		144	
1						16

$d = 5$

$2j_L \backslash 2j_R$	0	1	2	3	4	5	6	7
0		10		130		456		
1					10		130	
2								10

$d = 6$

$2j_L \backslash 2j_R$	0	1	2	3	4	5	6	7	8	9
0	16		160		736		1440		16	
1				16		176		736		
2							16		160	
3										16

$d = 7$

$2j_L \backslash 2j_R$	0	1	2	3	4	5	6	7	8	9	10	11	12
0		311		1345		3431		4726		257			
1			46		357		1602		3431		46		
2				1		46		357		1345		1	
3							1		46		311		
4										1		45	
5													1

$d = 8$

5.2. An alternative approach to the massless cases

Alternatively we use the Picard-Fuchs equations, the Yukawa couplings, i.e. the usual B-model methods, that also apply in the compact cases. As discussed in section 2.2.6, the complex geometry of the mirror manifolds are described by the Picard-Fuchs differential equations [32]

$$(\theta_z^2 + c_0 z \prod_{i=1}^{2} (\theta_z + 1 - a_i))\theta_z \int_{\gamma_i} \Omega = 0, \tag{5.2.1}$$

where z is the complex structure modulus in the mirror manifold and $\theta_z = z\partial_z$. a_1, a_2 and c_0 are classical constants of the the Calabi-Yau manifolds. c_0 is a normalization constant for the complex structure parameter z such that $t = \log(z) + \mathcal{O}(z)$ around $z \sim 0$ corresponds to the Kähler modulus in the large volume limit. The vectors $\vec{a} = (a_1, a_2)$ satisfy $a_1 + a_2 = 1$

CY	$\mathbb{P}^2$	$\mathbb{P}^1 \times \mathbb{P}^1$	D_5	E_6	E_7	E_8
c_0	27	-16	16	27	64	432
κ	$\frac{1}{3}$	1	4	3	2	1

Table 5.1.: The constants c_0 and κ for the Calabi-Yau models.

and are given as follows for various one-parameter families of Calabi-Yau manifolds. We consider

$$\begin{aligned} &\mathbb{P}^2 :\ \vec{a} = (\frac{1}{3}, \frac{2}{3}), \quad \mathbb{P}^1 \times \mathbb{P}^1 :\ \vec{a} = (\frac{1}{2}, \frac{1}{2}), \quad D_5 :\ \vec{a} = (\frac{1}{2}, \frac{1}{2}), \\ &E_6 :\ \vec{a} = (\frac{1}{3}, \frac{2}{3}), \quad E_7 :\ \vec{a} = (\frac{1}{4}, \frac{3}{4}), \quad E_8 :\ \vec{a} = (\frac{1}{6}, \frac{5}{6}). \end{aligned} \tag{5.2.2}$$

The E_n ($n = 5, 6, 7, 8$) del Pezzo surfaces can be represented as complete intersections of degree $(2, 2)$ in $\mathbb{P}^4$, a degree 3 hypersurface in $\mathbb{P}^3$, a degree 4 hypersurface in weighted projective space $\mathbb{P}^3(1, 1, 1, 2)$ and a degree six hypersurface in $P^3(1, 1, 2, 3)$. In these cases the normalization constant c_0 can be computed as $c_0 = (\prod_i d_i^{d_i})/(\prod_j w_j^{w_j})$ where d_i are the degree(s) of hypersurfaces or complete intersections, and w_j are weights of the ambient projective space (see also the discussion in section 4.1.1). The constant is $c_0 = 27$ for the $\mathbb{P}^2$ model and $c_0 = -16$ for the $\mathbb{P}^1 \times \mathbb{P}^1$ model.

The prepotential $F^{(0,0)}(t)$ is determined by the Picard-Fuchs (PF) equation (5.2.1) from the fact that the mirror map $t(z)$ and derivative $\partial_t F^{(0,0)}(t)$ are solutions to the PF equation besides the constant solution. The normalization of the prepotential is fixed by the classical intersection number κ as $F^{(0,0)}(t) = -\frac{\kappa}{6} t^3 + \cdots$. The intersection number can be calculated by the formula $\kappa = (\prod_i d_i)/(\prod_j w_j)$ in the E_n models. The numbers are $\kappa = \frac{1}{3}$ for the $\mathbb{P}^2$ model and $\kappa = 1$ for the $\mathbb{P}^1 \times \mathbb{P}^1$ model. We list the constants c_0 and κ for the Calabi-Yau models in Table 5.1.

We discuss next the genus one amplitudes $F^{(1,0)}$ and $F^{(0,1)}$. The $F^{(1,0)}$ amplitude is holomorphic while the amplitude $F^{(0,1)}$ has a holomorphic anomaly which is determined by the genus one holomorphic anomaly equation (2.3.17). Both amplitudes have logarithmic cuts for the discriminant $\Delta(z) = 1 + c_0 z$ whose coefficients are determined by the genus one gap boundary conditions at the conifold point $\Delta(z) = 0$. Furthermore, it turns out that the amplitudes also contain a logarithmic piece $\log(z)$. We can write the amplitudes as

$$\begin{aligned} F^{(1,0)} &= \frac{\log(\Delta(z)) - c^{(1,0)} \log(z)}{24}, \\ F^{(0,1)} &= -\frac{1}{2} \log(\partial_z t(z)) - \frac{1}{12} (\log(\Delta(z)) + c^{(0,1)} \log(z)), \end{aligned} \tag{5.2.3}$$

where we use the constants $c^{(1,0)}$ and $c^{(0,1)}$ to denote the coefficients for $\log(z)$ terms in the refined amplitudes. We determine the constants for the Calabi-Yau models and list them in Table 5.2.

The three-point Yukawa coupling and the Kähler metric in the moduli space are given up to an anti-holomorphic factor by

$$C_{zzz} = -\frac{\kappa}{z^3(1 + c_0 z)}, \quad G_{z\bar{z}} \sim \partial_z t \,. \tag{5.2.4}$$

CY	$\mathbb{P}^2$	$\mathbb{P}^1 \times \mathbb{P}^1$	D_5	E_6	E_7	E_8
$c^{(1,0)}$	1	2	8	9	10	11
$c^{(0,1)}$	7	7	4	3	2	1

Table 5.2.: The constants $c^{(1,0)}$ and $c^{(0,1)}$ for the Calabi-Yau models.

The Christoffel connection in the holomorphic limit $\Gamma^z_{zz} = \partial_t z(\partial_z^2 t)$ is not a rational function of z. There is a relation with the propagator which satisfies (3.3.7) $\partial_{\bar{z}} S^{zz} = \bar{C}^{zz}_{\bar{z}}$,

$$\Gamma^z_{zz} = -C_{zzz} S^{zz} + f_z \,, \tag{5.2.5}$$

where f_z is a rational function of z since the anti-holomorphic derivatives $\bar{\partial}_{\bar{z}}$ of both sides are the same. For the one-parameter models we simply denote the propagator as $S \equiv S^{zz}$. The rational function f_z is a holomorphic ambiguity that we can choose such that the propagator S has a nice behavior near the special singular points in the moduli space

$$f_z = -\frac{6a_1 + 5}{6z} - \frac{c_0}{6(1 + c_0 z)} \,, \tag{5.2.6}$$

where a_1 is the constant in (5.2.2) and c_0 is the normalization constant in table 5.1. With this choice of ambiguity f_z, the propagator S is regular at the conifold point $z = -\frac{1}{c_0}$. Near the orbifold point $z^{-1} \sim 0$, the propagator generically scales as $S \sim z^3$ and we have chosen the constant $(6a_1 + 5)$ in f_z to cancel the leading z^3 term so that the scaling behavior is less singular near the orbifold point as $S \sim z^2$. The cancellation can be seen by noting that the flat coordinate scales as $t \sim z^{-a_1}$ near the orbifold point $z^{-1} \sim 0$, and accordingly the Christoffel connection scales as $\Gamma^z_{zz} \sim -(a_1 + 1)z^{-1}$ and cancels the leading term in f_z.

The derivative of the propagator is constrained due to (3.3.7) as

$$D_z S = -C_{zzz} S^2 + \tilde{f}(z), \tag{5.2.7}$$

where the covariant derivative reads $D_z S = (\partial_z + 2\Gamma^z_{zz})S$. The holomorphic ambiguity $\tilde{f}(z)$ is a rational function with a simple pole at $\Delta(z)$, and it can be fixed by computing S and Γ^z_{zz} in the holomorphic limit.

The propagator S is the only an-holomorphic component in the higher genus amplitudes, and the generalized holomorphic anomaly for the refined theory is (3.3.1)

$$\partial_S F^{(n,g)}(S, z) = \frac{1}{2}[D_z^2 F^{(n,g-1)} + \sum_{n_1=0}^{n} \sum_{g_1=0}^{g} D_z F^{(n_1,g_1)} D_z F^{(n-n_1,g-g_1)}], \tag{5.2.8}$$

where the first term on the RHS is defined to be zero if $g = 0$, and the sum in the second term does not include the two cases $n_1 = g_1 = 0$ and $n_1 = n, g_1 = g$. Since the derivative of the propagator forms a closed algebra as seen in equation (5.2.7), the higher genus amplitudes $F^{(n,g)}$ with $n + g \geq 2$ are polynomials of the propagator S and the coefficients of the polynomials are rational function of z.

The holomorphic anomaly equation determines the S-dependent part in the higher genus amplitudes $F^{(n,g)}$, but not the S-independent holomorphic ambiguity which is a rational function of z and we can denote as $f_0^{(n,g)}(z)$. To further fix this function we consider the boundary conditions at the special points in the moduli space, the large volume point $z \sim 0$,

the conifold point $z \sim -\frac{1}{c_0}$ and the orbifold point $z \sim \infty$.

The behaviors near the large volume point and the conifold point are universal for all models. The amplitude $F^{(n,g)}$ and the ambiguity $f_0^{(n,g)}(z)$ approach a constant $\mathcal{O}(z^0)$ near the large volume point. The leading constant term in the conventional unrefined theory is the constant map contribution in Gromov-Witten theory. This constant does not affect the calculations of the refined GV invariants which only contribute to the world-sheet instantons of positive degrees, and here we will not determine the constant for the refined theory.

Near the conifold point, the amplitude $F^{(n,g)}$ satisfies the gap condition $F^{(n,g)} \sim \frac{1}{t_D^{2(n+g)-2}} + \mathcal{O}(t_D^0)$, where the t_D is the flat coordinate near the conifold point and scales like $t_D \sim z + \frac{1}{c_0}$, compare also the discussion in section 3.3.3. Accordingly the ambiguity scales as $f_0^{(n,g)}(z) \sim \frac{1}{(1+c_0 z)^{2(n+g)-2}}$ and the gap conditions fix $2(n+g)-2$ constants in the holomorphic ambiguity $f_0^{(n,g)}(z)$.

The boundary conditions near the orbifold point $z \sim \infty$ are more tricky, and needed to be classified into several cases, similar to the situation studied in [106].

For the $\mathbb{P}^2$ model, the higher genus amplitude $F^{(n,g)}$ is regular at the orbifold point. Since we have chosen the propagator S to have a nice scaling behavior $S \sim z^2$ at the orbifold point, there is no singularity at the orbifold point from the S-dependent part in $F^{(n,g)}$. Therefore the holomorphic ambiguity $f_0^{(n,g)}(z)$ is also regular at the orbifold point, and we can write an ansatz

$$f_0^{(n,g)}(z) = \sum_{k=0}^{2(n+g)-2} \frac{x_k}{(1+c_0 z)^k}. \tag{5.2.9}$$

The gap condition fixes the $2(n+g)-2$ constants x_k for $k = 1, 2, \cdots, 2(n+g)-2$, and we do not need to fix the constant x_0. So in this model we can in principle compute the refined topological string amplitudes to any genus and extract the corresponding refined GV invariants.

For the other five models, the amplitude $F^{(n,g)}$ is singular at the orbifold point but is less singular than $\frac{1}{t_o^{2(n+g)-2}}$, where t_o is the flat coordinate near the orbifold point and scales as $t_o \sim z^{-a_1}$, where a_1 is the fractional number in (5.2.2). So the ansatz for the ambiguity is

$$f_0^{(n,g)}(z) = \sum_{k=0}^{2(n+g)-2} \frac{x_k}{(1+c_0 z)^k} + \sum_{k=1}^{[2a_1(n+g-1)]} y_k z^k \,. \tag{5.2.10}$$

In these cases that are similar to the $\mathbb{P}^2$ model, the conifold gap condition fixes the $2(n+g)-2$ constants x_k for $k = 1, 2, \cdots, 2(n+g)-2$. However we still need to fix the $[2a_1(n+g-1)]$ constants y_k in order to solve the refined topological string amplitudes (up to a constant x_0).

For the $\mathbb{P}^1 \times \mathbb{P}^1$ model, there is also a further gap condition at the orbifold point similar to the conifold point which implies that $F^{(n,g)} \sim \frac{1}{t_o^{2(n+g)-2}} + \mathcal{O}(t_o^0)$. Since only even powers of t_o appear due to the leading scaling behavior $t_o \sim z^{-\frac{1}{2}}$, this provides $n+g-1$ boundary conditions which exactly fix the constants y_k with $k = 1, 2, \cdots, (n+g-1)$. So in this model we can also in principle compute the refined topological string amplitude to any genus.

For the remaining E_n ($n = 5, 6, 7, 8$) models, there is no nice boundary condition at the orbifold point to fix the constants y_k in (5.2.10). Here we can use the nice behavior of

refined GV invariants at the large volume point to provide boundary conditions to fix these constants. It is often the case that some low degree refined GV invariants $\tilde{n}^d_{g_L,g_R}$ vanish at a given genus g_L, g_R. If we have computed the refined GV invariants $\tilde{n}^d_{g_L,g_R}$ for all the genera $g_L+g_R \leq n+g$, $g_R \leq n$ and up to degree $d \leq [2a_1(n+g-1)]$, either by the B-model method or by their vanishing property, then we would have enough boundary conditions to fix the constants y_k with $k = 1, 2, \cdots, [2a_1(n+g-1)]$ in $f_0^{(n,g)}(z)$ in (5.2.10) and would have solved the refined amplitude $F^{(n,g)}$ as well. Using this technique we can solve the refined topological string amplitudes to some finite but not arbitrary high genus.

Using the B-model techniques we compute the refined topological string amplitudes to some higher genus and we fix the complete refined GV invariants up to some finite degrees for the various models. We list the results in the tables 5.1.4 - A.4.1. The refined GV invariants for the local $\mathbb{P}^2$ and $\mathbb{P}^1 \times \mathbb{P}^1$ models have been computed before in [30, 108]. Here we also include them for completeness. The blank elements in the tables represent vanishing GV invariants.

We discuss some salient features of the refined GV invariants. For degree d which is a positive integer as an element in $H_2(M, \mathbb{Z})$, there is a non-vanishing positive integer $n^d_{j_L,j_R} = \tilde{n}^d_{2j_L,2j_R}$ at the top genus $(2j_L, 2j_R) = (g_L^{top}, g_R^{top})$. All higher genus invariants vanish so the non-vanishing GV invariants form a rectangular matrix, and we find that the left top genus is always less than the right top genus $g_L^{top} \leq g_R^{top}$. For a Calabi-Yau model, the top genus of higher degree is always larger than that of the lower degree, i.e. we always find $g_L^{top}(d) \geq g_L^{top}(d-1)$ and $g_R^{top}(d) \geq g_R^{top}(d-1)$.

In the basis of integers $\tilde{n}^d_{g_L,g_R}$, the GV invariants do not generically vanish if the genus pair lies in the rectangular matrix, i. e. $g_L \leq g_L^{top}$ and $g_R \leq g_R^{top}$. So we can determine the top genus (g_L^{top}, g_R^{top}) as the smallest integer pair such that $\tilde{n}^d_{g_L^{top}+1,0} = \tilde{n}^d_{0,g_R^{top}+1} = 0$. The vanishing of a GV invariant $\tilde{n}^d_{g_L,g_R} = 0$ implies that its higher genus neighbors also vanish $\tilde{n}^d_{g_L+1,g_R} = \tilde{n}^d_{g_L,g_R+1} = 0$.

However in the j-spin basis $n^d_{j_L,j_R}$, there is furthermore a large number of vanishing GV invariants $n^d_{j_L,j_R}$ inside the rectangular matrix $2j_L \leq g_L^{top}$ and $2j_R \leq g_R^{top}$. The genus pairs of these non-vanishing integers follow certain patterns as we go up in higher degrees. More precisely, suppose at degree $d-1$ we find $n^{d-1}_{g_L/2,g_R/2} \neq 0$, then for the corresponding genus pair $(g'_L, g'_R) = (g_L + g_L^{top}(d) - g_L^{top}(d-1), g_R + g_R^{top}(d) - g_R^{top}(d-1))$ at degree d, we always find that the GV integer is also non-vanishing $n^d_{g'_L/2,g'_R/2} \neq 0$. On the the hand, if the integer $n^{d-1}_{g_L/2,g_R/2}$ vanishes, it is also usually but not always the case that the vanishing $n^d_{g'_L/2,g'_R/2} = 0$ also happens at the higher degree d.

The non-vanishing GV invariants seem to cluster together, but no two non-vanishing GV invariants are next neighbors to each others. More precisely, we define the distance as $|g_L - g'_L| + |g_R - g'_R|$ between two GV invariants $n^d_{g_L/2,g_R/2}$ and $n^d_{g'_L/2,g'_R/2}$. We find that the distance of a non-vanishing GV invariant $n^d_{g_L/2,g_R/2}$ to its nearest non-vanishing neighbor is almost always 2. Only two exceptions occur in the $\mathbb{P}^2$ model where the distance with the nearest non-vanishing neighbor is 4.

With the B-model method we can extract the GV invariants in the basis $\tilde{n}^d_{g_L,g_R}$ from the refined topological string amplitudes. We find that by utilizing the pattern in the j-spin basis, we do not need to solve all non-vanishing $\tilde{n}^d_{g_L,g_R}$ inside the top genus rectangular matrix in order to fix the complete GV invariants. It is still necessary to compute a number of non-vanishing $\tilde{n}^d_{g_L,g_R}$ from the B-model which is larger than the number of non-vanishing

$n^d_{j_L,j_R}$ in the j-spin basis. However, since we do not know a priori the number and the positions of the non-vanishing $n^d_{j_L,j_R}$ before we find that the solution, we usually need to compute the B-model to a few more genera higher. In practice, we find that we can usually fix the complete GV invariants when we compute the refined amplitudes $F^{(n,g)}$ up to the total genus $n+g$ a little bigger than the left top genus g_L^{top}. We consider a solution for the GV integers $n^d_{j_L,j_R}$ that passes non-trivial consistency checks, if the number of non-vanishing integers $\tilde{n}^d_{g_L,g_R}$ obtained from the B-model is larger than the number of non-vanishing integers $n^d_{j_L,j_R}$ in the solution.

5.3. The toric del Pezzo surfaces

In this section we discuss the calculation of refined BPS numbers of the toric del Pezzo surfaces F_0, $\mathbb{P}^2 \cong \mathcal{B}_0$, $\mathcal{B}_1$, $\mathcal{B}_2$ and $\mathcal{B}_3$ as well as an example for an almost Fano variety, namely F_2 which has only semi-positive first Chern class.

An important observation is that the GKZ-system (5.3.6) that can be easily determined from the toric diagram can be reduced to a single ordinary differential operator depending on only one variable u and some mass parameters m_i. The above discussed mass parameters correspond in this context to trivial solutions of the Picard-Fuchs equations[4]. We have determined this differential operator for the cases F_0 (5.3.15), $\mathbb{P}^2$ (5.3.9), $\mathcal{B}_1$ (5.3.28) and $\mathcal{B}_2$ (A.2.26).

As discussed in section 3.4, a crucial ingredient for the computation is the Weierstrass normal form of the mirror geometry that can be obtained by embedding the toric diagram into either one of the polyhedra 13, 15 or 16, see also the discussion in 4.4. This procedure is explicitly demonstrated for the embedding of the toric del Pezzo surfaces in the picture below (5.1) and is the starting point for the subsequent discussion. Following the procedure described in section 3.4, we have determined the free energies for the first genera. In the following we just discuss the important steps to set up the calculation and mostly restrict ourselves to just pointing out new phenomena when passing from one geometry to another.

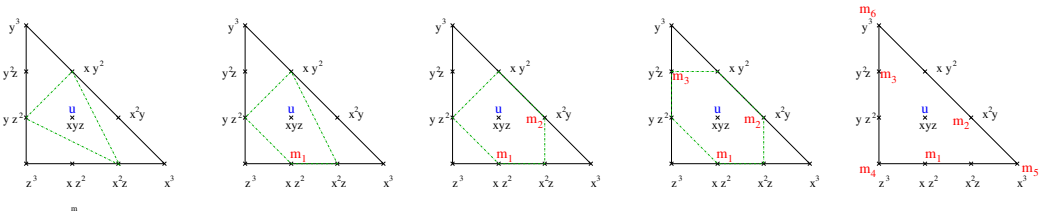

Figure 5.1.: Here we depict the polyhedral embedding of $\mathcal{B}_0, \ldots, \mathcal{B}_3$ into polyhedron 16. The Weierstrass form of the general Newton polynom to polyhedron 16 is calculated in Appendix A1.

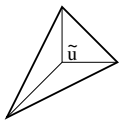

Figure 5.2.: The polyhedron 1 with the modulus $\tilde{u}$.

5.3.1. $\mathcal{O}(-K_{\mathbb{P}^2}) \to \mathbb{P}^2$

We start by providing the data of the Mori cone[5]

$$\begin{array}{c|ccc|c|} & \nu_i & & & l^{(1)} \\ D_u & 1 & 0 & 0 & -3 \\ D_1 & 1 & 1 & 0 & 1 \\ D_2 & 1 & 0 & 1 & 1 \\ D_3 & 1 & -1 & -1 & 1 \end{array} . \tag{5.3.1}$$

This gives us the invariant coordinate

$$z = \frac{a_1 a_2 a_3}{u^3} = \frac{1}{\tilde{u}^3}. \tag{5.3.2}$$

We set $a_1 = a_2 = a_3 = 1$ and denote the complex modulus by $\tilde{u}$. Note that the coordinate z is small at the large radius point, whereas the coordinate $\tilde{u}$ is small at the orbifold point. However, from the point of view of embedding the toric diagram of interest into either one of the polygons 13, 15 or 16, it more natural to use the coordinate $\tilde{u}$. As we proceed with blowing up $\mathbb{P}^2$ we will always use this coordinate and finally pass to the small coordinate $1/\tilde{u}^\alpha$ where α has to be suitably determined.

As explained above instead of starting like in [66] with (4.3.6) and eliminating X_i by (4.3.5) we solve this equations more geometrically by embedding Δ^* into polyhedra, so that the Newton polyhedron solves immediately the above constraints

$$XY^2 + YZ^2 + X^2Z + \tilde{u}XYZ = 0 \tag{5.3.3}$$

and yields the affine elliptic mirror curve $H(X, Y)$ by setting $Z = 1$. By Nagell's algorithm its Weierstrass normal form is given by

$$y^2 \;=\; x^3 + \frac{1}{12}\Big(- 24\tilde{u} - \tilde{u}^4\Big)x + \frac{1}{216}\Big(- 216 - 36\tilde{u}^3 - \tilde{u}^6\Big)\,. \tag{5.3.4}$$

It is easy to show that the period integrals $\int_\gamma \lambda$ over the meromorphic differential

$$\lambda = \log(x)\frac{dy}{y}, \tag{5.3.5}$$

which describe the closed string moduli fulfill the differential equations $i = 1, \ldots, \#$ moduli

[4] I.e. these solutions take the form of a linear combination of logarithms of the variables.
[5] The Mori cones of all two-dimensional reflexive polyhedra have been determined in [110].

$$\left(\prod_{l_k^{(i)}>0} \partial_{a_k}^{l_k^{(i)}} - \prod_{l_k^{(k)}<0} \partial_{a_k}^{-l_k^{(i)}} \right) \int_\gamma \lambda = 0 \ . \tag{5.3.6}$$

The a_i, $i = 1, \ldots, \#$ points are subject to symmetries of the geometry and can be 'gauge'-fixed to the variables z_i using $a_i \partial_{a_i} = l_i^{(k)} z_k \partial_{z_l}$. In the case at hand there is just one Picard Fuchs equation (5.3.6) which has third order

$$\mathcal{L}_{l.r.} = \theta^3 + 3z\theta(3\theta+1)(3\theta+2), \tag{5.3.7}$$

where θ denotes the logarithmic derivative $z\frac{d}{dz}$, s.t. (5.3.7) reads in terms of z

$$\mathcal{L}_{l.r.} = (1+60z)\,\partial_z + (3z+108z^2)\,\partial_z^2 + (z^2+27z^3)\,\partial_z^3. \tag{5.3.8}$$

Recall that the solutions to this differential operator give the periods at the large radius point. As already discussed above, it will often more natural to use the coordinate $\tilde{u}$, in which (5.3.8) takes the form

$$\mathcal{L}_{orb} = \tilde{u}\,\partial_{\tilde{u}} + 3\tilde{u}^2\,\partial_{\tilde{u}}^2 + \left(27+\tilde{u}^3\right)\partial_{\tilde{u}}^3. \tag{5.3.9}$$

The corresponding solutions give the periods at the orbifold point.

We end the discussion of $\mathbb{P}^2$ by writing down the prepotential up to degree 7 in Q_1, denoting $\mathrm{L}_\beta = \mathrm{Li}(Q_1^\beta)$, compare also (2.4.11)

$$F = \text{class} + 3\mathrm{L}_1 - 6\mathrm{L}_2 + 27\mathrm{L}_3 - 192\mathrm{L}_4 + 1695\mathrm{L}_5 - 17064\mathrm{L}_6 + 188454\mathrm{L}_7. \tag{5.3.10}$$

The refined invariants have already been calculated in [30] and indirectly in [108]. We list a few for reference with the blow-up cases. The connection to our solution of the $\frac{1}{2}K3$ is given by (6.4.3) and table 6.1.

5.3.2. $\mathcal{O}(-K_{F_0}) \to F_0$

With the two-parameter model given by the polyhedron 2, we discuss two perspectives of

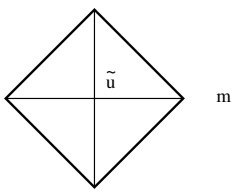

Figure 5.3.: The polyhedron 2 with the choice of the mass parameter m and the modulus $\tilde{u}$.

getting the mirror and performing the calculation of the BPS numbers. The first starts

d	$j_L \backslash j_R$	0	$\frac{1}{2}$	1	$\frac{3}{2}$	2	$\frac{5}{2}$	3	$\frac{7}{2}$	4	$\frac{9}{2}$	5	$\frac{11}{2}$	6	$\frac{13}{2}$	7	$\frac{15}{2}$	8	$\frac{17}{2}$	9	$\frac{19}{2}$	10	$\frac{21}{2}$	11	$\frac{23}{2}$	12	$\frac{25}{2}$	13	$\frac{27}{2}$
1	0			1																									
2	0					1																							
3	0							1																					
	$\frac{1}{2}$										1																		
4	0					1				1					1														
	$\frac{1}{2}$								1		1		1																
	2											1																	
	$\frac{3}{2}$															1													
5	0			1				1		1		2		2		2		1											
	$\frac{1}{2}$					1		1		2		2		3		2		1											
	1							1		1		2		2		2		1											
	$\frac{3}{2}$									1		1		2		1		1											
	2											1		1		1													
	$\frac{5}{2}$													1															
	3																	1											
6	0		1		1		3		2		6		4		8		5		7		2		2						
	$\frac{1}{2}$			1		2		3		5		6		9		9		10		7		5		1		1			
	1				1		1		3		3		7		7		11		9		9		4		2				
	$\frac{3}{2}$					1		1		3		4		7		7		10		6		4							
	2								1		1		3		4		7		6		6		2		1				
	$\frac{5}{2}$											1		1		3		3		5		3		2					
	3														1		1		3		3		3		1				
	$\frac{7}{2}$																	1		1		2		1		1			
	4																				1		1		1				
	$\frac{9}{2}$																							1					
	5																												1
d	j_L/j_R	0	$\frac{1}{2}$	1	$\frac{3}{2}$	2	$\frac{5}{2}$	3	$\frac{7}{2}$	4	$\frac{9}{2}$	5	$\frac{11}{2}$	6	$\frac{13}{2}$	7	$\frac{15}{2}$	8	$\frac{17}{2}$	9	$\frac{19}{2}$	10	$\frac{21}{2}$	11	$\frac{23}{2}$	12	$\frac{25}{2}$	13	$\frac{27}{2}$

Table 5.3.: Non-vanishing BPS numbers $N^d_{j_L,j_R}$ of local $\mathcal{O}(-3) \to \mathbb{P}^2$ up to $d = 7$.

with the Mori cone vectors, which correspond to the depicted triangulation in figure (5.3)

$$\begin{array}{c|ccc|cc} & \nu_i & & & l^{(1)} & l^{(2)} \\ D_u & 1 & 0 & 0 & -2 & -2 \\ D_1 & 1 & 1 & 0 & 1 & 0 \\ D_2 & 1 & 0 & 1 & 0 & 1 \\ D_3 & 1 & -1 & 0 & 1 & 0 \\ D_4 & 1 & 0 & -1 & 0 & 1 \end{array} . \tag{5.3.11}$$

Following (4.3.6) and eliminating coordinates by (4.3.5) and the $\mathbb{C}^*$-action on the Y_i we write the mirror curve in the remaining coordinates x, y as

$$H(x,y) = 1 + x + \frac{z_1}{x} + y + \frac{z_2}{y} = 0 \ , \tag{5.3.12}$$

where the z_i are defined as in (4.3.5). The Picard Fuchs equations (5.3.6) become in the case at hand with $\theta_i := z_i \frac{d}{dz_i}$

$$\begin{aligned} \mathcal{L}^{(1)} = &\quad \theta_1^2 - 2(\theta_1+\theta_2-1)(2\theta_1+2\theta_2-1)z_1 \\ \mathcal{L}^{(2)} = &\quad \theta_2^2 - 2(\theta_1+\theta_2-1)(2\theta_1+2\theta_2-1)z_2 \ . \end{aligned} \tag{5.3.13}$$

Let us come to the discussion of the mass parameter. To make contact with the latter one finds that at $z_i = 0$ one has a constant solution and two solutions, which are linear in $\log(z_i)$ and one solution, which is quadratic in $\log(z_i)$. As the two linear logarithmic solutions one finds $t_1 = \log(z_1) + \Sigma(z_1, z_2)$ and $t_2 = \log(z_2) + \Sigma(z_1, z_2)$ determining the Kähler parameters of the $\mathbb{P}^1$'s. Here $\Sigma(z_1, z_2)$ is the same holomorphic transcendental function. This suggests to change variables and introduce $z = z_1$ and $M = \log(z_1) - \log(z_2)$. The latter is a trivial solution. This is expected, as for a general Riemann surface the number of A- and B-cycles corresponds to the number of non-trivial logarithmic respectively double logarithmic solutions. Therefore we expect to find in all considered examples only one non-trivial logarithmic solution, while the other ones will have an interpretation as deformation parameters. In fact, we can be a bit more precise with the example at hand. Denote by C_1 and C_2 the two classes of $\mathbb{P}^1$'s respectively and by D the class of $\mathbb{P}^1 \times \mathbb{P}^1$ which corresponds to the double logarithmic solution. It is easy to check from the data of the Mori cone that

$$\#(C_1 \cap D) = -2 = \#(C_2 \cap D). \tag{5.3.14}$$

Therefore the class $C_1 - C_2$ has no compact dual as it has no intersection with D.

We now consider the differential left ideal generated by (5.3.13) up to homogeneous degree three in differentiations w.r.t. z and M. In this ideal one can eliminate all differential operators involving derivatives w.r.t. M and end up with a third order differential operator in z determining all non-trivial solutions of (5.3.13)

$$\begin{aligned} \mathcal{L} = &\quad \left(60\,(m-1)^2\,z^2 - 18\,(m+1)\,z + 1\right)\partial_z + z\left(80(m-1)^2z^2 - 32(m+1)z + 3\right)\partial_z^2 + \\ &\quad z^2\left(16(m-1)^2z^2 - 8(m+1)z + 1\right)\partial_z^3 \,. \end{aligned} \tag{5.3.15}$$

Here we understand $m = e^M$ now as a deformation parameter. Setting $m = 1$ imposes an identification of the complexified Kähler parameters $t_1 = t_2$ globally in the quantum moduli space. This leads to the diagonal model with $S = \mathbb{P}^1 \times \mathbb{P}^1$ as base, discussed in section (A.4.1). In particular (5.3.15) restricts for $m = 1$ to (5.2.1) with the appropriate parameters $c_0 = 16$ and $a_1 = \frac{1}{2}, a_2 = \frac{1}{2}$.

Instead of computing the mirror curve case by case via the $l^{(k)}$ vectors, the elliptic mirror curve is simply associated to the reflexive polyhedron as its Newton polynom, i.e. the coordinates of the points determine its positive exponents. In Appendix A we provide the Newton polynom of the biggest polyhedra so that all polyhedra can be embedded in at least one of them and provide the Weierstrass form for them. In this approach it is only necessary to specialize the general Weierstrass forms and to eventually rescale the $g_i \to g_i \lambda^i$ to ensure that the closed string period (3.4.4) has the right leading behavior. Note that according to the l vectors the right choice of large complex structure coordinates we get from (4.3.5) is

$$z_1 = \frac{m}{\tilde{u}^2} \quad z_2 = \frac{1}{\tilde{u}^2} \tag{5.3.16}$$

so that it is immediately clear that $z_1/z_2 = m$ and $\tilde{u} \to \infty$ is the large radius point.

In the $\mathbb{P}^1 \times \mathbb{P}^1$ case we can use the polytop for the cubic or the bi-quartic, the choice does not matter. Let us re-define $u = \frac{1}{\tilde{u}^2} = z_2$. Then we get

$$\begin{aligned} g_2 = &\quad 27u^4\left(16u^4\left(m^2-m+1\right)-8u^2(m+1)+1\right), \\ g_3 = &\quad -27u^6(-1+12(1+m)u^2-24(2+m+2m^2)u^4+32(2-3m-3m^2+2m^3)u^6)\ . \end{aligned} \tag{5.3.17}$$

This yields a j-invariant

$$j = \frac{\left(16\left(m^2-m+1\right)\tilde{u}^2-8(m+1)\tilde{u}+1\right)^3}{m^2\tilde{u}^4\left(16(m-1)^2\tilde{u}^2-8(m+1)\tilde{u}+1\right)}\ . \tag{5.3.18}$$

At the large radius we require $t(u,\underline{m}) = \log(u) + \mathcal{O}(u,\underline{m})$ and near the single zeros of Δ, $t_c(u,\underline{m}) = z_c(u,\underline{m}) + \mathcal{O}(z_c^2(u,\underline{m}))$, which fixes the scaling (3.4.5). We have calculated $F^{(n,g)}$ at the conifold to impose the gap condition. Other interesting limits are the Seiberg-Witten limit

$$z_1 \to \frac{1}{4}\exp(-4\epsilon^2 u), \quad z_2 \to \epsilon^4\Lambda^4 \tag{5.3.19}$$

in which

$$j = \frac{(3\Lambda^4-4u^2)^3}{27\Lambda^8(\Lambda^4-u^2)} \tag{5.3.20}$$

becomes the j-function of the massless $SU(2)$ Seiberg-Witten curve compare (5.4.1) and the Chern-Simons limit discussed for the refined case in [27].

We define a single-valued variable near the large radius as

$$Q_t = e^t = u + \mathcal{O}(u^2,\underline{m})\ , \tag{5.3.21}$$

which is easily inverted to $u(Q_f)$. From Kähler parameters of the two $\mathbb{P}^1$'s we define $Q_i = e^{t_i}$ and get the relation $Q_t = Q_2$ and $m = Q_1/Q_2$, which allows us to obtain for all expressions defined in section 3.4 the large radius expansion in terms of Q_i. The coefficients in (3.4.8,3.3.10) are given by $a_0 = 7, a_1 = \frac{7}{2}, b_0 = -2$ and $b_1 = -1$.

We have calculated the spin invariants and found the following series

$$N^{(1,d)}_{j_L,j_R} = \begin{cases} 1 & \text{if } \ j_L = 0, j_R = \frac{1}{2}+d \\ 0 & \text{otherwise} \end{cases} \tag{5.3.22}$$

Up to $d_1 + d_2 \leq 7$ the refined invariants are reported in Table 5.4.

5.3.3. $\mathcal{O}(-K_{\mathcal{B}_1}) \to \mathcal{B}_1$

The Mori cone is given by

	ν_i			$l^{(1)} = l^{(f)}$	$l^{(2)} = l^{(b)}$
D_u	1	0	0	−2	−1
D_1	1	1	0	1	0
D_2	1	0	1	0	1
D_3	1	−1	0	1	−1
D_4	1	−1	−1	0	1

. (5.3.23)

(d_1,d_2)	$j_L \backslash j_R$	0	$\frac{1}{2}$	1	$\frac{3}{2}$	2	$\frac{5}{2}$	3	$\frac{7}{2}$	4	$\frac{9}{2}$	5	$\frac{11}{2}$	6	$\frac{13}{2}$	7	$\frac{15}{2}$	8	$\frac{17}{2}$	9	$\frac{19}{2}$
$(2,2)$	0			1		1															
	$\frac{1}{2}$							1													
$(2,3)$	0			1		1		2													
	$\frac{1}{2}$							1		1											
	1											1									
$(2,4)$	0			1		1		2		2											
	$\frac{1}{2}$							1		1		2									
	1											1		1							
	$\frac{3}{2}$															1					
$(2,5)$	0			1		1		2		2		3									
	$\frac{1}{2}$							1		1		2		2							
	1											1		1		2					
	$\frac{3}{2}$															1		1			
	2																			1	
$(3,3)$	0			1		1		3		3		4									
	$\frac{1}{2}$					1		2		3		3		1							
	1							1		2		3									
	$\frac{3}{2}$									1		1									
	2													1							
$(3,4)$	0	1		1		3		4		7		6		7		1		1			
	$\frac{1}{2}$					1		2		4		6		8		2					
	1					1		2		5		6		7		1					
	$\frac{3}{2}$									1		2		4		1					
	2									1		2		3							
	$\frac{5}{2}$											1		1							
	3																	1			

Table 5.4.: Non-vanishing BPS numbers $N_{j_L,j_R}^{(d_1,d_2)}$ of local $\mathcal{O}(-2,-2) \to \mathbb{P}^1 \times \mathbb{P}^1$.

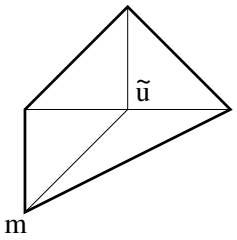

Figure 5.4.: The polyhedron 3 with the choice of the mass parameter m_1 and the modulus $\tilde{u}$.

The invariant coordinates are

$$z_1 = \frac{m}{\tilde{u}^2}, \quad z_2 = \frac{1}{\tilde{u}m}. \tag{5.3.24}$$

In our choice for the mass parameter we obtain from the embedding

$$XY^2 + YZ^2 + X^2Z + \tilde{u}XYZ + mXZ^2 = 0 \tag{5.3.25}$$

and its Weierstrass normal form is given by

$$\begin{aligned} y^2 &= x^3 + \frac{1}{12}\Big(-24\tilde{u} - \tilde{u}^4 + 8\tilde{u}^2 m - 16m^2\Big)x \\ &\quad + \frac{1}{216}\Big(-216 - 36\tilde{u}^3 - \tilde{u}^6 + 144\tilde{u}m + 12\tilde{u}^4 m - 48\tilde{u}^2 m^2 + 64m^3\Big)\,. \end{aligned} \tag{5.3.26}$$

As in the $\mathbb{P}^1 \times \mathbb{P}^1$ case, there is a trivial solution to the Picard Fuchs equation that reads

$$\varphi_1 = \log(z_1) - 2\log(z_2) = 3\log(m). \tag{5.3.27}$$

The third order differential operator is given in the case at hand as

$$\begin{aligned} \mathcal{L} &= (-12m^2 + 9\tilde{u} - 18m\tilde{u}^2 + 8m^2\tilde{u}^3)\partial_{\tilde{u}} + (-108m - 128m^4 + 144m^2\tilde{u} + 27\tilde{u}^2 \\ &\quad -64m^3\tilde{u}^2 - 52m\tilde{u}^3 + 24m^2\tilde{u}^4)\partial_{\tilde{u}}^2 + (-9 + 8m\tilde{u})(-27 + 16m^3 + 36m\tilde{u} \\ &\quad -8m^2\tilde{u}^2 - \tilde{u}^3 + m\tilde{u}^4)\partial_{\tilde{u}}^3\,. \end{aligned} \tag{5.3.28}$$

We followed the same logic as in the previous section to get the large radius expansion and obtain the spin invariants. Note that this equation reduces to the one for the $\mathbb{P}^2$ base in the blow-down limit $m = 0$. We note that the discriminant reads

$$\Delta = 1 - \tilde{u} - 8m_1\tilde{u}^2 + 36m_1\tilde{u}^3 - m_1(27 - 16m_1)\tilde{u}^4\,. \tag{5.3.29}$$

The prepotential is given as

$$\begin{aligned} F = \ & \text{class} + \mathrm{L}_{0,1} - 2\mathrm{L}_{1,0} + 3\mathrm{L}_{1,1} + 5\mathrm{L}_{2,1} - 6\mathrm{L}_{2,2} + 7\mathrm{L}_{3,1} - 32\mathrm{L}_{3,2} + 27\mathrm{L}_{3,3} + 9\mathrm{L}_{4,1} \\ & -110\mathrm{L}_{4,2} + 286\mathrm{L}_{4,3} - 192\mathrm{L}_{4,4} + 11\mathrm{L}_{5,1} - 288\mathrm{L}_{5,2} + 1651\mathrm{L}_{5,3} - 3038\mathrm{L}_{5,4} + 1695\mathrm{L}_{5,5} \\ & +13\mathrm{L}_{6,1} - 644\mathrm{L}_{6,2} + 6885\mathrm{L}_{6,3} - 25216\mathrm{L}_{6,4} + 35870\mathrm{L}_{6,5} - 17064\mathrm{L}_{6,6}\,. \end{aligned} \tag{5.3.30}$$

Again we have denoted $L_\beta = \mathrm{Li}_3(Q^\beta)$. Generally $N_{j_L,j_R}^{d_1,d_2} = 0$ for $d_1 < d_2$ and again there is an infinite series of spin invariants that can be given in a closed form [108]

$$N_{j_L,j_R}^{(d,1)} = \begin{cases} 1 & \text{if } \ j_L = 0, j_R = d \\ 0 & \text{otherwise} \end{cases}\,. \tag{5.3.31}$$

Up to $d_1 + d_2 \leq 7$ the refined invariants are reported in Table 5.5.

The Seiberg-Witten limit for $\mathbb{F}_1$ is

$$z_1 \to \frac{1}{4}\exp(-2\sqrt{2}\epsilon^2\tilde{u}), \quad z_2 \to \epsilon^4\Lambda^4\,. \tag{5.3.32}$$

5.3.4. $\mathcal{O}(-K_{F_2}) \to F_2$

We consider the two-parameter model given by the polyhedron 2 with the Mori cone vectors,

(d_1,d_2)	$j_L \backslash j_R$	0	$\frac{1}{2}$	1	$\frac{3}{2}$	2	$\frac{5}{2}$	3	$\frac{7}{2}$	4	$\frac{9}{2}$	5	$\frac{11}{2}$	6	$\frac{13}{2}$	7	$\frac{15}{2}$	8	$\frac{17}{2}$	9	$\frac{19}{2}$
$(2,2)$	0			1																	
$(3,2)$	0			1		1															
	$\frac{1}{2}$					1															
$(4,2)$	0			1		1		2													
	$\frac{1}{2}$					1		1		1											
	1									1											
$(5,2)$	0			1		1		2		2											
	$\frac{1}{2}$					1		1		2											
	1							1		1											
	$\frac{3}{2}$									1											
$(4,3)$	0		1		1		2		1		1										
	$\frac{1}{2}$				1		2		2		1										
	1						1		1												
	$\frac{3}{2}$								1		1										
$(5,3)$	0	1		1		3		3		5		3		2							
	$\frac{1}{2}$			1		2		4		5		5		1							
	1				1		2		4		3		1								
	$\frac{3}{2}$					1		2		3		1									
	2						1		1												
	$\frac{5}{2}$											1									

Table 5.5.: Non vanishing BPS numbers $N^{(d_1,d_2)}_{j_L,j_R}$ of local $\mathcal{O}(-2,-1) \to \mathbb{F}_1$.

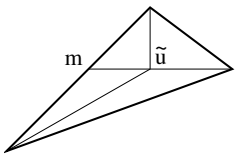

Figure 5.5.: The polyhedron 4 with the choice of the mass parameter m and the modulus $\tilde{u}$.

which correspond to the depicted triangulation

$$\left|\begin{array}{cccc|cc} & \nu_i & & & l^{(1)}=l^{(f)} & l^{(2)}=l^{(b)} \\ D_u & 1 & 0 & 0 & -2 & 0 \\ D_1 & 1 & 1 & 0 & 1 & 0 \\ D_2 & 1 & 0 & 1 & 0 & 1 \\ D_3 & 1 & -1 & 0 & 1 & -2 \\ D_4 & 1 & -2 & -1 & 0 & 1 \end{array}\right| . \tag{5.3.33}$$

Here we observe a new phenomenon namely a point on the edge, which corresponds to an almost Fano surface. The large structure coordinates are

$$z_1 = \frac{m}{\tilde{u}^2}, \qquad z_2 = \frac{1}{m^2} \ . \tag{5.3.34}$$

We cannot take simply a ratio between the two coordinates to get the non-dynamical pa-

rameter m. Let us define as before $u = \frac{1}{\tilde{u}^2}$, then we find by specialization of (A.1.10) for the appropriate rescaled g_i

$$\begin{aligned} g_2 = &\quad 27u^4\left((1-4mu)^2 - 48u^2\right), \\ g_3 = &\quad -27u^6\left(64m^3u^3 - 48m^2u^2 - 288mu^3 + 12mu + 72u^2 - 1\right) \ , \end{aligned} \tag{5.3.35}$$

which defines t_f. Let us denote the Kähler parameter of the base t_2 and the one of the fiber by t_1. As usual we also denote $Q_1 = e^{t_1}$ and $Q_2 = e^{t_2}$. Then we find

$$t_f = Q_1^{\frac{1}{2}} Q_2, \quad m = \frac{1+Q_2}{Q_2^{\frac{1}{2}}} \ . \tag{5.3.36}$$

So typically for the almost del Pezzo surfaces we find one transcendental mirror map $u(t_f)$ involving an elliptic integral and rational mirror maps for the mass parameters on the edges. The latter fact is simply due to the fact that the geometry on the edges is a rational geometry involving only Hirzebruch sphere trees of resolved ADE singularities. In fact in the toric case just A_n-singularities. One way to obtain the rational mirror map is to solve the Picard-Fuchs equations explicitly, see for this specific example also [176].

Now remarkably the spin invariants $N^{\beta}_{j_l,j_r}$ are the same however with a shift [101] in the classes so that $N^{d_f,d_b}_{j_l,j_r}(F_2) = N^{d_f-d_b,d_b}_{j_l,j_r}(F_0)$ and $N^{d_f,d_b}_{j_l,j_r}(F_2) = 0$ for $d_f < d_b$.

The Seiberg-Witten limit for F_2 is

$$z_1 \to \frac{1}{4}\exp(-2\epsilon^2\tilde{u}), \quad z_2 \to \epsilon^4\Lambda^4 \ . \tag{5.3.37}$$

5.3.5. $\mathcal{O}(-K_{\mathcal{B}_2}) \to \mathcal{B}_2$

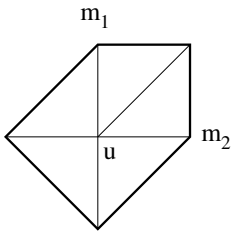

Figure 5.6.: The polyhedron 5 with the choice of the mass parameter m_1, m_2 and the modulus $\tilde{u}$.

The Mori cone is given by

	ν_i			$l^{(1)}$	$l^{(2)}$	$l^{(3)}$
D_u	1	0	0	−1	−1	−1
D_1	1	1	0	−1	1	0
D_2	1	1	1	1	−1	1
D_3	1	0	1	0	1	−1
D_4	1	−1	0	0	0	1
D_5	1	0	−1	1	0	0

. (5.3.38)

The invariant coordinates are given by

$$z_1 = \frac{m_1 m_2}{\tilde{u}}, \quad z_2 = \frac{1}{\tilde{u} m_2}, \quad z_3 = \frac{m_2}{\tilde{u}^2}. \tag{5.3.39}$$

The mirror curve reads

$$XY^2 + YZ^2 + X^2 Z + \tilde{u} XYZ + m_1 XZ^2 + m_2 X^2 Y = 0 \tag{5.3.40}$$

and the Weierstrass normal form is given by

$$\begin{aligned} y^2 \;=\; & x^3 + \frac{1}{12}\Big(-24\tilde{u} - \tilde{u}^4 + 8\tilde{u}^2 m_1 - 16 m_1^2 + 8\tilde{u}^2 m_2 + 16 m_1 m_2 - 16 m_2^2 \Big) x \\ & + \frac{1}{216}\Big(-216 - 36\tilde{u}^3 - \tilde{u}^6 + 144\tilde{u} m_1 + 12\tilde{u}^4 m_1 - 48\tilde{u}^2 m_1^2 + 64 m_1^3 + 144\tilde{u} m_2 \\ & + 12\tilde{u}^4 m_2 - 24\tilde{u}^2 m_1 m_2 - 96 m_1^2 m_2 - 48\tilde{u}^2 m_2^2 - 96 m_1 m_2^2 + 64 m_2^3 \Big). \end{aligned} \tag{5.3.41}$$

Also in this case a third order differential operator can be constructed. Note however, that in order to derive it one needs to take into account five l vectors out of which only three are linearly independent in order to make the ideal of differential operators close. This is due to the fact that linear dependent relations can give rise to further linear independent differential operators. The full differential operator may be found in appendix A.2.

Denoting as usual $L_\beta = \mathrm{Li}_3(Q^\beta)$, the prepotential is given as

$$\begin{aligned} F = \; & \text{class} + \mathrm{L}_{0,0,1} + \mathrm{L}_{0,1,0} - 2\mathrm{L}_{0,1,1} + 3\mathrm{L}_{1,1,1} - 4\mathrm{L}_{1,2,1} + 5\mathrm{L}_{1,2,2} - 6\mathrm{L}_{1,3,2} \\ & + 7\mathrm{L}_{1,3,3} - 8\mathrm{L}_{1,4,3} + 9\mathrm{L}_{1,4,4} - 6\mathrm{L}_{2,2,2} + 35\mathrm{L}_{2,3,2} - 32\mathrm{L}_{2,3,3} - 32\mathrm{L}_{2,4,2} \\ & + 135\mathrm{L}_{2,4,3} - 110\mathrm{L}_{2,4,4} + 27\mathrm{L}_{3,3,3} - 400\mathrm{L}_{3,4,3} + 286\mathrm{L}_{3,4,4} - 192\mathrm{L}_{4,4,4}\,. \end{aligned} \tag{5.3.42}$$

Note that there is a symmetry between the first and the third entry, so that we have omitted redundant terms.

5.3.6. $\mathcal{O}(-K_{\mathcal{B}_3}) \to \mathcal{B}_3$

This is the maximal still generic toric blow-up of $\mathbb{P}^2$ and is represented by the polyhedron 7. The Mori cone vectors, which correspond to the depicted triangulation are given below

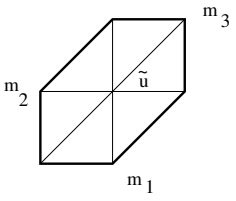

Figure 5.7.: The polyhedron 7 with the choice of the mass parameters m_1, m_2, m_3 and the modulus $\tilde{u}$.

$$\begin{array}{c|ccc|cccccc|} & \nu_i & & & l^{(1)} & l^{(2)} & l^{(3)} & l^{(4)} & l^{(5)} & l^{(6)} \\ D_u & 1 & 0 & 0 & -1 & -1 & -1 & -1 & -1 & -1 \\ D_1 & 1 & 1 & 0 & -1 & 1 & 0 & 0 & 0 & 1 \\ D_2 & 1 & 1 & 1 & 1 & -1 & 1 & 0 & 0 & 0 \\ D_3 & 1 & 0 & 1 & 0 & 1 & -1 & 1 & 0 & 0 \\ D_4 & 1 & -1 & 0 & 0 & 0 & 1 & -1 & 1 & 0 \\ \mathrm{D}_5 & 1 & -1 & -1 & 0 & 0 & 0 & 1 & -1 & 1 \\ D_6 & 1 & 0 & -1 & 1 & 0 & 0 & 0 & 1 & -1 \end{array} . \tag{5.3.43}$$

One finds the mirror curve

$$XY^2 + YZ^2 + X^2Z + \tilde{u}XYZ + m_1XZ^2 + m_2X^2Y + m_3Y^2Z = 0 \tag{5.3.44}$$

and the Weierstrass normal form

$$\begin{aligned} y^2 \;=\;& 4x^3 + \frac{1}{12}\Big(-16m_1^2 + 16m_1m_2 - 16m_2^2 + 16m_1m_3 + 16m_2m_3 - 16m_3^2 - 24\tilde{u} \\ & -24m_1m_2m_3\tilde{u} + 8m_1\tilde{u}^2 + 8m_2\tilde{u}^2 + 8m_3\tilde{u}^2 - \tilde{u}^4\Big) \\ & + \frac{1}{216}\Big(-216 + 64m_1^3 - 96m_1^2m_2 - 96m_1m_2^2 + 64m_2^3 - 96m_1^2m_3 - 48m_1m_2m_3 \\ & -96m_2^2m_3 - 96m_1m_3^2 - 96m_2m_3^2 - 216m_1^2m_2^2m_3^2 + 64m_3^3 + 144m_1\tilde{u} + 144m_2\tilde{u} \\ & +144m_3\tilde{u} + 144m_1^2m_2m_3\tilde{u} + 144m_1m_2^2m_3\tilde{u} + 144m_1m_2m_3^2\tilde{u} - 48m_1^2\tilde{u}^2 \\ & -24m_1m_2\tilde{u}^2 - 48m_2^2\tilde{u}^2 - 24m_1m_3\tilde{u}^2 - 24m_2m_3\tilde{u}^2 - 48m_3^2\tilde{u}^2 - 36\tilde{u}^3 \\ & -36m_1m_2m_3\tilde{u}^3 + 12m_1\tilde{u}^4 + 12m_2\tilde{u}^4 + 12m_3\tilde{u}^4 - \tilde{u}^6\Big) . \end{aligned} \tag{5.3.45}$$

In this case the Mori cone is not simplicial, but we will find a choice of these vectors, which truncates in the correct way to all possibilities of embedding all lower blow up cases into this model. This is only possible by using one non-integer combination of the Mori vectors $\tilde{l}^{(1)} = \frac{1}{3}\sum_{i=0}^{2}(l^{(2i+1)} - l^{(2i+2)})$ as well as $\tilde{l}^{(2)} = l^{(2)}$, $\tilde{l}^{(3)} = l^{(4)}$ and $\tilde{l}^{(4)} = l^{(6)}$. The corresponding large complex structure variables are

$$z_1 = m_1m_2m_3,\ z_2 = \frac{1}{m_1\tilde{u}},\ z_3 = \frac{1}{m_2\tilde{u}},\ z_4 = \frac{1}{m_3\tilde{u}} . \tag{5.3.46}$$

We can also calculate the ring of intersection numbers for the choice of basis of curves defined by $\tilde{l}^{(i)}$ and the dual divisors J_i as

$$R = J_1^2 + J_1J_2 + J_1J_3 + J_2J_3 + J_1J_4 + J_2J_4 + J_3J_4. \tag{5.3.47}$$

With this informations the instantons can be calculated following [101]. Alternatively, we can specialize either polyhedron 15 or 16, redefine $\tilde{u} \to u = 1/\tilde{u}$ and rescale $g_i \to \lambda^i g_i$ with $\lambda = 18u^4$. Then we obtain the mirror map (3.4.4) as

$$u = Q_t + (1 + m_1)Q_t^3 + 2m_3Q_t^4 + (1 - m_1 + m_1^2 - 3m_2)Q_t^5 + \mathcal{O}(Q_t^6) . \tag{5.3.48}$$

Here we have defined $Q_t = e^t = (Q_1Q_2Q_3Q_4)^{\frac{1}{3}}$. It follows from (5.3.46) that

$$m_1 = \frac{(Q_1Q_3Q_4)^{\frac{1}{3}}}{Q_2^{\frac{2}{3}}}, \quad m_2 = \frac{(Q_1Q_3Q_4)^{\frac{1}{3}}}{Q_3^{\frac{2}{3}}}, \quad m_3 = \frac{(Q_1Q_2Q_3)^{\frac{1}{3}}}{Q_4^{\frac{2}{3}}}. \tag{5.3.49}$$

This defines the large radius variables and allows to extract the BPS-numbers directly from the curve. For example we list here the prepotential up to multi-degree 16 in the instantons. With the notation $L_\beta = \mathrm{Li}_3(Q^\beta)$ we get

$$\begin{aligned} F = \quad & \text{class} + \mathrm{L}_{0,0,0,1} + \mathrm{L}_{1,0,0,1} - 2\mathrm{L}_{1,0,1,1} + 3\mathrm{L}_{1,1,1,1} + 3\mathrm{L}_{2,1,1,1} - 4\mathrm{L}_{2,1,1,2} + 5\mathrm{L}_{2,1,2,2} \\ & -6\mathrm{L}_{2,2,2,2} + 5\mathrm{L}_{3,1,2,2} - 6\mathrm{L}_{3,1,2,3} + 7\mathrm{L}_{3,1,3,3} - 36\mathrm{L}_{3,2,2,2} + 35\mathrm{L}_{3,2,2,3} - 32\mathrm{L}_{3,2,3,3} \\ & +27\mathrm{L}_{3,3,3,3} + 7\mathrm{L}_{4,1,3,3} - 8\mathrm{L}_{4,1,3,4} + 9\mathrm{L}_{4,1,4,4} - 6\mathrm{L}_{4,2,2,2} + 35\mathrm{L}_{4,2,2,3} - 32\mathrm{L}_{4,2,2,4} \\ & -160\mathrm{L}_{4,2,3,3} + 135\mathrm{L}_{4,2,3,4} - 110\mathrm{L}_{4,2,4,4} + 531\mathrm{L}_{4,3,3,3} - 400\mathrm{L}_{4,3,3,4} + 286\mathrm{L}_{4,3,4,4} \\ & -192\mathrm{L}_{4,4,4,4} \ . \end{aligned} \tag{5.3.50}$$

Note that there is a symmetry in the last three entries, so that we present only the β, which are ordered w.r.t these entries.

5.4. Almost del Pezzo surfaces

In this section we discuss some toric almost des Pezzo surfaces which correspond to blow-ups of the F_2 geometry and can be embedded into polyhedron 16. They are physically interesting as they correspond to the five-dimensional $SU(2)$ Seiberg-Witten theories with $N_f = 0, 1, 2, 3, 4$ matter multiplets in the fundamental representation. The Seiberg Witten curves with $N_f < 3$ are given by, see e.g. [77] (also for the $N_f = 4$ case)

$$y^2 = (x^2 - u^{sw})^2 - \Lambda^{4-N_f} \prod_{i=0}^{N_f} (x + m_i^{sw}) \ . \tag{5.4.1}$$

Four-dimensional Seiberg-Witten theory corresponds to the limit $R = \frac{1}{\epsilon} \to \infty$. The geometry $\mathcal{O}(-K_{F_2}) \to F_2$ corresponds to one of the five-dimensional realizations of the $SU(2)$ Seiberg-Witten theory with $N_f = 0$. Its limit in the moduli space of complex structure moduli was already given in (5.3.37).

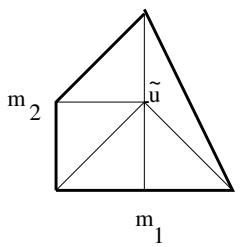

Figure 5.8.: The polyhedron 6 with the choice of the mass parameters m_1, m_2 and the modulus $\tilde{u}$.

The Mori cone vectors for this model are

$$\begin{array}{c|ccc|ccc|} & \nu_i & & & l^{(1)} & l^{(2)} & l^{(3)} \\ D_u & 1 & 0 & 0 & -1 & -1 & 0 \\ D_1 & 1 & 1 & -1 & 0 & 0 & 1 \\ D_2 & 1 & 0 & 1 & 1 & 0 & 1 \\ D_3 & 1 & -1 & 0 & -1 & 1 & 0 \\ D_4 & 1 & -1 & -1 & 1 & -1 & 1 \\ \mathrm{D}_5 & 1 & 0 & -1 & 0 & 1 & -2 \\ \end{array} \,. \tag{5.4.2}$$

From this we get the large volume variables

$$z_1 = \frac{1}{\tilde{u} m_2}, \quad z_2 = \frac{m_1 m_2}{\tilde{u}}, \quad z_3 = \frac{1}{m_1^2}\,. \tag{5.4.3}$$

In this case we define $Q_t = Q_1^{\frac{1}{2}} Q_2 Q_3^{\frac{1}{4}}$, so that the transcendental mirror map is

$$u = Q_t - m_1 Q_t^3 + 2 m_2 Q_t^4 + (-3 + m_1^2) Q_t^5 + \mathcal{O}(Q_t^7)\,. \tag{5.4.4}$$

The rational mirror maps are

$$\frac{z_1}{z_2} = \frac{Q_1}{(1+Q_3)Q_2}, \quad z_3 = \frac{Q_3}{(1+Q_3)^2}\ . \tag{5.4.5}$$

The Seiberg-Witten limit is given by

$$z_1 = \left(\exp 2^{\frac{2}{3}} m_1^{sw} \epsilon\right), \quad z_2 = \frac{1}{2}\exp\left(-2^{\frac{2}{3}}\epsilon(2^{\frac{2}{3}}\epsilon u^{sw} + m_1^{sw})\right), \quad z_3 = \Lambda^3 \epsilon^3\ . \tag{5.4.6}$$

The first rational Gromov-Witten invariants follow then from a suitable specialization of the biquartic curve (A.1.22) as

$$\begin{aligned} F = \ & \text{class} + L_{1,0,0} + L_{0,1,0} - 2L_{1,1,0} + L_{0,1,1} - 2L_{1,1,1} + 3L_{1,2,1} - 4L_{2,2,1} + 5L_{2,3,1} \\ & -6L_{3,3,1} + 7L_{3,4,1} - 8L_{4,4,1} + 9L_{4,5,1} - 10L_{5,5,1} + 11L_{5,6,1} - 12L_{6,6,1} + 13L_{6,7,1} \\ & +5L_{2,3,2} - 6L_{3,3,2} - 6L_{2,4,2} + 35L_{3,4,2} - 32L_{4,4,2} - 32L_{3,5,2} + 135L_{4,5,2} \\ & -110L_{5,5,2} - 110L_{4,6,2} + 385L_{5,6,2} - 288L_{6,6,2} - 288L_{5,7,2} + 7L_{3,4,3} - 8L_{4,4,3} \\ & -32L_{3,5,3} + 135L_{4,5,3} - 110L_{5,5,3} + 27L_{3,6,3} - 400L_{4,6,3} + 1100L_{5,6,3} + 286L_{4,7,3} \\ & +9L_{4,5,4} - 10L_{5,5,4} - 110L_{4,6,4}. \end{aligned} \tag{5.4.7}$$

Next we blow it up once more to get a model with three masses. The new feature we

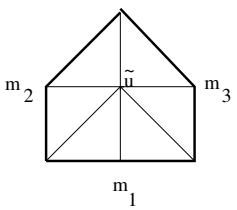

Figure 5.9.: The polyhedron 9 with the choice of the mass parameters m_1, m_2, m_3 and the modulus $\tilde{u}$.

want to discuss here is a non-simplicial Mori cone in a model with rational mirror maps

$$\begin{array}{c|ccc|ccccc|} & \nu_i & & & l^{(1)} & l^{(2)} & l^{(3)} & l^{(4)} & l^{(5)} \\ D_u & 1 & 0 & 0 & -1 & -1 & 0 & -1 & -1 \\ D_1 & 1 & 1 & -1 & 0 & 0 & 1 & -1 & 1 \\ D_2 & 1 & 0 & 1 & 1 & 0 & 1 & 0 & 1 \\ D_3 & 1 & -1 & 0 & -1 & 1 & 0 & 0 & 0 \\ D_4 & 1 & -1 & -1 & 1 & -1 & 1 & 0 & 0 \\ \mathrm{D}_5 & 1 & 0 & -1 & 0 & 1 & -2 & 1 & 0 \\ D_6 & 1 & 1 & 0 & 0 & 0 & 0 & 1 & -1 \\ \end{array} \quad . \tag{5.4.8}$$

The four large volume coordinates are redundantly given by

$$z_1 = \frac{1}{\tilde{u} m_2}, \quad z_2 = \frac{m_1 m_2}{\tilde{u}}, \quad z_3 = \frac{1}{\tilde{u}}, \quad z_4 = \frac{m_1 m_3}{\tilde{u}}, \quad z_5 = \frac{1}{\tilde{u} m_3} \ . \tag{5.4.9}$$

These coordinates fulfill the following non-trivial mirror maps $Q_t = (Q_1 Q_2 Q_3 Q_4 Q_5)^{\frac{1}{4}}$ and

$$z_3 = \frac{Q_3}{(1+Q_3)^2}, \quad \frac{z_1}{z_2} = \frac{Q_1}{Q_2(1+Q_3)}, \quad \frac{z_5}{z_1} = \frac{Q_5}{Q_4(1+Q_3)}, \quad Q_1 Q_2 = z_1 z_2 = z_4 z_5 = Q_4 Q_5 \ . \tag{5.4.10}$$

To extract the Gromov-Witten invariants from the specialized curve (A.1.22) we can solve the masses m_1, m_2, m_3 as well as Q_t either for Q_1, Q_2, Q_3, Q_4 or Q_2, Q_3, Q_4, Q_5, which corresponds to two chambers of the non-simplicial Kähler cone, which are symmetric under the exchange of $Q_1 Q_2 \leftrightarrow Q_4 Q_5$ and moreover specialize for $Q_4 = Q_5 = 0$ to the previously discussed model. In view of the symmetry we list only the invariants for Q_1, Q_2, Q_3, Q_4

$$\begin{aligned} F = \ & \text{class} + L_{0,0,0,1} + L_{0,0,1,1} + L_{0,1,0,0} + L_{0,1,1,0} - 2L_{0,1,1,1} + L_{1,0,0,0} - 2L_{1,1,0,0} \\ & -2L_{1,1,1,0} + 3L_{1,1,1,1} + 3L_{1,2,1,0} - 4L_{1,2,1,1} - 4L_{1,2,2,1} + 5L_{1,2,2,2} + 5L_{1,3,2,1} \\ & -6L_{1,3,2,2} - 4L_{2,2,1,0} + 5L_{2,2,1,1} + 5L_{2,2,2,1} - 6L_{2,2,2,2} + 5L_{2,3,1,0} - 6L_{2,3,1,1} \\ & +5L_{2,3,2,0} - 36L_{2,3,2,1} - 6L_{2,4,2,0} - 6L_{3,3,1,0} + 7L_{3,3,1,1} - 6L_{3,3,2,0} + 7L_{3,4,1,0} \end{aligned} \quad . \tag{5.4.11}$$

Again it is quite interesting to know the Seiberg-Witten limit. We define $z_f = z_1 z_2$ and obtain

$$z_1 = \frac{1}{2}\exp(-2\epsilon m_1^{sw}), \quad z_f = \frac{1}{4}\exp(-4\epsilon^2 u^{sw}), \quad z_3 = \Lambda^2\epsilon^2, \quad z_4 = \frac{1}{2}\exp(2\epsilon m_2^{sw}) \ . \tag{5.4.12}$$

We finally discuss a model with a simplicial Mori cone, which can be symmetrized like in the last case to the full D_5 del Pezzo.

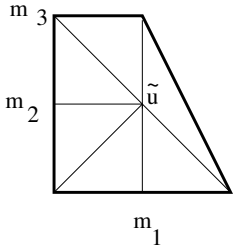

Figure 5.10.: The polyhedron 8 with the choice of the mass parameters m_1, m_2, m_3 and the modulus $\tilde{u}$.

The Mori cone vectors determine the large volume variables

$$\begin{array}{c|ccc|cccc|} & \nu_i & & & l^{(1)} & l^{(2)} & l^{(3)} & l^{(4)} \\ D_u & 1 & 0 & 0 & 0 & -1 & 0 & -1 \\ D_1 & 1 & 1 & -1 & 1 & 0 & 0 & 0 \\ D_2 & 1 & 0 & 1 & 0 & 0 & 0 & 1 \\ D_3 & 1 & -1 & 1 & 0 & 0 & 1 & -1 \\ D_4 & 1 & -1 & 0 & 0 & 1 & -2 & 1 \\ \mathrm{D}_5 & 1 & -1 & -1 & 1 & -1 & 1 & 0 \\ D_6 & 1 & 0 & -1 & -2 & 1 & 0 & 0 \\ \end{array} \,. \tag{5.4.13}$$

These read in terms of the m_i and $\tilde{u}$

$$z_1 = \frac{1}{m_1^2}, \quad z_2 = \frac{m_1 m_2}{\tilde{u}}, \quad z_3 = \frac{m_3}{m_2^2}, \quad z_4 = \frac{m_2}{\tilde{u} m_3} \,. \tag{5.4.14}$$

With $Q_t = Q_1^{\frac{1}{4}}(Q_2 Q_3 Q_4)^{\frac{1}{2}}$ we see as before that the variables z_i are not independent transcendental functions of the Kähler parameters rather one has the following relations

$$z_1 = \frac{Q_1}{(1+Q_1)^2}, \quad z_2 = \frac{z_4(1+Q_1)Q_2}{Q_4}, \quad z_3 = \frac{Q_3}{(1+Q_3)^2} \,. \tag{5.4.15}$$

$$\begin{aligned} F = \; & \text{class} + L_{0,0,0,1} + L_{0,0,1,1} + L_{0,1,0,0} + L_{0,1,1,0} - 2L_{0,1,1,1} + L_{1,1,0,0} + L_{1,1,1,0} \\ & -2L_{1,1,1,1} - 2L_{1,2,1,0} + 3L_{1,2,1,1} + 3L_{1,2,2,1} - 4L_{1,2,2,2} - 4L_{1,3,2,1} + 5L_{1,3,2,2} \\ & +5L_{1,3,3,2} - 6L_{1,3,3,3} - 6L_{1,4,3,2} + 7L_{1,4,3,3} + 7L_{1,4,4,3} - 4L_{2,3,2,1} + 5L_{2,3,2,2} \\ & +5L_{2,3,3,2} - 6L_{2,3,3,3} + 5L_{2,4,2,1} - 6L_{2,4,2,2} + 5L_{2,4,3,1} - 36L_{2,4,3,2} + 35L_{2,4,3,3} \\ & -6L_{2,4,4,2} - 6L_{2,5,3,1} + 35L_{2,5,3,2} - 6L_{3,4,3,2} - 6L_{3,5,3,1} \,. \end{aligned} \tag{5.4.16}$$

5.4.1. A mass deformation of the local E_8 del Pezzo surface

Let us consider the polyhedron 10. The Mori cone vectors, which correspond to the depicted

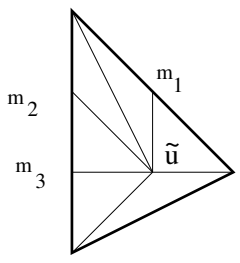

Figure 5.11.: The polyhedron 10 with the choice of the mass parameters m_1, m_2, m_3 and the modulus $\tilde{u}$.

triangulation are given below

$$\begin{array}{c|ccc|cccc|} & \nu_i & & & l^{(1)} & l^{(2)} & l^{(3)} & l^{(4)} \\ D_u & 1 & 0 & 0 & 0 & 1 & 0 & 0 \\ D_1 & 1 & 1 & 0 & 1 & 0 & 0 & 0 \\ D_2 & 1 & 0 & 1 & -2 & 1 & 0 & 0 \\ D_3 & 1 & -1 & 2 & 1 & -1 & 1 & 0 \\ D_4 & 1 & -1 & 1 & 0 & 1 & -2 & 1 \\ \mathrm{D}_5 & 1 & -1 & 0 & 0 & 0 & 1 & -2 \\ D_6 & 1 & -1 & -1 & 0 & 0 & 0 & 1 \\ \end{array} \ . \tag{5.4.17}$$

With the indicated mass parameters of the three non-renormalizable modes and the parameter $\tilde{u}$ the Mori vectors determine the large volume B-model coordinates

$$z_1 = \frac{1}{m_1^2}, \quad z_2 = \frac{m_1 m_2}{\tilde{u}}, \ z_3 = \frac{m_3}{m_2^2}, \ z_4 = \frac{m_2}{m_3^2} \ . \tag{5.4.18}$$

The anti-canonical class of the E_8 del Pezzo corresponds to an elliptic curve, which in turn has the following Mori vector

$$l_e = 3l^{(1)} + 6l^{(2)} + 4l^{(3)} + 2l^{(4)} = \sum_i a_i l^{(i)} \ . \tag{5.4.19}$$

This equation implies that $z_e = \frac{1}{u^6} = z_1^3 z_2^6 z_3^4 z_4^2$ is the correct large volume modulus for this curve independently of the masses. By specializing the expression in Appendix A.8 as $m_1 = 0, m_2 = 1, m_4 = 1, m_6 = 1, m_3 = m_2, m_5 = 0, a_1 = 0, a_2 = m_1, a_3 = m_3, \tilde{u} = \frac{1}{u}$ and scaling $g_i \to \lambda^i g_i$ with $\lambda = 18u^4$ we get

$$\begin{array}{rl} g_2 = & 27u^4(24m_1u^3 - 48m_2u^4 + 16m_3^2u^4 - 8m_3u^2 + 1)\,, \\ g_3 = & 27u^6(216m_1^2u^6 + 12m_3u^2(-12m_1u^3 + 24m_2u^4 - 1) + \\ & 36m_1u^3 - 72m_2u^4 - 64m_3^3u^6 + 48m_3^2u^4 - 864u^6 + 1)\,. \end{array} \tag{5.4.20}$$

The scaling is chosen so that $\frac{dt}{du} = \frac{1}{u} + 2m_3u + O(u^2)$ and $t(u,m)$ becomes the logarithmic solution $t(u,m) = \log(u) + \mathcal{O}(u)$ at infinity $z_e = 0$, which corresponds to $\frac{1}{j} \sim q \sim u^6$. Hence we get as the transcendental mirror map $u = Q_t - m_3 Q_t^3 + \mathcal{O}(Q_t^4)$, with $Q_t = (Q_e)^{\frac{1}{6}} = \sqrt{Q_1} Q_2 Q_3^{\frac{2}{3}} Q_4^{\frac{1}{3}}$. The non-transcendental rational mirror maps are

$$z_1 = \frac{Q_1}{(1+Q_2)^2}, \quad z_3 = Q_3 \frac{1 + Q_4 + Q_3 Q_4}{(1 + Q_3 + Q_3 Q_4)^2}, \quad z_4 = Q_4 \frac{1 + Q_3 + Q_3 Q_4}{(1 + Q_4 + Q_3 Q_4)^2} \ . \tag{5.4.21}$$

The existence of these rational solutions for the mirror maps can be proven from the system of differential equations that corresponds to the Mori vectors listed above. With the knowledge of these rational solutions the system of differential equations can be reduced to one third order differential equation in u parametrized by the m_i.

Such rational solutions exist for the differential operators associated to Mori vectors describing the linear relations of points on an (outer) edge of a toric diagram. One can understand their existence from the fact that this subsystem describes effectively a non-compact two-dimensional CY geometry, whose compact part is a Hirzebruch sphere tree, which has no non-trivial mirror maps.

This defines the Kähler parameters of the A-model geometry and relates them to the coordinates u, m_i. This allows to extract the BPS invariants for this mass deformation of the E_8 curve.

5.5. Solving the topological string on $\mathbb{C}^3/\mathbb{Z}_5$

So far only toric Calabi-Yau manifolds that are realized as the anti-canonical bundle over a Fano surface have been considered. While one expects no obstacle in carrying out the direct integration procedure, there are some interesting points that deserve attention. In analogy to the direct integration procedure based on the j-function of the elliptic curve, one can ask the question how the situation looks like for geometries whose mirror is given by a genus two curve[6]. These are characterized by three so-called Igusa invariants. We consider the example $\mathbb{C}^3/\mathbb{Z}_5$, which has for other purposes also been studied in [206–208] and use the Fourier expansion of these invariants to compute the complex structure moduli. It is demonstrated that the free energy at genus one can be written in terms of Siegel modular forms. The results of this section are based on [105].

5.5.1. Genus two curves and Igusa invariants

A genus two curve can always be brought into hyperelliptic form which can be shown using the Riemann Roch theorem. (Less rigorously one notices that the dimensions of the moduli space of hyperelliptic curves and genus two curves coincide.)

$$y^2 = v_0 x^5 - v_1 x^4 + v_2 x^3 - v_3 x^2 + v_4 x - v_5, \quad v_i \in \mathbb{C}. \tag{5.5.1}$$

A natural question is under which conditions two genus two curves being already in hyperelliptic form are equivalent. Given a genus two curve in hyperelliptic form (5.5.1) one associates with it a set of invariants that is given as

$$\begin{aligned}
A &= 40v_0v_4 - 16v_1v_3 + 6v_2^2, \\
B &= 300v_0^2v_3v_5 - 80v_0^2v_4^2 - 180v_0v_1v_2v_5 + 4v_0v_1v_3v_4 + 36v_0v_2^2v_4 - 12v_0v_2v_3^2 + 48v_1^3v_5 \\
&\quad -12v_1^2v_2v_4 + 4v_1^2v_3^2, \\
C &= 2250v_0^3v_2v_5^2 + 1600v_0^3v_3v_4v_5 - 320v_0^3v_4^3 - 900v_0^2v_1^2v_5^2 - 1860v_0^2v_1v_2v_4v_5 - 640v_0^2v_1v_3^2v_5 \\
&\quad +64v_0^2v_1v_3v_4^2 + 330v_0^2v_2^2v_3v_5 + 176v_0^2v_2^2v_4^2 + 26v_0^2v_2v_3^2v_4 - 36v_0^2v_3^4 + 616v_0v_1^3v_4v_5 \\
&\quad +492v_0v_1^2v_2v_3v_5 + 26v_0v_1^2v_2v_4^2 + 28v_0v_1^2v_3^2v_4 - 198v_0v_1^3v_2^2v_5 - 238v_0v_1v_2^2v_3v_4 \\
&\quad +76v_0v_1v_2v_3^3 + 72v_0v_2^4v_4 - 24v_0v_2^3v_3^2 - 160v_1^4v_3v_5 - 36v_1^4v_4^2 + 60v_1^3v_2^2v_5 + 76v_1^3v_2v_3v_4 \\
&\quad -24v_1^3v_3^3 - 24v_1^2v_2^3v_4 + 8v_1^2v_2^2v_3^2, \\
C' &= \frac{1}{2}(AB - 3C), \\
D &= v_0^2\Delta.
\end{aligned} \tag{5.5.2}$$

Here Δ denotes the discriminant of the curve. These invariants have degree two, four, six and ten and coordinize $\mathbb{P}^{(1,2,3,5)}$. Inhomogeneous coordinates are given in terms of

[6] Apart from conceptual reasons, the study of the direct integration of genus two mirrors is propably needed in order to understand the B-model geometry of the M-string [76, 218].

A, B, C, D as

$$x_1 = \frac{BC'}{D}, \quad x_2 = \frac{AB^2}{D}, \quad x_3 = \frac{B^5}{D^2}\,. \tag{5.5.3}$$

These invariants A, B, C, C', D have an expansion in terms of the generators of the ring of Siegel modular forms $E_4, E_6, \chi_{10}, \chi_{12}$ as [204, 205]

$$A = -8\frac{\chi_{12}}{\chi_{10}}, \quad B = 4E_4, \quad C' = 4E_6, \quad D = -2^{14}\chi_{10}\,. \tag{5.5.4}$$

5.5.2. The geometry and its mirror

We start by discussing the A-model geometry that is given as the resolution of the orbifold $\mathbb{C}^3/\mathbb{Z}_5$.

$$\left(\begin{array}{ccc|cc|l} 0 & 0 & 1 & 1 & -3 & \leftarrow \mathbb{P}^2 \\ 1 & 0 & 1 & -2 & 1 & \leftarrow F_3 \\ 2 & 0 & 1 & 1 & 0 & \\ 0 & 1 & 1 & 0 & 1 & \\ -1 & -1 & 1 & 0 & 1 & \\ & & & \uparrow & \uparrow & \\ & & & \mathbb{P}^1_f & \mathbb{P}^1_b & \end{array}\right) \tag{5.5.5}$$

By investigating the scaling relations, one easily sees that the divisor obtained by setting x_0 to 0 is given by a $\mathbb{P}^2$ while one obtains a F_3 from $x_1 = 0$.

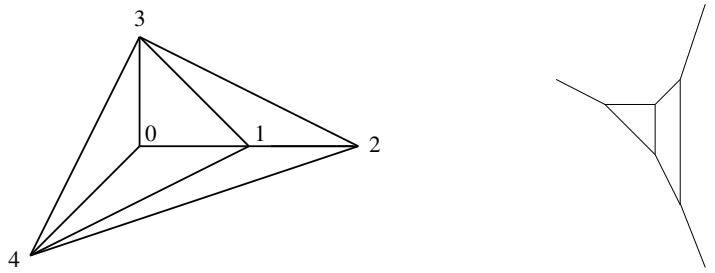

Figure 5.12.: The picture on the left shows the A-model geometry, which is the resolution of $\mathbb{C}^3/\mathbb{Z}_5$. On the right the dual diagram is shown. Upon thickening its lines [210], one obtains the Mirror curve which has genus two.

The toric diagram (5.5.5) provides us with the moduli

$$z_1 = \frac{X_0 X_2}{X_1^2}, \qquad z_2 = \frac{X_1 X_3 X_4}{X_0^3}\,. \tag{5.5.6}$$

The constraints can be easily solved by the following choice of coordinates

$$X_0 = xyz, \quad X_1 = z_2\, x^2 y, \quad X_2 = z_1 z_2^2\, \frac{x^3 y}{z}, \quad X_3 = y^2 z, \quad X_4 = xz^2. \tag{5.5.7}$$

In these coordinates it is easy to write down the mirror curve in hyperelliptic form

$$y^2 = -4x^5 + x^4 + 2x^3 z_2 + 2x^2 z_1 z_2^2 + x^2 z_2^2 + 2x z_1 z_2^3 + z_1^2 z_2^4\,. \tag{5.5.8}$$

From this one easily deduces the discriminant

$$\Delta = 256 z_1^5 z_2^{14} \left(1 + 27 z_2 + 3125 z_1^3 z_2^2 + 4 z_1^2 (4 + 125 z_2) - z_1 (8 + 225 z_2)\right) . \tag{5.5.9}$$

In addition, one finds the following Picard-Fuchs operators

$$\begin{aligned}
\mathcal{L}_1 &= (\Theta_1 - 3\Theta_2)\Theta_1 - z_1 \left[(2\Theta_1 - \Theta_2)^2 + 2\Theta_1 - \Theta_2\right] , \\
\mathcal{L}_2 &= (\Theta_2 - 2\Theta_1)\Theta_2^2 - z_2 \left[(\Theta_1 - 3\Theta_2)^3 - 3(\Theta_1 - 3\Theta_2)^2 + 2\Theta_1 - 6\Theta_2\right] , \\
\mathcal{L}_3 &= \Theta_1 \Theta_2^2 + z_1 z_2 \left(\Theta_1 - 3\Theta_2\right) \left(2\Theta_1 - \Theta_2\right) \left(\Theta_1 - 3\Theta_2 - 1\right) .
\end{aligned} \tag{5.5.10}$$

5.5.3. Extracting the complex structure moduli from the mirror

We compute the dependence of the period matrix

$$\tau = \begin{pmatrix} \tau_{11} & \tau_{12} \\ \tau_{12} & \tau_{22} \end{pmatrix} \tag{5.5.11}$$

from the moduli z_1, z_2. We denote $q_1 = \exp(\tau_{11})$, $q_2 = \exp(\tau_{22})$, $r = \exp(\tau_{12})$. To start one finds that the Igusa invariants are given as

$$\begin{aligned}
x_1 &= \frac{9\big(1 + 24 z_2 + 2400 z_1^3 z_2^2 - 8 z_1 (1 + 25 z_2) + z_1^2 (16 + 440 z_2 - 80 z_2^2)\big)}{\big(-1 + z_1 (4 + 40 z_2)\big)^2} , \\
x_2 &= 27\big(1 + 36 z_2 + 216 z_2^2 - 72 z_1^4 z_2^2 (197 + 1700 z_2) - 12 z_1 (1 + 37 z_2 + 228 z_2^2) \\
&\quad + 12 z_1^2 (4 + 155 z_2 + 988 z_2^2) + 16 z_1^3 (-4 - 165 z_2 - 876 z_2^2 + 1760 z_2^3)\big) \Big/ \big(-1 + z_1 (4 + 40 z_2)\big)^3 , \\
x_3 &= \frac{-243 z_1^5 z_2^4 (1 + 27 z_2 + 3125 z_1^3 z_2^2 + 4 z_1^2 (4 + 125 z_2) - z_1 (8 + 225 z_2))}{4\big(-1 + z_1 (4 + 40 z_2)\big)^5} .
\end{aligned} \tag{5.5.12}$$

Using the Fourier expansion in A.3.2 of the absolute Igusa invariants one finds accordingly

$$\begin{aligned}
q_1(z_1, z_2) &= -z_2^3 + z_1 z_2^3 + 45 z_2^4 - z_1^2 z_2^3 - 60 z_1 z_2^4 - 1512 z_2^5 + \mathcal{O}(z^6) , \\
q_2(z_1, z_2) &= z_1^5 z_2^2 + 16 z_1^6 z_2^2 - 5 z_1^5 z_2^3 + \mathcal{O}(z^9) , \\
r(z_1, z_2) &= -z_2 - 3 z_1 z_2 + 15 z_2^2 - 13 z_1^2 z_2 + 20 z_1 z_2^2 - 279 z_2^3 + \mathcal{O}(z^4) .
\end{aligned} \tag{5.5.13}$$

5.5.4. Periods and free energies at genus zero and one

At the large radius point one finds five solutions

$$\begin{aligned}
\omega_0 &= 1 , \\
t_1^A &= \frac{1}{2\pi i}\Big(\log(z_1) + 2 z_1 + 2 z_2 + 3 z_1^2 - 15 z_2^2 + \frac{20}{3} z_1^3 + 6 z_1 z_2^2 + \frac{560}{3} z_2^3 + \mathcal{O}(z^4)\Big) , \\
t_2^A &= \frac{1}{2\pi i}\Big(\log(z_2) - z_1 - 6 z_2 - \frac{3}{2} z_1^2 + 45 z_2^2 - \frac{10}{3} z_1^3 - 18 z_1 z_2^2 - 560 z_2^3 + \mathcal{O}(z^4)\Big) , \\
t_1^B &= \frac{1}{2\pi i}\Big(-\frac{1}{2}\log(z_2)^2 + X^{2,A}\log(z_2) + -2 z_1 - 9 z_2 - 4 z_1^2 + 3 z_1 z_2 + \frac{423}{4} z_2^2 - \frac{193}{18} z_1^3 \\
&\quad -3 z_1^2 z_2 - \frac{117}{2} z_1 z_2^2 1486 z_2^3 + \mathcal{O}(z^4)\Big) , \\
t_2^B &= \frac{1}{2\pi i}\Big(\big(\frac{3}{2}\log(z_1) + 5 z_1 + \frac{15 z_1^2}{2} + \frac{50 z_1^3}{3}\big)\log(z_1)\big) + X^{1,A}\log(z_2) + 4 z_1 + 3 z_2 \\
&\quad +13 z_1^2 - z_1 z_2 - \frac{141 z_2^2}{4} + \frac{328 z_1^3}{9} + z_1^2 z_2 + \frac{39 z_1 z_2^2}{2} + \frac{1486 z_2^3}{3} + \mathcal{O}(z^4)\Big) .
\end{aligned} \tag{5.5.14}$$

After introducing the monodromy invariant variables $Q_i = e^{2\pi i t_i^A}$ one obtains the mirror maps

$$\begin{aligned} z_1(Q_1,Q_2) &= Q_1 - 2Q_1^2 + 3Q_1^3 - 2Q_1Q_2 + 6Q_1^2Q_2 + 5Q_1Q_2^2 + \mathcal{O}(Q^4)\,, \\ z_2(Q_1,Q_2) &= Q_2 + Q_1Q_2 + 6Q_2^2 + 10Q_1Q_2^2 + 9Q_2^3 + \mathcal{O}(Q^4)\,. \end{aligned} \tag{5.5.15}$$

As described in in 2.2.6, one finds the prepotential

$$\begin{aligned} F^{(0,0)} &= -\frac{3}{10}t_1^{A\,3} - \frac{3}{10}t_1^{A\,2}t_2^A - \frac{1}{10}t_1^A t_2^{A\,2} - \frac{1}{15}t_2^{A\,3} - 2Q_1 + 3Q_2 - \frac{1}{4}Q_1^2 + 4Q_1Q_2 - \frac{45}{8}Q_2^2 \\ &\quad -\frac{2}{27}Q_1^3 + 3Q_1^2Q_2 - 10Q_1Q_2^2 + \frac{244}{9}Q_2^3 + \mathcal{O}(Q^4)\,. \end{aligned} \tag{5.5.16}$$

Denoting $K_{ij} = \partial_{t_i^A}\partial_{t_j^A}F^{(0,0)}$ one observes

$$\begin{aligned} \tau_{11} &= -K_{11} + 6K_{12} - 9K_{22} + c_{11}\,, \\ \tau_{22} &= -4K_{11} + 4K_{12} - K_{22} + c_{22}\,, \\ \tau_{12} &= -K_{11} + 7K_{12} - 3K_{22} + c_{12}\,, \end{aligned} \tag{5.5.17}$$

with $c_{ij} \in \mathbb{C}$. This result can be explained as follows. On a compact Riemann surface one could choose a symplectic basis, such that the B - periods would be just given as

$$t_B = \frac{\partial}{\partial t_i^A}F^{(0,0)} \tag{5.5.18}$$

and therefore

$$\tau_{ij} = \frac{\partial t_i^B}{\partial t_j^A} = \frac{\partial}{\partial t_i^A}\frac{\partial}{\partial t_j^A}F^{(0,0)}\,. \tag{5.5.19}$$

On a non-compact Riemann surface it is in contrast not possible to find a symplectic basis and the just discussed relation is not expected to hold anymore. One finds the Yukawa couplings

$$\begin{aligned} \tilde{\kappa}_{z_1z_1z_1} &= \frac{9 - 17z_1 + 4z_1^2 + 243z_2 - 540z_1z_2 + 225z_1^2z_2}{5z_1^3\Delta}\,, \\ \tilde{\kappa}_{z_1z_1z_2} &= \frac{3 - 14z_1 + 8z_1^2 + 81z_2 - 405z_1z_2 + 325z_1^2z_2}{5z_1^2z_2\Delta}\,, \\ \tilde{\kappa}_{z_1z_2z_2} &= \frac{1 - 8z_1 + 16z_1^2 + 27z_2 - 210z_1z_2 + 400z_1^2z_2}{5z_1z_2^2\Delta}\,, \\ \tilde{\kappa}_{z_2z_2z_2} &= \frac{2 - 16z_1 + 32z_1^2 + 9z_2 - 95z_1z_2 + 300z_1^2z_2}{5z_2^3\Delta}\,. \end{aligned} \tag{5.5.20}$$

With the help of a few known BPS numbers of the local $\mathbb{P}^2$ model the unknowns in (3.3.4) can be determined and one finds the refined free energies at genus one

$$F^{(1,0)} = \frac{1}{24}\log\left(\Delta z_1^{-3}z_2^{-2}\right) \qquad F^{(0,1)} = -\frac{1}{12}\log\left(\Delta z_1^{\frac{39}{5}}z_2^{-\frac{38}{5}}\right) + \frac{1}{2}\log\Big(\det(G_{i\bar{\jmath}})\Big)\,. \tag{5.5.21}$$

$$
\begin{aligned}
F^{(1,0)} &= -\frac{1}{8}t_1^{A\,2} - \frac{1}{12}t_2^A - \frac{1}{6}Q_1 + \frac{7}{8}Q_2 - \frac{1}{12}Q_1^2 + \frac{5}{6}Q_1Q_2 - \frac{129}{16}Q_2^2 \\
&\quad -\frac{1}{18}Q_1^3 + \frac{7}{8}Q_1^2Q_2 - \frac{65}{6}Q_1Q_2^2 + \frac{589}{6}Q_2^3 + \mathcal{O}(Q^4)\,, \\
F^{(0,1)} &= -\frac{3}{20}t_1^A - \frac{2}{15}t_2^A - \frac{1}{6}Q_1 + \frac{1}{4} - \frac{1}{12}Q_1^2 + \frac{1}{3}Q_1Q_2 - \frac{3}{8}Q_2^2 \\
&\quad -\frac{1}{18}Q_1^3 + \frac{1}{4}Q_1^2Q_2 - \frac{5}{6}Q_1Q_2^2 - \frac{23}{3}Q_2^3 + \mathcal{O}(Q^4)\,.
\end{aligned} \tag{5.5.22}
$$

By using the Fourier expansion of the Eisenstein series one finds that the free energy can be expressed as

$$
F^{(0,1)} = -\frac{1}{12}\log\Big(\big(\frac{C'E_6}{BE_4}\big)^8\chi_{10}\Big)\,. \tag{5.5.23}
$$

We list the BPS invariants in the appendix A.5

5.5.5. The propagator

In order to determine the higher genus free energies, we first calculate the propagators by solving (3.3.7). The ambiguities $A_i, f, \tilde{f}$ can be found in appendix A.5. The propagator reads

$$
S = \begin{pmatrix} S^{11}(z_1,z_2) & S^{12}(z_1,z_2) \\ S^{21}(z_1,z_2) & S^{22}(z_1,z_2) \end{pmatrix} \tag{5.5.24}
$$

where the components are explicitly given as

$$
\begin{aligned}
S^{11} &= -\frac{584z_1^2}{85} + \frac{2336z_1^3}{85} - \frac{77z_1^2z_2}{17} + \frac{583z_1^3z_2}{17} - 4z_1^4z_2 + 6z_1^2z_2^2 + \mathcal{O}(z^5)\,, \\
S^{12} &= \frac{2998z_1z_2}{255} - \frac{1718z_1^2z_2}{85} + \frac{141z_1z_2^2}{17} - \frac{1064z_1^2z_2^2}{17} + 2z_1^3z_2^2 - 18z_1z_2^3 + \mathcal{O}(z^5)\,, \\
S^{22} &= -\frac{z_2^2}{2} + \frac{1134z_1z_2^2}{85} - 9z_2^3 + \frac{2637z_1z_2^3}{17} + 54z_2^4 + \mathcal{O}(z^5)\,.
\end{aligned} \tag{5.5.25}
$$

It holds that $S^{12} = S^{21}$. According to (3.2.11) this has to transform like a vector-valued almost modular form of weight two. The fact that it fulfills two over-determined systems of equations provides evidence that one can give a meaningful interpretation to vector-valued second Eisenstein series of genus two.

6. The Refined BPS Invariants for the Half K3

In this chapter we discuss the computation of the refined stable pair invariants of the massless as well as massive half K3 surface. We start by reviewing the refined Göttsche formula as well as the unrefined modular anomaly equation due to Hosono, Saito and Takahashi. A presentation of the massless half K3 geometry in which only the moduli of the base and the fiber are realized is included. This discussion provides important background material for the computation of the refined BPS invariants of the massless half K3 surface in section 6.2. This includes in particular a proposal for a refined version of the modular anomaly equation. The results of the massless half K3 get generalized in section 6.3 where we consider all moduli of the half K3. In this case, the refined BPS invariants are not only classified by the respective degree in the fiber and base classes but also with respect to the Weyl orbits of the remaining moduli. This gives some insight into the structure of the refined BPS invariants of the massless half K3. Finally, we use the results of the massive half K3 to compute the refined BPS invariants of the remaining del Pezzo surfaces by taking suitable decoupling limits and blow-downs in section 6.4. The presentation follows closely [1].

6.1. The refined Göttsche formula and the unrefined HST recursion relation

A Hilbert scheme $\mathrm{Hilb}^p(S)$ of g points on a smooth surface S is given by $S^{\otimes g}$ divided by the permutation group Sym^g. In other words, it corresponds to the choice of g points that may be counted with multiplicities.

The Göttsche formula [100] describes the generating function for the Poincaré polynomials of the Hilbert scheme of g points on a complex surface S. It reads as follows

$$G(y,q) = \sum_{g=0}^{\infty} P(S^{[g]}, y) q^g = \prod_{n\geq 1} \frac{(1+y^{2n-1}q^n)^{b_1(S)}(1+y^{2n+1}q^n)^{b_1(S)}}{(1-y^{2n-2}q^n)^{b_0(S)}(1-y^{2n}q^n)^{b_2(S)}(1-y^{2n+2}q^n)^{b_0(S)}} \,. \tag{6.1.1}$$

This enjoys an interpretation [122] as the partition function of $b_1(S)$ chiral fermions and $b_0(S) + b_2(S)$ chiral bosons, whose oscillators are in addition also labeled by the SU(2) Lefshetz charge j_3. In particular for $y = -1$, one obtains the important limit

$$G(-1,q) = \sum_{g=0}^{\infty} e(S^{[g]}) q^g = \prod_{m=1}^{\infty} (1-q^m)^{-e(S)} = \frac{q^{\frac{e(S)}{24}}}{\eta(q)^{e(S)}} \tag{6.1.2}$$

where $e(S)$ denotes the Euler number of the surface S.

If $b_0(S) = 1$ and $b_1(S) = 0$ the Göttsche formula can be refined [34], see also [29], in that sense as it serves as the generating function for the Poincaré polynomials with respect to

the $\mathrm{SU}(2)_L \times \mathrm{SU}(2)_R$ Lefshetz decomposition, i.e. one assigns to the oscillator α_{-k} not the diagonal representation $(b_2(S)+1)[0]+[1]$ but instead the representations

$$b_2(S)\,[0,0] + \left[\frac{1}{2},\frac{1}{2}\right]. \tag{6.1.3}$$

The refined Göttsche formula reads explicitly

$$\begin{aligned} G^S(q,y_L,y_R) &= \sum_{g=0}^{\infty} P(S^{[g]},y_L,y_R)q^g \\ &= \prod_{n=1}^{\infty} \frac{1}{(1-(y_Ly_R)^{n-1}q^n)(1-(y_Ly_R)^{n+1}q^n)(1-(y_Ly_R)^nq^n)^{b_2(S)-2}} \\ &\quad \times \frac{1}{(1-y_R^2(y_Ly_R)^{n-1}q^n)(1-y_L^2(y_Ly_R)^{n-1}q^n)} \end{aligned} \tag{6.1.4}$$

and can be expressed in terms of Betti numbers as

$$G^S(q,y_L,y_R) = \sum_{d=0}^{\infty}\sum_{j_L,j_R} (-1)^{2j_L+2j_R} n^d_{j_L,j_R} \Big(\sum_{k=-j_L}^{j_L} y_L^{2k}\Big)\Big(\sum_{k=-j_R}^{j_R} y_R^{2k}\Big) q^d. \tag{6.1.5}$$

Here j_L, j_R denote the SU(2) spins and $n^d_{j_L,j_R}$ denote the refined Betti numbers of the Hilbert scheme of d points on S. Formula (6.1.5) can be used to extract the refined Betti numbers of the half K3. The results are listed in table A.2. These results have already appeared in [29].

We continue by a review of the (unrefined) recursion relation by Hosono, Saito and Takahashi[1] (HST) for the massless half K3, following [34] (see also [103]) and also using their notation. We start by considering a realization of the half K3 surface where only the moduli corresponding to the base and the elliptic fiber are realized. This can be constructed by considering a compact Calabi-Yau manifold X given as a hypersurface inside the ambient space $F_1 \times \mathbb{P}^2$. Coordinizing $\mathbb{P}^2$ by $[z_1 : z_2 : z_3]$, the base and fiber of F_1 by $[u_1 : u_2]$ and $[u_3 : u_4]$ respectively, the Calabi-Yau manifold X may be written as

$$g_{3,3}(z_i,u_1,u_2)u_3^2 + f_{3,1}(z_i,u_1,u_2)u_4^2 = 0\,, \tag{6.1.6}$$

where the subscript refers to the degree in the variables z_i and u_1, u_2. Indeed, by setting u_3 to zero, one obtains a half K3 geometry. The positive classes in $H_2(X,\mathbb{Z})$ are generated by the following divisors in X

$$H = \{z_1 = 0\} \cap X, \quad F = \{u_1 = 0\} \cap X, \quad D = \{u_4 = 0\} \cap X\,. \tag{6.1.7}$$

One also observes that the intersection of F with the half K3 surface $\mathcal{B}_9$ gives the class of the elliptic surface within $\mathcal{B}_9$. This relates to the basis of $H_2(\mathcal{B}_9,\mathbb{Z})$ in section 4.1

$$e_1, \ldots e_9, h \tag{6.1.8}$$

[1] In fact contributions into this direction have already appeared before, e.g. [31].

as follows[2]

$$H = h, \quad F = 3h - \sum e_i \,. \tag{6.1.9}$$

We consider the limit of infinite volume of the fiber class $\mathbb{P}^1$ which corresponds to taking the local limit of X. In this limit, only the Gromov Witten invariants of curves contained in the half K3 $\mathcal{B}_9$ survive. Also, we denote the corresponding Kähler moduli to the divisors in (6.1.7) by t_H, t_F and introduce $q = e^{2\pi i t_H}$, $p = e^{2\pi i t_F}$. We also need some notation concerning the genus g Gromov-Witten invariants $N_g(\beta)$ of class $\beta \in H_2(\mathcal{B}_9, \mathbb{Z})$. Denote by

$$N_{g,d,n} := \sum_{\substack{(\beta,H)=d \\ (\beta,F)=n}} N_g(\beta), \quad Z_{g,n}(q) := \sum_{d=0}^{\infty} N_{g,d,n} q^d, \quad F_g(q,p) := \sum_{n=0}^{\infty} Z_{g,n} p^n \,. \tag{6.1.10}$$

There are closed expressions for some of these generating functions. In reference [32] it was found that

$$Z_{0,1} = q^{\frac{3}{2}} \frac{\Theta_{\mathrm{E}_8}(t\gamma, 3t)}{\eta^{12}(q^3)} \qquad \gamma = (1, \ldots, 1, -1). \tag{6.1.11}$$

The E_8 theta function[3] is defined in (6.3.1). It is amusing to interpret the factors [177]. From a mathematical point of view the E_8 symmetry is traced back to the Weyl group, while the factor η^{12} comes from the twelve singular fibers of the elliptic fibration. In fact, when turning on the remaining mass parameters of the other blow-up divisors each of them gives rise to a section of the elliptic fibration that are governed by the Mordell Weyl group E_8. The physical interpretation in the E-String picture is relegated to section 8.1.

Furthermore, it was conjectured by [34] that the generating function takes the following form

$$Z_{g,n} = P_{2g+2n-2}(\phi, E_2, E_4, E_6)(Z_{0,1}(q))^n \,. \tag{6.1.12}$$

Here $P_{2g+2n-2}$ is a almost modular form of weight $2g + 2n - 2$ and ϕ denotes the fundamental solution (4.3.11) of the Picard-Fuchs equations at the large radius point. Note in particular that is does not become constant but is instead given by

$$\phi(x_e) = \sum_{n \geq 0} a_n x_e^n, \qquad a_n = \frac{\Gamma(1+3n)}{\Gamma(1+n)^3} \,. \tag{6.1.13}$$

This displays the fact that the half K3 is not rigid within X and gravity does not completely decouple. $Z_{g,n}$ is subject to the following recursion relation

$$\frac{\partial Z_{g,n}}{\partial E_2} = \frac{1}{72} \sum_{g'+g''=g} \sum_{s=1}^{n-1} s(s-n) Z_{g',s} Z_{g'',n-s} + \frac{n(n+1)}{72} Z_{g-1,n} \,. \tag{6.1.14}$$

In order to determine the amplitudes recursively using (6.1.14) one also needs to fix an integration constant at each step. The following observation [32] yields some boundary conditions. Consider a curve of the class

$$\mathcal{C}_g = dH - a_1 e_1 - \cdots - a_9 e_9 \,. \tag{6.1.15}$$

[2] Strictly speaking, we mean the restriction of H and F to $\mathcal{B}_9$.

[3] Again, for convenience, we review here the results by [34], which use a different notation than we do in the rest of this thesis.

One easily computes using the intersections in 4.1

$$(\mathcal{C}_g, F) = 3d - \sum a_i, \qquad g_a(\mathcal{C}_g) = \frac{(d-1)(d-2)}{2} - \sum_{i=1}^{9} \frac{a_i(a_i-1)}{2}. \tag{6.1.16}$$

The last quantity computes the arithmetic genus. Together these two formulae provide combinatorial vanishing conditions on some $N_{g,d,n}$ that can serve as boundary conditions. E.g. one finds that for $d < \frac{n}{3}$ $N_{0,n,d}$ has to vanish.

6.2. Refined BPS invariants for the massless half K3

In this section we want to show how a generalized version of the modular anomaly equation (6.1.14) can be used to compute refined BPS invariants. From now on we make a little change of basis. We parameterize base p and fiber f according to

$$p = e_9, \quad f = 3h - \sum_{i=1}^{9} e_i\,, \tag{6.2.1}$$

and denote[4] a general class by $\beta = n_b p + df$. Instead of the class of h, we consider the class of a section[5] of the elliptic fibration given by e_9 The main effect of this basis change is that one has to substitute $q^3 \mapsto q$ in the above formulae (6.1.10), (6.1.11), (6.1.12) and the prefactor 72 by 24 in the recursion relation (6.1.14). Also the weight of the modular forms (6.1.12) is now given by $6n_b + 2(g+n) - 2$ and the vanishing condition below (6.1.16) becomes that $N_{0,n_b,d}$ for $d < n_b$.

It was shown in [24, 29, 34] that the partition function of refined BPS invariants with wrapping number $n_b = 1$ take a particularly simple form

$$\mathcal{G}(\epsilon_1, \epsilon_2, q) = E_4(q) G^{\mathcal{B}_9}(q, y_L, y_R), \qquad y_{L/R} = \exp\left(\frac{\epsilon_1 \pm \epsilon_2}{2}\right). \tag{6.2.2}$$

Here the generating function is related to the refined BPS invariants as

$$\mathcal{G}(\epsilon_1, \epsilon_2, q) = \sum_{d=0}^{\infty} \sum_{j_L, j_R} (-1)^{2j_L + 2j_R} n_{j_L, j_R}^{p+df} \Big(\sum_{k=-j_L}^{j_L} y_L^{2k} \Big) \Big(\sum_{k=-j_R}^{j_R} y_R^{2k} \Big) q^d\,. \tag{6.2.3}$$

The reason for this is that the moduli space of such genus g curves takes a particularly simple form. These wrap the elliptic fiber over g points in the base. Choosing a connection on them corresponds by T-duality to picking a point on the fiber as well such one is naturally led to the problem of picking g points on the elliptic surface. In addition, the Mordell Weyl group accounts in the massless case for the factor E_4. This can be used to extract the refined BPS numbers and was already done in [29]. We cite the results in table A.3. Note that the results for the diagonal class $d + f$ are the same as for the massless E_8 del Pezzo surface. Indeed, the sum of the fiber and base class realizes the anti-canonical class of the del Pezzo surface after performing a flop transition as discussed in 8.1.4.

[4] Note that in the refined case the genus g splits into the pair (n, g). Therefore we denote in the following the wrapping number of the base by n_b.

[5] Note that also the class of a positive section $e_9 + f$ appears in the literature, see e.g. [103].

As the curves with wrapping numbers $n_b = 1$ cannot be affected by multi-cover contributions, there is an easy relation to the refined free energy

$$F(\epsilon_1, \epsilon_2, q) = \frac{\mathcal{G}(\epsilon_1, \epsilon_2, q)}{4\sinh(\frac{\epsilon_1}{2})\sinh(\frac{\epsilon_2}{2})}. \tag{6.2.4}$$

Building up onto the results of [34] one can show that

$$F(\epsilon_1, \epsilon_2, q) = \frac{q^{\frac{1}{2}}E_4(q)}{\eta^{12}(q)}\frac{1}{\epsilon_1\epsilon_2}\exp[-\sum_{k=1}^{\infty}\frac{B_{2k}}{2k(2k)!}(\epsilon_1^{2k}+\epsilon_2^{2k})E_{2k}(q)]. \tag{6.2.5}$$

The Eisenstein series E_{2k} for $k \geq 2$ are modular forms of $SL(2,\mathbb{Z})$ and can be written as polynomials of E_4 and E_6. E_2 is quasi-modular, and we can easily see the modular anomaly equation for $F(\epsilon_1, \epsilon_2, q)$ with respect to E_2 from the above formula,

$$\partial_{E_2}\log(F(\epsilon_1, \epsilon_2, q)) = -\frac{\epsilon_1^2+\epsilon_2^2}{24}, \tag{6.2.6}$$

where we have used the Bernoulli number $B_2 = \frac{1}{6}$. Our modular anomaly equation provides a refinement for the modular anomaly equation in [34] for the class $p + df$.

We can decompose the topological string generating function as in (2.4.19),

$$F(\epsilon_1, \epsilon_2, q) = \sum_{n,g=0}^{+\infty}(\epsilon_1+\epsilon_2)^{2n}(\epsilon_1\epsilon_2)^{g-1}F^{(n,g)}(q), \tag{6.2.7}$$

where $F^{(0,g)}$ are the conventional unrefined amplitudes. It is easy to see from (6.2.5) that the genus zero amplitude is

$$F^{(0,0)}(q) = \frac{q^{\frac{1}{2}}E_4(q)}{\eta^{12}(q)} \tag{6.2.8}$$

and the higher genus amplitudes divided by the genus zero amplitude $\frac{F^{(n,g)}(q)}{F^{(0,0)}(q)}$ are quasi-modular forms of weight $2(n+g)$. We can write down some explicit formulae at low genus

$$\begin{aligned} &F^{(0,1)} = \frac{E_2}{12}F^{(0,0)}, \quad F^{(1,0)} = -\frac{E_2}{24}F^{(0,0)}, \quad F^{(0,2)} = \frac{5E_2^2+E_4}{1440}F^{(0,0)}, \\ &F^{(1,1)} = -\frac{5E_2^2+2E_4}{1440}F^{(0,0)}, \quad F^{(2,0)} = \frac{5E_2^2+2E_4}{57600}F^{(0,0)}. \end{aligned} \tag{6.2.9}$$

The modular anomaly equation (6.2.6) can be written more explicitly for the higher genus amplitudes as

$$\partial_{E_2}F^{(n,g)} = \frac{1}{12}F^{(n,g-1)} - \frac{1}{24}F^{(n-1,g)}, \tag{6.2.10}$$

where the term $F^{(n,g-1)}$ is defined to be zero if $g = 0$, and similarly for $F^{(n-1,g)}$ if $n = 0$. We note that this modular anomaly equation seems quite different from the one we used before (3.3.1). It would be interesting to elucidate the connection.

It is a natural question how the modular anomaly equation (6.1.14) by HST generalizes to

the refined case. There are two hints. Obviously it has to reduce to the unrefined recursive relation in the corresponding limit. Also one knows due to (6.2.10) the refined recursion for case $n_b = 1$. A natural proposal for a refined modular anomaly equation is therefore

$$\begin{aligned}\partial_{E_2} F^{(n,g,n_b)} &= \frac{1}{24}\sum_{n_1=0}^{n}\sum_{g_1=0}^{g}\sum_{s=1}^{n_b-1} s(n_b-s)F^{(n_1,g_1,s)}F^{(n-n_1,g-g_1,n_b-s)} \\ &\quad + \frac{n_b(n_b+1)}{24}F^{(n,g-1,n_b)} - \frac{n_b}{24}F^{(n-1,g,n_b)}. \end{aligned} \tag{6.2.11}$$

Here $F^{(n,g,n_b)}$ are the refined topological string amplitudes with wrapping number n_b on the base, as appearing in the generating function

$$F = \sum_{n,g,n_b=0}^{\infty} (\epsilon_1+\epsilon_2)^{2n}(\epsilon_1\epsilon_2)^{g-1} e^{2\pi i t_b n_b} F^{(n,g,n_b)}(q), \tag{6.2.12}$$

where t_b is the Kähler modulus of the base $\mathbb{P}^1$, and $q = e^{2\pi i\tau}$ is the modulus of the fiber. We have guessed the factor $\frac{n_b}{24}$ in the last term in (6.2.11) by trials and tested by higher genus calculations, which we discuss below. Analogously to (6.1.12), is conjectured that $(\frac{\eta(q)^{12}}{\sqrt{q}})^{n_b}F^{(n,g,n_b)}(q)$ are quasi-modular forms of $SL(2,\mathbb{Z})$ of weight $6n_b+2(g+n)-2$, i. e. polynomials of the Eisenstein series $E_2(q), E_4(q), E_6(q)$, so that the partial derivative with respect to E_2 is well defined.

As already mentioned, our proposal (6.2.11) reduces to the HST modular anomaly equation (6.1.14) in the unrefined case of $n = 0$, which can be further reduced by setting $g = 0$ to the genus zero equation studied earlier in [38]. The generalizations to more elliptic Calabi-Yau manifolds have been studied recently in [82, 110]. The genus zero prepotential with base wrapping number n_b is also equivalent to the partition function of topological $N = 4$ $U(n_b)$ super Yang-Mills theory [31].

We can solve the higher genus refined amplitudes recursively in n, g, n_b by integrating the refined holomorphic anomaly equation. The integration constant is a polynomial of $E_4(q)$ and $E_6(q)$, and needs to be fixed by some boundary conditions. Here we will not use the gap conditions at the conifold locus, because it would require a careful analysis of the moduli space, which is quite complicated in multi-parameter models. Instead, we will utilize the boundary conditions due to vanishing GV invariants. We have mentioned before that if a GV integer vanishes $\tilde{n}^{\beta}_{g_L,g_R} = 0$, then the higher genus neighbors also vanish $\tilde{n}^{\beta}_{g_L+1,g_R} = \tilde{n}^{\beta}_{g_L,g_R+1} = 0$. In addition, at genus zero it is also known [32] that the GV invariants vanish $\tilde{n}^{n_b p+df}_{0,0} = 0$ if $n_b > d$, compare also (6.1.16), except for the case of $n_b = 1, d = 0$ where we have $\tilde{n}^{p}_{0,0} = 1$. The property was used in [38] to fix the integration constants for the genus zero modular anomaly equation.

In the special case of $n_b = 1$ studied previously, the integration of the modular anomaly equation by fixing the integration constants by vanishing GV invariants leads to a nice A-model type formula (6.2.4), related to the refined Göttsche formula (6.1.4) The A-model type formulae are exact to all genera, and are rather convenient for extracting the complete GV invariants $n^{\beta}_{j_L,j_R}$ for a fixed homology class β. Here in the general case with wrapping number $n_b > 1$, the A-model type formula is currently not available and therefore B-model calculations need to be done in order to extract the BPS invariants recursively.

We are able to compute the refined topological string amplitudes to some high genus $n+g$

and some high wrapping number n_b, and we can extract the complete refined GV invariants to some high degree for the base n_b and fiber. We provide some refined amplitudes $F^{(n,g,n_b)}$ for low genus $n+g$ and wrapping number $n_b \geq 2$. The genus zero amplitudes [38] for $n_b = 2, 3$ are

$$\begin{aligned} F^{(0,0,2)} &= \frac{q}{\eta(q)^{24}} \frac{E_4}{24}(E_2E_4 + 2E_6), \\ F^{(0,0,3)} &= \frac{q^{\frac{3}{2}}}{\eta(q)^{36}} \frac{E_4}{15552}(54E_2^2E_4^2 + 216E_2E_4E_6 + 109E_4^3 + 197E_6^2). \end{aligned} \tag{6.2.13}$$

The genus one amplitudes for $n_b = 2, 3$ are

$$\begin{aligned} F^{(0,1,2)} &= \frac{q}{\eta(q)^{24}} \frac{1}{1152}(10E_2^2E_4^2 + 9E_4^3 + 24E_2E_4E_6 + 5E_6^2), \\ F^{(1,0,2)} &= -\frac{q}{\eta(q)^{24}} \frac{1}{1152}(4E_2^2E_4^2 + 7E_4^3 + 8E_2E_4E_6 + 5E_6^2), \\ F^{(0,1,3)} &= \frac{q^{\frac{3}{2}}}{\eta(q)^{36}} \frac{78E_2^3E_4^3 + 299E_2E_4^4 + 360E_2^2E_4^2E_6 + 472E_4^3E_6 + 439E_2E_4E_6^2 + 80E_6^3}{62208}, \\ F^{(1,0,3)} &= -\frac{q^{\frac{3}{2}}}{\eta(q)^{36}} \frac{54E_2^3E_4^3 + 235E_2E_4^4 + 216E_2^2E_4^2E_6 + 776E_4^3E_6 + 287E_2E_4E_6^2 + 160E_6^3}{124416}. \end{aligned} \tag{6.2.14}$$

The genus two amplitudes for $n_b = 2$ are

$$\begin{aligned} F^{(0,2,2)} &= \frac{q}{\eta(q)^{24}} \frac{190E_2^3E_4^2 + 417E_2E_4^3 + 540E_2^2E_4E_6 + 356E_4^2E_6 + 225E_2E_6^2}{207360}, \\ F^{(1,1,2)} &= -\frac{q}{\eta(q)^{24}} \frac{25E_2^3E_4^2 + 79E_2E_4^3 + 60E_2^2E_4E_6 + 122E_4^2E_6 + 50E_2E_6^2}{34560}, \\ F^{(2,0,2)} &= \frac{q}{\eta(q)^{24}} \frac{10E_2^3E_4^2 + 37E_2E_4^3 + 20E_2^2E_4E_6 + 76E_4^2E_6 + 25E_2E_6^2}{69120}. \end{aligned} \tag{6.2.15}$$

We list some results for refined BPS invariants for $n_b > 1$ in the tables A.4 and A.5. The diagonal classes $n_b(p+f)$ correspond to the homology classes with degrees $d = n_b$ in the one-parameter E_8 del Pezzo model, and we check the matching of the corresponding BPS integers for the diagonal classes $n_b(p+f)$ with those in section 5.1.1. Our results demonstrate the compatibility of the refined version of the HST modular anomaly equation we proposed in (6.2.11) with the refined version of the BCOV holomorphic anomaly equation (3.3.1), see also (5.2.8).

In two special cases, namely the genus zero case $n+g=0$ and the case of wrapping number $n_b = 1$, it is clear that one can in principle solve the refined topological strings to all orders in the other directions, i.e. to all orders in n_b in the case of $n+g=0$ and all orders in n, g in the case of $n_b = 1$. It is tempting to wonder whether the vanishing conditions for GV invariants are sufficient in principle to fix the topological string amplitudes to all orders in both $n+g$ and n_b. Unfortunately this is not the case, even for the unrefined case $n=0$. The integration constant for the modular anomaly equation for $F^{(n,g,n_b)}$ is a polynomial of E_4 and E_6 of weighted degree $2(n+g)+6n_b-2$, so the number of unknown constant we need to fix is given by $[\frac{2(n+g)+6n_b-2}{12}]$ for odd $n+g+n_b$, or by $[\frac{2(n+g)+6n_b-8}{12}]$ for even $n+g+n_b$. On the other hand, we can also estimate the number of vanishing GV invariants $\tilde{n}_{g_L,g_R}^{n_bp+df}$

for given n_b, g_L, g_R. It is clear that the GV invariants vanish for $d < n_b$ since the genus zero invariants already vanish $\tilde{n}_{0,0}^{n_b p+df} = 0$ if $d < n_b$. Based on arguments from algebraic geometry, e.g. in [24, 106], we know that the left top genus for the diagonal class $n_b p + n_b f$ goes like quadratic power n_b^2 for large n_b, and this is also confirmed by our explicit results. The GV invariant $\tilde{n}_{g_L,g_R}^{n_b(p+f)}$ would not vanish if the total genus $g_L + g_R$ scaled as quadratic power n_b^2 at large n_b but was smaller than the left top genus. In this case we would have just n_b vanishing GV invariants $\tilde{n}_{0,0}^{n_b p+df}$ from $d = 0, 1, \cdots, n_b - 1$, but the number of unknown constants could be of the order of the quadratic power n_b^2 at large n_b. So eventually the boundary conditions from vanishing GV invariants would not be enough to fix the (refined) topological string amplitudes at large genus.

In fact, we can be a little more precise and show that the situation regarding fixing the ambiguity for the diagonal classes $n_b(p+f)$ is not better or worse than that of the E_8 model. This is rather surprising because in the case of the E_8 model we have utilized the conifold gap condition which is very powerful in fixing the holomorphic ambiguity, while in the half K3 model we do not use the conifold gap condition. In the E_8 model, we have $[\frac{2(n+g)-2}{6}]$ unknown constants in the holomorphic ambiguity in $F^{(n,g)}$ due to the singularity at the orbifold point. Suppose for the genus $g_L + g_R = n + g$ we can fix the (refined) GV invariants $\tilde{n}_{g_L,g_R}^{\beta}$ up to degree $d-1$, then in this case the number of conditions from GV invariants minus the number of unknown constants is $d - 1 - [\frac{2(n+g)-2}{6}]$. On the other hand, for the refined amplitude $F^{(n,g,n_b)}$ with $n_b = d$ in the half K3 model, based on the discussions in the previous paragraph, we can easily check that the number of conditions from GV invariants minus the number of ambiguous constants is up to ± 1 basically $\frac{1}{2}(d-1-[\frac{2(n+g)-2}{6}])$, i.e. one half of that of the E_8 model. So we see that the boundary conditions from GV invariants become insufficient to fix the ambiguity at about the same time for the E_8 model and for the diagonal classes in the half K3 model.

These arguments indicate that the vanishing of BPS invariants in the two-parameter half K3 model should imply the conifold gap conditions in the one-parameter E_8 model. It would interesting to understand this point more carefully.

6.3. The massive half K3

Based on the experience from the studies of higher genus terms in the Nekrasov function for $SU(2)$ Seiberg-Witten theory with $N_f = 4$ fundamental flavors or with one adjoint hypermultiplet in [30], we may hope that the mass deformation provides more boundary conditions for fixing the ambiguity comparing to the massless theory. There is one crucial difference with the studies in [30], where the mass parameters are not moduli parameters, and there is no enumerative geometric interpretation of the refined amplitudes in terms of the BPS invariants. In the present case, the mass parameters represent Kähler moduli of the E_8 part of the half K3 surface, and are part of the geometry of the moduli space. The refined BPS invariants have extra labels in terms of the corresponding wrapping degrees which are Weyl orbits of the E_8 lattice. In the mirror geometry, the mass parameters appear as polynomials in the Seiberg-Witten curve in [30], and in the present case they appear in exponential or trigonometric functions. This point was explained in [62].

We will need to use the theta function of the E_8 lattice Γ_8

$$\Theta(\vec{m},\tau)=\sum_{\vec{w}\in\Gamma_8}\exp(\pi i\tau\vec{w}^2+2\pi i\vec{m}\cdot\vec{w})=\frac{1}{2}\sum_{k=1}^{4}\prod_{j=1}^{8}\theta_k(m_j,\tau)\,, \tag{6.3.1}$$

where $\vec{m}=(m_1,m_2,\cdots,m_8)$ are the E_8 mass parameters. $\theta_k(m,\tau)$ is the ordinary Jacobi theta function and we provide the conventions in appendix A.3.1. The theta function $\Theta(\vec{m},\tau)$ of the E_8 lattice is a power series in $q=e^{2\pi i\tau}$, and from the well-known transformation properties of Jacobi theta functions, one can check that it has the following transformation behavior under a $SL(2,\mathbb{Z})$ transformation

$$\Theta(\frac{\vec{m}}{c\tau+d},\frac{a\tau+b}{c\tau+d})=(c\tau+d)^4\exp(\frac{i\sum_i m_i^2}{c\tau+d})\Theta(\vec{m},\tau). \tag{6.3.2}$$

We see that except for the modular phase, it has modular weight four under the $SL(2,\mathbb{Z})$ transformation. Furthermore, in the massless limit $\vec{m}=0$, the theta function $\Theta(\vec{m},\tau)$ is simply the E_4 Eisenstein series.

One can easily see that the E_8 theta function (6.3.1) is invariant under a Weyl group action[6] on the mass vector $\vec{m}$ since the lattice Γ_8 and the norm of a lattice vector are invariant under the action.

The Weyl orbit of a lattice vector consists of the lattice vectors generated by acting all the elements of the Weyl group $W(E_8)$ on the lattice vector. We can classify the E_8 lattice points into classes of Weyl orbits. It is clear that the lattice vectors in the same Weyl orbit have the same norm. We denote by $\mathcal{O}_{p,k}$ the Weyl orbit whose elements $\vec{w}$ have norm square $\vec{w}\cdot\vec{w}=2p$ and which has order $|\mathcal{O}_{p,k}|=k$. Since the Weyl orbits of the same norm usually have different numbers of elements, the notation should not cause any confusion. It is known that some low Weyl orbits are given as follows

$$\begin{aligned}&\mathcal{O}_{0,1},\quad \mathcal{O}_{1,240},\quad \mathcal{O}_{2,2160},\quad \mathcal{O}_{3,6720},\quad \mathcal{O}_{4,240},\mathcal{O}_{4,17280},\quad \mathcal{O}_{5,30240}\\ &\mathcal{O}_{6,60480},\quad \mathcal{O}_{7,13440},\mathcal{O}_{7,69120},\quad \mathcal{O}_{8,2160},\mathcal{O}_{8,138240},\quad \mathcal{O}_{9,240},\mathcal{O}_{9,181440},\\ &\mathcal{O}_{10,30240},\mathcal{O}_{10,241920},\quad \mathcal{O}_{11,138240},\mathcal{O}_{11,181440},\quad \mathcal{O}_{12,6720},\mathcal{O}_{12,483840},\\ &\mathcal{O}_{13,13440},\mathcal{O}_{13,30240},\mathcal{O}_{13,483840},\quad \cdots .\end{aligned} \tag{6.3.3}$$

We see that the lattice vectors with norm square $0,2,4,6,10,12$ consist of a single Weyl orbit respectively, while the lattice vectors with norm square $8,14,16,18,20,\cdots$ fall into multiple orbits. Any Weyl orbit $\mathcal{O}_{p,k}$ can be multiplied with a positive integer n and generates another Weyl orbit with the same order $\mathcal{O}_{n^2p,k}=\{n\vec{w}|\ \vec{w}\in\mathcal{O}_{p,k}\}$.

The E_8 theta function (6.3.1) can be written as sums over Weyl orbits

$$\Theta(\vec{m},q)=\sum_{\mathcal{O}_{p,k}}q^p\sum_{\vec{w}\in\mathcal{O}_{p,k}}\exp(2\pi i\vec{m}\cdot\vec{w}), \tag{6.3.4}$$

where $q=e^{2\pi i\tau}$. We will see that the (refined) topological string amplitudes in the massive half K3 model are constructed from the E_8 theta function, and can be also written as sums over the Weyl orbits. The refined BPS invariants are labelled by the class n_bp+df and the Weyl orbit $\mathcal{O}_{p,k}$, and denoted as $n_{j_L,j_R}^{n_bp+df,\mathcal{O}_{p,k}}$. We can compute the refined amplitudes in

[6]The Weyl group of E_8 is explicitly described in 4.1.

terms of refined BPS invariants with the formula (2.4.19) and by summing over the homology classes $\beta = (n_b p + df, \mathcal{O}_{p,k})$. As in the massless theory we denote the refined amplitudes by $F^{(n,g,n_b)}(q, \vec{m})$ as appearing in the generating function in (6.2.12). The arguments q and $\vec{m}$ represent the Kähler moduli of the fiber class f and Weyl orbits.

In the massless limit, the sum over a Weyl orbit $\mathcal{O}_{p,k}$, is simply the order $|\mathcal{O}_{p,k}| = k$. So the refined BPS invariants in the massless limit can be computed from the more general massive invariants by

$$(n_{j_L,j_R}^{n_b p+df})_{\text{massless}} = \sum_{\mathcal{O}_{p,k}} k \cdot n_{j_L,j_R}^{n_b p+df,\mathcal{O}_{p,k}}. \tag{6.3.5}$$

First we consider the case of wrapping number $n_b = 1$. In this case the refined Göttsche formula is still available as in the massless theory. We can simply replace the Eisenstein series E_4 with the theta function $\Theta(\vec{m}, \tau)$ for the generating function in (6.2.2) in the massless theory

$$\mathcal{G}(\epsilon_1, \epsilon_2, q) = \Theta(\vec{m}, q) G^{\mathcal{B}_9}(q, y_L, y_R). \tag{6.3.6}$$

Using the formula for the E_8 theta function (6.3.4), we find

$$\begin{aligned} \mathcal{G}(\epsilon_1, \epsilon_2, q) &= \sum_{d=0}^{\infty} \sum_{\mathcal{O}_{p,k}} \sum_{j_L, j_R} (-1)^{2j_L+2j_R} (n^{\mathcal{B}_9})_{j_L,j_R}^{d} \Big(\sum_{k=-j_L}^{j_L} y_L^{2k} \Big) \Big(\sum_{k=-j_R}^{j_R} y_R^{2k} \Big) \\ &\quad \times q^{d+p} \sum_{\vec{w} \in \mathcal{O}_{p,k}} \exp(2\pi i \vec{m} \cdot \vec{w}). \end{aligned} \tag{6.3.7}$$

We can then extract the refined Gopakumar-Vafa BPS invariants similarly as in (6.2.3) for the massless theory, with the additional sum over Weyl orbits

$$\begin{aligned} \mathcal{G}(\epsilon_1, \epsilon_2, q) &= \sum_{d=0}^{\infty} \sum_{\mathcal{O}_{p,k}} \sum_{j_L, j_R} (-1)^{2j_L+2j_R} n_{j_L,j_R}^{p+df,\mathcal{O}_{p,k}} \Big(\sum_{k=-j_L}^{j_L} y_L^{2k} \Big) \Big(\sum_{k=-j_R}^{j_R} y_R^{2k} \Big) \\ &\quad \times q^{d} \sum_{\vec{w} \in \mathcal{O}_{p,k}} \exp(2\pi i \vec{m} \cdot \vec{w}), \end{aligned} \tag{6.3.8}$$

where the sums over j_L, j_R are over non-negative half integers. To extract the BPS integers, we first use the formula (6.1.5) to write the Göttsche product $G^{\mathcal{B}_9}(q, y_L, y_R)$ in terms of the refined Betti numbers of the Hilbert schemes which have been computed in table A.2, and which we denote here by $(n^{\mathcal{B}_9})_{j_L,j_R}^{d}$ with the superscript $\mathcal{B}_9$ to avoid confusion with other BPS invariants.

Comparing (6.3.7) and (6.3.8), we find the BPS invariants in terms of the refined Betti numbers

$$n_{j_L,j_R}^{p+df,\mathcal{O}_{p,k}} = (n^{\mathcal{B}_9})_{j_L,j_R}^{d-p}, \quad \text{for } p \leq d \tag{6.3.9}$$

and it is understood that $n_{j_L,j_R}^{p+df,\mathcal{O}_{p,k}} = 0$ in the case of $p > d$.

We see from the formula (6.3.9) that the refined BPS invariants $n_{j_L,j_R}^{p+df,\mathcal{O}_{p,k}}$ are identical for the homology classes with the same $d - p$. Furthermore for a class $p + df$, the refined BPS invariants vanish if the square length for the Weyl orbits are sufficiently large. The

Weyl orbit with maximal length and non-vanishing BPS invariants will be called the top Weyl orbit(s). Here the top Weyl orbit for the class $p + df$ is the orbit $\mathcal{O}_{d,k}$.

As a check of the formalism, we can compute the refined BPS invariants for the half K3 model in the massless limit using the formula (6.3.5) and the Weyl orbits (6.3.3), in terms of the refined Betti numbers in table A.2. The results agree with those from direct calculations in table A.3. This is simply due to the fact that the E_8 theta function $\Theta(\vec{m}, q)$ is the Eisenstein series E_4 in the massless limit.

Similarly as in the massless theory, we can write down the genus zero amplitude for $n_b = 1$ by setting $y_L = y_R = 1$ in the Göttsche product

$$F^{(0,0,1)} = \frac{q^{\frac{1}{2}}\Theta(\vec{m}, q)}{\eta(q)^{12}}. \tag{6.3.10}$$

The formulae for the refined higher genus amplitudes and the modular anomaly equation for $n_b = 1$ are the same as in the massless theory in (6.2.9), (6.2.10).

Now we consider the case of wrapping number $n_b > 1$. The higher genus refined amplitude with an η function factor $(\frac{\eta(q)^{12}}{\sqrt{q}})^{n_b} F^{(n,g,n_b)}$ has modular weight $2(n + g) + 6n_b - 2$ as in the massless theory. However, the modular ambiguity is not simply a modular form of $SL(2, \mathbb{Z})$. Instead, the modular ambiguity can be written as a linear combination of level n_b E_8 characters, and the coefficients are mass-independent modular forms of $\Gamma_1(n_b)$ [31].

There is a convenient way to write the ansatz for the refined amplitudes. It is known that there are nine Weyl invariant Jacobi modular forms of the E_8 lattice, which can be constructed from the E_8 theta function (6.3.1), see e.g. [116]. The nine Jacobi forms are denoted by A_1, A_2, A_3, A_4, A_5 and B_2, B_3, B_4, B_6. Here $A_1 = \Theta(\vec{m}, \tau)$ is simply the E_8 theta function and we provide the detailed formulae for the other forms in appendix A.3.1. All the characters of the fundamental representation of the higher level E_8 algebra can then be written as polynomials in A_n and B_n, where the generators A_n or B_n contribute an E_8 level number n. For example, at level one there is only one polynomial A_1. There are three polynomials A_1^2, A_2, B_2 at level two, five polynomials $A_1^3, A_1A_2, A_1B_2, A_3, B_3$ at level three, and ten polynomials at level four.

The Jacobi form A_n has modular weight four and B_n has modular weight six, and they are simply the Eisenstein series E_4 and E_6 in the massless limit. Together with the quasi-modular forms E_2, E_4, E_6 of $SL(2, \mathbb{Z})$ which are independent of the mass parameters and have E_8 level number zero, we have all the ingredients for constructing the refined amplitudes.

It is natural to guess that similarly as in the massless theory, the scaled refined amplitude with η function factor $(\frac{\eta(q)^{12}}{\sqrt{q}})^{n_b} F^{(n,g,n_b)}$ can be written as polynomials of the nine E_8 Jacobi forms A_n, B_n and the $SL(2, \mathbb{Z})$ quasi-modular forms E_2, E_4, E_6, and it has E_8 level number n_b and modular weight $2(n + g) + 6n_b - 2$. We find that this is true for level $n_b \leq 4$. However, for level $n_b \geq 5$, the scaled amplitude $(\frac{\eta(q)^{12}}{\sqrt{q}})^{n_b} F^{(n,g,n_b)}$ is not exactly a modular form, but a rational function of modular forms with the powers in E_4 as the denominator. For example for the case of $n_b = 5$, we check that a denominator of E_4 is sufficient and the scaled amplitude $E_4(\frac{\eta(q)^{12}}{\sqrt{q}})^{n_b} F^{(n,g,n_b)}$ is again always a modular form, i.e. can be written as a polynomial of A_n, B_n and E_n.

In any case there is only a finite number of unknown constants in the ansatz for the amplitude. There is no further algebraic relation among the generators for generic mass parameters, so that the expression for a refined amplitude is unique. The E_2-dependent

part of the amplitudes is determined by the refined modular anomaly equation we proposed in (6.2.11). We can further fix the modular ambiguity by vanishing conditions of the refined BPS invariants. Here the vanishing conditions are $n_{0,0}^{n_b p+df,\mathcal{O}_{p,k}} = 0$ for $d < n_b$, except for the case $n_{0,0}^{p,\mathcal{O}_{0,1}} = 1$.

The generators A_n and B_n are sums over Weyl orbits, similarly as the theta function of the E_8 lattice in (6.3.4), as can be seen using their formulae in appendix A.3.1. On the other hand, the refined amplitudes are polynomials of the generators, and in order to extract the refined BPS invariants from the amplitudes, we must write the refined amplitudes as sums over Weyl orbits as in the general formula (2.4.19). So we need to decompose the product of sums over Weyl orbits into a sum of the sums over Weyl orbits as

$$(\sum_{\vec{w}\in\mathcal{O}_1} e^{2\pi i\vec{m}\cdot\vec{w}})(\sum_{\vec{w}\in\mathcal{O}_2} e^{2\pi i\vec{m}\cdot\vec{w}}) = \sum_i m_i \sum_{\vec{w}\in\mathcal{O}'_i} e^{2\pi i\vec{m}\cdot\vec{w}}, \tag{6.3.11}$$

where m_i are non-negative integers for the multiplicity in the decomposition. It is straightforward to compute the decompositions of the E_8 Weyl orbits. The product with the zero-length orbit is trivial $\mathcal{O}_{p,k}\otimes\mathcal{O}_{0,1} = \mathcal{O}_{p,k}$. Here we provide some decompositions for the low orbits

$$\begin{aligned}
\mathcal{O}_{1,240}\otimes\mathcal{O}_{1,240} &= 240\cdot\mathcal{O}_{0,1}\oplus 56\cdot\mathcal{O}_{1,240}\oplus 14\cdot\mathcal{O}_{2,2160}\oplus 2\cdot\mathcal{O}_{3,6720}\oplus\mathcal{O}_{4,240},\\
\mathcal{O}_{2,2160}\otimes\mathcal{O}_{1,240} &= 126\cdot\mathcal{O}_{1,240}\oplus 64\cdot\mathcal{O}_{2,2160}\oplus 27\cdot\mathcal{O}_{3,6720}\oplus 8\cdot\mathcal{O}_{4,17280}\oplus\mathcal{O}_{5,30240},\\
\mathcal{O}_{2,2160}\otimes\mathcal{O}_{2,2160} &= 2160\cdot\mathcal{O}_{0,1}\oplus 576\cdot\mathcal{O}_{1,240}\oplus 280\cdot\mathcal{O}_{2,2160}\oplus 144\cdot\mathcal{O}_{3,6720}\\
&\quad\oplus 126\cdot\mathcal{O}_{4,240}\oplus 70\cdot\mathcal{O}_{4,17280}\oplus 32\cdot\mathcal{O}_{5,30240}\oplus 10\cdot\mathcal{O}_{6,60480}\\
&\quad\oplus 2\cdot\mathcal{O}_{7,69120}\oplus\mathcal{O}_{8,2160},\\
\mathcal{O}_{3,6720}\otimes\mathcal{O}_{1,240} &= 56\cdot\mathcal{O}_{1,240}\oplus 84\cdot\mathcal{O}_{2,2160}\oplus 54\cdot\mathcal{O}_{3,6720}\oplus 56\cdot\mathcal{O}_{4,240}\oplus 28\cdot\mathcal{O}_{4,17280}\\
&\quad\oplus 12\cdot\mathcal{O}_{5,30240}\oplus 3\cdot\mathcal{O}_{6,60480}\oplus\mathcal{O}_{7,13440},\\
\mathcal{O}_{3,6720}\otimes\mathcal{O}_{2,2160} &= 756\cdot\mathcal{O}_{1,240}\oplus 448\cdot\mathcal{O}_{2,2160}\oplus 270\cdot\mathcal{O}_{3,6720}\oplus 168\cdot\mathcal{O}_{4,17280}\\
&\quad\oplus 92\cdot\mathcal{O}_{5,30240}\oplus 48\cdot\mathcal{O}_{6,60480}\oplus 27\cdot\mathcal{O}_{7,13440}\oplus 21\cdot\mathcal{O}_{7,69120}\\
&\quad\oplus 7\cdot\mathcal{O}_{8,138240}\oplus\mathcal{O}_{9,181440}.
\end{aligned} \tag{6.3.12}$$

We mention an identity for the order $|\mathcal{O}_{p_1,k_1}| = k_1$ and related multiplicities. Denote by $m_{p_1,k_1;p_2,k_2}^{p_3,k_3}$ the multiplicity of the Weyl orbit $\mathcal{O}_{p_3,k_3}$ in the decomposition of the product of the orbits $\mathcal{O}_{p_1,k_1}$ and $\mathcal{O}_{p_2,k_2}$. We can fix an element in $\mathcal{O}_{p_3,k_3}$, subtract from it all the elements in $\mathcal{O}_{p_1,k_1}$, and check which orbits the subtracted vectors belong to. We find an one-to-one correspondence of the elements in $\mathcal{O}_{p_1,k_1}$ with all multiplicities of the orbit $\mathcal{O}_{p_3,k_3}$ in the decomposition of $\mathcal{O}_{p_1,k_1}$ with another orbit

$$|\mathcal{O}_{p_1,k_1}| = \sum_{\mathcal{O}_{p_2,k_2}} m_{p_1,k_1;p_2,k_2}^{p_3,k_3}, \tag{6.3.13}$$

which is valid for any two orbits $\mathcal{O}_{p_1,k_1}$ and $\mathcal{O}_{p_3,k_3}$.

Different Weyl orbits with the same norm can be distinguished by their multiplicities in the decomposition of the product of two orbits. For example, we can see in (6.3.12) in the decomposition of $\mathcal{O}_{3,6720}\otimes\mathcal{O}_{2,2160}$, that the multiple orbits $\mathcal{O}_{p,k}$ in the cases of $p = 4, 7, 8, 9$ appear with different multiplicities.

We find that the vanishing conditions of the refined GV invariants over-determine the

modular ambiguity at low genus. The redundancy provides non-trivial tests of the consistency of the refined modular anomaly equation (6.2.11) and the refined amplitudes with generic mass parameters. As an example of an explicit check, we find that if we change the factor of $\frac{n_b}{24}$ in the last term in (6.2.11), there would be no solution at genus two to the modular ambiguity that satisfies the vanishing conditions.

We provide some low order formulae for the refined amplitudes. The genus zero results have been written down in [31], we also include them here for completeness. The formulae in terms of the Jacobi forms A_n and B_n are simpler than those in terms of the E_8 characters originally presented for genus zero case in [31]. The genus zero formulae are

$$\begin{aligned}
F^{(0,0,2)} &= \frac{q}{96\cdot\eta^{24}}[4E_2A_1^2+3E_6A_2+5E_4B_2],\\
F^{(0,0,3)} &= \frac{q^{\frac{3}{2}}}{15552\cdot\eta^{36}}[54A_1^3E_2^2-54A_1^3E_4+135A_1B_2E_2E_4+135A_1A_2E_4^2\\
&\quad +28A_3E_4^3+225A_1B_2E_6+81A_1A_2E_2E_6-28A_3E_6^2]. \qquad (6.3.14)
\end{aligned}$$

Some higher genus formulae are

$$\begin{aligned}
F^{(1,0,2)} &= -\frac{q}{1152\cdot\eta^{24}}[4A_1^2E_2^2+4A_1^2E_4+5B_2E_2E_4+3A_2E_4^2+5B_2E_6+3A_2E_2E_6],\\
F^{(0,1,2)} &= \frac{q}{1152\cdot\eta^{24}}[10A_1^2E_2^2+6A_1^2E_4+15B_2E_2E_4+3A_2E_4^2+5B_2E_6+9A_2E_2E_6],\\
F^{(1,0,3)} &= -\frac{q^{\frac{3}{2}}}{124416\cdot\eta^{36}}[54A_1^3E_2^3+18A_1^3E_2E_4+135A_1B_2E_2^2E_4+630A_1B_2E_4^2\\
&\quad +189A_1A_2E_2E_4^2-160B_3E_4^3+28A_3E_2E_4^3-72A_1^3E_6+315A_1B_2E_2E_6\\
&\quad +81A_1A_2E_2^2E_6+378A_1A_2E_4E_6+160B_3E_6^2-28A_3E_2E_6^2],\\
F^{(0,1,3)} &= \frac{q^{\frac{3}{2}}}{62208\cdot\eta^{36}}[78A_1^3E_2^3-54A_1^3E_2E_4+225A_1B_2E_2^2E_4+360A_1B_2E_4^2\\
&\quad +297A_1A_2E_2E_4^2-80B_3E_4^3+56A_3E_2E_4^3-24A_1^3E_6+495A_1B_2E_2E_6\\
&\quad +135A_1A_2E_2^2E_6+216A_1A_2E_4E_6+80B_3E_6^2-56A_3E_2E_6^2], \qquad (6.3.15)\\
F^{(2,0,2)} &= \frac{q}{138240\cdot\eta^{24}}[20A_1^2E_2^3+44A_1^2E_2E_4+25B_2E_2^2E_4+65B_2E_4^2+30A_2E_2E_4^2\\
&\quad +48A_1^2E_6\ +50B_2E_2E_6+15A_2E_2^2E_6+39A_2E_4E_6],\\
F^{(1,1,2)} &= -\frac{q}{69120\cdot\eta^{24}}[50A_1^2E_2^3+98A_1^2E_2E_4+75B_2E_2^2E_4+105B_2E_4^2+60A_2E_2E_4^2\\
&\quad +76A_1^2E_6+100B_2E_2E_6+45A_2E_2^2E_6+63A_2E_4E_6],\\
F^{(0,2,2)} &= \frac{q}{414720\cdot\eta^{24}}[380A_1^2E_2^3+564A_1^2E_2E_4+675B_2E_2^2E_4+315B_2E_4^2+270A_2E_2E_4^2\\
&\quad +208A_1^2E_6+450B_2E_2E_6+405A_2E_2^2E_6+189A_2E_4E_6]. \qquad (6.3.16)
\end{aligned}$$

In the massless limit the E_8 Jacobi forms simplify as $A_n = E_4, B_n = E_6$, and these formulae reduce to the ones previously obtained in (6.2.13), (6.2.14) and (6.2.15).

We list the refined BPS invariants for the case $n_b = 2$ in the tables A.6 and A.7. We see that the top Weyl orbit $\mathcal{O}_{p,k}$ for the class $2p + df$ is $p = 2d - 2$. This is easy to understand from the formula (6.3.4), which shows the Weyl orbits with maximal norm in the coefficient of q^d are $\mathcal{O}_{2d,k}$ in the level two E_8 characters $\Theta(2\vec{m}, 2\tau)$, $\Theta(\vec{m}, \frac{\tau}{2})$ and $\Theta(\vec{m}, \frac{\tau+1}{2})$, which appear in the formulae for the Jacobi forms A_2 and B_2. Our explicit results further show

that the contributions of the Weyl orbits $\mathcal{O}_{2d,k}$ and $\mathcal{O}_{2d-1,k}$ vanish, so that the top Weyl orbit turns out to be $\mathcal{O}_{2d-2,k}$. Another interesting feature is that the refined BPS invariants are similar for the classes $\beta = (2p+df, \mathcal{O}_{p,k})$ with the same value of $2d-2-p$. In particular, the refined BPS invariants have the smallest top genus, and are exactly identical for the top Weyl orbits $p = 2d-2$. The exact identifications gradually disappear for classes with higher values of $2d-2-p$.

Some refined BPS invariants for the cases $n_b = 3, 4$ are listed in the tables A.8 and A.9. We find that the general empirical formula of the top Weyl orbit $\mathcal{O}_{p,k}$ for the class $n_b p + df$ reads

$$p = n_b d - \frac{n_b(n_b+1)}{2} + 1. \tag{6.3.17}$$

Below the top Weyl orbit, the refined BPS invariants $n_{j_L,j_R}^{n_b p+df,\mathcal{O}_{p,k}}$ may still completely vanish for some homology classes with small non-negative values of $n_b d - \frac{n_b(n_b+1)}{2} + 1 - p$. However, there is at least one Weyl orbit $\mathcal{O}_{p,k}$ at each integer $p \leq n_b d - \frac{n_b(n_b+1)}{2} + 1$, where the refined BPS invariants do not completely vanish.

The non-vanishing refined BPS invariants at the top Weyl orbit have the top genus pair $(g_L, g_R)^{top} = (0, n_b - 1)$. Furthermore, the top genus pair for the classes with non-vanishing BPS invariants increases exactly at the same place as we lower the Weyl orbit. So the top genus pair for the class $(n_b p + df, \mathcal{O}_{p,k})$ with non-vanishing BPS invariants is

$$(g_L, g_R)^{top} = (n_b d - \frac{n_b(n_b+1)}{2} + 1 - p)(1,1) + (0, n_b - 1). \tag{6.3.18}$$

These formulae should come from the algebraic geometric properties of holomorphic curves in the half K3 surface.

Again as in the $n_b = 1$ case, we can reproduce the results for the massless theory of the half K3 model in tables A.4 and A.5 using the formula (6.3.5), the Weyl orbits (6.3.3) and the more general refined BPS invariants in tables A.6, A.7, A.8 and A.9 of the massive theory.

It is clear that in the massive theory it is easier to fix the modular ambiguity than in the massless theory. For example, for the case of genus $n + g = 1$ and $n_b = 1$, there is one modular ambiguity in the massless theory which is proportional to E_6, but there is no modular ambiguity in the massive theory since there is no E_8 level one holomorphic modular form of weight 6.

We discuss whether the vanishing conditions are sufficient for fixing the modular ambiguity in more detail. We have used the vanishing conditions $n_{0,0}^{n_b p+df,\mathcal{O}_{p,k}} = 0$ for $d < n_b$ (with the exception $n_{0,0}^{p,\mathcal{O}_{0,1}} = 1$). Surprisingly it turns out that there are also vanishing conditions available even for arbitrarily large fiber degree d, due to the the empirical formula for the top Weyl orbits (6.3.17). For a level n_b Jacobi modular form which is a polynomial of the generators A_n and B_n, one can check that the highest Weyl orbit appearing in the coefficient of q^d has the half norm square $p = n_b d$. The sum of the form $q^d \sum_{\vec{w} \in \mathcal{O}_{p,k}} e^{2\pi i \vec{w}\cdot\vec{m}}$ with $p = n_b d$ is non-vanishing in the Jacobi form for infinitely many fiber degrees d. For $n_b > 1$, this is higher than the top Weyl orbit with non-vanishing BPS invariants according to our formula (6.3.17). So the vanishing of the BPS invariants $n_{j_L,j_R}^{n_b p+df,\mathcal{O}_{p,k}} = 0$ for $p > n_b d - \frac{n_b(n_b+1)}{2} + 1$ should impose constraints on the ansatz for the level n_b refined topological amplitudes for these fiber degrees.

However, one can construct a certain ansatz for the modular ambiguity at level $n_b \geq 2$, such that the sums of the form $q^d \sum_{\vec{w}\in\mathcal{O}_{p,k}} e^{2\pi i \vec{w}\cdot\vec{m}}$ do not appear for all degrees d and Weyl orbits with $p > n_b d - \frac{n_b(n_b+1)}{2} + 1$. For example, we can consider the case of $n_b = 2$ and genus $n + g = 3$. The modular ambiguity is a Jacobi form of level $n_b = 2$ and weight 16, multiplied by the factor of $\frac{q}{\eta(q)^{24}}$. The level 2 forms A_2, B_2 and A_1^2 can be written in terms of sums of the form $q^d \sum_{\vec{w}\in\mathcal{O}_{p,k}} e^{2\pi i \vec{w}\cdot\vec{m}}$, where the Weyl orbit $p \leq 2d$. We can look at an example of a modular ambiguity $\frac{q(\mathrm{E}_6^2 - E_4^3)}{\eta^{24}} A_2 \sim q A_2$. Due to the extra factor of q, now the modular ambiguity qA_2 is written as a sum of the form $q^d \sum_{\vec{w}\in\mathcal{O}_{p,k}} e^{2\pi i \vec{w}\cdot\vec{m}}$, where $p \leq 2d-2$. So this ambiguity cannot be fixed by the vanishing conditions of BPS invariants due to the top Weyl orbit formula (6.3.17).

6.4. Flow to the del Pezzo models

One can take some limits of the mass parameters and flow from the E_8 model to E_n ($n = 5, 6, 7$) models [62]. We consider the diagonal class $\beta = (d(p+f), \mathcal{O}_{p,k})$ where the base number n_b equals d, and denote the parameter q as the combined Kähler parameter of the base and fiber classes. We have discussed that the E_8 model is simply the massless limit of the diagonal classes in half K3 model. For the E_n ($n = 5, 6, 7$) model, one performs the following scalings of q and the mass parameters

$$\begin{aligned} &q \to e^{2\pi(8-n)\Lambda} q, \quad m_j \to i\Lambda + \mu, \quad (j = n, \cdots, 7), \\ &m_8 \to -i(8-n)\Lambda + \mu\,. \end{aligned} \tag{6.4.1}$$

The refined amplitudes of the half K3 model consist of sums over the Weyl orbits of the E_8 lattice of the form $\sum_{\vec{w}\in\mathcal{O}_{p,k}} q^d e^{2\pi i \vec{w}\cdot\vec{m}}$. To flow to the E_n model, we keep only the terms which are independent of the scaling parameter Λ under the scaling (6.4.1). We denote by $\mathcal{O}_{p,k}^{\mathrm{E}_n,d}$ the subset of the E_8 Weyl orbit $\mathcal{O}_{p,k}$, whose elements satisfy the condition

$$\mathcal{O}_{p,k}^{\mathrm{E}_n,d} := \{\vec{w} \in \mathcal{O}_{p,k} | \sum_{j=n}^{7} w_j - (8-n) w_8 = (8-n) d \}. \tag{6.4.2}$$

This condition is also compatible with multiple cover contributions in the refined topological amplitudes, namely if a lattice vector $\vec{w} \in \mathcal{O}_{p,k}^{\mathrm{E}_n,d}$, then it is also true that $r\vec{w} \in \mathcal{O}_{r^2 p,k}^{\mathrm{E}_n,rd}$ for any multi-covering positive integer r.

To compare with the results in section 5.1, we further take the massless limit for the remaining mass parameters $\mu \to 0$ and $m_j \to 0$ ($j = 1, \cdots, n-1$). The sum over the subset $\mathcal{O}_{p,k}^{\mathrm{E}_n,d}$ of the E_8 Weyl orbit is then simply the order, i.e. the number of elements of the subset. Similar to the formula (6.3.5), we can compute the refined BPS invariants for the E_n models by the formula

$$(n_{j_L,j_R}^d)_{\mathrm{E}_n} = \sum_{\mathcal{O}_{p,k}} |\mathcal{O}_{p,k}^{\mathrm{E}_n,d}| \cdot n_{j_L,j_R}^{d(p+f),\mathcal{O}_{p,k}}. \tag{6.4.3}$$

It is straightforward to check the elements in the E_8 Weyl orbits (6.3.3) and to compute the subset $\mathcal{O}_{p,k}^{\mathrm{E}_n,d}$ for various degrees d and E_n models. We list the data for the orders of the subset for some low orbits and degrees for the $\mathrm{D}_5, \mathrm{E}_6, \mathrm{E}_7$ models in the table 6.1.

We can then compute the refined BPS invariants for the E_n models using the formula (6.4.3), the orders of the Weyl orbits in table 6.1, and the refined BPS invariants for the diagonal classes $n_b = d$ for the E_8 model in tables A.6, A.7, A.8 and A.9. We reproduce the results in the corresponding tables for D_5, E_6 and E_7 up to $d \leq 5$ in section 5.1.

We note the following inequality for the element $\vec{w}$ in $\mathcal{O}_{p,k}^{\mathrm{E}_n,d}$

$$\begin{aligned}(8-n)^2 d^2 &= (\sum_{j=n}^{7} w_j - (8-n)w_8)^2 \leq (\sum_{j=n}^{7} 1 + (8-n)^2)(\sum_{j=n}^{8} w_j^2) \\ &\leq 2(8-n)(9-n)p\,. \end{aligned} \tag{6.4.4}$$

Therefore the orbit must satisfy $p \geq \frac{(8-n)d^2}{2(9-n)}$, otherwise the subset $\mathcal{O}_{p,k}^{\mathrm{E}_n,d}$ would be empty. This is also confirmed explicitly by the data in table 6.1. Furthermore, the top Weyl orbit with non-vanishing BPS invariants is $p \leq \frac{d(d-1)}{2}+1$ for the diagonal classes $n_b = d$ according to (6.3.17). So the argument in the sum in the formula for the E_n model (6.4.3) is only non-vanishing for the E_8 Weyl orbits $\mathcal{O}_{p,k}$ in the range $\frac{(8-n)d^2}{2(9-n)} \leq p \leq \frac{d(d-1)}{2}+1$ for the half square length p of the orbit.

We can also flow to the $\mathbb{P}^1 \times \mathbb{P}^1$ and $\mathbb{P}^2$ models. For the $\mathbb{P}^1 \times \mathbb{P}^1$ model, we set $n = 1$ in the subset (6.4.2) of the E_8 Weyl orbits

$$\mathcal{O}_{p,k}^{\mathbb{P}^1\times\mathbb{P}^1,d} := \{\vec{w} \in \mathcal{O}_{p,k} |\ \sum_{j=1}^{7} w_j - 7w_8 = 7d\ \}. \tag{6.4.5}$$

As the point $\vec{w}$ lies in the E_8 lattice, the sum $\sum_{j=1}^{8} w_j$ is an even integer and w_j is an integer or half integer, we see that $\mathcal{O}_{p,k}^{\mathbb{P}^1\times\mathbb{P}^1,d}$ is an empty set for odd degree d. The formula for the refined BPS invariants (6.4.3) is modified to depend on only even degree invariants from the half K3 model

$$(n_{j_L,j_R}^{d})_{\mathbb{P}^1\times\mathbb{P}^1} = \sum_{\mathcal{O}_{p,k}} |\mathcal{O}_{p,k}^{\mathbb{P}^1\times\mathbb{P}^1,2d}| \cdot n_{j_L,j_R}^{2d(p+f),\mathcal{O}_{p,k}}. \tag{6.4.6}$$

We also list the data for $|\mathcal{O}_{p,k}^{\mathbb{P}^1\times\mathbb{P}^1,d}|$ for even d in table 6.1, and reproduce the results for $d = 1, 2$ in table A.4.1 in appendix A.4.1. Similarly as for the E_n models, we find that the argument in the sum (6.4.6) is non-vanishing in the range $\frac{7}{4}d^2 \leq p \leq 2d^2 - d + 1$.

For the $\mathbb{P}^2$ model, the subset of Weyl orbits is defined as

$$\mathcal{O}_{p,k}^{\mathbb{P}^2,d} := \{\vec{w} \in \mathcal{O}_{p,k} |\ \sum_{j=1}^{7} w_j - w_8 = 8d\ \}. \tag{6.4.7}$$

We also list the data for $|\mathcal{O}_{p,k}^{\mathbb{P}^2,d}|$ in table 6.1. The refined invariants from the half K3 model only contribute when the degree d is divisible by 3

$$(n_{j_L,j_R}^{d})_{\mathbb{P}^2} = \sum_{\mathcal{O}_{p,k}} |\mathcal{O}_{p,k}^{\mathbb{P}^2,d}| \cdot n_{j_L,j_R}^{3d(p+f),\mathcal{O}_{p,k}}. \tag{6.4.8}$$

Similarly as in the other models, the argument in the sum (6.4.8) is non-vanishing in the range $4d^2 \leq p \leq \frac{3d(3d-1)}{2} + 1$. Our results for the massive half K3 model are available for

d \ orbits	$\mathcal{O}_{0,1}$	$\mathcal{O}_{1,240}$	$\mathcal{O}_{2,k}$	$\mathcal{O}_{3,k}$	$\mathcal{O}_{4,k_1}$	$\mathcal{O}_{4,k_2}$	$\mathcal{O}_{5,k}$	$\mathcal{O}_{6,k}$	$\mathcal{O}_{7,k_1}$	$\mathcal{O}_{7,k_2}$	$\mathcal{O}_{8,k_1}$	$\mathcal{O}_{8,k_2}$
1	0	16	176	640	0	1296	2416	4336	976	4960	0	8272
2	0	0	10	140	16	576	1052	2710	508	2704	176	6336
3	0	0	0	0	0	16	176	640	208	1088	0	2416
4	0	0	0	0	0	0	0	1	6	40	10	320
5	0	0	0	0	0	0	0	0	0	0	0	0

The D_5 model

d \ orbits	$\mathcal{O}_{0,1}$	$\mathcal{O}_{1,240}$	$\mathcal{O}_{2,k}$	$\mathcal{O}_{3,k}$	$\mathcal{O}_{4,k_1}$	$\mathcal{O}_{4,k_2}$	$\mathcal{O}_{5,k}$	$\mathcal{O}_{6,k}$	$\mathcal{O}_{7,k_1}$	$\mathcal{O}_{7,k_2}$	$\mathcal{O}_{8,k_1}$	$\mathcal{O}_{8,k_2}$
1	0	27	270	891	54	1944	3564	5724	1350	7560	432	12096
2	0	0	27	270	27	864	1998	3564	972	4752	270	8640
3	0	0	0	1	2	72	414	1260	434	1944	144	4032
4	0	0	0	0	0	0	0	27	54	216	27	864
5	0	0	0	0	0	0	0	0	0	0	0	0

The E_6 model

d \ orbits	$\mathcal{O}_{0,1}$	$\mathcal{O}_{1,240}$	$\mathcal{O}_{2,k}$	$\mathcal{O}_{3,k}$	$\mathcal{O}_{4,k_1}$	$\mathcal{O}_{4,k_2}$	$\mathcal{O}_{5,k}$	$\mathcal{O}_{6,k}$	$\mathcal{O}_{7,k_1}$	$\mathcal{O}_{7,k_2}$	$\mathcal{O}_{8,k_1}$	$\mathcal{O}_{8,k_2}$
1	0	56	576	1512	0	4032	5544	12096	1568	12096	0	24192
2	0	1	126	756	56	2016	4158	7560	1512	10080	576	16128
3	0	0	0	56	0	576	1512	4032	1512	4032	0	12096
4	0	0	0	0	1	0	126	756	56	2016	126	4032
5	0	0	0	0	0	0	0	0	56	0	0	576

The E_7 model

d \ orbits	$\mathcal{O}_{0,1}$	$\mathcal{O}_{1,240}$	$\mathcal{O}_{2,k}$	$\mathcal{O}_{3,k}$	$\mathcal{O}_{4,k_1}$	$\mathcal{O}_{4,k_2}$	$\mathcal{O}_{5,k}$	$\mathcal{O}_{6,k}$	$\mathcal{O}_{7,k_1}$	$\mathcal{O}_{7,k_2}$	$\mathcal{O}_{8,k_1}$	$\mathcal{O}_{8,k_2}$
2	0	0	2	84	0	422	784	2184	420	2380	0	5266
4	0	0	0	0	0	0	0	0	0	1	2	42
6	0	0	0	0	0	0	0	0	0	0	0	0

The $\mathbb{P}^1 \times \mathbb{P}^1$ model

d \ orbits	$\mathcal{O}_{0,1}$	$\mathcal{O}_{1,240}$	$\mathcal{O}_{2,k}$	$\mathcal{O}_{3,k}$	$\mathcal{O}_{4,k_1}$	$\mathcal{O}_{4,k_2}$	$\mathcal{O}_{5,k}$	$\mathcal{O}_{6,k}$	$\mathcal{O}_{7,k_1}$	$\mathcal{O}_{7,k_2}$	$\mathcal{O}_{8,k_1}$	$\mathcal{O}_{8,k_2}$
1	0	0	0	0	0	1	56	420	168	728	70	2296
2	0	0	0	0	0	0	0	0	0	0	0	0

The $\mathbb{P}^2$ model

Table 6.1.: The orders of subsets $|\mathcal{O}_{p,k}^{X,d}|$ for $X = \mathrm{D}_5, \mathrm{E}_6, \mathrm{E}_7, \mathbb{P}^1 \times \mathbb{P}^1, \mathbb{P}^2$ models. Here $k_i = |\mathcal{O}_{p,k_i}|$ are the orders of the E_8 Weyl orbits available in (6.3.3), and we sort them by increasing order in the case of multiple orbits with the same norm.

checking only the $d = 1$ result in table 5.3 in section 5.3.

We can check the top genus pairs for the refined BPS invariants $n^d_{j_L,j_R}$ using the formulae (6.4.3), (6.4.6) and (6.4.8) for the del Pezzo models. Using the general top genus formula (6.3.18) for the massive half K3 model and specializing to the diagonal classes $n_b = d$, we find that the top genus pairs for $n^d_{j_L,j_R}$ are realized at the smallest integer p for which the orbit $\mathcal{O}^{X,d}_{p,k}$ is non-empty, where $X = \mathrm{D}_5, \mathrm{E}_6, \mathrm{E}_7, \mathrm{E}_8, \mathbb{P}^1 \times \mathbb{P}^1, \mathbb{P}^2$ represents the del Pezzo models. We have discussed all the models except E_8, for which there is no constraint for Weyl orbits and the lower bound is simply $p \geq 0$. From our discussions we find the top genus pairs for various models

$$(g_L, g_R)^{top} = \begin{cases} ([\frac{d^2}{2(9-n)} - \frac{d}{2}])(1,1) + (1,d), & \text{for the } \mathrm{D}_5, \mathrm{E}_6, \mathrm{E}_7, \mathrm{E}_8 \text{ models}, \\ ([\frac{d^2}{4}] - d)(1,1) + (1,2d), & \text{for the } \mathbb{P}^1 \times \mathbb{P}^1 \text{ model}, \\ (\frac{(d-1)(d-2)}{2}, \frac{d(d+3)}{2}), & \text{for the } \mathbb{P}^2 \text{ model}. \end{cases} \tag{6.4.9}$$

The formula agrees with all results in the corresponding tables that can be found in section 5.1 for the groups D_5, E_6, E_7 and E_8, in section 5.3 for the group $\mathbb{P}^2$ and in section A.4.1 for the diagonal $\mathbb{P}^1 \times \mathbb{P}^1$-model.

Furthermore, we can now explain certain patterns for the refined BPS invariants at the top genus for the del Pezzo models from the general formulae (6.4.3), (6.4.6) and (6.4.8). One can observe in the just cited tables that the top genus refined invariants follow a periodicity of $9 - n$ for the E_n ($n = 5, 6, 7$) models and a periodicity of two for the $\mathbb{P}^1 \times \mathbb{P}^1$ model, while the top genus numbers are always 1 for the E_8 and $\mathbb{P}^2$ models. The top genus numbers in the D_5, E_6, E_7 models are exactly the dimensions of the smallest irreducible representations of the groups $SO(10)$, E_6, E_7.

We observe from the tables A.6, A.7, A.8, A.9 that for the massive half K3 model, the top genus invariants are always 1. So the patterns for the del Pezzo models should come from the orders of orbits $|\mathcal{O}^{X,d}_{p,k}|$ in the formulae (6.4.3) and (6.4.8), or $|\mathcal{O}^{X,2d}_{p,k}|$ in (6.4.6) for the $X = \mathbb{P}^1 \times \mathbb{P}^1$ case. According to (6.3.18) we should consider the lowest Weyl orbits which have the largest top genus. In the following we will assume that the top genus numbers from the massive half K3 models for the lowest non-empty orbits are always 1, so the top genus number for the del Pezzo models is simply the order of the lowest non-empty orbit, or their sum if there are multiple non-empty lowest orbits with the same length. With this assumption for the massive half K3 model, we explain the patterns and compute the top genus numbers case by case.

For the E_8 model there is no constraint therefore the lowest orbit is simply $\mathcal{O}_{0,1}$, and the top genus number is always $|\mathcal{O}_{0,1}| = 1$.

For the E_7 model, we have discussed that according to the inequality (6.4.4) the lowest orbit $\mathcal{O}^{\mathrm{E}_7,d}_{p,k}$ for degree d is achieved for the smallest integer $p \geq \frac{d^2}{4}$. We discuss the situation according to the divisibility of d by 2.

1. d is an even integer. In this case the norm square of the lowest orbit is $L^2 = 2p = \frac{d^2}{2}$. There is a unique lattice vector $\vec{w} \in \mathcal{O}^{\mathrm{E}_7,d}_{p,k}$, which is $\vec{w} = (0,0,0,0,0,0,\frac{d}{2},-\frac{d}{2})$, and the order is $\sum_k |\mathcal{O}^{\mathrm{E}_7,d}_{p,k}| = 1$. So the top genus number is 1.

2. d is an odd integer. In this case the norm square of the lowest orbit is $L^2 = 2p = \frac{d^2+3}{2}$. There are two classes of the lattice vectors $\vec{w} \in \mathcal{O}^{\mathrm{E}_7,d}_{p,k}$. Firstly, we can use $(w_7, w_8) = (\frac{d}{2}, -\frac{d}{2}) \pm (\frac{1}{2}, \frac{1}{2})$, and all w_i ($i = 1, 2, \cdots, 6$) are 0 except one of them is 1 or -1. There

are $2 \cdot 6 \cdot 2 = 24$ elements in this class. Secondly, we can use $(w_7, w_8) = (\frac{d}{2}, -\frac{d}{2})$, and the w_i $(i = 1, 2, \cdots, 6)$ are either $\frac{1}{2}$ or $-\frac{1}{2}$ with an odd number of them being positive to satisfy the E_8 lattice condition. This class contributes 32 elements. In total we find $\sum_k |\mathcal{O}_{p,k}^{E_7,d}| = 24 + 32 = 56$, which is exactly the top genus number for odd degrees observed in the tables for E_7 in subsection 5.1.2.

For the E_6 model, the lowest orbit $\mathcal{O}_{p,k}^{E_6,d}$ of degree d lies at the smallest integer $p \geq \frac{d^2}{3}$. We discuss the situation according to the remainder of d divided by 3. We successfully derive the top genus numbers in tables for E_6 in subsection 5.1.3 for all cases.

1. $d \equiv 0 \mod 3$. In this case the norm square of the lowest orbit is $L^2 = 2p = \frac{2d^2}{3}$. There is a unique lattice vector $\vec{w} \in \mathcal{O}_{p,k}^{E_6,d}$, which is $\vec{w} = (0, 0, 0, 0, 0, \frac{d}{3}, \frac{d}{3}, -\frac{2d}{3})$, and the order is $\sum_k |\mathcal{O}_{p,k}^{E_6,d}| = 1$. So the top genus number is 1.

2. $d \equiv 1 \mod 3$. In this case the norm square of the lowest orbit is $L^2 = 2p = \frac{2d^2+4}{3}$. There are several classes of the lattice vectors $\vec{w} \in \mathcal{O}_{p,k}^{E_6,d}$. Firstly, we can set $(w_6, w_7, w_8) = (\frac{d}{3}, \frac{d}{3}, -\frac{2d}{3}) - \frac{1}{3}(1, 1, 1)$, and the other w_i $(i = 1, 2, \cdots, 5)$ being 0 except one of them is 1 or -1. There are 10 such vectors. Secondly, we look at $(w_6, w_7, w_8) = (\frac{d}{3}, \frac{d}{3}, -\frac{2d}{3}) + \frac{1}{6}(1, 1, 1)$, the other w_i $(i = 1, 2, \cdots, 5)$ are $\pm\frac{1}{2}$ with even number of them positive. There are 16 such vectors. Finally there is the vector with $(w_6, w_7, w_8) = (\frac{d}{3}, \frac{d}{3}, -\frac{2d}{3}) + \frac{2}{3}(1, 1, 1)$ and all other $w_i = 0$ $(i = 1, 2, \cdots, 5)$. In total we find $\sum_k |\mathcal{O}_{p,k}^{E_6,d}| = 10 + 16 + 1 = 27$.

3. $d \equiv 2 \mod 3$. The norm square of the lowest orbit is also $L^2 = 2p = \frac{2d^2+4}{3}$. This case is similar to the case of $d \equiv 1 \mod 3$. By completely similar reasoning we also find $\sum_k |\mathcal{O}_{p,k}^{E_6,d}| = 27$.

For the D_5 model, the lowest orbit $\mathcal{O}_{p,k}^{D_5,d}$ of degree d lies at the smallest integer $p \geq \frac{3d^2}{8}$. We discuss the situation according to the remainder of d divided by 4, and find complete agreement with the pattern in table 5.1.4.

1. $d \equiv 0 \mod 4$. In this case the norm square of the lowest orbit is $L^2 = 2p = \frac{3d^2}{4}$. There is a unique lattice vector $\vec{w} \in \mathcal{O}_{p,k}^{D_5,d}$, which is $\vec{w} = (0, 0, 0, 0, \frac{d}{4}, \frac{d}{4}, \frac{d}{4}, -\frac{3d}{4})$, and the order is $\sum_k |\mathcal{O}_{p,k}^{D_5,d}| = 1$. So the top genus number is 1.

2. $d \equiv 1 \mod 4$. In this case the norm square of the lowest orbit is $L^2 = 2p = \frac{3d^2+5}{4}$. There are two classes of the lattice vectors $\vec{w} \in \mathcal{O}_{p,k}^{D_5,d}$. Firstly, we can set $(w_5, w_6, w_7, w_8) = (\frac{d}{4}, \frac{d}{4}, \frac{d}{4}, -\frac{3d}{4}) - \frac{1}{4}(1, 1, 1, 1)$, and the other w_i $(i = 1, 2, 3, 4)$ are 0 except one of them is 1 or -1. There are 8 such vectors. Secondly, we look at $(w_5, w_6, w_7, w_8) = (\frac{d}{4}, \frac{d}{4}, \frac{d}{4}, -\frac{3d}{4}) + \frac{1}{4}(1, 1, 1, 1)$, the other w_i $(i = 1, 2, 3, 4)$ are $\pm\frac{1}{2}$ with odd number of them positive to satisfy the E_8 lattice condition. There are 8 such vectors. In total we find $\sum_k |\mathcal{O}_{p,k}^{D_5,d}| = 8 + 8 = 16$.

3. $d \equiv 2 \mod 4$. The norm square of the lowest orbit is also $L^2 = 2p = \frac{3d^2+4}{4}$. Firstly, we find 2 vectors in the orbit with $(w_1, w_2, w_3, w_4) = (0, 0, 0, 0)$ and $(w_5, w_6, w_7, w_8) = (\frac{d}{4}, \frac{d}{4}, \frac{d}{4}, -\frac{3d}{4}) \pm \frac{1}{2}(1, 1, 1, 1)$. Secondly, we consider $(w_5, w_6, w_7, w_8) = (\frac{d}{4}, \frac{d}{4}, \frac{d}{4}, -\frac{3d}{4})$, the other w_i $(i = 1, 2, 3, 4)$ are $\pm\frac{1}{2}$ with even number of them positive to satisfy the E_8 lattice condition. There are 8 such vectors. In total we find $\sum_k |\mathcal{O}_{p,k}^{D_5,d}| = 2 + 8 = 10$ in this case.

4. $d \equiv 3 \bmod 4$. The norm square of the lowest orbit is also $L^2 = 2p = \frac{3d^2+5}{4}$. This case is similar to the case of $d \equiv 1 \bmod 4$. By completely similar reasoning we also find $\sum_k |\mathcal{O}_{p,k}^{\mathrm{D}_5,d}| = 16$.

For the $\mathbb{P}^1 \times \mathbb{P}^1$ model, the lowest orbit $\mathcal{O}_{p,k}^{\mathbb{P}^1\times\mathbb{P}^1,2d}$ of degree d lies at the smallest integer $p \geq \frac{7d^2}{4}$. If d is even, the norm square is $L^2 = 2p = \frac{7d^2}{2}$. There is a unique lattice vector in the orbit $\vec{w} = \frac{d}{4}(1,1,1,1,1,1,1,-7)$. If d is odd, the norm square is $L^2 = 2p = \frac{7d^2+1}{2}$. There are 2 lattice vectors $\vec{w} = \frac{d}{4}(1,1,1,1,1,1,1,-7) \pm \frac{1}{4}(1,1,1,1,1,1,1,1)$. This agrees with the top genus numbers, which are 2 for odd degrees and 1 for even degrees in table A.4.1.

Finally for the $\mathbb{P}^2$ model, the lowest orbit $\mathcal{O}_{p,k}^{\mathbb{P}^2,d}$ of degree d lies at the smallest integer $p \geq 4d^2$. The norm square of the lattice vectors is $L^2 = 2p = 8d^2$. There is a unique vector $\vec{w} = (d,d,d,d,d,d,d,-d)$ in the orbit, implying that the top genus numbers are always 1.

Part II.

Corrections and Nonperturbative Phenomena in F-theory

7. Basic Concepts of F-Theory

In the first chapter of this second part, we discuss some basic background material in F-theory, such as its interpretation as the strong coupling regime of Type IIB string theory and its relation to M-theory and the Heterotic string.

7.1. F-theory as the strong coupling regime of Type IIB

It is well-known that type IIB string theory possesses an SL(2,$\mathbb{Z}$) symmetry that maps the strongly coupled regime of the theory to a different weak-coupling description. More precisely, given the axiodilaton $\tau = C_0 + \frac{i}{g_s}$ and the two-form fields B_2, C_2 coupling to the fundamental as well as to the D1 string, the theory is conjectured to be invariant under

$$\begin{pmatrix} C_2 \\ B_2 \end{pmatrix} \mapsto \begin{pmatrix} C_2' \\ B_2' \end{pmatrix} = M \begin{pmatrix} C_2 \\ B_2 \end{pmatrix}, \qquad \tau \mapsto \frac{a\tau + b}{c\tau + d}, \quad \begin{pmatrix} a & b \\ c & d \end{pmatrix} \in \mathrm{SL}(2,\mathbb{Z})\,. \tag{7.1.1}$$

Classically, the symmetry group would be SL(2,$\mathbb{R}$), but this gets broken to SL(2,$\mathbb{Z}$) due to D(-1) instantons. This symmetry leads in particular to the notion of $[p,q]$-strings which the usual F-string transforms into after applying a general SL(2,$\mathbb{Z}$)-transformation. These have an interpretation as bound states of fundamental and D1-strings. Analogously, one is lead to consider (p,q)7-branes and in general a $[p,q]$-string is allowed to end on a (p,q)7-brane.

That these states have to enter the discussion is also clear from a different perspective. The axiodilaton profile around a usual D7-brane is given[1] by

$$\tau(z) = \frac{1}{2\pi i} \ln(z) \tag{7.1.2}$$

and passing once around the brane with an F1-string will transform it by

$$M = \begin{pmatrix} 1 & 1 \\ 0 & 1 \end{pmatrix}. \tag{7.1.3}$$

This has among others two immediate consequences. First of all (7.1.2) implies that one is inevitably[2] taken out of the weak coupling regime where the perturbative description of type IIB string theory is valid. Also the profile cannot hold globally as it implies a negative string coupling constant far away from the brane and diverges close to it. While the profile gets corrected by the presence of other 7-branes far away from this brane, this picture breaks down close to the 7-brane where the weakly coupled IIB description becomes valid. In fact we discover corrections that render the profile finite from the F-theory side when discussing the gauge coupling function of seven-branes from the F-theory perspective in section 9.

The general idea of F-theory [11] is to geometrize the SL(2,$\mathbb{Z}$) symmetry by considering it as the group of large diffeomorphisms of an auxiliary torus which is fibered over the

[1] This is simply the fundamental solution for a co-dimension two point source.

[2] Apart from the case of local tadpole cancellation, compare the discussion of the Sen limit.

space-time and encodes a non-perturbative profile of the string coupling constant. Loci, where the fibration becomes singular, are identified with the positions of 7-branes. The easiest setup is in eight dimensions which corresponds to a compactification of F-theory on an elliptically fibered K3 manifold. The base of this is fibration is given by a $\mathbb{P}^1$ and locally the fibration reads[3]

$$y^2 = x^3 + f(z)x + g(z)\,. \tag{7.1.4}$$

Here z denotes the coordinate on the base and f and g are sections of $\mathcal{O}(8)$ and $\mathcal{O}(12)$ respectively. The discriminant

$$\Delta = 27g^2 + 4f^3 \tag{7.1.5}$$

has accordingly 24 zeros which describe the positions of 7-branes. At such a zero the j-function

$$j(z) = \frac{4(24f)^3}{\Delta} \tag{7.1.6}$$

becomes singular and via its Fourier expansion

$$j(q) = \frac{1}{q} + 744 + \ldots, \qquad q = e^{2\pi i \tau} \tag{7.1.7}$$

one also finds at a single zero of the discriminant that

$$\tau = \frac{1}{2\pi i}\ln(z)\,. \tag{7.1.8}$$

This setup describes generically 24 seven-branes distributed among the S^2 which from the type IIB perspective can be argued for by noting that each seven-brane gives rise to a deficit angle of $\frac{\pi}{6}$. An easy monodromy argument also shows that not all seven-branes can be considered as D7-branes at the same time. In fact measuring one D7-brane charge with a loop on $\mathbb{P}^1$, the charges of the other 23 7-branes have to sum up to -1. When one moves zeros together, which physically corresponds to forming brane stacks, one obtains higher singularities that give rise to SU(N), SO(N) as well as exceptional gauge groups. The respective gauge group can be read off from the Kodaira classification (7.1) of singularities [137].

Roughly speaking the following happens. The resolution of these singularities introduces a Hirzebruch-Jung tree of $\mathbb{P}^1$'s that intersect as the negative of the Cartan matrix of the corresponding ADE group. These correspond to Cartan generators of the gauge group while the roots are given by M2-branes wrapping these $\mathbb{P}^1$'s that become massless when one blows down this configuration in order to re-obtain the corresponding singularity. It was even before the birth of F-theory shown by Schwarz [159] that M2 branes that wrap (p, q)-cycles of a torus compactification of M-theory gives rise to $[p, q]$-strings after performing a T-duality transformation.

In higher-dimensional F-theory compactifications one obtains in general singularities over divisors and the classification of possible singularities is still a subject of current research, e.g. [161]. In particular, it becomes possible that different discriminant loci of (7.1.5) intersect which leads to an enhancement of the singularities and in addition to the generation of matter (co-dimension two) and Yukawa couplings (co-dimension three) [160].

[3]Note that we use different conventions than in (3.4.1) which are however more common to the F-theory literature.

order (f)	order (g)	order (Δ)	singularity
≥ 0	≥ 0	0	none
0	0	n	A_{n-1}
≥ 1	1	2	none
1	≥ 2	3	A_1
≥ 2	2	4	A_2
2	≥ 3	$n+6$	D_{n+4}
≥ 2	3	$n+6$	D_{n+4}
≥ 3	4	8	E_6
3	≥ 5	9	E_7
≥ 4	5	10	E_8

Table 7.1.: The Kodaira classification of singular fibers. Here f and g are the coefficients of the Weierstrass normal form, Δ is the discriminant as defined in (7.1.5) and order refers to their order of vanishing at a particular zero.

7.2. Embedding F-theory into the web of string dualities

Unfortunately, there is no microscopic description of F-theory which could be used to compute the effective action upon compactifying on Calabi-Yau manifolds. Besides its high conceptual relevance, it is therefore important to understand how F-theory is connected to other string theories in order to perform such computations. In the next two sections we briefly review the two most important dualities, namely M-/F-theory duality and Heterotic F-theory duality.

7.2.1. M/F-Theory duality

The bosonic part of the eleven-dimensional supergravity action that constitutes the low-energy approximation of M-theory is given[4] by

$$S_{\mathrm{M}}^{(11)} = -2\pi \int_{\mathcal{M}_{11}} \tfrac{1}{2} R * 1 + \tfrac{1}{4} G_4 \wedge * G_4 + \tfrac{1}{12} C_3 \wedge G_4 \wedge G_4 - 2\pi \int_{\mathcal{M}_{11}} C_3 \wedge X_8 + \sum_k S_{\mathrm{M2}}^k \quad (7.2.1)$$

where locally $G_4 = dC_3$ is the field strength of the M-theory three-form C_3, and X_8 is a fourth order polynomial in the Riemann curvature of the eleven-dimensional space-time. The last term includes the coupling to M2-branes with action S_{M2}^k. The G_4 field strength, the curvature X_8, and M2-branes can serve as sources in the C_3 equations of motion

$$d * G_4 = \tfrac{1}{2} G_4 \wedge G_4 - X_8 + \sum_k \delta^{(8)}(\Sigma_3^k)\,, \quad (7.2.2)$$

where $\delta^{(8)}(\Sigma_3^k)$ is an eight-form current localizing to the world-volumes Σ_3^k of the M2-branes. To make contact with F-theory, one compactifies down to nine dimensions on a two-torus with metric

$$ds_M^2 = \frac{v}{\tau_2}\Big((dx + \tau_1)^2 + \tau_2^2 dy^2\Big) + ds_9^2\,. \quad (7.2.3)$$

[4] We omit in general dimensions for actions in this thesis. Compare also to appendix A for the conventions used.

We identify the x-direction as the M-theory circle while a T-duality is performed along the y-direction. To identify the axiodilaton one recalls that the circle connection corresponds to the C_1 field in type IIA and gets T-dualized into the C_0 field, while the IIA coupling is related to the radius of the M-theory circle, see [47] for a detailed calculation:

$$\tau = C_0 + \frac{i}{g_{IIB}}, \quad ds^2_{IIB,E} = -(dx^0)^2 + (dx^1)^2 + (dx^2)^2 + \frac{l_s^4}{v} dy^2 + ds^2_{B_6}. \tag{7.2.4}$$

The F-Theory limit corresponds to taking the volume v to zero which shows that in this limit one obtains as expected a ten-dimensional compactification. Higher-dimensional compactifications are obtained by fibering this duality over a base manifold B_n, i.e. they have to be performed on an elliptically fibered Calabi-Yau manifold. Although the main idea is simple, there are in general many subtleties in this limit. We do not want to discuss this issue here at length but point out two important examples. Typically one is interested in F-theory on singular Calabi-Yau manifolds as these engineer gauge theories. In contrast, M-theory is only well defined on smooth manifolds and therefore one has to first resolve all singularities. However, in the F-theory lift the blow-down is necessarily taken and the Coulomb branch cannot be approached from the F-theory side. Also, in order to compute the effective action of an F-theory compactification [138] down to $2n$ dimensions, it is not possible to extract the data of the $2n$-dimensional action directly, but one has to compactify this further on a circle and compare this with the corresponding M-theory compactification. In addition, one has to identify on both sides the limit in the moduli space that corresponds to the F-theory lift.

We continue the discussion with supersymmetric backgrounds for M-theory compactifications on general Calabi-Yau fourfolds. In order to specify a consistent background, one not only needs to specify a compactification geometry but also a background flux $\mathcal{G}_4$ being supported on homologically non-trivial cycles. Supersymmetric compactifications on Calabi-Yau fourfolds have been investigated in detail in [140] and a non-trivial background was found in which allows for an internal Calabi-Yau geometry Y_4 times a flat space $\mathbb{R}^{(2,1)}$ and a background flux for the field strength G_4. We follow this discussion as it will be quite relevant for the discussion of the F-theoretic derivation of the 7-brane gauge coupling function in section 9.

The metric in the presence of such flux has to include a non-trivial warp factor e^A, and is given by

$$ds^2_{(11)} = e^{-A}\eta_{\mu\nu}dx^\mu dx^\nu + e^{A/2}g_{a\bar{b}}dy^a d\bar{y}^{\bar{b}} \ , \tag{7.2.5}$$

with $g_{a\bar{b}}$ being the metric on the Calabi-Yau manifold Y_4. The warp factor only depends on the coordinates $y^a, \bar{y}^b$ of Y_4. The non-trivial field strength G_4 splits into a contribution with three flat indices $(G_4)_{\mu\nu\rho m}$ and an internal G_4-flux $\mathcal{G}_4$ with indices only along Y_4. Supersymmetry implies that the background component of G_4 with flat indices is determined by the warp factor

$$(G_4)_{\mu\nu\rho m} = \epsilon_{\mu\nu\rho}\partial_m e^{3A/2}\,, \tag{7.2.6}$$

where the derivative is taken with respect to the internal coordinates. The equations (7.2.6) and (7.2.2) require that the warp factor has to fulfill the Laplace equation

$$\Delta_{Y_4}(e^{3A/2}) = *_{Y_4}(\tfrac{1}{2}\mathcal{G}_4 \wedge \mathcal{G}_4 - X_8|_{Y_4} + \sum_k \delta^{(8)}(\Sigma_3^k)) \ , \tag{7.2.7}$$

where $\Delta_{Y_4}, *_{Y_4}$ is the Laplacian and the Hodge-star evaluated in the Calabi-Yau metric $g_{a\bar{b}}$.

The last term in (7.2.7) needs to be included if the background contains M2-branes which fill the non-compact space-time $\mathbb{R}^{(2,1)}$ and are pointlike in Y_4. There are further constraints by supersymmetry and the equations of motion on the background flux $\mathcal{G}_4$. It can be shown that $\mathcal{G}_4$ has to be self-dual and primitive,

$$*_{Y_4}\mathcal{G}_4 = \mathcal{G}_4\,, \qquad J \wedge \mathcal{G}_4 = 0\,, \tag{7.2.8}$$

where J is the Kähler form on the fourfold Y_4.

Let us stress that for compact geometries the Laplace equation (7.2.7) implies a non-trivial consistency condition when integrated over Y_4. This is the famous M2-brane tadpole condition

$$\frac{\chi(Y_4)}{24} = \frac{1}{2}\int_{Y_4} \mathcal{G}_4 \wedge \mathcal{G}_4 + N_{\mathrm{M2}}\,, \tag{7.2.9}$$

where $\chi(Y_4)$ is the Euler number of Y_4, and N_{M2} is the number of space-time filling M2-branes. The condition (7.2.9) together with (7.2.8) implies that in a compact setting the corrections due to X_8 leading to $\chi(Y_4)$ in (7.2.9) are crucial to find supersymmetric vacua with $\mathcal{G}_4$ flux.

7.2.2. Heterotic/F-theory duality

Heterotic F-theory duality [36, 83] conjectures that F-theory compactified on an elliptically fibered K3 surface is equivalent to the $\mathrm{E}_8 \times \mathrm{E}_8$ Heterotic string compactified on a torus. Let us start with the Heterotic side by considering the moduli of this compactification. There are two moduli coming from the torus and in addition there are sixteen further moduli coming from Wilson lines on the torus. These parametrize the moduli space

$$\mathcal{M}_{\mathrm{Het}} = \mathrm{SO}(18,2,\mathbb{Z})\backslash\mathrm{SO}(18,2)/\mathrm{SO}(18)\times\mathrm{SO}(2)\times\mathbb{R}_+ \tag{7.2.10}$$

which is just the moduli space of the sixteen-dimensional Heterotic lattice extended by two further pairs of compact dimensions of Lorentzian signature (1,1). The last factor parametrizes the string coupling constant.

On the F-theory side the K3 is described by an elliptic fibration over a $\mathbb{P}^1$, coordinized by z, which reads

$$y^2 = x^3 + f(z)x + g(z)\,. \tag{7.2.11}$$

As this fibration should have generically 24 singular fibers one obtains 9+13 parameters out of which 3+1 can be deleted due to the SL(2,$\mathbb{Z}$) invariance of the base and a rescaling of the equation, which gives eighteen parameters in total which are in fact also parametrized by (7.2.10) [36]. Here the half-line factor gets identified with the size of the base.

To match the moduli it is useful to turn off all Wilson lines on the Heterotic side leaving us with two moduli and the full $\mathrm{E}_8 \times \mathrm{E}_8$ symmetry. On the F-theory side the elliptic fibration is accordingly specialized to the two moduli curve

$$y^2 = x^3 + \alpha z^4 x + (z^5 + \beta z^6 + z^7)\,. \tag{7.2.12}$$

According to table (7.1) this has indeed an E_8 singularity at $z = 0$ and it is easy to check that this is also the case for $z = \infty$. Moreover, if one makes the K3 degenerate by taking the limit $\alpha, \beta \longrightarrow \infty$ while keeping the ratio α^3/β^2 fixed one obtains a constant coupling constant all over the base except near to the two poles. Technically what happens in this limit is

that the K3 degenerates into a chain of three surfaces. The two end surfaces are found to be half K3 surfaces that intersect both with an elliptic scroll, i.e. the product of a rational curve with an elliptic curve. This is called the stable degeneration limit [36, 162, 163]. On the Heterotic side the torus also degenerates by becoming very large, while the complex structure becomes identified with that of the elliptic curve on F-theory side.

Heterotic/F-theory duality in six dimensions

Heterotic/F-theory duality in six dimensions is basically established by compactifying the eight-dimensional duality over a common $\mathbb{P}^1$, i.e. one compactifies F-theory on a K3-fibered threefold, where the K3 is itself elliptically fibered and the Heterotic string is compactified on an elliptically fibered K3 as well. In the following we denote by z_1 and z_2 the coordinates of the base $\mathbb{P}^1_b$ and fiber $\mathbb{P}^1_f$ respectively. Globally, these have to glue together to a Hirzebruch surface F_n. On the Heterotic side anomaly cancellation demands that

$$c_2(V) = c_2(T_{K3}) \tag{7.2.13}$$

where V denotes the Heterotic gauge bundle and accordingly, one has to turn on 24 instantons. It was found in [36], that the distribution of these instantons among the two E_8-bundles corresponds to $(12+n, 12-n)$. A good starting point to match the moduli on both sides is assume point like instantons. The elliptic fibration of the threefold can accordingly be written as [36, 83]

$$y^2 = x^3 + \sum_{k=-4}^{4} f_{8-nk}(z_1) z_2^{4-k} x + \sum_{k=-6}^{6} g_{12-nk}(z_1) z_2^{6-k}\,. \tag{7.2.14}$$

Here the subscript denotes the degree of the polynomial with the convention that those with negative degrees vanish. The extension of this local description to a global one demands that the two $\mathbb{P}^1$'s have to fiber as a Hirzebruch surface F_n. This explicit form makes the structure very transparent, one easily sees that one has for fixed z_1 a K3 which is itself elliptically fibered. Moreover, one observes that the generic singularity is destroyed at zeros of $f_{8-nk}(z_1)$, which corresponds just to the location of the instantons. Giving these instantons a finite size corresponds to blowing-up the base.

We do not delve deeper into the discussion here, but refer to the beautiful original expositions [36, 83] or the review article [139].

8. Counting Non-Perturbative States in F-Theory

In this chapter we discuss two interesting physical applications of the refined BPS invariants within F-theory which are given by the F-dual description of the E-string in section 8.1 and $[p, q]$-strings in section 8.2.

8.1. Counting refined BPS states of the E-string

In this section we show that the refined topological string is able to count BPS states of the E-String and to predict their space-time spin and gauge theory quantum numbers. We start by reviewing some aspects of the construction of the E-string. Afterwards, we discuss (unrefined) BPS state counting via the Green-Schwarz string description in six and five dimensions and also in the dual F-theory setup. Finally, we explain how the refined topologcial string considerably improves the understanding of BPS states of the E-string.

8.1.1. Zero-sized Heterotic instantons

We consider the Heterotic SO(32) string compactified down to six dimensions on a K3 surface. Anomaly cancellation demands in the absence of M5-branes that

$$c_2(V) = c_2(T_{K3}) \tag{8.1.1}$$

where V denotes the Heterotic gauge bundle which implies that one has to turn on 24 instantons. If one of these instantons shrinks to zero size [41], space-time develops a deep throat in which one obtains a diverging dilaton - irrespectively of its profile outside the throat - and in addition an SP(1) $\cong$ SU(2) gauge enhancement giving rise to hypermultiplets in the representation (**32,2**) under SO(32) $\times$ SU(2). If all instantons shrink within one point one obtains an SP(24) enhancement. As there is no vector multiplet moduli space in six dimensions, the dynamics is completely governed by the Higgs effect.

In contrast, the effect of a zero-sized instanton in the $E_8 \times E_8$ Heterotic string cannot be understood by the Higgs effect as the representations of E_8 are too large compared to the dimension of a single E_8 instanton which is 29. Instead the E_8 case is governed by a six-dimensional tensionless string [39, 40]. This can be inferred by noticing in a first step the following chain of dualities [90]

$$\text{Het}\, E_8 \times E_8/S^1 \simeq \text{M-theory}/I \times S^1 \simeq \text{Type IA}/I \overset{\text{T}}{\simeq} \text{Typ I}/S^1 \overset{\text{S}}{\simeq} \text{Het SO(32)}/S^1\,. \tag{8.1.2}$$

In particular, one notices that a Heterotic SO(32) instanton is mapped to a D5-brane in the dual Type I theory. As the D5-brane carries SU(2) Chan-Paton indices [41], one also recovers here the (**32,2**) hypermultiplets, coming from D5-D9 open strings. In addition, the D5-D9 system is via T-duality equivalent to the D0-D4 system whose moduli space is

known to have two branches: On the Coulomb branch the D0-brane is separated from the D4-brane while in contrast the D0-brane has dissolved into flux on the D4-branes on the Higgs-branch.

The upshot of a careful analysis of these dualities is, that the analogon of this process in Heterotic M-theory is an M5-M9 brane configuration with a M2-brane stretching between them. This induces a string, called E-string, in the world-volume of the M9-brane which becomes tensionless, once the M5-brane approaches the M9-brane and corresponds to the pointlike Heterotic $E_8 \times E_8$ instanton. Also in this case the M5-brane can dissolve into a finite-sized instanton.

It is crucial to note that this rather simple chain of dualities is based on the additional compactification on a circle. However, once compactified on a circle, the two Heterotic theories share a common moduli space anyway. It is therefore not apriori clear that the five-dimensional analysis can be lifted to a six-dimensional picture. To give one example, after the circle compactification, one obtains the (**16,2**) hypermultiplet from the Heterotic SO(32) theory, but the decomposition of the representations of E_8 under the subgroup SO(16) do not provide a fundamental representation of SO(16). These states cannot be there in the six-dimensional $E_8 \times E_8$ theory and only arise after the compactification. These issues were carefully analyzed and a consistent six-dimensional picture was provided in [39].

Their analysis also showed that the low energy field content of the E-String is governed by the eleven-dimensional supergravity in the bulk, super E_8 Yang-Mills theory in ten dimensions on the fixed point, a tensor[1] as well as a hyper multiplet, the reduction of the world-volume U(1) field of the two-brane, an E_8 level one current from the boundary of the two-brane on the nine-brane and anomaly cancellation finally suggests that there is nothing coming from the intersection of the two-brane with the five-brane.

8.1.2. The E-String in six and five dimensions

So far, no Lagrangian description is known to describe the physics of the E-string. A first step towards unraveling its nature can be done by carefully understanding its BPS spectrum which was initiated in [32] (see also [65]). As the quantum field theories based on strings are not well understood, it is useful to consider the situation compactified on a circle, where one can again analyse particles. There are two ways to attack this problem: The first one uses a Green-Schwarz description of the six-dimensional exceptional string which gets compactified on a circle. This can be used to compute parts of the partition function of the E-string. The second way approaches the problem using Heterotic/F-theory duality. These dualities are compactly summarized in figure 8.1.

In a nut-shell the analysis of the five-dimensional theory reveals the following. It exhibits different phases which are parameterized by the string tension. In the first phase, both, the excitations of the wrapped and of the un-wrapped E-string are massive. Due to a quantum mechanical effect the tension of the wrapped string is smaller than that of the un-wrapped string and one approaches a point where the wrapped string becomes tensionless, while the unwrapped string has still positive tension. After this transition point, the tension of the wrapped string becomes formally negative and one finally hits a second transition point, where also the un-wrapped string becomes tensionless. At this point one obtains a whole tower of massless particles interacting with the tensionless string.

[1] This disappears when the five-brane gets stuck on the 9-brane as its multiplet hosts the scalar that describes the transverse motions.

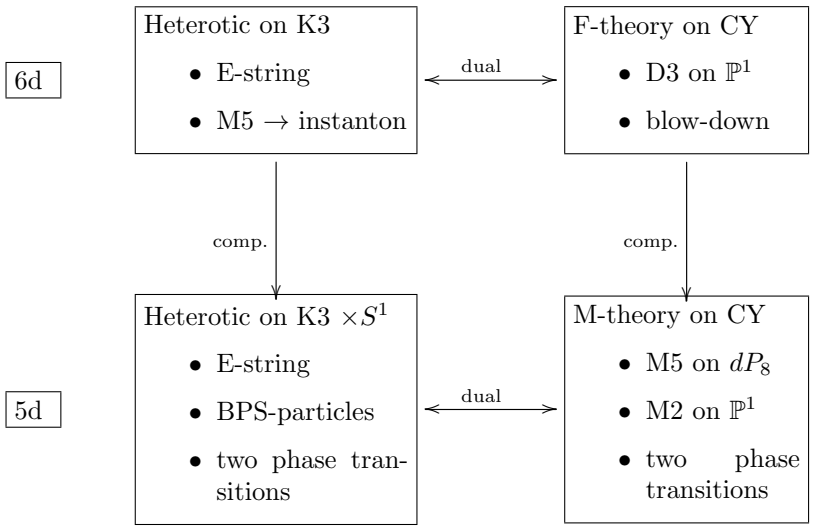

Figure 8.1.: The description of the E-string in six and five dimensions using Heterotic/F-theory duality.

This is geometrically reflected in F-theory as points in the moduli space where first only a two-cycle vanishes and afterwards a four-cycle collapses and together with it all possible curves inside this divisor. In the next two sections we elaborate on this picture and finally present how the space-time spin content and quantum numbers of the BPS-particles are encoded in refined stable pair invariants.

8.1.3. The Green-Schwarz string

It was argued in [32] that the degrees of freedom of the E-String are governed by the Green-Schwarz string in six dimensions. Its degrees of freedom consist of a left-running E_8 current algebra and right-moving spinor of O(4) and the external four bosonic oscillators

$$4(0,0) \oplus (\frac{1}{2},0) \oplus (0,\frac{1}{2})\,. \tag{8.1.3}$$

As it is easier to count the particle states one compactifies the six-dimensional string on a circle of radius R giving rise to light stringy and particle states in five dimensions. The mass of a BPS state is given by

$$M = \left|\frac{n}{2R} + mRT\right|, \tag{8.1.4}$$

where T is the string tension and n, m denote the momentum and winding quantum number respectively. The partition function for the states with $m = 1$ reads

$$q^{-\frac{1}{2}} \sum_{n=0}^{\infty} d(n) q^n = \frac{\theta_{\mathrm{E}_8}(q)}{\eta(q)^{12}}, \tag{8.1.5}$$

where the exponent twelve reflects four space-time oscillators and eight internal ones coming from the lattice. $\theta_{\mathrm{E}_8}(q)$ organizes the summation over the lattice momenta and is defined

in (A.3.3). This implies that the degeneracies

$$d(0) = 1, \quad d(1) = 252, \quad d(2) = 5130, \ldots \tag{8.1.6}$$

When an instanton shrinks to zero size the E_8 symmetry is expected to be restored at least locally and therefore the BPS states should be classified by their E_8 as well as their space-time quantum numbers. Whereas one finds at level zero a hypermultiplet in the trivial representation of E_8, the momentum number $n = 1$ gives the following field content

$$\left[\mathbf{248}; 4(0,0) \oplus \left(\frac{1}{2}, 0\right) \oplus \left(0, \frac{1}{2}\right)\right] + \left[\mathbf{1}; 4\left(\frac{1}{2}, \frac{1}{2}\right) \oplus \left(1, \frac{1}{2}\right) \oplus \left(\frac{1}{2}, 1\right) \oplus \left(0, \frac{1}{2}\right) \oplus \left(\frac{1}{2}, 0\right)\right] . \tag{8.1.7}$$

All these states are generically massive, except if one allows for a negative tension, which gives a whole tower of massless states. The interpretation of the latter gets clarified once one passes to the dual F-theory description, which is the subject of the next section.

8.1.4. The F-theory perspective

From the F-theory perspective, the transition of a M5-brane into a zero-sized instanton is reflected by performing a blow-down from F_1 to $\mathbb{P}^2$ in the base of the elliptic fibration. As previously discussed, the tower of massless states comes from a shrinking four-cycle, which is in the case of an E_8 instanton a dP_8 del Pezzo surface[2]. An elliptically fibered Calabi-Yau three-fold with basis F_1 can be constructed using the Batyrev method described in 4.3.1. If one chooses an E_8 fiber, one finds for the dual polyhedron Δ^*

$$\begin{pmatrix} 0 & 0 & & 0 \\ & -2 & & -3 \\ \Delta_3 & & \vdots & \\ & -2 & & -3 \\ & & & \\ 0 & & \Delta_{10} & \end{pmatrix}, \qquad \left(\begin{array}{cccc|ccc} & & & & l^{(\mathcal{E})} & l^{(F_1^F)} & l^{(F_1^B)} \\ 0 & 0 & 0 & 0 & -6 & 0 & 0 \\ 1 & 0 & -2 & -3 & 0 & 1 & 0 \\ -1 & 0 & -2 & -3 & 0 & 1 & -1 \\ 0 & 1 & -2 & -3 & 0 & 0 & 1 \\ -1 & -1 & -2 & -3 & 0 & 0 & 1 \\ 0 & 0 & -2 & -3 & 1 & -2 & -1 \\ 0 & 0 & 1 & 0 & 2 & 0 & 0 \\ 0 & 0 & 0 & 1 & 3 & 0 & 0 \end{array}\right) \tag{8.1.8}$$

Here Δ_3 and Δ_{10} are the two-dimensional polyhedra from figure 4.1. This is also a toric realization of the compact model for the half K3 discussed in 6.1 but with a different ambient space to realize the elliptic fiber. The Mori cone is spanned by the elliptic fiber class E with Kähler class k_E and charge vector $l^{(\mathcal{E})}$, the base of F_1 given by $l^{(F_1^B)}$, and $l^{(F_1^F)}$ denotes the charge vector of the fiber class D of F_1 (which is also the base of the half K3) where we denote the Kähler class by k_D. Next one performs a flop transition by which one enters the extended Kähler cone [32, 36, 37]. The basis for the new Kähler cone is given by $l^{(1)} = l^{(\mathcal{E})} + l^{(F_1^F)}$ which corresponds to the canonical class of the dP_8 del Pezzo surface, $l^{(2)} = -l^{(F_1^F)}$ which belongs to the flopped curve and finally $l^{(3)} = l^{(F_1^B)} + l^{(F_1^F)}$, which is the hyperplane class of $\mathbb{P}^2$. Technically speaking the elliptic fibration has a section in the first

[2] For general reasons, a four-cycle that shrinks at the boundary of the Kähler cone of a Calabi-Yau manifold to zero must be a del Pezzo surface, if the shrinking surface has no singularities on it. Moreover, the condition, to have a shrinkable curve within a Hirzebruch surface restricts n to be a divisor of four. See [36] for the discussion of the other cases.

phase which gets flopped out in the second phase such that one obtains an elliptic pencil with one base point, i.e. a dP_8 surface[3].

Via the M/F-theory duality, the compactification of the E-string on a circle is better described by the compactification of M-theory on the elliptically fibered Calabi-Yau threefold, where the F-theory lift corresponds as usual to taking the volume of the elliptic fiber to zero. It is interesting to see [32], how the above described geometry reflects the fact that there is just one phase in six dimensions, namely when the E-string becomes tensionless, but two phases in five dimensions, when either a particle or the tensionless string becomes light. In fact, in the first geometrical phase it is not possible to blow down the del Pezzo surface without blowing down the elliptic fiber at the same time - this is only possible in the second geometrical phase. However, this distinction makes no sense in six dimensions as the fiber acquires necessarily zero volume. This is illustrated in figure 8.2.

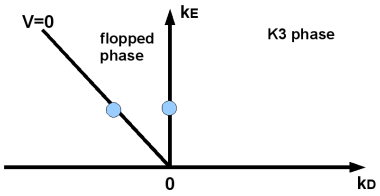

Figure 8.2.: There is just one phase transition in six dimensions, but two in five dimensions. V denotes the volume of the four-cycle.

Finally, one can make quantitative contact with the Green-Schwarz description of the tensionless string by the identification

$$k_E = \frac{1}{2R}, \qquad k_D = RT. \tag{8.1.9}$$

and use the Gromov-Witten invariants to count the states that correspond to a certain winding and momentum number. One finds for the dP_8 geometry the following genus zero Gromov Witten invariants [32]

	d_E	0	1	2	3
d_D					
0			480	480	480
1		1	252	5130	54760
2				-9252	-673760
3					848628

First of all one notices that the results for the winding number one perfectly match with the results from the Green Schwarz string in (8.1.6). Furthermore, the Gromov-Witten invariants predict $252, -9252, \ldots$ massless states. However this counting can be at best an index as negative integers appear and moreover there is no obvious decomposition into E_8-representations. In the next section we show how the refined BPS invariants resolve this problem.

[3]See e.g. [32] for models with multi-sections that lead to lower del Pezzo surfaces.

8.1.5. Refined stable pair invariants solve the problem

It turns out that all this information is stored within the refined BPS numbers. For convenience we recall the results of the massless dP_8 surface from section 5.1.1. One finds e.g. for the multiplicities $d = 1, 2$ of the canonical class

$2j_L \backslash 2j_R$	0	1
0	248	
1		1

$d = 1 \qquad N_{0,1} = 252$

$2j_L \backslash 2j_R$	0	1	2	3
0		3876		
1			248	
2				1

$d = 2 \qquad N_{0,2} = -9252$

The result for $d = 1$ perfectly matches with (8.1.7) once we tensor with the two hypermultiplets from the right-running ground state. The second table gives a prediction for the spin and E_8-representation content. Note that is explains in particular the negative counting from the Gromov-Witten invariants. If the refined spin quantum numbers are indeed to be identified with the space-time quantum numbers of the massless E-String states the sum over all dimensions of the E_8 (Weyl group) representations weighted by the dimensions of the corresponding spin representations has to give back the Gromov-Witten invariants which is true by construction of the refined string.

As already noticed in [32], already at the first level one obtains an additional light gravitino state and it is obvious that the higher level states give rise to light even higher spin states. We therefore have a quite concrete proposal for the spectrum of a conformal higher spin theory of type recently analyzed in [91, 92].

We close by discussing one little issue. These BPS states have been counted by performing calculations at the large radius point while the E-String states appear at the conifold locus where the del Pezzo shrinks. It can therefore not rigorously be proven that these states are stable in this limit. However as shown in section 5.1.2 the spectrum at the conifold point is identical to that at the large radius point due to the self-duality of the E_8-lattice, which underlines the claim that we have indeed found the spectrum of the tensionless string!

8.2. Counting $[p, q]$-strings using refined invariants

The aim of this section is to argue that the refined BPS invariants contain some information about $[p, q]$-string states within F-theory. The reason for this is the following chain of observations. It is well-known that F-theory on certain orbifolds - most notably $T^4/\mathbb{Z}_2$ has a type IIB description with constant coupling. In these cases one can identify the $[p, q]$-strings easily. Moreover, if one places a D3-probe brane near one fixed point of the latter, this system has an interpretation as SU(2) Seiberg-Witten theory with four fundamental matters transforming under the flavor group SO(8). In addition, it is possible to identify $[p, q]$-strings as geodesics in the base which is matched with the BPS state condition in Seiberg-Witten theory. Finally, it can be argued, that the geodesic condition is also equivalent to having a

lift to a holomorphic curve into F-theory compactification geometry. But these curves are counted by the refined BPS invariants.

In the following discussion we review these aspects and draw finally our conclusion.

8.2.1. The Seiberg-Witten description of the Sen limit

The Sen limit [167] describes F-theory in the background, which is specified by the following Weierstrass normal form (7.1.4)

$$f^3 = \alpha\phi^2, \qquad g = \phi^3, \qquad \Delta = (4\alpha^3 + 27)\phi^6, \qquad \phi = \prod_{i=1}^{4}(z - z_i)\,. \tag{8.2.1}$$

The j-function (7.1.7) therefore only depends on α, which allows for a globally constant coupling that can be tuned small to make contact with type IIB string theory. Moreover, there is a monodromy around each of the four z_i given by

$$\begin{pmatrix} -1 & 0 \\ 0 & -1 \end{pmatrix} \tag{8.2.2}$$

which shows that the base of the elliptic fibration is given by $T^2/\mathbb{Z}_2$ and in addition the action on the fields can be identified with the transformation $(-1)^{F_L} \cdot \Omega$ such that this setup gets identified with a type IIB orientifold compactification on T^2 modded out by $(-1)^{F_L} \cdot \Omega \cdot \mathbb{Z}_2$. As usual, F_L and Ω denote the left-running fermion number and the world-sheet parity operator respectively. An inspection of the Kodaira table (7.1) yields that at each fixed point there is a SO(8) gauge group. In addition, this setup is dual to type I theory by T-dualizing both circles of T^2.

In a next step we consider the neighborhood of one fixed point z_i and put a D3-brane, which is un-effected by the SL(2,$\mathbb{Z}$) action, into this setup. We display how the relevant objects are extended into the various directions in figure 8.3. This $(8, 9)$-plane is now

	x^0	x^1	x^2	x^3	x^4	x^5	x^6	x^7	x^8	x^9
O7	×	×	×	×	×	×	×	×		
D7	×	×	×	×	×	×	×	×		
D3	×	×	×	×						

Figure 8.3.: Extension of the O7, D7 and D3 brane into the various directions.

identified [164] with the moduli space of SU(2) Seiberg-Witten (SW) theory[4] with four flavors and flavor group SO(8). The position u_0 of the D3-brane gets identified with the expectation value of the SU(2) adjoint scalar. Indeed, if the D3-brane is at the origin, it can be identified with a D5-brane in the dual type I setup which carries SU(2) Chan-Paton factors. Moreover, the positions u_i of the D7-branes correspond to the masses of the fundamental matter multiplets that arise from open strings stretching between the D3- and the D7-branes. These make up for four points of the singularities of the torus fibration, while the other two zeros correspond to the quantum-mechanical splitting of the classical SU(2) enhancement point into a (0,1)-monopole and a (1,-1)-dyon. In general, the (p, q)-type of the string encodes the charge in SW theory.

[4] See the original papers [19] or [87, 88] for a nice review.

A crucial observation is that the BPS condition in Seiberg-Witten theory is equivalent to the condition of being a geodesic in the basis of the elliptic fibration [166]. In general the mass of a BPS state in Seiberg-Witten theory is given by

$$m_{p,q}^{\mathrm{SW}} = |pa(z) + qa_D(z) + \sum_i m_i S_i| \,. \tag{8.2.3}$$

Here z is the gauge invariant coordinate, $a(z)$ and $a_D(z)$ are a symplectic pair of periods of the SW curve while m_i and S_i denote the bare masses and global U(1) charges carried by the BPS state respectively. If a BPS state becomes at $\tilde{u}$ massless, one obtains

$$m_{p,q}^{\mathrm{SW}} = |pa(u) + qa_D(u) - pa(\tilde{u}) + qa_D(\tilde{u})| \,. \tag{8.2.4}$$

On the other hand the tension of a $[p,q]$-string is given by

$$T_{p,q} = \frac{1}{\sqrt{\tau_2}}|p + q\tau_2| \tag{8.2.5}$$

where as usual $\tau = \tau_1 + i\tau_2$ and $1/\tau_2$ is identified with the string coupling constant. The mass of a $[p,q]$-string stretched along the curve C is accordingly given by

$$m_{p,q} = \int_C |\eta(\tau)^2 \prod_{i=1}^{6} (u - u_i)^{-\frac{1}{12}} (p + q\tau)| dz \,. \tag{8.2.6}$$

The formula (8.2.4) resembles (8.2.6) by proving that [166]

$$da = \eta(\tau)^2 \prod_{i=1}^{6} (u - u_i)^{-\frac{1}{12}}, \qquad da_D = \tau da. \tag{8.2.7}$$

8.2.2. Generalizations

This easy picture needs to be extended. In general, $[p,q]$-strings are not sufficient [43–46] to explain gauge enhancements on strongly coupled 7-brane stacks. Instead, these are traced back to string junctions which are bound states of $[p,q]$-strings. These string junctions are created analogously to the Hanany-Witten effect when a $[p,q]$-string crosses the branch cut of a (r,s)7-brane. In the M-/F-theory picture a $[p,q]$-string is lifted to a complex curve that wraps a mixed class in fiber and base. It was investigated in [127, 128] under which conditions string junctions which are eventually bound to $[p,q]$7-branes can be lifted to holomorphic curves in the total space of a complex two-dimensional elliptic fibration $\mathcal{E}$. In fact this is possible if certain stability conditions are fulfilled. The latter can be translated in easy intersection conditions on the holomorphic curves, e.g. that holomorphic curves are required to have positive intersection. Moreover, it was shown that the geodesic minimality in the base is equivalent to the condition that the lifted curve is holomorphic. Altogether one finds that string junctions have to obey the following rules

- J.1 String junctions are configurations of $\begin{bmatrix} p \\ q \end{bmatrix}_i$-strings $i = 1, \ldots, N$, which meet in a

single point, subject to a non-force condition

$$\sum_{i=1}^{N} \left[\begin{array}{c} p \\ q \end{array} \right]_i = 0\,. \tag{8.2.8}$$

- J.2 Two $[p,q]$-strings can end on each other iff they are compatible

$$\left[\begin{array}{c} p \\ q \end{array} \right]_i \wedge \left[\begin{array}{c} p \\ q \end{array} \right]_k = p_i q_k - q_i p_k = \pm 1\ , \tag{8.2.9}$$

  the sign depending on the orientation of the corresponding cycle in $H_1(\mathcal{E},\mathbb{Z})$. 3-junctions are BPS configurations iff (8.2.9) holds for each pair [127].

- J.3 Each $[p,q]$-string line emerging from the junction can end on a $[p,q]$ 7-brane, where $\gamma = \left[\begin{array}{c} p \\ q \end{array} \right] \in H_1(\mathcal{E},\mathbb{Z})$ shrinks.

8.2.3. Counting $[p,q]$-strings in the half K3

The half K3 surface arises in the stable degeneration limit of F-theory compactifications and we claim to be able to provide some insight into the corresponding BPS states corresponding to $[p,q]$-strings. As we have seen in the previous discussion these correspond to lifts of geodesics in the base to holomorphic curves in the total space with components in the fiber and base. The homology of the massless half K3 is precisely spanned by the base class b and fiber class f and we find e.g. for the lowest diagonal class $b+f$, where es recall the result for convenience in table 8.1 that the 248 splits according to formula (6.3.5) and the

$2j_L \backslash 2j_R$	0	1
0	248	
1		1

$d = 1$

Table 8.1.: The splitting of the lowest diagonal class of the half K3

Weyl action into $240+8$. This is precisely the gauge content of the adjoint representation of E_8 which should be established by the $[p,q]$-strings. In addition, the refined invariants in the diagonal classes of the half K3 are precisely those that correspond to multiples of the canonical class of the dP_8 del Pezzo surface. The latter is associated to a Seiberg-Witten curve [59, 63] (A.2.1) with eight mass parameters that enjoy an E_8-flavor symmetry. Setting all these mass parameters to zero, one simply obtains an elliptic E_8 singularity, while turning on the masses breaks the flavor group accordingly. In addition, it was argued in [178], that the probe brane picture also extends to the strongly coupled F-theory setups where no Lagrangian description exists. It is therefore tempting to identify the E_8 flavor symmetry of the Seiberg-Witten theory with the E_8 gauge symmetry of the F-theory setup and to conclude that the mass parameters correspond to the position moduli of the seven-branes. All this provides some evidence to assume that the excitations of the $[p,q]$-string are encoded within the (j_L, j_R) spin content. As discussed in section 2.4.3, the flavor symmetries of the system can be used to modify the Ω-background [129] which results in shifts in the

association of mass and spin. A further analysis is therefore needed in order to clarify the matching of BPS state and space-time spin values.

9. The Sevenbrane Gauge Coupling Function in F-Theory

So far we have counted non-perturbative objects in F-theory which were constituted by $[p, q]$-strings and the dual description of E-string excitations. These calculations were possible since the considered states are protected by holomorphicity against the decay in the strong coupling regime. In this chapter we change to some extent gears and consider four-dimensional effective actions with $\mathcal{N} = 1$ supersymmetry. These also contain protected terms which have only a holomorphic dependence on the moduli. Such terms are given by the superpotential and the gauge coupling function, see [130] for a review and references therein. They do not receive corrections beyond the tree- respectively the one-loop level in perturbation theory and one therefore expects that they can be computed in a controlled way. While the superpotential of $\mathcal{N} = 1$ effective actions (of F-theory) has already been considered quite extensively [131–135], not much is known about the gauge coupling function so far.

We focus in particular on the F-theory reproduction of corrections to the 7-brane gauge coupling function that arises in the $\mathcal{N} = 1$ effective action of Type IIB orientifold compatifications. While this quantity can be derived in the latter setup from the reduction of the Chern-Simons respectively the Dirac-Born-Infeld action including α'-corrections, only the leading term given by the volume of the wrapped divisor in the orientifold can be easily reproduced within F-theory. We show that the subleading flux corrections to the 7-brane gauge coupling functions can be reproduced in a warped compactification[1]. The warp factor takes into account the backreaction of G_4-flux, M2-branes and curvature as discussed in section 7 and modifies the Kaluza-Klein reduction ansatz. Taking this into account, we are able to reproduce the weak coupling corrections and perform first steps towards a computation beyond the weak coupling regime. The following discussion follows closely [2] and is organized as follows.

We start with a review of the gauge coupling on a stack of D7-branes in Type IIB in section 9.1. As a crucial ingredient we present the $\mathcal{N} = 1$ effective action in terms of linear multiplets in section 9.1.1 that we compactify on a circle to three dimensions in section 9.1.2. This is necessary to compare to the three-dimensional theory obtained from the warped compactification of M-theory on a fourfold with G_4-flux as reviewed in section 7. We embed k D6-branes as multi-center Taub-NUT spaces into M-theory in section 9.2.1 and compactify on S^1 by constructing an infinite periodic array of multi-center Taub-NUT TN_k^∞ in section 9.2.2. In section 9.3 we turn to the calculation of the 7-brane gauge coupling. Then we determine the leading gauge coupling on a general compact fourfold in section 9.3.2. We extend the M-theory reduction to include a back-reaction of the G_4-flux on the three-form reduction ansatz in section 9.3.3. With these preparations we derive the full flux-corrected gauge coupling in section 9.3.4. We first obtain the real part from the back-reaction of the G_4-flux on the warp factor that we determine as a closed expression on

[1] See also [125, 126] for the derivation of F^4-terms in F-theory compactications on K3 with constant string coupling constant.

TN_k^∞ and then for the imaginary part by taking into account the altered reduction ansatz for the three-form that we also explicitly determine.

9.1. Motivation: D7-brane gauge coupling function

In this section we discuss the aspects of the four-dimensional effective theory on a stack of D7-branes in a weakly coupled orientifold compactification. We first recall in section 9.1.1 the expression of the D7-brane gauge coupling function as determined by a reduction of the D7-brane action. In section 9.1.2 we perform the reduction to three dimensions. This three-dimensional result will be later useful to compare to the F-theory gauge coupling function derived via M-theory.

9.1.1. D7-brane gauge couplings in 4d: Calabi-Yau orientifolds

We begin by recalling the basics from the computation of the four-dimensional D7-brane effective action in Type IIB $\mathcal{N}=1$ compactifications on a Calabi-Yau orientifold $B_3 = Z_3/\sigma$ with O7-planes [141, 146].[2] Here Z_3 denotes the Calabi-Yau threefold covering space of the orientifold B_3 that is obtained by modding out an holomorphic involution $\sigma : Z_3 \to Z_3$. For appropriately chosen involution the fix point locus of σ is a holomorphic divisor D_{O7} that supports the O7-orientifold planes. The divisor D_{O7} has to be homologous to -8 times the divisors S in Z_3 wrapped by the D7-branes due to tadpole cancellation.

String theory on the orientifold is specified by the orientifold action $\mathcal{O} = \Omega(-1)^{F_L}\sigma$ acting on the fields, with Ω being the world sheet parity operator, and F_L the left-moving fermion number. The spectrum of orientifold invariant states together with the twisted sector states, that can be matched with the open string degrees of freedom, determine the physical spectrum. To obtain the four-dimensional effective theory, all massless fields both of the bulk and the D7-brane have to be expanded in zero-modes that are counted by appropriate cohomology groups. Then these expansions are inserted into the ten-dimensional Type IIB supergravity and eight-dimensional D7-brane effective action, that are dimensionally reduced to four dimensions by integration over the internal directions and keeping only the orientifold invariant terms, to obtain the $\mathcal{N}=1$ effective four-dimensional action.

Let us outline the gauge sector of this effective theory focusing on a stack of k D7-branes with an eight-dimensional U(k) gauge theory on $\mathbb{R}^{(3,1)} \times S_\mathrm{b}$. If the divisor S_b has a non-trivial topology, one can consider flux configurations $\mathcal{F}$ for the field strength F_{D7} on the D7-brane. More precisely, we split in the Kaluza-Klein ansatz the D7-brane field strength as

$$F_{\mathrm{D7}} = F + \mathcal{F} = (F^0 + \mathcal{F}^0)\mathbf{1} + (F^i + \mathcal{F}^i)T_i + (F^A + \mathcal{F}^A)\tilde{T}_A \ , \tag{9.1.1}$$

where $F = dA + A \wedge A$ is the U(k) field strength in the four-dimensional effective theory, and $\mathcal{F}$ is a background two-form flux on the D7-brane divisor S_b. The field strength F_{D7} is a general element in the adjoint of U(k), that we have expanded in the generators $\tilde{T}_\mathcal{A} = (\mathbf{1}, T_i, \tilde{T}_A)$ of the adjoint. Here $T_I = (T_i, \mathbf{1})$, $i = 1, \ldots, k-1$, are the k Cartan generators of U(k) =U(1)×SU(k), while $\tilde{T}_A$ denote the generators associated to the roots of SU(k).

In the absence of flux $\mathcal{F}$ it can be shown by a straightforward reduction of the D7-brane

[2] See [95, 147, 148] for a similar derivation of the dual D5- respectively D6-brane effective action.

worldvolume action using the expansion (9.1.1) that the kinetic term for F takes the form

$$S^{(4)}_{F^2_{\rm D7}} = -2\pi \int_{\mathcal{M}_4} \tfrac{1}{2}{\rm Re} f_{\mathcal{A}\mathcal{B}}\, F^{\mathcal{A}} \wedge *F^{\mathcal{B}} + \tfrac{1}{2}{\rm Im} f_{\mathcal{A}\mathcal{B}}\, F^{\mathcal{A}} \wedge F^{\mathcal{B}} \tag{9.1.2}$$

in the conventions (A.6.3) of appendix A.6. Here $f_{\mathcal{A}\mathcal{B}}$ denotes the gauge coupling function that is a holomorphic function of the chiral fields in the $\mathcal{N}=1$ effective theory, and has adjoint indices $\mathcal{A}, \mathcal{B}$. The adjoint indices arise as we will show soon from the two traces

$$\mathcal{C}_{\mathcal{A}\mathcal{B}} = {\rm Tr}(\tilde{T}_{\mathcal{A}}\tilde{T}_{\mathcal{B}}) \ , \qquad \tilde{\mathcal{C}}_{\mathcal{A}\mathcal{B}} = \tfrac{1}{2}\,{\rm sTr}(\tilde{T}_{\mathcal{A}}\tilde{T}_{\mathcal{B}}\tilde{T}_{\mathcal{C}}\tilde{T}_{\mathcal{D}}) \int_{S_{\rm b}} \mathcal{F}^{\mathcal{C}} \wedge \mathcal{F}^{\mathcal{D}} \ , \tag{9.1.3}$$

where $\mathcal{F}^{\mathcal{C}}$ are the fluxes localized on the internal part $S_{\rm b}$ of the D7-brane and sTr(.) denotes the symmetrized trace defined as the sum over all permutations σ,

$${\rm sTr}(\tilde{T}_{\mathcal{A}}\tilde{T}_{\mathcal{B}}\tilde{T}_{\mathcal{C}}\tilde{T}_{\mathcal{D}}) = \frac{1}{4!}\sum_{\sigma} {\rm Tr}(\tilde{T}_{\sigma(\mathcal{A})}\tilde{T}_{\sigma(\mathcal{B})}\tilde{T}_{\sigma(\mathcal{C})}\tilde{T}_{\sigma(\mathcal{D})}) \, . \tag{9.1.4}$$

In the case at hand the chiral superfields are given by the the axiodilaton $\tau = C_0 + ie^{-\phi}$, the combination $G^a = \int_{\Sigma_a} C_2 - \tau \mathcal{B}_2$ and the Kähler moduli [146]

$$T_\alpha = \int_{D_\alpha} \tfrac{1}{2}(J\wedge J - e^{-\phi}B_2\wedge B_2) + i(C_4 - C_2\wedge B_2 + \tfrac{1}{2}C_0 B_2\wedge B_2) \ , \tag{9.1.5}$$

where Σ_a, D_α denote a homology basis of odd curves respectively even divisors in Z_3 w.r.t. the involution σ. The Kähler form on Z_3 is given by J, while C_p denote the R-R p-forms, and B_2 is the NS-NS B-field. For simplicity we have frozen out the position and Wilson line moduli of the D7-brane and refer to [141] for the open string corrected chiral coordinates.

In order to proceed we will need to recall some additional facts about the D7-brane theories following [141, 149, 150]. In particular, one finds that in the weak coupling description the gauge group is actually U(k) =SU(k)×U(1). However, if the D7-brane and its orientifold image are not in the same cohomology class on Z_3, one finds that a geometric Stückelberg term is induced which renders the overall U(1) massive. More precisely, the moduli G^a are gauged due to the geometric Stückelberg coupling, and ReG^a is eaten by the overall U(1) which thus becomes massive. The mass of the massive vector multiplet containing the U(1) and ImG^a is of the order of the Kaluza-Klein scale. In the following we will make the simplifying assumption that for each stack of D7-branes there is exactly one G^a which becomes massive together with the overall U(1). While a detailed derivation of the effective action would require to actually integrate out this massive vector multiplets, we will in the following mostly drop it in our consideration. In other words, we will consider an SU(k) gauge theory and no G^a moduli.

Given these preliminaries we are now in the position to display the gauge coupling function $f_{\mathcal{A}\mathcal{B}}$ for a stack of D7-branes. This generalizes the results given for a single D7-brane [141]. Using the traces (9.1.3) one finds [3]

$$\begin{aligned} f_{\mathcal{A}\mathcal{B}} &= \tfrac{1}{4}\left(\delta^\alpha_S T_\alpha \mathcal{C}_{\mathcal{A}\mathcal{B}} - i\tau\,\tilde{\mathcal{C}}_{\mathcal{A}\mathcal{B}}\right) \\ &\equiv f^{\rm c}(T)\,\mathcal{C}_{\mathcal{A}\mathcal{B}} + f^{\rm flux}_{\mathcal{A}\mathcal{B}}(\tau) \ . \end{aligned} \tag{9.1.6}$$

[3] We have set $2\pi\alpha' = 1$ in the following.

where δ_S^α are the coefficients in the expansion of $S = \delta_S^\alpha D_\alpha$ in a homology basis of orientifold-even divisors. Note that the general $\mathcal{N} = 1$ effective action (9.1.2) with the gauge coupling (9.1.6) is not a standard $\mathcal{N} = 1$ action due to the presence of the flux correction in (9.1.6). These fluxes actually break the gauge group in the eight-dimensional world volume theory of the D7-branes. To make this more explicit we display the action splitting into a flux-independent and a flux-dependent part as

$$\begin{aligned} S^{(4)}_{F^2_{\rm D7}} &= -2\pi \int_{\mathcal{M}_4} \tfrac{1}{2}{\rm Re}f^c\,{\rm Tr}(F\wedge *F) + \tfrac{1}{2}{\rm Im}f^c\,{\rm Tr}(F\wedge F) \\ &\qquad + \tfrac{1}{2}{\rm Re}f^{\rm flux}_{\mathcal{A}\mathcal{B}}\,F^{\mathcal{A}}\wedge *F^{\mathcal{B}} + \tfrac{1}{2}{\rm Im}f^{\rm flux}_{\mathcal{A}\mathcal{B}}\,F^{\mathcal{A}}\wedge F^{\mathcal{B}}\ . \end{aligned} \tag{9.1.7}$$

Clearly, a standard $\mathcal{N} = 1$ action can be found if the fluxes are zero and the gauge group is completely unbroken. A second possibility is to consider the breaking of the group, for example by moving the D7-branes apart on Z_3. Then one finds a standard $\mathcal{N} = 1$ action for a gauge group $\mathrm{U}(1)^k$. For completeness we will summarize the result in this phase. Later on we will T-dualize the D7-branes to D6-branes which can then be moved apart in the T-dualized direction.

Assuming that we can move the D7-branes apart on different internal cycles in the same class $[S_{\rm b}]$. The gauge coupling function can be given for each individual brane labeled by $I = 1, \ldots, k$. Fluxes are now only located on each separate D7-brane, which is reflected in the structure of adjoint indices. Indeed, in evaluating $\mathcal{C}_{IJ}$ and $\tilde{\mathcal{C}}_{IJ}$ from (9.1.3) we use the basis $E_I = {\rm diag}(0, \ldots, 0, 1, 0, \ldots, 0)$ with 1 at the I-the position that is related to the $T_I = (T_i, \mathbf{1})$ by a basis transformation. We then readily evaluate (9.1.3) as

$$\mathcal{C}_{IJ} = \delta_{IJ}\,, \qquad \tilde{\mathcal{C}}_{IJ} = \frac{1}{2}\delta_{IJ}\delta_{KL}\delta_{IK}\int_{S_{\rm b}} \mathcal{F}^K\wedge\mathcal{F}^L = \frac{1}{2}\delta_{IJ}n^I\,, \tag{9.1.8}$$

where we exploited that the E_I commute to evaluate the symmetrized trace sTr(.). Here $\mathcal{F}^I$ denotes the internal flux on the Ith D7-brane. The numbers n^I characterize the topology of the gauge configuration on the I-th brane. They are related to the integral instanton number k^I of the U(1) on the I-th brane as $n^I = -8\pi^2 k^I$. Using these results the gauge coupling function on the I-th D7-brane is given by

$$f_I = \tfrac{1}{4}\left(\delta_S^\alpha T_\alpha - i\tfrac{1}{2}\tau\, n^I\right)\,. \tag{9.1.9}$$

As we will see in section 9.3 for the comparison of the D7-brane action with the M-theory fourfold compactification it turns out to be convenient to dualize certain scalars into form fields. More precisely, we replace in four dimensions the chiral multiplet containing the complex scalars T_α with a linear multiplet containing the bosonic fields $(L^\alpha, \mathcal{C}_2^\alpha)$. Here L^α are real scalars dual to the real part ${\rm Re}T_\alpha$ and the imaginary part ${\rm Im}T_\alpha$ is dual due to its shift symmetry to a two-form $\mathcal{C}_2^\alpha$. It will then be crucial to follow the terms involving $f_{\mathcal{A}\mathcal{B}}$ through the dualization. As outlined in detail in appendix A.7 this procedure dualizes the classical coupling ${\rm Im}f^{\rm c}(T){\rm Tr}(F\wedge F)$ in (9.1.7) into a modification of the field strength strength $\mathcal{H}_3^\alpha$ of $\mathcal{C}_2^\alpha$ by the Chern-Simons form $\omega_{\rm CS}$ to ${\rm Tr}(F\wedge F)$,

$$\mathcal{H}_3^\alpha = d\mathcal{C}_2^\alpha + \tfrac{1}{8}\delta_S^\alpha\omega_{\rm CS}\ , \qquad \omega_{\rm CS} = A\wedge dA + \tfrac{2}{3}A\wedge A\wedge A\,. \tag{9.1.10}$$

The complete dual action as given in (A.7.6) of appendix A.7 then contains all terms in (9.1.7) except the term involving ${\rm Im}f^{\rm c}(T)$ which is replaced, together with the kinetic term

for the $\mathrm{Im}T_\alpha$, by a kinetic term for $\mathcal{H}^\alpha$. Of course all other fields that do not couple to $\mathrm{Im}T_\alpha$ like τ and $\mathrm{Re}T_\alpha$ or its dual L^α are unaffected. For the later comparison to M-theory it is important to keep in mind the Kähler potential $\tilde{K}$ for L^α and τ obtained by Legendre transformation of $K(\tau|T)$ as

$$\tilde{K}(\tau|L) = K + L^\alpha \,\mathrm{Re}T_\alpha = \log(\tfrac{1}{6} L^\alpha L^\beta L^\gamma \mathcal{K}_{\alpha\beta\gamma}) - \log(\tau - \bar{\tau})\,. \tag{9.1.11}$$

9.1.2. Dimensional reduction to three dimensions

In this subsection we discuss the circle reduction of the four-dimensional effective action of a D7-brane in an orientifold compactification to three dimensions. The final result will later be compared to the M-theory reduction on a Calabi-Yau fourfold when restricted to the weak coupling limit. It is important to stress that the M-theory reduction is performed on a smooth geometry at large volume. In the three-dimensional effective theory this yields a gauge theory on the Coulomb branch. In 4d F-theory compactified on an extra circle new terms in the effective theory are generated due to the necessity to integrate out massive vector multiplets containing the W-bosons and charged chiral matter multiplets [54, 151].

In the D7-brane picture we consider a reduction on a circle of circumference r. Moving on the Coulomb branch is achieved by giving the scalars in the three-dimensional vector multiplets a vacuum expectation value. In order to make this more precise we make the following reduction ansatz for the four-dimensional fields,

$$g^4_{\mu\nu} = \begin{pmatrix} g_{pq} + r^2 A^0_q A^0_p & r^2 A^0_q \\ r^2 A^0_p & r^2 \end{pmatrix}, \qquad A = (A_3 - A^0\zeta, \zeta)\,. \tag{9.1.12}$$

Here A_3 and ζ are a three-dimensional vector and a three-dimensional scalar both transforming in the adjoint of the gauge group G. The Coulomb branch is obtained by giving ζ a vev, and splitting

$$\mathrm{U}(k) \;\to\; \mathrm{U}(1)^k\,, \qquad A \;\to\; A^I\,, \qquad \zeta \;\to\; \zeta^I\,, \tag{9.1.13}$$

where $I = 1, ..., k$ runs only over the Cartan generators T_I of $\mathrm{U}(k)$. In this split one can now evaluate the traces (9.1.3). By the basis change to the $E_I = \mathrm{diag}(0, \ldots, 1, \ldots, 0)$ the traces can be written, by the same calculations leading to (9.1.8), as

$$\mathcal{C}_{IJ} = \delta_{IJ}\,, \qquad \tilde{\mathcal{C}}_{IJ} = \tfrac{1}{2}\delta_{IJ} n^I\,, \tag{9.1.14}$$

where we used the numbers n^I introduced before. The couplings of the gauge-fields are thus encoded by

$$f_{IJ} = \tfrac{1}{4}(C^\alpha_{IJ} T_\alpha - i\tfrac{1}{2}\tau\delta_{IJ} n^I)\,, \qquad C^\alpha_{IJ} = \delta^\alpha_S \mathcal{C}_{IJ}\,. \tag{9.1.15}$$

Note that this breaking has a natural interpretation in the T-dual picture, where the T-duality is performed along the reduction circle. In this duality the D7-branes become D6-branes localized on points of the reduction circle. The Coulomb branch corresponds to moving the D6-branes apart. The ζ^I can then be reinterpreted as positions on the circle.

Since we are reducing an $\mathcal{N} = 1$ supersymmetric action in four dimensions, we obtain an

action with $\mathcal{N}=2$ supersymmetry in three dimensions. It can be brought into the form

$$S^{(3)} = 2\pi \int_{\mathcal{M}_3} -\tfrac{1}{2}R_3 * 1 - \tilde{K}_{a\bar{b}} dM^a \wedge *d\bar{M}^{\bar{b}} + \tfrac{1}{4}\tilde{K}_{\Lambda\Sigma} d\xi^\Lambda \wedge *d\xi^\Sigma + \tfrac{1}{4}\tilde{K}_{\Lambda\Sigma} F^\Lambda \wedge *F^\Sigma + F^\Lambda \wedge \mathrm{Im}(\tilde{K}_{\Lambda a} dM^a), \tag{9.1.16}$$

where one has to perform the Weyl-rescaling $g_{pq} \to r^2 g_{pq}$ to the Einstein-frame metric, and to make the following identifications,

$$R = r^{-2}\,, \qquad \xi^\Lambda = (R, R\zeta^I)\,, \qquad A^\Lambda = (A^0, A^I)\,, \tag{9.1.17}$$

with $\Lambda = 0, 1, \ldots, k$. Here, the M^a collectively denote four-dimensional chiral multiplets. The three-dimensional kinetic potential $\tilde{K}$ depends on M^a, $\bar{M}^{\bar{b}}$ as well as ξ^Λ and reads

$$\tilde{K} = K(M, \bar{M}) + \log R - \frac{1}{R}\mathrm{Re} f_{IJ}(M)\xi^I \xi^J\,, \tag{9.1.18}$$

where $K(M, \bar{M})$ is the four-dimensional Kähler potential evaluated for the three-dimensional fields. This kinetic potential contains also the gauge kinetic function since the third component of the four-dimensional vectors have become scalars ξ^I in three dimensions as is obvious from (9.1.12).

Let us be more concrete by reducing the four-dimensional action (A.7.6) with linear multiplets. Since we are considering not only chiral and vector multiplets, but also linear multiplets containing $\mathcal{C}_2^\alpha$, the form of the kinetic action in three dimensions we will obtain will be different from (9.1.16).[4] Incorporating two-forms we specify the reduction ansatz for $\mathcal{C}_2^\alpha$ such that

$$\mathcal{H}_3^\alpha \quad \to \quad (\tilde{F}^\alpha + \tfrac{1}{4}C_{IJ}^\alpha \zeta^I F^J) \wedge dy\,, \tag{9.1.19}$$

where we introduced the field strength $\tilde{F}^\alpha = d\mathcal{A}^\alpha$ in three dimensions. Physically this means that the fields T_α, of which $\mathrm{Im}T_S = \delta_S^\alpha T_\alpha$ constitutes the leading part of the D7-brane gauge coupling, will occur after dualization into two-forms and dimensional reduction as vectors in three dimensions. Plugging that into the action (A.7.6) and performing a Weyl rescaling $g_{\mu\nu} \to r^2 g_{\mu\nu}$ we integrate out the circle coordinate y to obtain

$$S^{(3)}_{F^I, F^\alpha} = 2\pi \int_{\mathcal{M}_3} \tilde{K}_{\alpha\beta}(\tilde{F}^\alpha + \tfrac{1}{4}C_{IJ}^\alpha \zeta^I F^J) \wedge *(\tilde{F}^\beta + \tfrac{1}{4}C_{IJ}^\beta \zeta^I F^J) - \tfrac{1}{2R}\mathrm{Re} f_{IJ}(F^I \wedge *F^J + d\xi^I \wedge *d\xi^J) - \mathrm{Im} f_{IJ}^{\mathrm{flux}} d\zeta^I \wedge F^J \tag{9.1.20}$$

where we used the kinetic potential (9.1.18) with the four-dimensional Kähler potential (9.1.11). As one can easily check this matches the structure anticipated in (9.1.16) which is supplemented by additional terms involving the vectors $\tilde{F}^\alpha$ contributed by the linear multiplets. The terms to determine f_{IJ} are:

(1) the kinetic term $F^I \wedge *F^J$ to determine the complete $\mathrm{Re} f_{IJ}$,

(2) the mixed terms $F^I \wedge *\tilde{F}^\alpha$ to determine the classical part of $\mathrm{Im} f_{IJ}$ proportional to $\mathrm{Im}T_\alpha$,

(3) the term $d\zeta^I \wedge F^J$ to obtain $\mathrm{Im} f_{IJ}^{\mathrm{flux}}$.

[4] However, we note that an action including linear multiplets can be brought in the standard form using duality of vectors and scalars in three dimensions.

Let us close this section by commenting on another choice of Cartan generators for U(k) which naturally appears in M-theory. This choice is associated to the split U(k) = SU(k) × U(1) and yields the trace $\mathcal{C}_{IJ}$ in (9.1.3) as

$$\mathcal{C}_{ij} = C_{ij}, \qquad \mathcal{C}_{00} = k \ , \qquad \mathcal{C}_{i0} = 0 \ , \tag{9.1.21}$$

where $i, j = 1, ..., k-1$ label the Cartan generators $T_i = E_i - E_{i+1}$ of SU(k) and C_{ij} is the Cartan matrix of SU(k). Decoupling the overall U(1) of $\tilde{T}_0 = \mathbf{1}$ in U(k) as in [149, 150], the classical part of the three-dimensional gauge coupling function (9.1.6) splits for the Cartan U(1)'s of SU(k) as

$$f_{ij} = \tfrac{1}{4}\, C_{ij}^{\alpha}\, T_{\alpha} \ , \qquad\qquad C_{ij}^{\alpha} = C_{ij}\delta_S^{\alpha} \ . \tag{9.1.22}$$

It was this coupling which was found in [138] in a dimensional reduction of M-theory on a resolved Calabi-Yau fourfold. We will recall this reduction briefly in section 9.3.2.

9.2. M-theory compactifications and Taub-NUT geometries

In order to understand the gauge kinetic function of 7-branes in F-theory, we have to extend the Type IIB effective action discussed in the last section away from the weak coupling limit. This is achieved by considering F-theory as a limit of M-theory with G_4-fluxes.

It was shown in section 7.2.1 that the G_4-background flux induces a non-trivial warp factor. We will show later on that this back-reaction corrects the gauge coupling function. Since we will be interested in the gauge dynamics of one stack of 7-branes it will be necessary to introduce the dual local M-theory geometries. For a stack of k D7-branes the form of this local M-theory geometry can be inferred via string duality. First we note that in compactifying Type IIB on a circle one can T-dualize the D7-branes into k D6-branes. These D6-branes lift in M-theory to the geometry of Kaluza-Klein monopoles. Since the metric and cohomology of Kaluza-Klein monopoles in M-theory is just given by a Taub-NUT[5] space TN_k with k indicating the number of monopoles, we can explicitly analyze their local geometry in subsection 9.2.1.

Having introduced the multi-Taub-NUT spaces we discuss in subsection 9.2.2 a further compactification on a circle on which one can perform a T-duality to the F-theory setup. The resulting geometry will serve as a local model of the singular elliptic fibration of the M-/F-theory fourfold Y_4 with a 7-brane located on a divisor $S_{\rm b}$ in the base. The compactification of the Taub-NUT geometry is achieved by considering an infinite chain of Kaluza-Klein monopoles with period a, denoted TN_k^{∞}, and later considering the quotient. Technically, this process involves a resummation of certain divergent infinite sums in the corresponding metric.

9.2.1. Kaluza-Klein-monopoles: TN$_k$-spaces in M-theory

In this section we like to identify local geometries in Y_4 which would correspond to D6-branes at weak coupling. Note that our geometries Y_4 will be elliptic fibrations in which such a weak coupling limit can be performed. The D6-branes are located at the points where the elliptic fiber pinches. In particular, a D6-brane will wrap the divisors $S_{\rm b}$ in the base B_3 if the elliptic fiber pinches over this divisor. Clearly it is very hard to evaluate the

[5] This name is due to Taub and Newman, Unti and Tamburino (NUT), but can also be traced back to nut at the origin which is the terminus for an isometrical fixed point introduced by Hawking.

warp factor equation (7.2.7) for the full geometry Y_4. To proceed we therefore will focus on a local model denoted as $\mathcal{Y}_4$ which arises in a patch of Y_4 near $S_{\rm b}$.

Before considering the periodic case with an additional circle let us first recall some classical facts about the origin of D6-branes in M-theory. The D6-brane lifts in M-theory to a Kaluza-Klein monopole that is a solution to eleven-dimensional supergravity [152]. Roughly speaking, this monopole solution is an asymptotically locally flat circle fibration[6] over $\mathbb{R}^3$ with degeneration loci at a point in $\mathbb{R}^3$. The asymptotic circumference of the circle fibration will be denoted by $r_{\rm A}$, and corresponds to the Type IIA string coupling

$$g_s^{\rm IIA} = \frac{r_{\rm A}}{2\pi} \ . \tag{9.2.1}$$

In the weak coupling limit $r_{\rm A} \to 0$ the M-theory setup reduces to the Type IIA string with a D6-brane located at the point where the monopole circle pinches.

We will directly consider the case of multiple Kaluza-Klein monopoles since we will need to consider periodic arrays later on. The solution with k Kaluza-Klein monopoles will be denoted by TN_k. The metric of TN_k is given by

$$ds^2_{TN_k} = \frac{1}{V}(dt + U)^2 + V d\vec{r}^{\,2} \ , \tag{9.2.2}$$

where $t \sim t + r_{\rm A}$ is a periodic coordinate on a circle S^1 of circumference $r_{\rm A} = 4\pi m$ with m being the mass of the Taub-NUT solution. The flat part of TN_k is $\mathbb{R}^3$ with coordinates $\vec{r} = (x, y, z)$. The one-form U on $\mathbb{R}^3$ is the S^1 connection. In this metric one has the functions

$$V = 1 + \sum_{i=1}^{k} V_I, \qquad U = \sum_{I=1}^{k} U_I, \qquad V_I = \frac{m}{|\vec{r} - \vec{r}_I|}, \qquad *_3\, dU_I = -dV_I \,, \tag{9.2.3}$$

where $\vec{r}_I$ denote the positions of the k monopoles, and $*_3$ is the Hodge star in $\mathbb{R}^3$. We denote this space as TN_k. We see that the circle fibration degenerates at the k points $\vec{r}_I$ in $\mathbb{R}^3$. Note that one has to use two patches around each monopole in order to obtain a globally well-defined connection U_I. Furthermore, one has to have the same mass m for all monopoles in order to get a smooth solution. The multi-center solution TN_k admits k anti-selfdual two-forms locally defined by

$$\Omega_I = d\eta_I = \frac{1}{4\pi m} d\Big(\frac{V_I}{V}(dt + U) - U_I\Big), \qquad I = 1, \ldots, k \ . \tag{9.2.4}$$

It is straightforward although technically involved to check that

$$\int_{TN_k} \Omega_I \wedge \Omega_J = -\delta_{IJ} \,, \tag{9.2.5}$$

as was noted in [153] and is shown in detail in appendix A.8.

Let us comment on the topology of TN_k. One can introduce the following real two-dimensional subvarieties of TN_k defined as

$$S_i = \big\{\ (t, \vec{r}) \,|\, \exists p \in [0,1] \text{ s. t. } \vec{r} = (1-p)\vec{r}_i + p\vec{r}_{i+1}\big\}, \qquad i = 1, \ldots, k-1 \ . \tag{9.2.6}$$

[6] The geometry approaches an S^1-bundle over $S^2 \times \mathbb{R}$ at infinity in $\mathbb{R}^3$.

These subvarieties are indeed closed two-cycles by noting the degeneration of the S^1-fiber at the position of the monopoles which gives them the topology of a sphere $S^2 = \mathbb{P}^1$. The generators $S_1, \ldots, S_{k-1}$ span the second homology of TN_k that is thus given by $\mathbb{Z}^{k-1}$. Furthermore these surfaces intersect each other as the negative Cartan matrix C_{ij} of A_{k-1} which matches the fact that these geometries give $SU(k)$ gauge theories [154]. To see this one notices that S_i and S_j, $i \neq j$, intersect each other exactly once if and only if $i = j-1$ but with reversed orientation. To find the self-intersection of S_i, deform the base curve generically, which intersects the old one precisely at $\vec{r}_i$ and at $\vec{r}_{i+1}$ this time with the same orientation resulting in the self-intersection two. If we add the cycle S_0 connecting $\vec{r}_1$ and $\vec{r}_k$, that is minus the sum of the S_i, we obtain the Cartan matrix of affine A_{k-1}. This is consistent with the fact, that TN_k is for generic moduli the resolution of an A_{k-1}-singularity[7]. In summary $H_2(TN_k, \mathbb{Z})$ is isomorphic to the weight lattice of A_{k-1}.

The Poincaré dual of $H_2(TN_k, \mathbb{Z})$ is given by $H^2_{\text{cpct}}(TN_k, \mathbb{Z})$, the second cohomology with compact support. Hence it is isomorphic to $\mathbb{Z}^{k-1}$ and its generators are given by [155]

$$\hat{\omega}_i = \Omega_i - \Omega_{i+1} \ . \tag{9.2.7}$$

These fulfill the following conditions, see appendix A.8,

$$\int_{TN_k} \hat{\omega}_i \wedge \hat{\omega}_j = -C_{ij}, \quad \int_{S_i} \hat{\omega}_j = -C_{ij}. \tag{9.2.8}$$

This concludes our discussion of the space TN_k. It will be crucial in a next step to generalize these geometries to have infinitely many centers in order to describe periodic configurations.

9.2.2. S^1-compactification of TN_k: TN_k^∞-space in M-theory

Our goal is to to eventually describe 7-branes F-theory and to derive their gauge coupling function. At weak Type IIB string coupling the corresponding D7-branes T-dualize to D6-branes localized on a circle, which we termed the B-circle. In order to describe this situation in M-theory we consider an infinite array of Kaluza-Klein monopoles separated by a distance r_{B} in the z-direction of $\mathbb{R}^3$ introduced in (9.2.2). To effectively compactify this z-direction on a circle we mod out the relation $z \sim z + r_{\text{B}}$. This is analogous to the geometries considered in [144, 156, 157].

We first introduce the metric structure on the infinite array denoted by TN_k^∞ in the following. This space is obtained as follows. We first consider the special situation of TN_k with centers located in the (x, y)-origin but separated along the z-coordinate in (9.2.2) by a distance z_I. This implies that we take the vectors $\vec{r}_I$ in (9.2.3) of the form

$$\vec{r}_I = (0, 0, z_I) \ , \qquad 0 \leq z_I < r_{\text{B}} \ . \tag{9.2.9}$$

Next we periodically extend this space to TN_k^∞ in the z-direction with period r_{B}. The metric for such a configuration still takes the form

$$ds^2_{TN_k^\infty} = \frac{1}{V}(dt + U)^2 + V d\vec{r}^{\,2}, \tag{9.2.10}$$

[7] Indeed if all monopoles approach each other the area of the S_i vanishes and the space develops a $\mathbb{Z}_{k-1}$-singularity. To see this one expands the metric along the lines as was done for the case of the single monopole. The configuration which arises by squeezing all monopoles together corresponds to a monopole of charge nm which equippes ψ with a periodicity of $\frac{4\pi}{k}$ what shows the desired deficit angle.

where V is a harmonic function on $\mathbb{R}^3$ except at the points $\vec{r}_I$ and U a connection one-form,

$$V = 1 + \sum_{I=1}^{k} V_I \,, \qquad U = \sum_{I=1}^{k} U_I \ . \tag{9.2.11}$$

Since we consider an infinite array V_I, U_I are of the form

$$V_I = \frac{r_{\rm A}}{4\pi} \sum_{\ell\in\mathbb{Z}} \frac{1}{\sqrt{\rho^2 + (z + \ell\, r_{\rm B} - z_I)^2}} - \frac{r_{\rm A}}{4\pi} \sum_{l\in\mathbb{Z}^*} \frac{1}{r_{\rm B}|\ell|} \,, \qquad *_3\, dU_I = -dV_I \ . \tag{9.2.12}$$

where $r_{\rm A} = 4\pi m$, $\mathbb{Z}^* = \mathbb{Z}\backslash\{0\}$, and $\rho = \sqrt{x^2 + y^2}$. The first term in V_I is just the potential of a periodic configuration of monopoles along the z-axis with spacing $r_{\rm B}$. The second term in V_I is a regulator which ensures convergence and can be modified by any finite constant. This metric is also called the Ooguri-Vafa metric, that was initially constructed in the analysis of the hypermultiplet moduli space of Type II string theory [144]. To see that the metric (9.2.10) defined with V and U in (9.2.11) is smooth for finite and different $z_I \neq z_J$ for $I \neq J$ one notices that locally near the singularities of V the space looks like that of one single Kaluza-Klein monopole which is known to be smooth. For our later discussion it will be crucial to introduce the rescaled coordinates

$$\hat{t} = \frac{t}{r_{\rm A}} \,, \qquad \hat{z} = \frac{z}{r_{\rm B}} \,, \qquad \hat{z}^I = \frac{z^I}{r_{\rm B}} \,, \qquad \hat{\rho} = \frac{\rho}{r_{\rm B}} \,. \tag{9.2.13}$$

Note that in these coordinates one has the periodic identifications

$$\hat{t} = \hat{t} + 1 \,, \qquad \hat{z} = \hat{z} + 1 \,, \qquad \hat{z}^I = \hat{z}^I + 1 \ . \tag{9.2.14}$$

To obtain a better understanding of the regularity and the physical meaning of the solution one has to perform a Poisson resummation of V and U [144, 145]. The details of the calculations are relegated to appendix A.9. Finally we may then write

$$\begin{aligned} V_I &= -\frac{r_{\rm A}}{2\pi r_{\rm B}} \Big(\log\Big(\frac{\rho}{\Lambda r_{\rm B}}\Big) - \sum_{\ell\in\mathbb{Z}^*} K_0\Big(\frac{2\pi\rho}{r_{\rm B}}|\ell|\Big)\ e^{2\pi i\ell(z-z_I)/r_{\rm B}} \Big) \\ &= -\frac{r_{\rm A}}{2\pi r_{\rm B}} \Big(\log\Big(\frac{\hat{\rho}}{\Lambda}\Big) - 2\sum_{\ell>0} K_0(2\pi\hat{\rho}\,\ell)\ \cos(2\pi\ell(\hat{z} - \hat{z}_I)) \Big) \,, \end{aligned} \tag{9.2.15}$$

where Λ is a constant which can be chosen arbitrarily in the regularization of (9.2.12). [8] The function $K_0(x)$ is the zeroth Bessel function of second kind. Let us note that V_I satisfies the Poisson equation

$$\Delta_3 V_I = -\frac{r_{\rm A}}{r_{\rm B}\,\hat{\rho}}\ \delta(\hat{z} - \hat{z}_I)\delta(\hat{\rho})\delta(\varphi) \ , \tag{9.2.16}$$

where $\Delta_3 = \frac{\partial^2}{\partial\hat{\rho}^2} + \frac{1}{\hat{\rho}}\frac{\partial}{\partial\hat{\rho}} + \frac{1}{\hat{\rho}^2}\frac{\partial^2}{\partial\varphi^2} + \frac{\partial^2}{\partial\hat{z}^2}$ is the Laplacian in cylinder coordinates. One can also perform a Poisson resummation for U, as we do in appendix A.9, finding up to an ambiguity

[8] In appendix A.9 we have fixed $1/\Lambda = \pi e^{2\gamma}$ with $\gamma \approx 0.577$ denoting the Euler-Mascheroni constant.

of an exact form

$$\begin{aligned} U_I &= \frac{r_{\rm A}}{4\pi}\Big(-1 - 2(\hat{z}-\hat{z}_I) + 2i\hat{\rho}\sum_{\ell\in\mathbb{Z}^*}\mathrm{sign}(\ell)K_1\Big(2\pi\hat{\rho}|\ell|\Big)e^{2\pi i\ell(\hat{z}-\hat{z}_I)}\Big)d\varphi \\ &= -\frac{r_{\rm A}}{4\pi}\Big(1 + 2(\hat{z}-\hat{z}_I) + 4\hat{\rho}\sum_{\ell>0}K_1(2\pi\hat{\rho}\ell)\sin\big(2\pi\ell(\hat{z}-\hat{z}_I)\big)\Big)d\varphi\ , \end{aligned} \tag{9.2.17}$$

for $\hat{z}_I \le \hat{z} < \hat{z}_I + 1$, where $\varphi = \arctan(y/x)$, and K_1 is the first Bessel function of second kind. In the first term in this expression we have included an integration constant $\hat{z}_I$ which arises when solving (9.2.12). Note that this form is gauge equivalent to U_I with leading term given by $U_I = \frac{r_{\rm A}}{2\pi}(\varphi_0+\varphi)d\hat{z} + \dots$ by the gauge transformation by $d(\hat{z}\varphi)$. It will turn out below that it is important for the F-theory interpretation to define the full circle connection U in this gauge reading

$$U = \frac{k}{2\pi}r_{\rm A}(\varphi+\varphi_0)d\hat{z} - \frac{r_{\rm A}}{2\pi}\Big(2\hat{\rho}\sum_{\ell>0}K_1(2\pi\hat{\rho}\ell)\sin\big(2\pi\ell(\hat{z}-\hat{z}_I)\big)\Big)d\varphi\,. \tag{9.2.18}$$

Here we introduced an integration constant φ_0. As we will show next this choice of integration constant is required when matching the local geometry with an asymptotic elliptic fibration required in F-theory and equivalently for the identification of the three-dimensional RR-form $C_0 \equiv k\varphi_0$.

For completeness we note that also the definition of the two-forms Ω_i can be extended to TN_k^∞. They are given by

$$\Omega_I^\infty = d\eta_I = \frac{1}{r_{\rm A}}d\Big(\frac{V_I}{V}(dt+U) - U_I\Big). \tag{9.2.19}$$

As demonstrated in appendix A.9 these forms still satisfy

$$\int_{TN_k^\infty}\Omega_I^\infty\wedge\Omega_J^\infty = -\delta_{IJ}\ , \qquad *_4\Omega_I^\infty = -\Omega_I^\infty\ , \tag{9.2.20}$$

where the Hodge-star $*_4$ is in the TN_k^∞ metric (9.2.10). In addition, we introduce the generalization of the forms introduced in in (9.2.7) to the geometry TN_k^∞,

$$\omega_i^\infty = \Omega_i^\infty - \Omega_{i+1}^\infty\,. \tag{9.2.21}$$

As on the the Taub-NUT space TN_k we expect them to generate the second cohomology with compact support $H^2_{\rm cpct}(TN_k^\infty,\mathbb{Z})$ and to be dual to the connecting $\mathbb{P}^1$ between z_i and z_{i+1} of the resolved A_{k-1} singularity. In particular, the intersections are given by the Cartan matrix C_{ij} as in (9.2.8).

To close this section, let us now discuss the limit of large $\hat{\rho}$, which means that we are moving away from the centers of the monopoles. In this limit one can expand

$$K_0(x) \sim \sqrt{\frac{\pi}{2x}}e^{-x}, \quad x \gg 1\,, \tag{9.2.22}$$

so that the terms involving the Bessel functions in (9.2.15) and (9.2.17) are exponentially suppressed as $e^{-2\pi\hat{\rho}|\ell|} \to 0$ for large $\hat{\rho}$. Since the z_I are the positions in the z-direction with period $r_{\rm B}$ this is equivalent to smearing one Kaluza-Klein monopole along the z-direction

in the base $\mathbb{R}^3$ to obtain a new isometrical direction.[9] One can then use this isometry to gauge away two components of the connection U keeping only the component U_3 in the z-direction. We therefore obtain the approximate potential and gauge connection

$$V = 1 - \frac{k}{2\pi}\frac{r_{\rm A}}{r_{\rm B}}\log\Big(\frac{\hat\rho}{\Lambda}\Big)\,, \quad U = \frac{k}{2\pi} r_{\rm A}(\varphi+\varphi_0)d\hat z\,, \tag{9.2.23}$$

up to leading order in $r_{\rm B}$. Clearly, this means simply that we have dropped the exponentials in (9.2.15) and (9.2.18). In the limit (9.2.23) we can rewrite the metric (9.2.10) as

$$ds^2_{TN^\infty_k} \approx \frac{1}{V}\big((dt+U_z dz)^2 + V^2 dz^2\big) + V(d\rho^2+\rho d\varphi^2)\,, \tag{9.2.24}$$

where the coordinates have periods $(t,z) = (t+r_{\rm A}, z+r_B)$. In the next step we show that this is simply a two-torus bundle over the $(\hat\rho,\varphi)$-plane with metric

$$ds^2 = \frac{v_0}{{\rm Im}\tau}\big((d\hat t + {\rm Re}\tau\, d\hat z)^2 + ({\rm Im}\tau)^2 d\hat z^2\big) + ds^2_{\rm base}\,, \tag{9.2.25}$$

where v_0 is the volume of the two-torus fiber. The rescaled coordinates $\hat t$ and $\hat z$ with integral periods were introduced already in (9.2.13). Note that this torus structure is present due to the careful choice of boundary conditions, involving the constant φ_0 only, in the determination of (9.2.23). Comparing (9.2.24) and (9.2.25) volume of the torus fiber is given by

$$v_0 = r_{\rm A} r_{\rm B}\,. \tag{9.2.26}$$

The complex structure of the torus-fiber at a fixed point $u = \rho\, e^{i\varphi}$ in the $(\hat\rho,\varphi)$-plane, is given by

$$\tau(u) = \frac{k}{2\pi}(\varphi_0+\varphi) + i\Big(\frac{r_{\rm B}}{r_{\rm A}} - \frac{k}{2\pi}\log\Big(\frac{\hat\rho}{\Lambda}\Big)\Big) = \tau + \frac{k}{2\pi i}\log\Big(\frac{u}{\Lambda}\Big)\,. \tag{9.2.27}$$

Furthermore, the condition $dV = -*\,dU$ ensures that τ is a holomorphic function in u. Recalling the discussion in the introductory section 7, we thus obtain precisely the expected monodromy of the the axio-dilaton in an F-theory with k D7-branes at $u=0$. We identify the background value $\tau = C_0 + i g_s^{-1}$ as

$$C_0 = \frac{1}{2\pi}k\varphi_0\,, \qquad g_s = \frac{r_{\rm A}}{r_{\rm B}}\,. \tag{9.2.28}$$

We also introduce the notation

$$\tau_I(u) = \frac{1}{2\pi}(\varphi+\varphi_0) - i\frac{1}{2\pi}\log\Big(\frac{\hat\rho}{\Lambda}\Big)\,. \tag{9.2.29}$$

That the right-hand side of the equation carries no index is explained by the fact that we have neglected the subleading corrections.

For completeness and later reference we list the leading parts of the anti-selfdual two-form Ω. Inserting (9.2.23) and (9.2.27) into (9.2.19) we obtain

$$\eta^\infty_I = \frac{{\rm Im}\tau_I}{{\rm Im}\tau}(d\hat t + {\rm Re}\tau d\hat z) - {\rm Re}\tau_I d\hat z, \qquad \Omega^\infty_I = d\eta^\infty_I. \tag{9.2.30}$$

[9] In the picture of point particles in $\mathbb{R}^3$ this corresponds to a charged wire extended along the z-axis.

For the case of just one monopole we reproduce (in cohomology) the model discussed in [47] to describe a local 7-brane geometry.

$$\eta^{\infty} = \frac{r_{\mathrm{B}}}{r_{\mathrm{A}}}\frac{1}{\mathrm{Im}\tau}(d\hat{t} + \mathrm{Re}\tau d\hat{z}), \qquad \Omega^{\infty} = d\eta^{\infty}. \tag{9.2.31}$$

As a next step one would have to construct the forms $\omega_i^{\infty} = \Omega_{i+1}^{\infty} - \Omega_i^{\infty}$ as in (9.2.21). However, having neglected the subleading corrections depending on the z-coordinate the forms ω_i^{∞} would vanish identically for the forms (9.2.30). In other words, if we want to localize fluxes or gauge fields along the forms ω_i^{∞} it will be crucial to include the non-trivial z-dependence in (9.2.15).

We conclude by interpreting the geometric meaning of the subleading exponential sums in (9.2.15) and (9.2.17). Approaching $\rho = 0$ where the fiber torus degenerates, we note that the leading term of V does not "know" about the position of the degeneration of the fibration of the A-circle *on* the z-direction. The corresponding degenerated torus that arises from the leading term only, i.e. the metric (9.2.24), merely looks like a very thin tire. However, the degenerated torus that arises from M-/F-theory should look like a torus that pinches at a point only, so that the pinched torus forms a $\mathbb{P}^1$. These two different pictures of the degeneration of the torus are called the "differential geometric" and the "algebraic geometric" degeneration in reference [162]. Including now the exponential corrections in V and U, however, localizes the A-cyle degeneration and thus the torus degeneration at the point $z = 0$ on the B-cycle, which reconciles the differential and algebraic geometric pictures.

9.3. 7-brane gauge coupling functions in warped F-theory

In this section we turn to the computation of the gauge-coupling function of a stack of 7-branes in F-theory by using the dual M-theory. In order to do that we first recall some basics about F-theory on singular elliptically fibered Calabi-Yau fourfolds with an A_{k-1} singularity along a divisor S_{b} in section 9.3.1. This setup leads to an SU(k) gauge theory in the effective four-dimensional theory, and has a weak coupling limit introduced in section 9.1. In section 9.3.2 we use the map of F-theory to a dual three-dimensional M-theory compactification on a resolved Calabi-Yau fourfold to compute the leading gauge coupling function as in [138]. In order to include the corrections due to brane fluxes we perform a refined but local reduction in section 9.3.4, and include a non-trivial warp factor and a back-reacted M-theory three-form as introduced in section 9.3.3. The resulting correction to the D7-brane gauge coupling can be matched with the weak coupling result of section 9.1.

9.3.1. The effective action of F-theory

As briefly discussed in 7, the special subloci of the base of the fibration B_3 where the discriminant Δ of the elliptic fiber vanishes indicate the presence of objects charged under τ. These loci geometrically describe divisors in B_3 over which the elliptic fiber becomes singular. In Type IIB string theory these divisors are wrapped by (p, q)7-branes. The particular type of fiber degeneration leads to different monodromies of τ around the discriminant loci that encode the type of (p, q)7-branes and the gauge groups on these branes. As an example we consider a singular Y_4 with an A_{k-1} singularity in the elliptic fiber over a divisor $S_{\mathrm{b}} \subset B_3$

which describes a stack of k D7-branes on $S_{\rm b}$. In other words we consider the split of the class $[\Delta]$ of the discriminant as

$$[\Delta] = k[S_{\rm b}] + [\Delta'] \ , \tag{9.3.1}$$

where $[\Delta']$ is the residual part of Δ wrapped by a single complicated 7-brane. While Δ' might intersect $S_{\rm b}$ the new physics at these intersections will not be of crucial importance to the discussion of this work. We will mainly focus on a local model near $S_{\rm b}$ and concentrate on the back-reaction of the flux on the geometry. In this local model we introduce a local complex coordinate u such that $S_{\rm b}$ is given by $u = 0$. In the vicinity of $S_{\rm b}$ we have the local behavior

$$j(\tau(\vec{w})) = a\frac{1}{u^k} + b \quad \Rightarrow \quad \tau(\vec{w}) = \begin{cases} j^{-1}(b) & \text{far away from the D7-branes} \\ -i\frac{k}{2\pi}\log(u) & \text{near the D7-branes} \end{cases} \tag{9.3.2}$$

where we have used that $j(\tau) \sim e^{-2\pi i\tau}$ for large $\mathrm{Im}(\tau)$. This is precisely the naively expected dilaton in the neighborhood of a D7-brane in perturbative Type IIB theory. As was already briefly mentioned in section 7, one has to resolve Y_4 to obtain a smooth geometry $\hat{Y}_4$, on which one can Kaluza-Klein reduce eleven-dimensional supergravity (7.2.1) in order to derive the couplings in F-theory. Geometrically this yields $k-1$ new exceptional divisors D_i in $\hat{Y}_4$ resolving the A_{k-1} singularity over $S_{\rm b}$. We denote the Poincaré dual two-forms to D_i by ω_i. The Kaluza-Klein reduction of M-theory to three dimensions requires to expand the Kähler form J of Y_4, as well as the M-theory three-form potential C_3 into harmonic modes. Explicitly, one has [10]

$$\begin{aligned} \frac{J}{\mathcal{V}} &= R\,\omega_0 + L^\alpha\omega_\alpha + \xi^i\omega_i \\ C_3 &= A^0\wedge\omega_0 + A^\alpha\wedge\omega_\alpha + A^i\wedge\omega_i \ , \end{aligned} \tag{9.3.3}$$

where $\mathcal{V}$ is the volume of the Calabi-Yau fourfold $\hat{Y}_4$. Here we have included the two-form ω_0 Poincaré dual to the base B_3, and the two-forms ω_α Poincaré dual to divisors $D_\alpha = \pi^{-1}(D^{\rm b}_\alpha)$ inherited from divisors $D^{\rm b}_\alpha$ of the base. The coefficients (R, L^α, ξ^i), and $(A^{\mathcal{A}}) = (A^0, A^\alpha, A^i)$, with $\mathcal{A} \in \{\alpha, 0, i\}$, are real scalars and vectors in the three-dimensional effective theory. In the F-theory limit to four dimensions, the vector multiplet with bosonic components (R, A^0) becomes part of the four-dimensional metric, and one identifies

$$R = r_{\rm B}^2 \ , \tag{9.3.4}$$

where $r_{\rm B}$ is the circumference of the circle on which the T-duality to Type IIB is performed, and $\mathcal{V}$ is the volume of $\hat{Y}_4$. The vector A^0 is the Kaluza-Klein vector in the four-dimensional metric as in (9.1.12). The vector multiplets with bosonic components (L^α, A^α) lift to complex scalars T_α in the F-theory limit, just as in appendix A.7. Finally, the vector multiplets with bosonic components (ξ^i, A^i) lift to four-dimensional U(1) vector multiplets gauging the Cartan generators T_i of the four-dimensional SU(k) gauge group as in section 9.1.1.

In order to proceed further in the discussion, let us recall the behavior of the fields in the F-theory lift. The latter is given by the vanishing of the fiber volume and the blow-down

[10] Note that we restrict to Calabi-Yau fourfolds with $h^{2,1}(\hat{Y}_4) = 0$, such that no extra scalars arise from C_3.

map from $\hat{Y}_4$ to Y_4. To make this more precise we introduce the following ϵ-scaling [138]

$$r_{\rm B} \mapsto \epsilon\, r_{\rm B}\ , \qquad R \mapsto \epsilon^2 R\ , \qquad \zeta^i \equiv \frac{\xi^i}{R} \mapsto \epsilon^{2/3}\zeta^i\ , \qquad L^\alpha = 2L^\alpha_{\rm IIB}\ , \tag{9.3.5}$$

where the scalars L^α do not scale with ϵ but are identified with a factor two with the Type IIB variables $L^\alpha_{\rm IIB}$ used in appendix A.7. Note that the Type IIB string coupling is given by $g_s^{\rm IIB} = r_{\rm A}/r_{\rm B}$ as can be inferred by using the T-duality rules applied to the Type IIA coupling (9.2.1). Since $g_s^{\rm IIB}$ should not scale in the F-theory limit, we find that also $r_{\rm A} \mapsto \epsilon\, r_{\rm A}$. We note in addition that this identification of the string coupling perfectly agrees with (9.2.28) from M-theory on TN_k^∞.

We can thus give a diagrammatic summary of the limit we will consider. Recalling all identifications from M-theory on TN_∞^k in section 9.2,

$$v^0 = r_{\rm A} r_{\rm B}, \qquad g_s^{\rm IIA} = \frac{r_{\rm A}}{2\pi}\ , \qquad g_s^{\rm IIB} = \frac{r_{\rm A}}{r_{\rm B}}\ , \tag{9.3.6}$$

we consider the following limits:

$$\begin{array}{ccc} \text{M-theory on } TN_\infty & \xrightarrow[v^0\to 0]{\text{F-limit}} & \text{10d F-theory} \\ r_{\rm A},\, r_{\rm B} \text{ finite} & & g_s^{\rm IIB} \text{ finite} \\ \Big\downarrow {\scriptstyle g_s^{\rm IIA}\to 0} & & \Big\downarrow {\scriptstyle g_s^{\rm IIB}\to 0} \\ \text{Type IIA in 9d} & \xrightarrow[v^0\to 0]{\text{F-limit}} & \text{weakly coupled 10d IIB} \\ r_{\rm A} \text{ finite},\, g_s^{\rm A}\sim 0 & & g_s^{\rm IIB}\sim 0\,. \end{array} \tag{9.3.7}$$

Understanding the geometry and the physics of the four corners of this diagram is essential for the calculations of the corrections to the gauge kinetic function in section 9.3.4.

It is important for us to also follow the space TN_k^∞ through the M-theory to F-theory lift. In fact, since the space TN_k corresponds in Type IIA to k parallel D6-branes, the space TN_k^∞ yields an infinite array of periodically repeating parallel D6-branes. The periodic coordinate in section 9.2.2 was $z = z + r_{\rm B}$, which we normalized to have integer periods by setting $\hat{z} = z/r_{\rm B}$. In the z-direction the monopoles are separated by distances $z_{i+1} - z_i$, where z_I are the locations of the k monopoles. Without loss of generality we will take in the following $z_1 = 0$, setting the location of the first monopole to be the origin. We identify the blow-up modes ξ^i in (9.3.3) with the normalized differences as we will later justify in section 9.3.4 as

$$\xi^i = r_{\rm B}(z_{i+1} - z_i)\ . \tag{9.3.8}$$

In the F-theory limit $\epsilon \to 0$ the vanishing of the ξ^i requires to also moving the centers on top of each other by sending $z_{i+1} \to z_i$, i.e. one has to send $z_I \to 0$.

9.3.2. Leading 7-brane gauge coupling functions

In this section we recall how the classical volume parts of the 7-brane gauge coupling function can be derived in F-theory via M-theory. This derivation only involves topological methods and can therefore be treated in a rigorous global picture of a compact Calabi-Yau fourfold Y_4. We return to a local analyis when deriving the corrections to the gauge-coupling function in section 9.3.4.

Let us note that the field strength of C_3 given in (9.3.3) is given by

$$G_4 = F^{\mathcal{A}} \wedge \omega_{\mathcal{A}} = F^0 \wedge \omega_0 + F^\alpha \wedge \omega_\alpha + F^i \wedge \omega_i \ . \tag{9.3.9}$$

In this expression $F^{\mathcal{A}} = dA^{\mathcal{A}}$ are the field strengths of the three-dimensional $U(1)$ gauge fields. The three-dimensional effective action is computed by inserting the expansion (9.3.9) into the eleven-dimensional supergravity action (7.2.1). Since we are interested in the leading flux-independent gauge coupling function we assume here that the metric is not warped by demanding that the warp factor $e^{3A/2}$ in (7.2.5) is constant, and we set the background flux $\mathcal{G}_4 = 0$. Here we are interested in the reduction of the kinetic term of G_4, and derive

$$S^{(11)}_{\rm kin} = \frac{\pi}{2}\int G_4 \wedge *G_4 \cong 2\pi \int_{\mathbb{R}^{(2,1)}} \mathcal{G}_{\mathcal{AB}}\, F^{\mathcal{A}} \wedge *F^{\mathcal{B}} \tag{9.3.10}$$

where in the second equality we have performed a Weyl rescaling of the three-dimensional metric $g^{(3)} \to \mathcal{V}^2 g^{(3)}$ in order to bring the action into the Einstein frame, and introduced the metric

$$\mathcal{G}_{\mathcal{AB}} = \frac{\mathcal{V}}{4}\int_{\hat{Y}_4} \omega_{\mathcal{A}} \wedge *\omega_{\mathcal{B}} \ , \qquad \omega_{\mathcal{A}} = (\omega_0, \omega_i, \omega_\alpha)\,. \tag{9.3.11}$$

In the following we compute the metric $\mathcal{G}_{\mathcal{AB}}$ explicitly and discuss the matching with (9.1.20) in order to read off the gauge-coupling function.

In order to compute the metric $\mathcal{G}_{\mathcal{AB}}$ explicitly we need some information about the intersections of the various forms $\omega_{\mathcal{A}}$. We define $\mathcal{K}_{\mathcal{ABCD}} = \int_{\hat{Y}_4} \omega_{\mathcal{A}} \wedge \omega_{\mathcal{B}} \wedge \omega_{\mathcal{C}} \wedge \omega_{\mathcal{D}}$. Due to the elliptic fibration structure one has $\mathcal{K}_{\alpha\beta\gamma\delta} = 0$. In addition we have $\omega_i \wedge \omega_0 = 0$ in cohomology. We will need the following non-vanishing intersections[11]

$$\mathcal{K}_{0\alpha\beta\gamma} \equiv \tfrac{1}{2}\mathcal{K}_{\alpha\beta\gamma}\,, \qquad \mathcal{K}_{ij\alpha\beta} = -\tfrac{1}{2}C^\gamma_{ij}\,\mathcal{K}_{\alpha\beta\gamma}\ , \qquad C^\gamma_{ij} \equiv C_{ij}C^\gamma\ , \tag{9.3.12}$$

where C_{ij} denotes the Cartan matrix of G as above in section 9.1. We recall that in the M-theory reduction the complex coordinates are given by

$$\begin{aligned} T_\alpha &= \tfrac{1}{6}\int_{D_\alpha} J\wedge J\wedge J + i\int_{D_\alpha} C_6 && (9.3.13)\\ &= \tfrac{1}{4}\mathcal{V}^3\mathcal{K}_{\alpha\beta\gamma}\big(L^\beta L^\gamma R - C^\gamma_{ij}L^\beta\xi^i\xi^j\big) + i\rho_\alpha + \dots\ , && (9.3.14)\end{aligned}$$

where we have used (9.3.3). Using the intersections (9.3.12) one evaluates [12]

$$\begin{aligned} \mathcal{G}_{ij} &= \frac{C^\alpha_{ij}}{4R}{\rm Re}T_\alpha + \mathcal{G}_{\alpha\beta}\frac{C^\alpha_{ik}C^\beta_{jl}\xi^k\xi^l}{R^2} + \dots\ , && (9.3.15)\\ \mathcal{G}_{i\alpha} &= -\frac{\mathcal{G}_{\alpha\beta}}{R}C^\beta_{ij}\xi^j + \dots\ , && (9.3.16)\end{aligned}$$

where the dots indicate terms which are of higher power in R. Inserting these expressions

[11] We note the additional factor of $\frac{1}{2}$ in (9.3.12) in the definition of the intersection numbers $\mathcal{K}$ that was included in [150] to identify with the intersections of the orientifold geometry $B_3 = Z_3/\mathcal{O}$ in the upstairs-picture.

[12] Strictly speaking, a precise match requires a coordinate redefinition of the L^α with a term proportional to $C^\alpha_{ij}\xi^i\xi^j/R$ as in reference [151]. We will omit this here for simplicity. The factors can be fixed by matching the terms which are unaffected by this shift.

into (9.3.10) we find the action

$$S^{(3)}_{\rm kin} = -2\pi \int \mathcal{G}_{\alpha\beta}(F^\alpha - R^{-1}\xi^i C^\alpha_{ij} F^j)\wedge *(F^\beta - R^{-1}\xi^i C^\beta_{ij} F^j) + \tfrac{1}{4R} C^\alpha_{ij} {\rm Re} T_\alpha F^i \wedge * F^j \ . \quad (9.3.17)$$

Comparing this action with (9.1.20) we infer that the leading gauge coupling function is simply given by

$$f_{ij} = \tfrac{1}{2} C^\alpha_{ij} T_\alpha = \tfrac{1}{4} C^\alpha_{ij} T^{0\,\rm IIB}_\alpha \ , \quad (9.3.18)$$

where we recall from (9.3.5) that we have to identify $T_\alpha = \frac{1}{2} T^{0\,\rm IIB}_\alpha$. Note that this expression agrees with the weak coupling result (9.1.22) if we drop the correction term Q_α containing the flux. It will be the task of the final subsection to also reproduce this correction.

Let us conclude this section by noting that the expression (9.3.18) can also be directly inferred from an M-theory kinetic potential $\tilde{K}$. It was shown in [150] that for an elliptic fibration it takes the form

$$\tilde{K}^{\rm M} = \log\Big(\tfrac{1}{12} R L^\alpha L^\beta L^\gamma \mathcal{K}_{\alpha\beta\gamma} - \tfrac{1}{8}\xi^i\xi^j C^\alpha_{ij} L^\beta L^\gamma \mathcal{K}_{\alpha\beta\gamma} + \dots\Big). \quad (9.3.19)$$

and can be obtained from a Kähler potential given by $K^{\rm M} = -3\log\mathcal{V}$ via a Legendre transform. If one Taylor expands (9.3.19) around the F-theory point in moduli space with small ξ^i one finds

$$\tilde{K}^{\rm M} = \log\big(\tfrac{1}{12} L^\alpha L^\beta L^\gamma K_{\alpha\beta\gamma}\big) + \log(R) - \frac{C^\alpha_{ij}\mathcal{K}_{\alpha\beta\gamma} L^\beta L^\gamma}{\frac{1}{3}\mathcal{K}_{\alpha\beta\gamma} R L^\alpha L^\beta L^\gamma}\xi^i\xi^j. \quad (9.3.20)$$

with $\mathcal{K}_{\alpha\beta\gamma}$ the intersection numbers (9.3.12). Comparing this form with the general expression (9.1.18) of a three-dimensional kinetic potential one confirms the identification (9.3.18) of the classical gauge coupling function.

9.3.3. On dimensional reduction with fluxes and warp factor

In this subsection we discuss the dimensional reduction of M-theory with a warp factor and background four-form fluxes $\mathcal{G}_4$. Our main focus will be on the modifications arising in the reduction of the M-theory three-form. Our results will extend the discussion in [136].

Let us now perform the reduction including the warp factor. For simplicity we will not include higher curvature corrections and mobile M2-branes in the supergravity action (7.2.1). We will focus on the terms involving G_4 only, i.e. the kinetic terms and the Chern-Simons term. For the M-theory three-form C_3 itself we make the reduction Ansatz

$$C_3 = A^{\mathcal{A}} \wedge \tilde{\omega}_{\mathcal{A}} + \beta(M^\Sigma) \ , \quad (9.3.21)$$

where $\tilde{\omega}_{\mathcal{A}}$ are two-forms and β is a three-form on $\hat{Y}_4$. The fluctuations are parameterized by three-dimensional vectors $A^{\mathcal{A}}$ and scalars M^Σ, which change the geometry of $\hat{Y}_4$. To restrict to the case of massless vectors $A^{\mathcal{A}}$ we demand in the following

$$d\tilde{\omega}_{\mathcal{A}} = 0 \ . \quad (9.3.22)$$

We introduce the three-forms

$$\beta_\Sigma = \frac{\partial\beta}{\partial M^\Sigma} \ . \quad (9.3.23)$$

The three-form β is only patchwise defined, since we demand that in cohomology $d_8\beta$ encodes the topologically non-trivial background flux $\mathcal{G}_4$. This yields the field strength

$$G_4 = F^{\mathcal{A}} \wedge \tilde{\omega}_{\mathcal{A}} + dM^{\Sigma} \wedge \beta_{\Sigma} + \mathcal{G}_4 \ . \tag{9.3.24}$$

On next inserts the expressions (9.3.21) and (9.3.24) in the 11d supergravity action

$$S^{(11)}_{G_4} = 2\pi \int \frac{1}{4} G_4 \wedge *G_4 + \frac{1}{12} C_3 \wedge G_4 \wedge G_4 \ , \tag{9.3.25}$$

using the warped metric (7.2.5). In order to bring the Einstein-Hilbert term into the standard 3d from one has to perform a Weyl rescaling with the warped volume

$$\mathcal{V}_w = \int_{\hat{Y}_4} e^{3A/2} J \wedge J \wedge J \wedge J \ . \tag{9.3.26}$$

As a result one finds the 3d action [13]

$$\begin{aligned} S^{(3)}_{G_4} \ = \ & 2\pi \int_{\mathcal{M}_3} \mathcal{G}^w_{\mathcal{A}\mathcal{B}} F^{\mathcal{A}} \wedge *F^{\mathcal{B}} + d^w_{\Sigma\Lambda} dM^{\Sigma} \wedge *dM^{\Lambda} + V_w \ * 1 \\ & + \tfrac{1}{4} \Theta_{\mathcal{A}\mathcal{B}} A^{\mathcal{A}} \wedge F^{\mathcal{B}} + d_{\mathcal{A}\Sigma\Lambda} (M^{\Sigma} dM^{\Lambda} \wedge F^{\mathcal{A}}) \ . \end{aligned} \tag{9.3.27}$$

We discuss the various terms appearing in this action in turn. Firstly, there is the kinetic term for the vectors $A^{\mathcal{A}}$ with coupling

$$\mathcal{G}^w_{\mathcal{A}\mathcal{B}} = \frac{\mathcal{V}_w}{4} \int_{\hat{Y}_4} e^{3A/2} \tilde{\omega}_{\mathcal{A}} \wedge *\tilde{\omega}_{\mathcal{B}} \ . \tag{9.3.28}$$

Note that in contrast to (9.3.11) a warp factor appears in the integral. By solving the warp factor equation (7.2.7) we will later show that this induces a flux correction to the gauge coupling function. The term involving $d^w_{\Sigma\Lambda}$ is a correction to the kinetic term of the scalars M^{Σ}. Its explicit form reads

$$d^w_{\Sigma\Lambda} = \frac{1}{\mathcal{V}_w} \int_{\hat{Y}_4} \beta_{\Sigma} \wedge *\beta_{\Lambda} \, , \tag{9.3.29}$$

where we have performed a Weyl rescaling and the Hodge star refers to the unwarped metric, i.e. this term happens to be independent of the warp factor. Moreover, there is the well-known 3d potential V_w introduced by the background flux $\mathcal{G}_4$.

The terms in the second line of (9.3.27) arise from the reduction of the 11d Chern-Simons coupling. The term proportional to $\Theta_{\mathcal{A}\mathcal{B}}$ is a three-dimensional Chern-Simons term with constant coefficient $\Theta_{\mathcal{A}\mathcal{B}} = \int_{\hat{Y}_4} \mathcal{G}_4 \wedge \tilde{\omega}_{\mathcal{A}} \wedge \tilde{\omega}_{\mathcal{B}}$. Depending on the index structure this Chern-Simons term either induces a gauging for non-trivial $\Theta_{i\alpha}$ in the dual 4d F-theory compactification [138, 150, 168], or for Θ_{ij} generated at one loop by the four-dimensional

[13] Note that the reduction of the Chern-Simons term is complicated by the fact that the M-theory potential C_3 appears without derivatives. We suppress terms of the form $\beta \wedge \partial_{M^{\Lambda}} \beta_{\Sigma}$ which are manifestly not gauge invariant. Terms of this type appear in Chern-Simons couplings for D-branes and it would be interesting to interpret them. These terms can be computed explicitly in our example and vanish for the derivatives w.r.t. the M^{Σ} we study.

chiral matter [54]. Finally, the last term in (9.3.27) contains the coupling

$$d_{\mathcal{A}\Sigma\Lambda} = -\frac{1}{4}\int_{\hat{Y}_4} \tilde{\omega}_{\mathcal{A}} \wedge \beta_\Sigma \wedge \beta_\Lambda \ . \tag{9.3.30}$$

We will later show that coupling induces a flux correction to the imaginary part of the F-theory gauge coupling function.

9.3.4. Calculation of corrections to the gauge kinetic function

Finally we are well equipped in order to derive the correction to the gauge kinetic function induced by a non-trivial background flux $\mathcal{G}_4$. We will show that these corrections match in the weak coupling limit the well-known corrections to the gauge kinetic function due to D7-brane flux.

The basic idea to compute the corrections to the real part of the gauge coupling function (9.3.18) is to derive the gravitational back-reaction of the fluxes on the warp factor in M-theory via (7.2.7). This computation requires an explicit knowledge of the metric on the M-/F-theory fourfold $\hat{Y}_4$. We describe the elliptic fourfold $\hat{Y}_4 \to Y_4$ with a resolved SU(k) singularity in the elliptic fibration locally in the vicinity of the resolved singularity by the local geometry constructed in section 9.2.2,

$$\mathcal{Y}_4 = S_\mathrm{b} \times TN_k^\infty \, . \tag{9.3.31}$$

Here S_b is that divisor in the base B_3 of the elliptic fibration[14] Y_4 with the SU(k)-fiber singularity. TN_k^∞ is the periodic chain of multi-center Taub-NUT spaces with metric (9.2.10), that locally describes the normal space in $\hat{Y}_4$ to the resolved singularity over S_b. As discussed in section 9.2.2, the metric on TN_k^∞ is known and governed by the function $V = 1+\sum_{I=1}^k V_I$ and the gauge connection U of (9.2.15) respectively (9.2.17).

In a brane picture in Type IIA and IIB or F-theory, the compactification of M-theory on $\mathcal{Y}_4$ describes the Coulomb branch with U(1)^k gauge symmetry of the 3-dimensional gauge theory from k parallel space-time-filling 6-branes or T-dual, fluxed k 7-branes wrapping $S_\mathrm{b} \times \mathcal{M}_3$ respectively $S_\mathrm{b} \times S^1 \times \mathcal{M}_3$[15], where S^1 denotes the circle in the basis of Taub-NUT TN_k^∞, $\mathbb{R}^2 \times S^1$. In this picture we also introduce the localized $\mathcal{G}_4$-flux in M-theory. This flux is identified with two-form flux $\hat{\mathcal{F}}^I$ of the I-th 6-brane on S_b or its T-dual 7-brane that is valued in the U(1) gauge group of the corresponding brane. It can be embedded into the Cartan sub-algebra of the enhanced gauge group U(1)×SU(k) by defining new fluxes $\mathcal{F}^0$ and $\mathcal{F}^i$, $i = 1, \ldots, k-1$, as

$$\hat{\mathcal{F}}^m = \mathcal{F}^0 + \mathcal{F}^m - \mathcal{F}^{m-1} \, , \qquad \hat{\mathcal{F}}^1 = \mathcal{F}^0 + \mathcal{F}^1 \, , \qquad \hat{\mathcal{F}}^k = \mathcal{F}^0 - \mathcal{F}^{k-1} \, , \tag{9.3.32}$$

where $m = 2, \ldots, k-1$. The flux on $\mathcal{Y}_4$ is thus of the form

$$\mathcal{G}_4 = \hat{\mathcal{F}}^I \wedge \Omega_I^\infty = \mathcal{F}^i \wedge \omega_i^\infty + \mathcal{F}^0 \wedge \sum_J \Omega_J^\infty \, , \tag{9.3.33}$$

[14] We focus here on SU(k)-singularities only in co-dimension 1 in B_3, i.e. S_b is the full internal world-volume of the wrapped branes in a D-brane picture.

[15] Note that the flux on the 7-brane is T-dual to the separation of 6-branes on S^1, i.e. has one leg on $\mathcal{M}_3$ and one leg on S^1. It breaks $U(k) \to U(1)^k$ and is not to be confused with the fluxes $\mathcal{F}^i$ introduced next in (9.3.33).

where the second equality can be checked easily using (9.3.32) and where $I = 1, \ldots, k$ and $i = 1, \ldots, k-1$. Recall that $\omega_i^\infty = \Omega_i^\infty - \Omega_{i+1}^\infty$ are two-forms on TN_k^∞ which have been introduced already in (9.2.21), and satisfy $\int_{TN_k^\infty} \omega_i^\infty \wedge \omega_j^\infty = -C_{ij}$. Note that these forms should be identified with the blow-up forms ω_i appearing in (9.3.3) in the global embedding. Note that the two-form in the expansion with $\mathcal{F}^0$ is trivial in cohomology in TN_k^∞, which matches the fact that the corresponding diagonal U(1) in the enhancement to gauge group U(k) is massive and frozen in the effective theory.

Corrections to the real part of the gauge coupling function

We first calculate the correction to the real part of the gauge coupling function from the back-reaction of the $\mathcal{G}_4$-flux (9.3.33) on the warp factor. We find this corrected warp factor analytically for the full metric (9.2.10) on the local geometry $\mathcal{Y}_4$ with fluxes $\mathcal{G}_4$. Qualitatively, the corrected warp factor then modifies all integrals over the internal space $\hat{Y}_4$, in particular (9.3.10), and thus corrects the gauge kinetic function.

The warp factor equation (7.2.7) on $\mathcal{Y}_4$ is given by

$$\Delta_{\mathcal{Y}_4} e^{3A/2} = *_{\mathcal{Y}_4}(\tfrac{1}{2}\mathcal{G}_4 \wedge \mathcal{G}_4), \tag{9.3.34}$$

where on the right hand side we have only included the background flux $\mathcal{G}_4$ and dropped the remaining terms in (7.2.7). In general the precise expression of the the two-forms $\hat{\mathcal{F}}^I$ on S_b will induce a non-trivial behavior of the warp factor on S_b. However, for simplicity we will neglect the non-trivial profile of $\hat{\mathcal{F}}^I$ on S_b by averaging over S_b as

$$\big\langle \hat{\mathcal{F}}^I \wedge \hat{\mathcal{F}}^J \big\rangle_{S_\mathrm{b}} = \delta^{IJ} \frac{1}{\mathcal{V}_{S_b}} \int_{S_\mathrm{b}} \hat{\mathcal{F}}^I \wedge \hat{\mathcal{F}}^I = \delta^{IJ} \frac{n^I}{\mathcal{V}_{S_\mathrm{b}}}, \tag{9.3.35}$$

where $\mathcal{V}_{S_\mathrm{b}} = \frac{1}{2}\int_{S_\mathrm{b}} J \wedge J$ for J denoting the Kähler form on S_b. Note that we additionally assumed that the off-diagonal elements $I \neq J$ vanish identically. In the brane picture the numbers n^I are then related to the instanton numbers on S_b in the U(1) of the I-th brane, respectively, as discussed below (9.1.8). Similarly we average over the dependence of the warp factor $e^{3A/2}$ on S_b by integrating the right hand side of the warp factor equation (9.3.34) over the S_b. Then we obtain an equation between four-forms on TN_k^∞ reading

$$d *_4 d\, e^{3A/2} = \frac{n^I}{2\mathcal{V}_{S_\mathrm{b}}}\, \Omega_I^\infty \wedge \Omega_I^\infty\,, \tag{9.3.36}$$

where d and $*_4$ denote the exterior derivative respectively the Hodge star on TN_k^∞. In order to solve the warp factor equation (9.3.34) we first evaluate

$$\Omega_I^\infty \wedge \Omega_J^\infty = \frac{2}{r_\mathrm{A}^2} V d\Big(\frac{V_I}{V}\Big) \wedge (dt + U) \wedge *_3 d\Big(\frac{V_J}{V}\Big) = -\frac{2}{r_\mathrm{A}^2} V d\Big(\frac{V_I}{V}\Big) \wedge *_4 d\Big(\frac{V_J}{V}\Big)\,, \tag{9.3.37}$$

where we used the relation $*_3 dU_I = -dV_I$ and $*_4 dV_I = -(dt+U) \wedge *_3 dV_I$ where the latter follows from (A.9.24) and the orientation on TN_k^∞ specified there. Then it is straightforward to show that (9.3.36) is solved by

$$e^{3A/2} = 1 - \frac{n^I}{2r_\mathrm{A}^2 \mathcal{V}_{S_\mathrm{b}}} \Big(\frac{V_I^2}{V} - V_I\Big)\,, \tag{9.3.38}$$

where we made use of $\Delta_3 V_I \sim \delta(z - z_I)$ on the three- dimensional base of the Taub- NUT geometry TN_k^∞ as well as

$$\frac{V_I}{V}(\hat{z} = \hat{z}_J, \hat{\rho} = 0) = \delta_{IJ}\,. \tag{9.3.39}$$

The integration constant in (9.3.38) is chosen to be 1 to reproduce the unwarped case.[16] With this convention the boundary behavior of the warp factor is analyzed as follows. First we introduce a cutoff M "at infinity" in the $\hat{\rho}$-direction so that

$$V_I|_{\hat{\rho}=M} = 0\,, \qquad e^{3A/2}\Big|_{\hat{\rho}=M} = 1\,. \tag{9.3.40}$$

Indeed, this behavior at large $\hat{\rho}$ is necessary to glue the local model $\mathcal{Y}_4$ into a compact Calabi-Yau fourfold $\hat{Y}_4$. Then we evaluate the warp factor on the locus $\hat{Z}_J := (\hat{\rho} = 0, \hat{z} = \hat{z}_J)$ of one monopole in TN_k^∞. We obtain the warp factor

$$\begin{aligned}(e^{3A/2} - 1)\Big|_{\hat{Z}_J} &= \frac{n^I}{2r_{\rm A}^2\mathcal{V}_{S_{\rm b}}}\frac{V_I}{V}\big(1 + \sum_{K\neq I} V_K\big)\Big|_{\hat{Z}_J} = \frac{n^I}{2r_{\rm A}^2\mathcal{V}_{S_{\rm b}}}\big[\delta_{IJ}\big(1 + \sum_{K\neq I} V_K\big) + V_I \sum_{K\neq I}\delta_{KJ}\big]\Big|_{\hat{Z}_J} \\ &= \frac{1}{2r_{\rm A}^2\mathcal{V}_{S_{\rm b}}}\big[n^J + \sum_{K\neq J}(n^J + n^K)V_K|_{\hat{Z}_J}\big]\,,\end{aligned} \tag{9.3.41}$$

which is finite since the potentials V_K are regular at $\hat{Z}_J$ for $K \neq J$. This result is expected since in the one-monopole case the warp factor at the position of the 6-brane should only see the localized flux n^J on that brane and fall off to 1 at distances $\hat{\rho}$ far away from the brane. However, we see from (9.3.41) that in the case of k monopoles, besides this back-reaction of the localized flux n^J on the same 6-brane at $\hat{Z}_J$ the gravitational back-reaction of the localized fluxes n^K from different branes, $K \neq J$, also affects the warp factor at $\hat{Z}_J$ with a suppression factor $V_K|_{\hat{Z}_J}$.

Now we are able to calculate the gauge coupling function. This is carried out by considering the kinetic term (9.3.10) corrected by the warp factor in the general metric ansatz (7.2.5). Following the same logic as for the flux $\mathcal{G}_4$ in (9.3.33) we include a three-dimensional field strength in the expansion of G_4 as

$$G_4 = \hat{F}^I \wedge \Omega_I^\infty + \mathcal{G}_4 = F^i \wedge \omega_i^\infty + F^0 \wedge \sum_J \Omega_J^\infty + \mathcal{G}_4\,, \tag{9.3.42}$$

where $I = 1, \ldots, k$ and $i = 1, \ldots, k-1$. Then, the three-dimensional gauge fields are embedded into $\mathrm{U}(k)$ as

$$\hat{F}^m = F^0 + F^m - F^{m-1}\,, \qquad \hat{F}^1 = F^0 + F^1\,, \qquad \hat{F}^k = F^0 - F^{k-1}\,, \tag{9.3.43}$$

for $m = 2, \ldots, k-1$, which is completely analogous to (9.3.33). The three-dimensional kinetic term for $\hat{F}^I$ is evaluated in the warped background as in section 9.3.3, and contains the warped metric (9.3.28). Focusing on the warped metric in the local fourfold $\mathcal{Y}_4$ we obtain

$$\mathcal{G}_{IJ}^w = \frac{\mathcal{V}_w}{4}\int_{\mathcal{Y}_4} e^{3A/2}\Omega_I^\infty \wedge *_{\mathcal{Y}_4}\Omega_J^\infty = -\frac{\mathcal{V}_w\mathcal{V}_{S_{\rm b}}}{4}\int_{TN_k^\infty} e^{3A/2}\Omega_I^\infty \wedge \Omega_J^\infty \tag{9.3.44}$$

[16] In general the precise linear combination of the two solutions to the homogeneous equation $d *_4 dg = 0$ we have to add has to be determined by global boundary conditions on $e^{3A/2}$.

which is the corrected version of (9.3.11). Here we used that the Hodge star on $\mathcal{Y}_4$ acts as $\frac{1}{2}J^2 *_4$ and in addition the anti-selfduality (9.2.20) of Ω_I^∞. Noting that the forms Ω_I^∞ are constant over S_b we readily integrate out the Kähler form to obtain a volume factor $\mathcal{V}_{S_\mathrm{b}}$. Then we read off the gauge coupling function $\mathrm{Re}f_{IJ}$ simply as the coefficient of the kinetic term $\hat{F}^I \wedge *\hat{F}^J$ in (9.1.20) from which we see that we have to take into account an additional factor of $-2R = -2v^0/\mathcal{V}_w$. In addition we note that the Type IIB volume $\mathrm{Re}T_S = 2\mathcal{V}_{S_\mathrm{b}}$. Since the warp factor only appears linearly in (9.3.44) we insert the solution (9.3.38) for $e^{3A/2}$ to obtain

$$\mathrm{Re}\, f_{IJ} \equiv -2\frac{v^0}{\mathcal{V}_w}\mathcal{G}^w_{IJ} = \tfrac{1}{4}v^0 \mathrm{Re}T_S\delta_{IJ} - \frac{v^0}{4r_\mathrm{A}^2}n^K\int_{TN_k^\infty}\Big(\frac{V_K^2}{V} - V_K\Big)\Omega_I^\infty \wedge \Omega_J^\infty\,, \tag{9.3.45}$$

where we used the property (9.2.20) of the Ω_I on the first term to obtain the proportionality to δ_{IJ}.

We immediately recognize the first term in (9.3.45) as the leading part of the gauge coupling function (9.1.15) on the Coulomb branch of the three-dimensional gauge theory. The second term in (9.3.45) already resembles the real part of the flux induced contribution $\mathrm{Re}f_{IJ}^\mathrm{flux}$ to the gauge coupling (9.1.6) respectively (9.1.15). We obtain the final expression for the gauge coupling function by evaluating the integral in (9.3.45) over the local geometry TN_k^∞. However, instead of evaluating this in general, which is hard due to complicated integrand, we focus on the weak coupling result $g_s \sim 0$. For small g_s, as discussed rigorously in appendix A.8, we can use the localization property

$$\Omega_I^\infty \wedge \Omega_J^\infty \;\to\; -\frac{1}{2\pi}\delta_{IJ}\delta(\hat{\rho})\delta(\hat{z}-\hat{z}_I)d\hat{t}\wedge d\hat{\rho}\wedge d\varphi\wedge d\hat{z} \tag{9.3.46}$$

in local coordinates $\hat{z}$ on the quotient $\mathbb{R}/\mathbb{Z} = S^1$. Then we evaluate the integral in (9.3.45) as

$$\begin{aligned}\mathrm{Re}f_{IJ}^\mathrm{flux} &= -\frac{v^0}{4r_\mathrm{A}^2}n^K\int_{TN_k^\infty}\Big(\frac{V_K^2}{V}-V_K\Big)\Omega_I^\infty\wedge\Omega_J^\infty = \frac{1}{2}\delta_{IJ}v_0\mathcal{V}_{S_\mathrm{b}}(e^{3A/2}-1)\Big|_{\hat{Z}_I}\\ &= \frac{1}{8}g_s^{-1}\delta_{IJ}\big[n^I_{IIB} + \sum_{K\neq I}(n^I_{IIB}+n^K_{IIB})V_K|_{\hat{Z}_I}\big]\,,\end{aligned} \tag{9.3.47}$$

where we used the evaluation of the warp factor (9.3.41) in the last equality and the basic relation $\frac{v^0}{r_\mathrm{A}^2} = g_s^{-1}$ following from (9.3.6). Moreover the remaining integrals over $\hat{t}$ and φ yield a factor 1 respectively 2π. In addition we identified the flux number $n^K_{IIB} = 2n^K$ due to the orientifolding as noted already in (9.3.5).

We note, that in the result (9.1.15) for $\mathrm{Re}f_{IJ}^\mathrm{flux}$ that we obtained by dimensional reduction of the D7-brane effective action to three dimensions we only see the first term in (9.3.47) proportional to n^I. However, this is perfectly consistent recalling that $V_K \sim g_s$, cf. (9.2.15), which reveals the corrections proportional to V_K in (9.3.47) as one loop corrections to the gauge coupling f_{IJ}. These are *not* visible in the string-tree-level D7-brane effective action obtained in section 9.1. More precisely the corrections are suppressed by g_s and the separation $|\hat{z}_I - \hat{z}_k|$ between the branes as

$$V_K|_{\hat{Z}_I} = \frac{g_s}{4\pi}\Big(\frac{1}{|\hat{z}_I-\hat{z}_K|} - 2\gamma - \psi(1-|\hat{z}_I-\hat{z}_K|) - \psi(1+|\hat{z}_I-\hat{z}_K|)\Big)\,, \tag{9.3.48}$$

where we used (9.2.12) and introduced Euler's constant $\gamma = 0.577216\ldots$ as well as $\psi(x)$ denoting the digamma function. The function $\psi(x)$ is well-defined except at $x \in \{0, -1, -2, \ldots\}$ and since $0 < |\hat{z}_I - \hat{z}_K| < 1$, the composition $\psi(1 - |\hat{z}_I - \hat{z}_K|)$ is finite [17]. We note, however, that this implies that the corrections in (9.3.47) diverge as $\frac{1}{|\hat{z}_I - \hat{z}_K|}$ in the case that the branes move on top of each other $\hat{z}_K = \hat{z}_I$. Intuitively this is clear since the integral (9.3.36) calculates formally the self-energy $E = \int \phi \varrho dV$ of charges in three dimensions by identifying $e^{3A/2}$ with the electric potential ϕ and $\Omega_I^\infty \wedge \Omega_I^\infty$ with the charge density ϱ. Thus, by using the approximation (9.3.46) we formally calculate the self-energy of a point charge, that is infinite. However, the self-energy i.e. the integral (9.3.36) is regularized in M-theory by the smooth forms Ω_I^∞ that smear out the charge density ϱ.

Corrections to the imaginary part of the gauge coupling function

In this final section we calculate the flux-induced corrections to the imaginary part of the gauge coupling function. These corrections originate from the 11-dimensional Chern-Simons term $C_3 \wedge G_4 \wedge G_4$ with an altered reduction ansatz (9.3.21) in the presence of a non-trivial flux $\mathcal{G}_4$. Following the logic of section 9.3.3 the dependence of the new three-form $\beta(M^\Sigma)$ on the moduli M^Σ of the compactification geometry is crucial to obtain the coupling $d_{\mathcal{A}\Sigma\Lambda}$ in (9.3.27). It is a Chern-Simons term in three dimensions and is identified with the reduction of the topological term $\mathrm{Tr}(F \wedge F)$ of the four-dimensional gauge theory to three dimensions in (9.1.20). We demonstrate this identification and the reproduction of the right flux correction to the imaginary part of the gauge coupling and obtain a perfect match in the weak coupling limit where we reproduce the flux correction $\sim n^I$ in (9.1.15) to the D7-brane gauge coupling.

First we have to identify the appropriate form for the three-form β that we defined in (9.3.24) as the Chern-Simons form of the flux $\mathcal{G}_4 = d_8\beta$. From the expansion (9.3.33) and recalling $\Omega_I^\infty = d_4\eta_I$ we make the ansatz

$$\beta = \mathcal{F}^I \wedge \eta_I(\varphi_0, \underline{\hat{z}})\,, \tag{9.3.49}$$

where we indicated the moduli dependence of β on the angle φ_0 and the position of the k periodic monopoles $\underline{\hat{z}} = (\hat{z}_I)$ through the one-forms η_I. From this it follows that the relevant terms in the three-dimensional action (9.3.27) take the form

$$S_{G_4}^{(3)} \supset 2\pi \int_{\mathcal{M}_3} \left(d_{IC_0K} C_0 d\hat{z}^K \wedge \hat{F}^I + d_{IKC_0} \hat{z}^K dC_0 \wedge \hat{F}^I \right), \tag{9.3.50}$$

where we identified the RR-axion $\frac{k}{2\pi}\varphi_0 = C_0$ as before in the definition of the axio-dilaton (9.2.28) and set $\tilde{\omega}_I = \Omega_I$ as in (9.3.42). Then the coupling d_{IC_0K} is given by

$$d_{IC_0K} = -\tfrac{1}{4} \int_{\hat{Y}_4} \Omega_I^\infty \wedge \frac{\partial \beta}{\partial C_0} \wedge \frac{\partial \beta}{\partial \hat{z}^K} = -\tfrac{1}{4} n^J \delta^{JL} \int_{TN_k^\infty} \Omega_I^\infty \wedge \partial_{C_0}\eta_L \wedge \partial_{\hat{z}_K}\eta_J\,. \tag{9.3.51}$$

Here we replaced the compact fourfold $\hat{Y}_4$ by our local geometry $\mathcal{Y}_4$ that by its direct product structure $\mathcal{Y}_4 = S_\mathrm{b} \times TN_k^\infty$ allowed us to pull out the integral of the flux over S_b. We note that the two terms in (9.3.50) are equal, up to a term proportional to $d(d_{IC_0K})C_0\hat{z}^K\hat{F}^I$, by

[17] In contrast the Poisson re-summed V_K in (9.2.15) diverges at $\rho = 0$, though, since Poisson re-summation breaks down for $\rho = 0$ and (9.2.15) is not valid at $\rho = 0$.

partial integration and by virtue of the antisymmetry of d_{IC_0K} in the last two indices. In general this can yield further subleading correction to $\mathrm{Im} f_{IJ}$ that we ignore in the following.

In order to show that (9.3.50) reproduces the flux correction to the imaginary part of the gauge coupling we have to evaluate (9.3.51). This is a lengthy but straight forward calculation. Omitting the details we obtain up to exact forms the result

$$\begin{aligned}\Omega_I\wedge\partial_{C_0}\eta_L\wedge\partial_{\hat{z}_K}\eta_J &= \frac{1}{2}\Big[-\frac{V_J}{V}\Big(\frac{V_K}{V}-\delta_{KJ}\Big)\Omega_L\wedge\Omega_I-\frac{V_L}{V}\frac{V_K}{V}\Omega_J\wedge\Omega_I \\ &\quad +2\frac{V_L}{V}V_K\Big(\frac{V_J}{V}-\delta_{KJ}\Big)\sum_S\Omega_I\wedge\Omega_S\Big] \\ &\quad +\frac{r_{\mathrm{B}}}{r_{\mathrm{A}}^2}\frac{V_L}{V}\frac{V_J}{V}\left(\frac{V_K}{V}-\delta_{KJ}\right)\left(\Delta V_I-\frac{V_I}{V}\Delta V\right)dt\wedge\hat{\rho}d\hat{\rho}\wedge d\varphi\wedge d\hat{z}\,,\end{aligned} \tag{9.3.52}$$

where we ommited the superscript $^\infty$ for brevity. In the derivation we first recall from (9.2.18) that $U = r_{\mathrm{A}}C_0 d\hat{z}$ and evaluate $\partial_{C_0}\eta_L = \frac{V_L}{V}d\hat{z}$ that follows from (9.2.19). Thus we can drop all terms in $\Omega_I^\infty\wedge\partial_{\hat{z}_K}\eta_J$ which are proportional to $d\hat{z}$. Next we plug in the definitions for these forms and formally calculate the derivatives in local coordinates. We note that due to the dependence of V_I and U_I in (9.2.15), (9.2.17) on only the combination $(\hat{z}-\hat{z}_I)$ we can write

$$\partial_{\hat{z}_K}V_I = -\delta_{IK}\partial_{\hat{z}}V_I\,,\qquad \partial_{\hat{z}_K}U_I = -\delta_{IK}\partial_{\hat{z}}U_I\,. \tag{9.3.53}$$

Next we write the relation $*_3 dU_I = -dV_I$ in local coordinates for the φ-component U_I^φ of U_I as

$$r_{\mathrm{B}}\hat{\rho}\partial_{\hat{\rho}}V_I = \partial_{\hat{z}}U_I^\varphi\,,\qquad r_{\mathrm{B}}\hat{\rho}\partial_{\hat{z}}V_I = -\partial_{\hat{\rho}}U_I^\varphi\,, \tag{9.3.54}$$

which is of course in perfect agreement with (9.2.15), (9.2.17), to recast every term in (9.3.52) as a function of derivatives of V_I and V multiplying the top-form $dt\wedge\hat{\rho}d\hat{\rho}\wedge d\varphi\wedge d\hat{z}$. Then we perform partial integrations, ignoring boundary terms, until every single partial derivative acts only on fractions $\frac{V_I}{V}$. Comparing to (9.3.37) in local coordinates,

$$\Omega_I^\infty\wedge\Omega_J^\infty = -\frac{2r_{\mathrm{B}}V}{r_{\mathrm{A}}^2}\left[\partial_{\hat{\rho}}\Big(\frac{V_I}{V}\Big)\partial_{\hat{\rho}}\Big(\frac{V_J}{V}\Big)+\partial_{\hat{z}}\Big(\frac{V_I}{V}\Big)\partial_{\hat{z}}\Big(\frac{V_J}{V}\Big)\right]dt\wedge\hat{\rho}d\hat{\rho}\wedge d\varphi\wedge d\hat{z} \tag{9.3.55}$$

where we used $*_4 d\hat{\rho} = -\hat{\rho}(dt+U)\wedge d\varphi\wedge d\hat{z}$ and $*_4 d\hat{z} = -\hat{\rho}(dt+U)\wedge d\hat{\rho}\wedge d\varphi$ exploiting the vierbein formalism (A.9.24), allows us to obtain the first two terms in (9.3.52). However, partial integration in addition produces a term

$$\frac{r_{\mathrm{B}}}{r_{\mathrm{A}}^2}\frac{V_L}{V}V_J\Big(\frac{V_K}{V}-\delta_{KJ}\Big)\Delta_3\Big(\frac{V_I}{V}\Big)dt\wedge\hat{\rho}d\hat{\rho}\wedge d\varphi\wedge d\hat{z}\,. \tag{9.3.56}$$

Applying $\Delta_3 = *_3 d *_3 d$ we obtain the last two terms in (9.3.52) and the mixed terms with derivatives acting on different terms can be rewritten using

$$\sum_S\Omega_I^\infty\wedge\Omega_S^\infty = \frac{2}{r_{\mathrm{A}}^2V}dV\wedge(dt+U)\wedge *_3 d\Big(\frac{V_I}{V}\Big) = -\frac{2}{r_{\mathrm{A}}^2V}dV\wedge *_4 d\Big(\frac{V_I}{V}\Big) \tag{9.3.57}$$

and $*_4 dV_I = -(dt+U)\wedge *_3 dV_I$ yielding the third term in (9.3.52).

With the result (9.3.52) we can now evaluate the coupling d_{IC_0K} in (9.3.51). According

to (9.1.15), (9.1.20) and (9.3.50) it is related to the imaginary part of the flux correction to the the gauge coupling function in the Coulomb branch of $U(k)$ as $\frac{1}{2}\text{Im}f_{IJ}^{\text{flux}}$ if we identify

$$\hat{z}_I = \zeta^I = \frac{\xi^I}{r_{\text{B}}^2}\,. \tag{9.3.58}$$

Again we focus on the extraction of the weak coupling behavior $g_s \sim 0$ where the integral (9.3.51) for d_{IC_0K} can be evaluated explicitly. We recall first the limit (9.3.46) and note that the potentials V, V_I obey the Poisson equation (9.2.16). As in the evaluation of the real part (9.3.47) we then replace all four-forms in (9.3.52) by delta-functions and by integration we just have to evaluate the different pre-factors at points. Then only the second and third term in (9.3.52) contribute yielding $n^J\delta_{JL}\frac{V_L}{V}\frac{V_K}{V}\Omega_J\wedge\Omega_I \to -\delta_{IK}n^I$ respectively

$$n^J\delta_{JL}\frac{V_LV_K}{V}\Big(\frac{V_J}{V}-\delta_{KJ}\Big)\sum_S\Omega_I\wedge\Omega_S \to \delta_{IK}\big[n^I+n^I\sum_{S\neq I}V_S|_{\hat{Z}_I}\big]+(\delta_{IK}-1)n^IV_K|_{\hat{Z}_I}\,, \tag{9.3.59}$$

where it is important for the latter formula to separately consider the cases $I = K$ and $I \neq K$ and to split the sum over J into $J \neq I$ and $J = I$. Thus we obtain the imaginary part of the flux correction to f_{IJ} as

$$\text{Im}f_{IJ}^{\text{flux}} \cong 2d_{IC_0K} = -\tfrac{1}{8}C_0\Big[\delta_{IJ}\big(3n^I_{IIB}+2\sum_{K\neq I}n^I_{IIB}V_K|_{\hat{Z}_I}\big)+2n^I_{IIB}V_J|_{\hat{Z}_I}(\delta_{IJ}-1)\Big]\,, \tag{9.3.60}$$

where we used as before the definition $\hat{Z}_I := (\hat{\rho}=0, \hat{z}=\hat{z}_I)$ and the relation $n^K_{IIB} = 2n^K$. Note that the structure is similar to the real part however a precise matching requires to keep all terms, most importantly those related to the terms in (9.3.50) by partial integration[18], in the reduced action (9.3.27). We emphasize that we not only obtain the expected flux correction to the imaginary part of f_{IJ} in (9.1.15) but also subleading corrections proportional to g_s via $V_J \sim g_s$. These corrections are analogous to the to those of the real part in (9.3.47) and are accordingly identified as one-loop corrections that are absent in the strict weak coupling limit and in particular in the the tree-level result (9.1.15) of the D7-brane gauge coupling. Using the finite expression (9.3.48) for $V_K|_{\hat{Z}_I}$ we can predict some of this leading loop correction.

Summary

Let us summarize the results of this chapter. Using a dual M-theory description, we have computed corrections to the four-dimensional effective action of F-theory which were induced by G_4-flux. The latter encodes the 7-brane flux and backreacts onto the geometry. This results on the one hand side in a non-trivial warp-factor and in a modification of the Kaluza-Klein reduction ansatz on the other hand side. To investigate the backreaction we have considered an analytic model of the local neighborhood of the 7-brane geometry which is in M-theory given by an infinite chain of Kaluza-Klein monopoles. This enabled us to obtain closed expressions for the warp factor and the M-theory three-form. These closed expressions were used to show that the warp factors induces quadratic flux corrections to the real part of the gauge coupling function while the imaginary part is traced back to the

[18] In particular the factor 3 in (9.3.60) arises precisely by partial integration and should be canceled by the omitted terms in (9.3.27) that are also obtained by partial integration.

modified M-theory three-form. The dependence on the position moduli on the type IIB circle was crucial in this discussion. These corrections were shown to reproduce the known Type IIB weak-coupling expressions while they further modify the 7-brane gauge coupling away from the weak coupling limit.

10. Conclusion and Outlook

In the first part of this thesis, we have determined the refined BPS invariants of local del Pezzo surfaces and the half K3 surface using multi-pronged approaches, such as the refined holomorphic anomaly equations, modularity and the refined modular anomaly equations. In the second part we discussed three applications to compute corrections and non-perturbative effects in F-theory compactifications, which are constituted by E-strings, $[p, q]$-strings and flux-corrections to the 7-brane gauge coupling function. While the first two topics rely on the results obtained in the first part, the third one is derived from an analysis of the backreacted geometry due to G_4-flux.

We have systematically calculated the refined BPS invariants of local del Pezzo surfaces and the half K3 surface using various techniques. The first method we have used applies if a toric description of the del Pezzo surface is available, which is generically the case for the geometries F_0 and up to three blow-ups of $\mathbb{P}^2$, as well as for (almost) del Pezzo surfaces with blow-ups at non-generic points. The formalism enjoys a high degree of universality and is based on the Weierstrass normal form of the elliptic mirror geometry together with a meromorphic differential. This mirror curve depends on only one complex structure modulus and additional non-normalizable mass parameters. The latter possess trivial or at least rational mirror maps and effectively allow for the reduction of an n-parameter to a one-parameter problem, which e.g. is demonstrated by the fact that the GKZ system is reduced to one differential operator of third order. While one has in general to solve a system of at least n Picard-Fuchs equations in order to obtain the periods, we make use of the fact that there are closed expressions for the periods of an elliptic curve which can be directly obtained from the data of the Weierstrass normal form. In addition, this formalism also drastically simplifies the finding of good conifold coordinates and allows to perform the direct integration procedure up to high order. Here we used the gap condition in order to fix the holomorphic ambiguity. In addition, we spelled out the limits in the complex structure moduli space that correspond to five and four-dimensional Seiberg-Witten theories. This exemplifies the fact that our framework is due to its analytic nature applicable everywhere in the moduli space. Besides providing the refined stable pair invariants for the toric del Pezzo geometries, these calculations also serve as a consistency check of the refined holomorphic anomaly equations that have a local B-model interpretation but miss a rigorous derivation.

Next we went on and considered the massless and massive half K3 surface which serves as a master geometry encoding all other del Pezzo surfaces as certain limits. In order to perform these calculations, we used the fact that the generating function for refined invariants that wrap the base of the half K3 only once is basically given by the refined Göttsche formula. In addition, we proposed a refinement of the modular anomaly equation. In this case the boundary conditions were fixed by using geometric constraints on the structure of the refined invariants and the restricted structure of the ring of Jacobi modular forms. The finding of the refined BPS invariants of the half K3 can be seen as a highly non-trivial check of the refined modular anomaly equation. In fact, we were also able to show by comparison to the results of different massless del Pezzo geometries that the refined modular anomaly equation is compatible with the formalism of the refined holomorphic anomaly equations.

By performing suitable flop transitions and blow-downs we were able to derive the refined stable pair invariants of the non-toric del Pezzo surfaces. Besides that, we demonstrated how the physical spin decomposition reflects the beautiful group theory of the exceptional groups that govern the homological structure of the del Pezzo surfaces.

Furthermore, we have performed first steps to extend the above formalism based on the Weierstrass normal form to mirror curves of genus two. We discussed the geometry $\mathbb{C}^3/\mathbb{Z}_5$ and derived the period matrix from the Fourier expansion of the Igusa invariants which provide the analogue of the Weierstrass normal form for genus two curves. Notably, we were able to rewrite the free energy at genus one in terms of Siegel modular forms of genus two and checked the existence of a vector-valued Siegel modular form that has according to the formalism by [33] to transform with weight two, i.e. serves as a candidate for an extension of the definition of the second Eisenstein series to genus two.

In the second part of the thesis we discussed diverse applications of these results to F-theory. In particular, we were able to show that the refined stable pair invariants count the massless excitations of the tensionless string. These arise, if a dP_8 del Pezzo surface collapses within the compactification geometry. By comparing to the results obtained by [32] we could explain the space-time spin of these excitations as well as their splitting into representations of E_8. This is based on the fact that the refined stable pair do not average over the five-dimensional spins in contrast to the Gopakumar Vafa invariants, but are even able to resolve the Weyl orbits of curves inside the geometry.

Also we provided some evidence that the refined BPS invariants are able to count the massless vector bosons that generate the (microscopic) gauge theory sector in F-theory. Additionally, the refined BPS invariants are assumed to count infinite towers of massive BPS states which are present in the geometry of non-local 7-branes. This proposal is based on the observation that flavor and gauge group get exchanged in the probe brane picture. Moreover, in the probe brane picture it is possible to identify $[p, q]$-strings with BPS states of Seiberg-Witten theory which in turn correspond to geodesics in the base that can be lifted to holomorphic curves under certain conditions. The latter are precisely counted by the refined stable pair invariants. However, we also pointed out that a further analysis is required in order to match the spins of the refined stable pair invariants with the physical quantum numbers of the $[p, q]$-string.

Independently from the refined BPS state counting we discussed the derivation of the 7-brane gauge coupling function within F-theory by investigating the backreaction of G_4-flux onto the geometry. This backreaction was responsible for a non-trivial warpfactor as well as for a modification of the Kaluza-Klein reduction ansatz. To explicitly evaluate this backreaction, we considered the dual M-theory set-up and constructed a local, analytical model of an A_n-singularity. This was used to explicitly solve the warp factor equation and the M-theory three-form field. The dependence of these quantities on the directions of the Type IIB cycle that gets decompactified in the F-theory lift was crucial in this discussion. The warp factor and the modified three-form field were proven to be responsible for quadratic corrections in the 7-brane flux to the gauge coupling function. These were shown to reproduce the known weak coupling result but also display further corrections that become important away from the weak coupling limit.

There are many directions this work could be continued into.

It would be very interesting to extent the techniques presented here in order compute more corrections within F-theory compactifications. While it would clearly be desirable to get a consistent picture played by the refined stable pair invariants in the counting of (the excitations of) $[p, q]$-strings, it would also be very interesting to explore whether the

backreaction computations can be used to also extract other known type IIB corrections such as curvature terms on the 7-branes.

Apart from concrete physical applications, it would also be attractive to improve the understanding of some conceptual questions. Topological string theory enjoys many dualities to other theories, such as Chern-Simons theory, Matrix models, ABJM theory [67, 68], to name a few examples. The investigation to which extent these can be lifted on the refined level[1] is certainly an exciting question.

It would clearly also be desirable to explore how the formalism of the refined holomorphic anomaly equations together with its proposed local B-model interpretation connects to the other approaches to refinement such as the fluxbrane picture [216] or the world-sheet description proposed by [217]. A much more difficult question is to ask whether one can give any meaningful interpretation to the refinement on compact Calabi-Yau manifolds. While the additional $\mathrm{U}(1)_{\mathcal{R}}$ symmetry is not present on compact Calabi-Yau manifolds one does not expect the refined partition function to be an index. However, it might be that one could evaluate these invariants for a fixed complex structure and control the jumping by some kind of "wall-crossing" phenomena. One application of this program would be an extension of the refined OSV conjecture of [80] to the compact case.

[1] For the first two theories, some progress has already appeared in [81].

A. Appendix

A.1. The general Weierstrass forms for the cubic, the quartic and the bi-quadratic

In this section we discuss the Weierstrass normal forms corresponding to the curves that are associated to the polyhedra 13, 15 and 16 in figure 4.1. This is turn corresponds to determining the Weierstrass normal form of a general quartic, bi-quadratic and cubic curve respectively. The corresponding algorithms are well-known in the literature. We briefly present them here for convenience and completing the discussion. The respective coefficients are translated as follows

Curve	$\tilde{u}$	a_1	a_2	a_3	m_1	m_2	m_3	m_4	m_5	m_6	m_7	m_8
Cubic	s_6	s_5	s_3	s_9	s_8	s_2	s_7	s_{10}	s_1	s_4	-	-
Quartic	l_7	l_9	l_6	l_4	l_8	-	l_3	l_5	-	l_2	l_1	-
Bi-quadratic	a_{11}	a_{22}	a_{01}	a_{10}	a_{21}	a_{12}	a_{00}	a_{20}	-	-	-	a_{02}

.

A.1.1. The Weierstrass normal form of cubic curves

We consider a cubic curve in projective space $\mathbb{P}^2 = \{[x : y : z]\}$ that is given by

$$\begin{aligned} 0 &= s_1x^3 + s_2x^2y + s_3xy^2 + s_4y^3 + s_5x^2z + s_6xyz + s_7y^2z + s_8xz^2 + s_9yz^2 + s_{10}z^3 \\ &= F_1(x,y) + F_2(x,y)z + F_3(x,y)z^2 + s_{10}z^3\,. \end{aligned} \tag{A.1.1}$$

The algorithm that brings this curve into Weierstrass normal form is called Nagell's algorithm. We review only the most important steps here and refer to the literature [118] for an extensive discussion. By a coordinate transformation $x \to x + p$, we can achieve that $s_{10} = 0$. Without loss of generality we assume that $s_9 \neq 0$. We define

$$e_i = F_i(s_9, -s_8). \tag{A.1.2}$$

Next, the coordinate transformation

$$(x,y) \longmapsto \begin{cases} \left(x - s_9\frac{e_2}{e_3}\,y, y + s_8\frac{e_2}{e_3}\,x\right) & \text{if } e_3 \neq 0 \\ (x - s_9\,y, y + s_8x) & \text{if } e_3 = 0 \end{cases} \tag{A.1.3}$$

is applied in order to map the rational point to the origin. Having brought the curve into this form, it is re-written as

$$x^2f_3'(1,t) + x'f_2'(1,t) + f_1'(1,t) = 0, \quad t = y/x, \tag{A.1.4}$$

where the f_i denote the homogeneous parts of degree i. The solution to this quadratic

equation is given by

$$x = \frac{-f_2'(1,t) \pm \sqrt{\delta}}{2f_3'(1,t)}, \quad \delta = f_2'(1,t)^2 - 4f_3'(1,t)f_1'(1,t)\,. \tag{A.1.5}$$

One zero of δ is given by $t_0 = -s_8/s_9$. By introducing

$$t = t_0 + \frac{1}{\tau}, \tag{A.1.6}$$

one obtains a cubic polynomial

$$\rho = \tau^4 \delta, \tag{A.1.7}$$

which is easily brought into Weierstrass normal form

$$Y^2 = 4X^3 - g_2 X - g_3\,. \tag{A.1.8}$$

Its explicit form in terms of the coefficients s_i reads

$$
\begin{aligned}
Y^2 \;=\;& 4X^3 - \frac{1}{12}\Big(s_6^4 - 8s_5s_6^2s_7 + 16s_5^2s_7^2 + 24s_4s_5s_6s_8 - 8s_3s_6^2s_8 - 16s_3s_5s_7s_8 + 24s_2s_6s_7s_8 \\
& -48s_1s_7^2s_8 + 16s_3^2s_8^2 - 48s_2s_4s_8^2 - 48s_4s_5^2s_9 + 24s_3s_5s_6s_9 - 8s_2s_6^2s_9 - 16s_2s_5s_7s_9 \\
& +24s_1s_6s_7s_9 - 16s_2s_3s_8s_9 + 144s_1s_4s_8s_9 + 16s_2^2s_9^2 - 48s_1s_3s_9^2 - 48s_3^2s_5s_{10} \\
& +144s_2s_4s_5s_{10} + 24s_2s_3s_6s_{10} - 216s_1s_4s_6s_{10} - 48s_2^2s_7s_{10} + 144s_1s_3s_7s_{10}\Big)X \\
& -\frac{1}{216}\Big(s_6^6 - 12s_5s_6^4s_7 + 48s_5^2s_6^2s_7^2 - 64s_5^3s_7^3 + 36s_4s_5s_6^3s_8 - 12s_3s_6^4s_8 - 144s_4s_5^2s_6s_7s_8 \\
& +24s_3s_5s_6^2s_7s_8 + 36s_2s_6^3s_7s_8 + 96s_3s_5^2s_7^2s_8 - 144s_2s_5s_6s_7^2s_8 - 72s_1s_6^2s_7^2s_8 \\
& +288s_1s_5s_7^3s_8 + 216s_4^2s_5^2s_8^2 - 144s_3s_4s_5s_6s_8^2 + 48s_3^2s_6^2s_8^2 - 72s_2s_4s_6^2s_8^2 + 96s_3^2s_5s_7s_8^2 \\
& -144s_2s_4s_5s_7s_8^2 - 144s_2s_3s_6s_7s_8^2 + 864s_1s_4s_6s_7s_8^2 + 216s_2^2s_7^2s_8^2 - 576s_1s_3s_7^2s_8^2 \\
& -64s_3^3s_8^3 + 288s_2s_3s_4s_8^3 - 864s_1s_4^2s_8^3 - 72s_4s_5^2s_6^2s_9 + 36s_3s_5s_6^3s_9 - 12s_2s_6^4s_9 \\
& +288s_4s_5^3s_7s_9 - 144s_3s_5^2s_6s_7s_9 + 24s_2s_5s_6^2s_7s_9 + 36s_1s_6^3s_7s_9 + 96s_2s_5^2s_7^2s_9 \\
& -144s_1s_5s_6s_7^2s_9 - 144s_3s_4s_5^2s_8s_9 - 144s_3^2s_5s_6s_8s_9 + 720s_2s_4s_5s_6s_8s_9 + 24s_2s_3s_6^2s_8s_9 \\
& -648s_1s_4s_6^2s_8s_9 + 48s_2s_3s_5s_7s_8s_9 - 1296s_1s_4s_5s_7s_8s_9 - 144s_2^2s_6s_7s_8s_9 \\
& +720s_1s_3s_6s_7s_8s_9 - 144s_1s_2s_7^2s_8s_9 + 96s_2s_3^2s_8^2s_9 - 576s_2^2s_4s_8^2s_9 + 864s_1s_3s_4s_8^2s_9 \\
& +216s_3^2s_5^2s_9^2 - 576s_2s_4s_5^2s_9^2 - 144s_2s_3s_5s_6s_9^2 + 864s_1s_4s_5s_6s_9^2 + 48s_2^2s_6^2s_9^2 \\
& -72s_1s_3s_6^2s_9^2 + 96s_2^2s_5s_7s_9^2 - 144s_1s_3s_5s_7s_9^2 - 144s_1s_2s_6s_7s_9^2 + 216s_1^2s_7^2s_9^2 \\
& +96s_2^2s_3s_8s_9^2 - 576s_1s_3^2s_8s_9^2 + 864s_1s_2s_4s_8s_9^2 - 64s_2^3s_9^3 + 288s_1s_2s_3s_9^3 - 864s_1^2s_4s_9^3 \\
& -864s_4^2s_5^3s_{10} + 864s_3s_4s_5^2s_6s_{10} - 72s_3^2s_5s_6^2s_{10} - 648s_2s_4s_5s_6^2s_{10} + 36s_2s_3s_6^3s_{10} \\
& +540s_1s_4s_6^3s_{10} - 576s_3^2s_5^2s_7s_{10} + 864s_2s_4s_5^2s_7s_{10} + 720s_2s_3s_5s_6s_7s_{10} \\
& -1296s_1s_4s_5s_6s_7s_{10} - 72s_2^2s_6^2s_7s_{10} - 648s_1s_3s_6^2s_7s_{10} - 576s_2^2s_5s_7^2s_{10} \\
& +864s_1s_3s_5s_7^2s_{10} + 864s_1s_2s_6s_7^2s_{10} - 864s_1^2s_7^3s_{10} + 288s_3^3s_5s_8s_{10} \\
& -1296s_2s_3s_4s_5s_8s_{10} + 3888s_1s_4^2s_5s_8s_{10} - 144s_2s_3^2s_6s_8s_{10} + 864s_2^2s_4s_6s_8s_{10} \\
& -1296s_1s_3s_4s_6s_8s_{10} - 144s_2^2s_3s_7s_8s_{10} + 864s_1s_3^2s_7s_8s_{10} - 1296s_1s_2s_4s_7s_8s_{10} \\
& -144s_2s_3^2s_5s_9s_{10} + 864s_2^2s_4s_5s_9s_{10} - 1296s_1s_3s_4s_5s_9s_{10} - 144s_2^2s_3s_6s_9s_{10} \\
& +864s_1s_3^2s_6s_9s_{10} - 1296s_1s_2s_4s_6s_9s_{10} + 288s_2^3s_7s_9s_{10} - 1296s_1s_2s_3s_7s_9s_{10} \\
& +3888s_1^2s_4s_7s_9s_{10} + 216s_2^2s_3^2s_{10}^2 - 864s_1s_3^3s_{10}^2 - 864s_2^3s_4s_{10}^2 + 3888s_1s_2s_3s_4s_{10}^2 \\
& -5832s_1^2s_4^2s_{10}^2\Big)\,. \qquad \text{(A.1.9)}
\end{aligned}
$$

A.1.2. The Weierstrass normal form of quartic curves

We start by considering homogeneous quartic curves [118] in $\mathbb{P}^{(1,1,2)}$ that have the form

$$0 = l_1p^4 + l_2p^3q + l_3p^2q^2 + l_4pq^3 + l_5q^4 + l_6p^2r + l_7pqr + l_8q^2r + l_9r^2\,. \qquad \text{(A.1.10)}$$

By setting $q = 1$ we obtain the affine part, which reads after a change of coordinates

$$v^2 = \tilde{l}_1p^4 + \tilde{l}_2p^3 + \tilde{l}_3p^2 + \tilde{l}_4p + \tilde{l}_5. \qquad \text{(A.1.11)}$$

The constant term can be eliminated by shifting $p \longmapsto p + a$, a being a root of (A.1.11). After applying the final coordinate transformation

$$v \longmapsto \frac{v}{p^2}, \quad p \longmapsto \frac{1}{p} \tag{A.1.12}$$

the curve is takes the form of a cubic

$$y^2 + a_1xy + a_3y = x^3 + a_2x^2 + a_4x + a_6, \tag{A.1.13}$$

where the a_i can be expressed in terms of $\tilde{l}_i$ as

$$a_1 = \frac{\tilde{l}_4}{\sqrt{\tilde{l}_5}}, \quad a_2 = c - \frac{\tilde{l}_4^2}{4\tilde{l}_5}, \quad a_3 = 2\sqrt{\tilde{l}_5}\tilde{l}_2, \quad a_4 = -4\tilde{l}_5\tilde{l}_1, \quad a_6 = a_2a_4\,. \tag{A.1.14}$$

Nagell's algorithm can be applied to this form and one finds the Weierstrass normal form

$$\begin{aligned} Y^2 \;=\; & 4X^3 - \frac{1}{12}\Big(l_7^4 - 8l_6l_7^2l_8 + 16l_6^2l_8^2 + 48l_5l_6^2l_9 - 24l_4l_6l_7l_9 + 8l_3l_7^2l_9 + 16l_3l_6l_8l_9 - 24l_2l_7l_8l_9 \\ & +48l_1l_8^2l_9 + 16l_3^2l_9^2 - 48l_2l_4l_9^2 + 192l_1l_5l_9^2\Big)X - \frac{1}{216}\Big(l_7^6 - 12l_6l_7^4l_8 + 48l_6^2l_7^2l_8^2 \\ & -64l_6^3l_8^3 + 72l_5l_6^2l_7^2l_9 - 36l_4l_6l_7^3l_9 + 12l_3l_7^4l_9 - 288l_5l_6^3l_8l_9 + 144l_4l_6^2l_7l_8l_9 - 24l_3l_6l_7^2l_8l_9 \\ & -36l_2l_7^3l_8l_9 - 96l_3l_6^2l_8^2l_9 + 144l_2l_6l_7l_8^2l_9 + 72l_1l_7^2l_8^2l_9 - 288l_1l_6l_8^3l_9 + 216l_4^2l_6^2l_9^2 \\ & -576l_3l_5l_6^2l_9^2 - 144l_3l_4l_6l_7l_9^2 + 864l_2l_5l_6l_7l_9^2 + 48l_3^2l_7^2l_9^2 - 72l_2l_4l_7^2l_9^2 - 576l_1l_5l_7^2l_9^2 \\ & +96l_3^2l_6l_8l_9^2 - 144l_2l_4l_6l_8l_9^2 - 1152l_1l_5l_6l_8l_9^2 - 144l_2l_3l_7l_8l_9^2 + 864l_1l_4l_7l_8l_9^2 + 216l_2^2l_8^2l_9^2 \\ & -576l_1l_3l_8^2l_9^2 + 64l_3^3l_9^3 - 288l_2l_3l_4l_9^3 + 864l_1l_4^2l_9^3 + 864l_2^2l_5l_9^3 - 2304l_1l_3l_5l_9^3\Big)\,. \end{aligned} \tag{A.1.15}$$

A.1.3. The Weierstrass normal form for a bi-quadratic curve

We follow the discussion in [119] and consider a general homogeneous bi-quadratic curve p in $\mathbb{P}^1 = \{[s:t]\} \times \mathbb{P}^1 = \{[v:w]\}$.

$$\begin{aligned} 0 \;=\; & a_{00}s^2w^2 + a_{10}stw^2 + a_{01}s^2vw + a_{20}t^2w^2 + a_{11}stvw + a_{02}s^2v^2 + a_{21}t^2vw \\ & +a_{12}stv^2 + a_{22}t^2v^2. \end{aligned} \tag{A.1.16}$$

The affine part of p reads in the chart $s = 1, w = 1$

$$0 = a_{00} + a_{10}t + a_{01}v + a_{20}t^2 + a_{11}tv + a_{02}v^2 + a_{21}t^2v + a_{12}tv^2 + a_{22}t^2v^2\,. \tag{A.1.17}$$

We denote by

$$\Delta_2(p) = \Big(\sum_{i=0}^{2} s^it^{2-i}a_{i1}\Big)^2 - 4\Big(s^it^{2-i}a_{i0}\Big)\Big(s^it^{2-i}a_{i2}\Big) \tag{A.1.18}$$

the discriminant with respect to the second variable (v, w). The discriminant with respect to the first variable $\Delta_1(p)$ is defined analogously. To proceed we need to introduce some more notation. Consider a homogeneous quartic in two variables (x_0, x_1)

$$f = a_0x_1^4 + 4a_1x_0 + 6a_2x_0^2x_1^2 + 4a_3x_0^3x_1 + a_4x_0^4\,. \tag{A.1.19}$$

Next we introduce the so-called Eisenstein invariants of (A.1.19) which are projective invariants under the action of $GL(2,\mathbb{C})$ and defined as

$$\begin{aligned} D &= a_0a_4 3a_2^2 - 4a_1a_3\,, \\ E &= a_0a_3^2 + a_1^2a_4 - a_0a_2a_4 - 2a_1a_2a_3 + a_2^3\,. \end{aligned} \tag{A.1.20}$$

It can be shown that the coefficients g_2, g_3 of the Weierstrass normal form are given as

$$g_2 = D(\Delta_2(p)), \quad g_3 = -E(\Delta_2(p))\,. \tag{A.1.21}$$

The general Weierstrass form of a bi-quadratic curve is finally found to be

$$\begin{aligned} Y^2 &= 4X^3 - \frac{1}{12}\Big(a_{11}^4 - 8a_{10}a_{11}^2a_{12} + 16a_{10}^2a_{12}^2 - 8a_{02}a_{11}^2a_{20} - 16a_{02}a_{10}a_{12}a_{20} \\ &\quad +24a_{01}a_{11}a_{12}a_{20} - 48a_{00}a_{12}^2a_{20} + 16a_{02}^2a_{20}^2 + 24a_{02}a_{10}a_{11}a_{21} - 8a_{01}a_{11}^2a_{21} \\ &\quad -16a_{01}a_{10}a_{12}a_{21} + 24a_{00}a_{11}a_{12}a_{21} - 16a_{01}a_{02}a_{20}a_{21} + 16a_{01}^2a_{21}^2 - 48a_{00}a_{02}a_{21}^2 \\ &\quad -48a_{02}a_{10}^2a_{22} + 24a_{01}a_{10}a_{11}a_{22} - 8a_{00}a_{11}^2a_{22} - 16a_{00}a_{10}a_{12}a_{22} - 48a_{01}^2a_{20}a_{22} \\ &\quad +224a_{00}a_{02}a_{20}a_{22} - 16a_{00}a_{01}a_{21}a_{22} + 16a_{00}^2a_{22}^2\Big)X - \frac{1}{216}\Big(a_{11}^6 - 12a_{10}a_{11}^4a_{12} \\ &\quad +48a_{10}^2a_{11}^2a_{12}^2 - 64a_{10}^3a_{12}^3 - 12a_{02}a_{11}^4a_{20} + 24a_{02}a_{10}a_{11}^2a_{12}a_{20} + 36a_{01}a_{11}^3a_{12}a_{20} \\ &\quad +96a_{02}a_{10}^2a_{12}^2a_{20} - 144a_{01}a_{10}a_{11}a_{12}^2a_{20} - 72a_{00}a_{11}^2a_{12}^2a_{20} + 288a_{00}a_{10}a_{12}^3a_{20} \\ &\quad +48a_{02}^2a_{11}^2a_{20}^2 + 96a_{02}^2a_{10}a_{12}a_{20}^2 - 144a_{01}a_{02}a_{11}a_{12}a_{20}^2 + 216a_{01}^2a_{12}^2a_{20}^2 \\ &\quad -576a_{00}a_{02}a_{12}^2a_{20}^2 - 64a_{02}^3a_{20}^3 + 36a_{02}a_{10}a_{11}^3a_{21} - 12a_{01}a_{11}^4a_{21} - 144a_{02}a_{10}^2a_{11}a_{12}a_{21} \\ &\quad +24a_{01}a_{10}a_{11}^2a_{12}a_{21} + 36a_{00}a_{11}^3a_{12}a_{21} + 96a_{01}a_{10}^2a_{12}^2a_{21} - 144a_{00}a_{10}a_{11}a_{12}^2a_{21} \\ &\quad -144a_{02}^2a_{10}a_{11}a_{20}a_{21} + 24a_{01}a_{02}a_{11}^2a_{20}a_{21} + 48a_{01}a_{02}a_{10}a_{12}a_{20}a_{21} \\ &\quad -144a_{01}^2a_{11}a_{12}a_{20}a_{21} + 720a_{00}a_{02}a_{11}a_{12}a_{20}a_{21} - 144a_{00}a_{01}a_{12}^2a_{20}a_{21} \\ &\quad +96a_{01}a_{02}^2a_{20}^2a_{21} + 216a_{02}^2a_{10}^2a_{21}^2 - 144a_{01}a_{02}a_{10}a_{11}a_{21}^2 + 48a_{01}^2a_{11}^2a_{21}^2 \\ &\quad -72a_{00}a_{02}a_{11}^2a_{21}^2 + 96a_{01}^2a_{10}a_{12}a_{21}^2 - 144a_{00}a_{02}a_{10}a_{12}a_{21}^2 - 144a_{00}a_{01}a_{11}a_{12}a_{21}^2 \\ &\quad +216a_{00}^2a_{12}^2a_{21}^2 + 96a_{01}^2a_{02}a_{20}a_{21}^2 - 576a_{00}a_{02}^2a_{20}a_{21}^2 - 64a_{01}^3a_{21}^3 + 288a_{00}a_{01}a_{02}a_{21}^3 \\ &\quad -72a_{02}a_{10}^2a_{11}^2a_{22} + 36a_{01}a_{10}a_{11}^3a_{22} - 12a_{00}a_{11}^4a_{22} + 288a_{02}a_{10}^3a_{12}a_{22} \\ &\quad -144a_{01}a_{10}^2a_{11}a_{12}a_{22} + 24a_{00}a_{10}a_{11}^2a_{12}a_{22} + 96a_{00}a_{10}^2a_{12}^2a_{22} - 576a_{02}^2a_{10}^2a_{20}a_{22} \\ &\quad +720a_{01}a_{02}a_{10}a_{11}a_{20}a_{22} - 72a_{01}^2a_{11}^2a_{20}a_{22} - 480a_{00}a_{02}a_{11}^2a_{20}a_{22} - 144a_{01}^2a_{10}a_{12}a_{20}a_{22} \\ &\quad -960a_{00}a_{02}a_{10}a_{12}a_{20}a_{22} + 720a_{00}a_{01}a_{11}a_{12}a_{20}a_{22} - 576a_{00}^2a_{12}^2a_{20}a_{22} \\ &\quad -576a_{01}^2a_{02}a_{20}^2a_{22} + 2112a_{00}a_{02}^2a_{20}^2a_{22} - 144a_{01}a_{02}a_{10}^2a_{21}a_{22} - 144a_{01}^2a_{10}a_{11}a_{21}a_{22} \\ &\quad +720a_{00}a_{02}a_{10}a_{11}a_{21}a_{22} + 24a_{00}a_{01}a_{11}^2a_{21}a_{22} + 48a_{00}a_{01}a_{10}a_{12}a_{21}a_{22} \\ &\quad -144a_{00}^2a_{11}a_{12}a_{21}a_{22} + 288a_{01}^3a_{20}a_{21}a_{22} - 960a_{00}a_{01}a_{02}a_{20}a_{21}a_{22} + 96a_{00}a_{01}^2a_{21}^2a_{22} \\ &\quad -576a_{00}^2a_{02}a_{21}^2a_{22} + 216a_{01}^2a_{10}^2a_{22}^2 - 576a_{00}a_{02}a_{10}^2a_{22}^2 - 144a_{00}a_{01}a_{10}a_{11}a_{22}^2 \\ &\quad +48a_{00}^2a_{11}^2a_{22}^2 + 96a_{00}^2a_{10}a_{12}a_{22}^2 - 576a_{00}a_{01}^2a_{20}a_{22}^2 + 2112a_{00}^2a_{02}a_{20}a_{22}^2 \\ &\quad +96a_{00}^2a_{01}a_{21}a_{22}^2 - 64a_{00}^3a_{22}^3\Big). \end{aligned} \tag{A.1.22}$$

A.2. Some more details on del Pezzo surfaces

In this appendix we discuss some further interesting aspects of del Pezzo surfaces. In particular, we concentrate on the relation to the E_n-curves that are considered in [63] starting with the E_8-curve.

A.2.1. E_n-curves as Cubic curves

The E_8-curve has been given in [63]

$$\begin{aligned}
y^2 \;=\;& 4x^3 + \Big(-\frac{1}{12}\tilde{u}^4 + \big(\frac{2}{3}\chi_1^{\mathrm{E}_8} - \frac{50}{3}\chi_8^{\mathrm{E}_8} + 1550\big)\tilde{u}^2 + \big(-70\chi_1^{\mathrm{E}_8} + 2\chi_2^{\mathrm{E}_8} - 12\chi_7^{\mathrm{E}_8} \\
&+1840\chi_8^{\mathrm{E}_8} - 115010\big)\tilde{u} - \frac{4}{3}\chi_1^{\mathrm{E}_8}\chi_1^{\mathrm{E}_8} + \frac{8}{3}\chi_1^{\mathrm{E}_8}\chi_8^{\mathrm{E}_8} + 1824\chi_1^{\mathrm{E}_8} - 112\chi_2^{\mathrm{E}_8} + 4\chi_3^{\mathrm{E}_8} - 4\chi_6^{\mathrm{E}_8} \\
&+680\chi_7^{\mathrm{E}_8} - \frac{28}{3}\chi_8^{\mathrm{E}_8}\chi_8^{\mathrm{E}_8} - 50744\chi_8^{\mathrm{E}_8} + 2399276\Big)x \\
&-\frac{1}{216}\tilde{u}^6 + 4\tilde{u}^5 + \big(\frac{1}{18}\chi_1^{\mathrm{E}_8} + \frac{47}{18}\chi_8^{\mathrm{E}_8} - \frac{5177}{6}\big)\tilde{u}^4 + \big(-\frac{107}{6}\chi_1^{\mathrm{E}_8} + \frac{1}{6}\chi_2^{\mathrm{E}_8} + 3\chi_7^{\mathrm{E}_8} \\
&-\frac{1580}{3}\chi_8^{\mathrm{E}_8} + \frac{504215}{6}\big)\tilde{u}^3 + \big(-\frac{2}{9}\chi_1^{\mathrm{E}_8}\chi_1^{\mathrm{E}_8} - \frac{20}{9}\chi_1^{\mathrm{E}_8}\chi_8^{\mathrm{E}_8} + \frac{5866}{3}\chi_1^{\mathrm{E}_8} - \frac{112}{3}\chi_2^{\mathrm{E}_8} + \frac{1}{3}\chi_3^{\mathrm{E}_8} \\
&+\frac{11}{3}\chi_6^{\mathrm{E}_8} - \frac{1450}{3}\chi_7^{\mathrm{E}_8} + \frac{196}{9}\chi_8^{\mathrm{E}_8}\chi_8^{\mathrm{E}_8} + 39296\chi_8^{\mathrm{E}_8} - \frac{12673792}{3}\big)\tilde{u}^2 + \big(\frac{94}{3}\chi_1^{\mathrm{E}_8}\chi_1^{\mathrm{E}_8} \\
&-\frac{2}{3}\chi_1^{\mathrm{E}_8}\chi_2^{\mathrm{E}_8} + \frac{718}{3}\chi_1^{\mathrm{E}_8}\chi_8^{\mathrm{E}_8} - \frac{270736}{3}\chi_1^{\mathrm{E}_8} - \frac{10}{3}\chi_2^{\mathrm{E}_8}\chi_8^{\mathrm{E}_8} + 2630\chi_2^{\mathrm{E}_8} - 52\chi_3^{\mathrm{E}_8} + 4\chi_5^{\mathrm{E}_8} \\
&-416\chi_6^{\mathrm{E}_8} + 16\chi_7^{\mathrm{E}_8}\chi_8^{\mathrm{E}_8} + 25880\chi_7^{\mathrm{E}_8} - \frac{7328}{3}\chi_8^{\mathrm{E}_8}\chi_8^{\mathrm{E}_8} - \frac{3841382}{3}\chi_8^{\mathrm{E}_8} + 107263286\big)\tilde{u} \\
&\frac{8}{27}\chi_1^{\mathrm{E}_8}\chi_1^{\mathrm{E}_8}\chi_1^{\mathrm{E}_8} + \frac{28}{9}\chi_1^{\mathrm{E}_8}\chi_1^{\mathrm{E}_8}\chi_8^{\mathrm{E}_8} - 1065\chi_1^{\mathrm{E}_8}\chi_1^{\mathrm{E}_8} + \frac{118}{3}\chi_1^{\mathrm{E}_8}\chi_2^{\mathrm{E}_8} - \frac{4}{3}\chi_1^{\mathrm{E}_8}\chi_3^{\mathrm{E}_8} + \frac{4}{3}\chi_1^{\mathrm{E}_8} \\
&\chi_6^{\mathrm{E}_8} - \frac{8}{3}\chi_1^{\mathrm{E}_8}\chi_7^{\mathrm{E}_8} - \frac{40}{9}\chi_1^{\mathrm{E}_8}\chi_8^{\mathrm{E}_8}\chi_8^{\mathrm{E}_8} - \frac{19264}{3}\chi_1^{\mathrm{E}_8}\chi_8^{\mathrm{E}_8} + \frac{4521802}{3}\chi_1^{\mathrm{E}_8} - \chi_2^{\mathrm{E}_8}\chi_2^{\mathrm{E}_8} \\
&+\frac{572}{3}\chi_2^{\mathrm{E}_8}\chi_8^{\mathrm{E}_8} - 59482\chi_2^{\mathrm{E}_8} - \frac{20}{3}\chi_3^{\mathrm{E}_8}\chi_8^{\mathrm{E}_8} + 1880\chi_3^{\mathrm{E}_8} + 4\chi_4^{\mathrm{E}_8} - 232\chi_5^{\mathrm{E}_8} + \frac{8}{3}\chi_6^{\mathrm{E}_8}\chi_8^{\mathrm{E}_8} \\
&+11808\chi_6^{\mathrm{E}_8} - \frac{2740}{3}\chi_7^{\mathrm{E}_8}\chi_8^{\mathrm{E}_8} - 460388\chi_7^{\mathrm{E}_8} + \frac{136}{27}\chi_8^{\mathrm{E}_8}\chi_8^{\mathrm{E}_8}\chi_8^{\mathrm{E}_8} + \frac{205492}{3}\chi_8^{\mathrm{E}_8}\chi_8^{\mathrm{E}_8} \\
&+\frac{45856940}{3}\chi_8^{\mathrm{E}_8} - 1091057493
\end{aligned} \tag{A.2.1}$$

We have denoted the characters of E_n by

$$\chi_i^{\mathrm{E}_n} = \sum_{\vec{\nu}\in\mathcal{R}_i} e^{i\vec{m}\vec{\nu}}. \tag{A.2.2}$$

$\mathcal{R}_i$ denotes the representation with highest weight being the ith fundamental one and $\vec{m}$ takes values in the $\mathbb{C}$-extended root space and have an interpretation as Wilson line parameters. In particular if all the masses are zero the χ_i become just the dimensions of the corresponding weight modules given in (5.1.3). Starting from the E_8-curve, one obtains successively the E_n-curves whose maximal singularity is an E_n-singularity. Fur this purpose, one decomposes the characters of E_n into representations of

$$\mathrm{E}_n \longrightarrow E_{n-1} \times U(1), \tag{A.2.3}$$

factors out the $U(1)$ part L and finally takes the leading part in L. For the present case of E_8 the scaling relations are explicitly given as

$$\begin{aligned}&\big(\chi_1^{\mathrm{E}_8},\chi_2^{\mathrm{E}_8},\chi_3^{\mathrm{E}_8},\chi_4^{\mathrm{E}_8},\chi_5^{\mathrm{E}_8},\chi_6^{\mathrm{E}_8},\chi_7^{\mathrm{E}_8},\chi_8^{\mathrm{E}_8}\big)\\ \longmapsto\ &\big(L^2\chi_1^{\mathrm{E}_7},L^3\chi_2^{\mathrm{E}_7},L^4\chi_3^{\mathrm{E}_7},L^6\chi_4^{\mathrm{E}_7},L^5\chi_5^{\mathrm{E}_7},L^4\chi_6^{\mathrm{E}_7},L^3\chi_7^{\mathrm{E}_7},L^2\big),\\ &(\tilde u,x,y)\longmapsto(L\tilde u,L^2x,L^3y),\quad L\to\infty\,.\end{aligned}\tag{A.2.4}$$

Accordingly one finds the E_7-curve

$$\begin{aligned}y^2 &= 4x^3+\Big(-\frac{1}{12}\tilde u^4+(\frac{2}{3}\chi_1^{\mathrm{E}_7}-\frac{50}{3})\tilde u^2+(2\chi_2^{\mathrm{E}_7}-12\chi_7^{\mathrm{E}_7})\tilde u-\frac{4}{3}\chi_1^{\mathrm{E}_7}\chi_1^{\mathrm{E}_7}+\frac{8}{3}\chi_1^{\mathrm{E}_7}\\ &\quad+4\chi_3^{\mathrm{E}_7}-4\chi_6^{\mathrm{E}_7}-\frac{28}{3}\Big)x\\ &\quad-\frac{1}{216}\tilde u^6+(\frac{1}{18}\chi_1^{\mathrm{E}_7}+\frac{47}{18})\tilde u^4+(\frac{1}{6}\chi_2^{\mathrm{E}_7}+3\chi_7^{\mathrm{E}_7})\tilde u^3+\big(-\frac{2}{9}\chi_1^{\mathrm{E}_7}\chi_1^{\mathrm{E}_7}-\frac{20}{9}\chi_1^{\mathrm{E}_7}+\frac{1}{3}\chi_3^{\mathrm{E}_7}\\ &\quad+\frac{11}{3}\chi_6^{\mathrm{E}_7}+\frac{196}{9}\big)\tilde u^2+\big(-\frac{2}{3}\chi_1^{\mathrm{E}_7}\chi_2^{\mathrm{E}_7}-\frac{10}{3}\chi_2^{\mathrm{E}_7}+4\chi_5^{\mathrm{E}_7}+16\chi_7^{\mathrm{E}_7}\big)\tilde u+\frac{8}{27}\chi_1^{\mathrm{E}_7}\chi_1^{\mathrm{E}_7}\chi_1^{\mathrm{E}_7}\\ &\quad+\frac{28}{9}\chi_1^{\mathrm{E}_7}\chi_1^{\mathrm{E}_7}-\frac{4}{3}\chi_1^{\mathrm{E}_7}\chi_3^{\mathrm{E}_7}+\frac{4}{3}\chi_1^{\mathrm{E}_7}\chi_6^{\mathrm{E}_7}-\frac{40}{9}\chi_1^{\mathrm{E}_7}-\chi_2^{\mathrm{E}_7}\chi_2^{\mathrm{E}_7}-\frac{20}{3}\chi_3^{\mathrm{E}_7}+4\chi_4^{\mathrm{E}_7}\\ &\quad+\frac{8}{3}\chi_6^{\mathrm{E}_7}+\frac{136}{27}\,,\end{aligned}\tag{A.2.5}$$

as well as the E_6-curve

$$\begin{aligned}y^2 &= 4x^3+\Big(-\frac{1}{12}\tilde u^4+\frac{2}{3}\chi_1^{\mathrm{E}_6}\tilde u^2+\big(-12+2\chi_2^{\mathrm{E}_6}\big)\tilde u+4\chi_3^{\mathrm{E}_6}-4\chi_6^{\mathrm{E}_6}-\frac{4}{3}\chi_1^{\mathrm{E}_6}\chi_1^{\mathrm{E}_6}\Big)x\\ &\quad-\frac{1}{216}\tilde u^6+\frac{1}{18}\chi_1^{\mathrm{E}_6}\tilde u^4+\big(3+\frac{1}{6}\chi_2^{\mathrm{E}_6}\big)\tilde u^3+\big(-\frac{2}{9}\chi_1^{\mathrm{E}_6}\chi_1^{\mathrm{E}_6}+\frac{1}{3}\chi_3^{\mathrm{E}_6}+\frac{11}{3}\chi_6^{\mathrm{E}_6}\big)\tilde u^2\\ &\quad+\big(4\chi_5^{\mathrm{E}_6}-\frac{2}{3}\chi_1^{\mathrm{E}_6}\chi_2^{\mathrm{E}_6}\big)\tilde u+\frac{8}{27}\chi_1^{\mathrm{E}_6}\chi_1^{\mathrm{E}_6}\chi_1^{\mathrm{E}_6}-\chi_2^{\mathrm{E}_6}\chi_2^{\mathrm{E}_6}-\frac{4}{3}\chi_1^{\mathrm{E}_6}\chi_3^{\mathrm{E}_6}+4\chi_4^{\mathrm{E}_6}+\frac{4}{3}\chi_1^{\mathrm{E}_6}\chi_6^{\mathrm{E}_6}\,.\end{aligned}\tag{A.2.6}$$

The E_6-curve can be mapped onto the general Weierstrass normal form of the cubic (A.1.9) provided one chooses a different gauge. Instead of setting three of the inner points of the one-dimensional faces to 1, which is convenient for the description of local $\mathbb{P}^2$ and its blow-ups, one has to set the coefficients of the monomials x^3,y^3,z^3 to -1. The characters χ_i may then be written in terms of a_1,a_2,a_3,m_1,m_2,m_3 as follows

$$\begin{aligned}\chi_1 &= m_3a_1+m_1a_2+m_2a_3,\\ \chi_2 &= -3-m_1m_2m_3+m_1a_1+m_2a_2+m_3a_3-a_1a_2a_3,\\ \chi_3 &= -m_1^2m_2-m_2^2m_3-m_1m_3^2-2m_2a_1-2m_3a_2+m_1m_3a_1a_2-a_1a_2^2-2m_1a_3\\ &\quad+m_2m_3a_1a_3-a_1^2a_3+m_1m_2a_2a_3-a_2a_3^2,\\ \chi_4 &= 9-m_1^3-m_2^3-m_3^3-6m_1a_1-m_1^2m_2m_3a_1-m_2^2m_3^2a_1-2m_2m_3a_1^2-a_1^3\\ &\quad-6m_2a_2-m_1m_2^2m_3a_2-m_1^2m_3^2a_2+m_1m_2a_1a_2-2m_3^2a_1a_2-2m_1m_3a_2^2\\ &\quad-m_3a_1^2a_2^2-a_2^3-m_1^2m_2^2a_3-6m_3a_3-m_1m_2m_3^2a_3-2m_2^2a_1a_3+m_1m_3a_1a_3\\ &\quad-2m_1^2a_2a_3+m_2m_3a_2a_3+m_1m_2m_3a_1a_2a_3-m_1a_1^2a_2a_3-m_2a_1a_2^2a_3\\ &\quad-2m_1m_2a_3^2-m_2a_1^2a_3^2-m_3a_1a_2a_3^2-m_1a_2^2a_3^2-a_3^3,\end{aligned}$$

$$\begin{aligned}\chi_5 &= -m_1m_2^2 - m_1^2m_3 - m_2m_3^2 - 2m_3a_1 - 2m_1a_2 + m_2m_3a_1a_2 - a_1^2a_2 - 2m_2a_3 \\ &\quad + m_1m_2a_1a_3 + m_1m_3a_2a_3 - a_2^2a_3 - a_1a_3^2, \\ \chi_6 &= m_2a_1 + m_3a_2 + m_1a_3. \end{aligned} \tag{A.2.7}$$

Repeating the above procedure one finds the D_5-curve

$$\begin{aligned}y^2 &= 4x^3 + \Big(-\frac{1}{12}\tilde{u}^4 + \frac{2}{3}\chi_1^{\mathrm{D}_5}\tilde{u}^2 + 2\chi_2^{\mathrm{D}_5}\tilde{u} - \frac{4}{3}\chi_1^{\mathrm{D}_5}\chi_1^{\mathrm{D}_5} + 4\chi_3^{\mathrm{D}_5} - 4\Big)x \\ &\quad -\frac{1}{216}\tilde{u}^6 + \frac{1}{18}\chi_1^{\mathrm{D}_5}\tilde{u}^4 + \frac{1}{6}\chi_2^{\mathrm{D}_5}\tilde{u}^3 + \big(\frac{11}{3} - \frac{2}{9}\chi_1^{\mathrm{D}_5}\chi_1^{\mathrm{D}_5} + \frac{1}{3}\chi_3^{\mathrm{D}_5}\big)\tilde{u}^2 + \big(4\chi_5^{\mathrm{D}_5} - \frac{2}{3}\chi_1^{\mathrm{D}_5}\chi_2^{\mathrm{D}_5}\big)\tilde{u} \\ &\quad + \frac{4}{3}\chi_1^{\mathrm{D}_5} + \frac{8}{27}\chi_1^{\mathrm{D}_5}\chi_1^{\mathrm{D}_5}\chi_1^{\mathrm{D}_5} - \chi_2^{\mathrm{D}_5}\chi_2^{\mathrm{D}_5} - \frac{4}{3}\chi_1^{\mathrm{D}_5}\chi_3^{\mathrm{D}_5} + 4\chi_4^{\mathrm{D}_5}, \end{aligned} \tag{A.2.8}$$

the E_4-curve

$$\begin{aligned}y^2 &= 4x^3 + \Big(-\frac{1}{12}\tilde{u}^4 + \frac{2}{3}\chi_1^{E_4}\tilde{u}^2 + 2\chi_2^{E_4}\tilde{u} + 4\chi_3^{E_4} - \frac{4}{3}\chi_1^{E_4}\chi_1^{E_4}\Big)x \\ &\quad -\frac{1}{216}\tilde{u}^6 + \frac{1}{18}\chi_1^{E_4}\tilde{u}^4 + \frac{1}{6}\chi_2^{E_4}\tilde{u}^3 + \big(\frac{1}{3}\chi_2^{E_3} - \frac{2}{9}\chi_1^{E_4}\chi_1^{E_4}\big)\tilde{u}^2 + \big(4 - \frac{2}{3}\chi_1^{E_4}\chi_2^{E_4}\big)\tilde{u} \\ &\quad + \frac{8}{27}\chi_1^{E_4}\chi_1^{E_4}\chi_1^{E_4} - \chi_2^{E_4}\chi_2^{E_4} - \frac{4}{3}\chi_1^{E_4}\chi_3^{E_4} + 4\chi_4^{E_4}, \end{aligned} \tag{A.2.9}$$

and finally the E_3-curve

$$\begin{aligned}y^2 &= 4x^3 + \Big(-\frac{1}{12}\tilde{u}^4 + \frac{2}{3}\chi_1^{E_3}\tilde{u}^2 + 2\chi_2^{E_3}\tilde{u} + 4\chi_3^{E_3} - \frac{4}{3}\chi_1^{E_3}\chi_1^{E_3}\Big)x \\ &\quad -\frac{1}{216}\tilde{u}^6 + \frac{1}{18}\chi_1^{E_3}\tilde{u}^4 + \frac{1}{6}\chi_2^{E_3}\tilde{u}^3 + \big(\frac{1}{3}\chi_3^{E_3} - \frac{2}{9}\chi_1^{E_3}\chi_1^{E_3}\big)\tilde{u}^2 - \frac{2}{3}\chi_1^{E_3}\chi_2^{E_3}\tilde{u} \\ &\quad - \frac{4}{3}\chi_1^{E_3}\chi_3^{E_3} + \frac{8}{27}\chi_1^{E_3}\chi_1^{E_3}\chi_1^{E_3} - \chi_2^{E_3}\chi_2^{E_3} + 4. \end{aligned} \tag{A.2.10}$$

The case of the E_3 is distinguished in the following sense. It is the last curve that is toric, but it is the first curve for which the identification of the orthogonal complement to the canonical class inside the homology lattice can be identified with the root lattice of E_3. In the following we illustrate this correspondence explicitly. As a first step we recall the toric data of $\mathcal{B}_3$, i.e. the generators of the Mori cone (5.3.43) and make the identification of points in the toric diagram with divisors explicit. Note that we omit the non-compact direction, i.e. we are not considering the CY geometry here, but just its base for simplicity. Therefore curves and divisors are the same in this case.

$l^{(1)}$	$l^{(2)}$	$l^{(3)}$	$l^{(4)}$	$l^{(5)}$	$l^{(6)}$	Divisor Class
-1	-1	-1	-1	-1	-1	
-1	1	0	0	0	1	e_1
1	-1	1	0	0	0	$h - e_1 - e_2$
0	1	-1	1	0	0	e_2
0	0	1	-1	1	0	$h - e_2 - e_3$
0	0	0	1	-1	1	e_3
1	0	0	0	1	-1	$h - e_1 - e_3$
e_1	$h - e_1 - e_2$	e_2	$h - e_2 - e_3$	e_3	$h - e_1 - e_3$	

here we have denoted by h the hyperplane class in $\mathbb{P}^2$ and by e_1, e_2, e_3 the classes of the

three blow-up divisors.

As it was already explained in the discussion in the main text, the Mori as well as the Kähler cone are non-simplicial. It is sufficient for our purposes to only search for a dual basis of the first four generators $l^{(1)}, ..., l^{(4)}$. The dual generators read in terms of h, e_1, e_2, e_3

$$\left|\begin{array}{c|c} \text{Generator} & \text{Dual generator} \\ e_1 & h-e_1-e_3 \\ h-e_1-e_2 & h-e_3 \\ e_2 & h-e_2 \\ h-e_2-e_3 & e_3 \end{array}\right| .$$

The Kähler form enjoys accordingly an expansion

$$J = v_1(h-e_1-e_3) + v_2(h-e_3) + v_3(h-e_2) + v_4 e_3 \,. \tag{A.2.11}$$

The moduli are given by the relations corresponding to the $l^{(i)}$

$$\log(v_1) = \frac{a_1 a_3}{\tilde{u} m_1}, \quad \log(v_2) = \frac{m_1 m_2}{\tilde{u} a_1}, \quad \log(v_3) = \frac{a_1 a_2}{\tilde{u} m_2}, \quad \log(v_4) = \frac{m_2 m_3}{\tilde{u} a_2}, \tag{A.2.12}$$

where we have used the leading mirror map at large radius. Using this, one easily computes the volumes of a divisor D as

$$\text{vol}(D) = \int_D J = J \cdot D. \tag{A.2.13}$$

and obtains explicitly

$$\text{vol}(h) = \log(v_1 v_2 v_3), \quad \text{vol}(e_1) = \log(v_1), \quad \text{vol}(e_2) = \log(v_3), \quad \text{vol}(e_3) = \log\Big(\frac{v_1 v_2}{v_4}\Big) . \tag{A.2.14}$$

For convenience we recall explicitly the homology of the $\mathcal{B}_3$ surface. The orthogonal complement of the canonical class of $\mathcal{B}_3$ reads

$$K = -3h + e_1 + e_2 + e_3 \,. \tag{A.2.15}$$

The simple roots of $\mathcal{B}_3$ are given in terms of divisors as

$$\alpha_1 = e_1 - e_2, \quad \alpha_2 = e_2 - e_3, \quad \alpha_3 = h - e_1 - e_2 - e_3. \tag{A.2.16}$$

Note that the roots intersect precisely as the Cartan matrix of $A_2 \times A_1$

$$\alpha_i \cdot \alpha_j = \begin{pmatrix} -2 & 1 & 0 \\ 1 & -2 & 0 \\ 0 & 0 & -2 \end{pmatrix} . \tag{A.2.17}$$

From these one can determine the corresponding fundamental weights $\mathcal{V}_i$ which are defined as

$$2\frac{\alpha_i \cdot \mathcal{V}_j}{\alpha_i \cdot \alpha_i} = \delta_{ij} \quad \Leftrightarrow \quad \alpha_i \cdot \mathcal{V}_j = -\delta_{ij} \,. \tag{A.2.18}$$

One obtains

$$\mathcal{V}_1 = \frac{1}{3}\big(2e_1 - e_2 - e_3\big), \quad \mathcal{V}_2 = \frac{1}{3}\big(e_1 + e_2 - 2e_3\big), \quad \mathcal{V}_3 = -\frac{1}{2}\big(-h + e_1 + e_2 + e_3\big) \,. \tag{A.2.19}$$

Acting with the roots on the highest weights, one can work out the representations. E.g. taking $\mathcal{V}_1$ as the highest weight, one obtains the fundamental representation of A_2 which consists out of the following weights

$$\nu_1 = \mathcal{V}_1, \quad \nu_2 = \mathcal{V}_1 - \alpha_1, \quad \nu_3 = \mathcal{V}_1 - \alpha_1 - \alpha_2 \,. \tag{A.2.20}$$

By pairing the roots (that are still given in terms of divisors) with the Kähler form and exponentiating the result, one can work out the characters of the representation and compare with (A.2.2). For $\mathcal{V}_1$ one obtains

$$\begin{aligned} \chi_1 &= \Big(\frac{a_1 a_3 m_2 m_3}{a_2^2 m_1^2}\Big)^{\frac{1}{3}} + \Big(\frac{a_1 a_2 m_1 m_3}{a_3^2 m_2^2}\Big)^{\frac{1}{3}} + \Big(\frac{a_2 a_3 m_1 m_2}{a_1^2 m_3^2}\Big)^{\frac{1}{3}}, \\ \chi_2 &= \Big(\frac{a_1^2 m_3^2}{a_2 a_3 m_1 m_2}\Big)^{\frac{1}{3}} + \Big(\frac{a_3^2 m_2^2}{a_1 a_2 m_1 m_3}\Big)^{\frac{1}{3}} + \Big(\frac{a_2^2 m_1^2}{a_1 a_3 m_2 m_3}\Big)^{\frac{1}{3}}, \\ \chi_3 &= \Big(\frac{a_1 a_2 a_3}{m_1 m_2 m_3}\Big)^{-\frac{1}{2}} + \Big(\frac{a_1 a_2 a_3}{m_1 m_2 m_3}\Big)^{\frac{1}{2}} . \end{aligned} \tag{A.2.21}$$

We obtain a matching of the curve (A.2.10) with (A.1.9), with m_4, m_5, m_6 vanishing, provided we make the following identification

$$a_1 \mapsto \frac{1}{m_1}, \quad a_2 \mapsto \frac{1}{m_2}, \quad a_3 \mapsto \frac{1}{m_3}. \tag{A.2.22}$$

In this case the characters read explicitly

$$\begin{aligned} \chi_1 &= \frac{m_1}{m_3} + \frac{m_2}{m_1} + \frac{m_3}{m_2}, \\ \chi_2 &= \frac{m_1}{m_2} + \frac{m_2}{m_3} + \frac{m_3}{m_1}, \\ \chi_3 &= \frac{1}{m_1 m_2 m_3} + m_1 m_2 m_3 \,. \end{aligned} \tag{A.2.23}$$

Note that this is just one possible identification, e.g. the identification

$$a_1 \mapsto \frac{1}{m_2}, \quad a_2 \mapsto \frac{1}{m_3}, \quad a_3 \mapsto \frac{1}{m_1}. \tag{A.2.24}$$

leads to the characters of the complex conjugate representation. We conclude by noting that the identification on the level of Wilson line parameters $\tilde{m}_1, \tilde{m}_2, \tilde{m}_3$ is given as

$$M_1 = \frac{m_3}{m_1}, \quad M_2 = \frac{m_2}{m_1}, \quad M_3 = \frac{1}{m_1 m_2 m_3}, \quad M_i = e^{\tilde{m}_i}. \tag{A.2.25}$$

A.2.2. The third order differential operator for $\mathcal{B}_2$

The third order differential operator for $\mathcal{B}_2$ is given by

$$\begin{aligned}\mathcal{L} \;=\; & (-12m_1^2+12m_1m_2+16m_1^4m_2-12m_2^2-12m_1^3m_2^2-12m_1^2m_2^3+16m_1^5m_2^3+16m_1m_2^4\\
&-32m_1^4m_2^4+16m_1^3m_2^5+9\tilde{u}+24m_1^2m_2\tilde{u}+24m_1m_2^2\tilde{u}-32m_1^4m_2^2\tilde{u}+56m_1^3m_2^3\tilde{u}\\
&-32m_1^2m_2^4\tilde{u}-18m_1\tilde{u}^2-18m_2\tilde{u}^2-4m_1^3m_2\tilde{u}^2-68m_1^2m_2^2\tilde{u}^2-4m_1m_2^3\tilde{u}^2-4m_1^4m_2^3\tilde{u}^2\\
&-4m_1^3m_2^4\tilde{u}^2+8m_1^2\tilde{u}^3+36m_1m_2\tilde{u}^3+8m_2^2\tilde{u}^3+28m_1^3m_2^2\tilde{u}^3+28m_1^2m_2^3\tilde{u}^3+8m_1^4m_2^4\tilde{u}^3\\
&-16m_1^2m_2\tilde{u}^4-16m_1m_2^2\tilde{u}^4-16m_1^3m_2^3\tilde{u}^4+7m_1^2m_2^2\tilde{u}^5)\partial_{\tilde{u}}+(-108m_1-128m_1^4\\
&-108m_2+64m_1^3m_2-264m_1^2m_2^2-192m_1^5m_2^2+64m_1m_2^3+128m_1^4m_2^3-128m_2^4\\
&+128m_1^3m_2^4-128m_1^6m_2^4-192m_1^2m_2^5+256m_1^5m_2^5-128m_1^4m_2^6+144m_1^2\tilde{u}\tilde{u}\\
&+450m_1m_2+288m_1^4m_2\tilde{u}+144m_2^2\tilde{u}+240m_1^3m_2^2\tilde{u}+240m_1^2m_2^3\tilde{u}+288m_1^5m_2^3\tilde{u}\tilde{u}\\
&+288m_1m_2^4\tilde{u}-320m_1^4m_2^4\tilde{u}+288m_1^3m_2^5\tilde{u}+27\tilde{u}^2-64m_1^3\tilde{u}^2-384m_1^2m_2\tilde{u}^2\tilde{u}\\
&-384m_1m_2^2\tilde{u}^2-336m_1^4m_2^2\tilde{u}^2-64m_2^3\tilde{u}^2-240m_1^3m_2^3\tilde{u}^2-336m_1^2m_2^4\tilde{u}^2-64m_1^5m_2^4\tilde{u}^2\tilde{u}\\
&-64m_1^4m_2^5\tilde{u}^2-52m_1\tilde{u}^3-52m_2\tilde{u}^3+112m_1^3m_2\tilde{u}^3+172m_1^2m_2^2\tilde{u}^3+112m_1m_2^3\tilde{u}^3\tilde{u}\\
&+112m_1^4m_2^3\tilde{u}^3+112m_1^3m_2^4\tilde{u}^3+24m_1^2\tilde{u}^4+100m_1m_2\tilde{u}^4+24m_2^2\tilde{u}^4+12m_1^3m_2^2\tilde{u}^4\tilde{u}\\
&+12m_1^2m_2^3\tilde{u}^4+24m_1^4m_2^4\tilde{u}^4-46m_1^2m_2\tilde{u}^5 46m_1m_2^2\tilde{u}^5-46m_1^3m_2^3\tilde{u}^5+21m_1^2m_2^2\tilde{u}^6)\partial_{\tilde{u}}^2\\
&+(-9-4m_1^2m_2-4m_1m_2^2+8m_1\tilde{u}+8m_2\tilde{u}+8m_1^2m_2^2\tilde{u}-7m_1m_2\tilde{u}^2)(-27+16m_1^3\tilde{u}\\
&-24m_1^2m_2-24m_1m_2^2+16m_1^4m_2^2+16m_2^3-32m_1^3m_2^3+16m_1^2m_2^4+36m_1\tilde{u}+36m_2\tilde{u}\tilde{u}\\
&-16m_1^3m_2\tilde{u}+64m_1^2m_2^2\tilde{u}-16m_1m_2^3\tilde{u}-8m_1^2\tilde{u}^2-46m_1m_2\tilde{u}^2-8m_2^2\tilde{u}^2-8m_1^3m_2^2\tilde{u}^2\tilde{u}\\
&-8m_1^2m_2^3\tilde{u}^2-\tilde{u}^3+8m_1^2m_2\tilde{u}^3+8m_1m_2^2\tilde{u}^3+m_1\tilde{u}^4+m_2\tilde{u}^4+m_1^2m_2^2\tilde{u}^4-m_1m_2\tilde{u}^5)\partial_{\tilde{u}}^3\,.\end{aligned} \tag{A.2.26}$$

We note the limits $\mathcal{B}_1$ and $\mathbb{P}^2$ in the case of one respectively two vanishing mass parameters.

A.3. Jacobi and Siegel modular forms

In this appendix we summarize some information on Jacobi and Siegel modular forms which are needed for the main discussion.

A.3.1. Weyl invariant Jacobi modular forms for E_8 lattice

Our convention for the theta functions are

$$\begin{aligned}\theta_1(m,\tau) &= -i\sum_{n\in\mathbb{Z}}(-1)^n \exp[\pi i m(2n+1)]\exp[\pi i\tau(n+\frac{1}{2})^2],\\
\theta_2(m,\tau) &= \sum_{n\in\mathbb{Z}}\exp[\pi i m(2n+1)]\exp[\pi i\tau(n+\frac{1}{2})^2],\\
\theta_3(m,\tau) &= \sum_{n\in\mathbb{Z}}\exp(2\pi i m n)\exp(\pi i\tau n^2),\\
\theta_4(m,\tau) &= \sum_{n\in\mathbb{Z}}(-1)^n\exp(2\pi i m n)\exp(\pi i\tau n^2).\end{aligned} \tag{A.3.1}$$

We use the notation $\theta_i(\tau) \equiv \theta_i(0,\tau)$ for the massless theta functions. We define a modular form $h(\tau)$ as

$$h(\tau) = \theta_2(2\tau)\theta_2(6\tau) + \theta_3(2\tau)\theta_3(6\tau) = 1 + 6q + 6q^3 + 6q^4 + 12q^7 + \mathcal{O}(q^9), \qquad \text{(A.3.2)}$$

where the parameter is $q = e^{2\pi i\tau}$.

The nine Weyl invariant Jacobi forms can be written in terms of the theta function of the E_8 lattice

$$\Theta(\vec{m},\tau) = \sum_{\vec{w}\in\Gamma_8} \exp(\pi i\tau\vec{w}^2 + 2\pi i\vec{m}\cdot\vec{w}) = \frac{1}{2}\sum_{k=1}^{4}\prod_{j=1}^{8}\theta_k(m_j,\tau)\,. \qquad \text{(A.3.3)}$$

We also introduce the notation $\theta_{\mathrm{E}_8}(\tau) = \Theta(\vec{0},\tau)$. The formulae read as follows

$$\begin{aligned}
A_1 &= \Theta(\vec{m},\tau), \qquad A_4 = \Theta(2\vec{m},\tau),\\
A_n &= \frac{n^3}{n^3+1}[(\Theta(n\vec{m},n\tau) + \frac{1}{n^4}\sum_{k=0}^{n-1}\Theta(\vec{m},\frac{\tau+k}{n})], \quad n = 2,3,5,\\
B_2 &= \frac{8}{15}[(\theta_3(\tau)^4+\theta_4(\tau)^4)\Theta(2\vec{m},2\tau) - \frac{1}{2^4}(\theta_2(\tau)^4+\theta_3(\tau)^4)\Theta(\vec{m},\frac{\tau}{2})\\
&\quad +\frac{1}{2^4}(\theta_2(\tau)^4-\theta_4(\tau)^4)\Theta(\vec{m},\frac{\tau+1}{2})],\\
B_3 &= \frac{81}{80}[h(\tau)^2\Theta(3\vec{m},3\tau) - \frac{1}{3^5}\sum_{k=0}^{2}h(\frac{\tau+k}{3})^2\Theta(\vec{m},\frac{\tau+k}{3})],\\
B_4 &= \frac{16}{15}[\theta_4(2\tau)^4\Theta(4\vec{m},4\tau) - \frac{1}{2^4}\theta_4(2\tau)^4\Theta(2\vec{m},\tau+\frac{1}{2}) - \frac{1}{4^5}\sum_{k=0}^{3}\theta_2(\frac{\tau+k}{2})^4\Theta(\vec{m},\frac{\tau+k}{4})],\\
B_6 &= \frac{9}{10}[h(\tau)^2\Theta(6\vec{m},6\tau) + \frac{h(\tau)^2}{2^4}\sum_{k=0}^{1}\Theta(3\vec{m},\frac{3\tau+3k}{2}) - \frac{1}{3^5}\sum_{k=0}^{2}h(\frac{\tau+k}{3})^2\Theta(2\vec{m},\frac{2(\tau+k)}{3})\\
&\quad -\frac{1}{3\cdot 6^4}\sum_{k=0}^{5}h(\frac{\tau+k}{3})^2\Theta(\vec{m},\frac{\tau+k}{6}).
\end{aligned} \qquad \text{(A.3.4)}$$

A.3.2. Siegel modular forms of genus two

In this section we introduce the basics of Siegel modular forms of genus two. See also [201–204] for further reference.

The Siegel upper halfplane is denoted by

$$\mathfrak{S}_2 = \left\{\tau \in \mathbb{C}^{2\times 2} \mid \tau^T = \tau, \quad \mathrm{Im}\,\tau \geq 0\right\} \qquad \text{(A.3.5)}$$

on which the homogeneous modular group $\Gamma_2 = \mathrm{Sp}(4,\mathbb{Z})$ operates by

$$\tau \mapsto \big(A\tau + B\big)\big(C\tau + D\big)^{-1}, \qquad \begin{pmatrix} A & B \\ C & D \end{pmatrix} \in \mathrm{Sp}(4,\mathbb{Z}). \qquad \text{(A.3.6)}$$

The quotient $\mathfrak{S}_2$ by this action is called the Siegel fundamental domain $\mathcal{F}_2 = \Gamma_2\backslash\mathfrak{S}_2$. A Siegel modular form of weight w is a holomorphic function $f : \mathfrak{S}_2 \longrightarrow \mathbb{C}$, such that for all

$\tau \in \mathfrak{S}_2$ and $\gamma \in \Gamma_2$

$$f(\gamma\tau) = \det\big(C\tau + D\big)^w f(\tau), \quad \gamma = \begin{pmatrix} A & B \\ C & D \end{pmatrix} \tag{A.3.7}$$

holds. The space of all Siegel modular forms of weight w is denoted by $M_w(\mathfrak{S}_2)$. As $\begin{pmatrix} \mathbb{1} & \mathbb{1} \\ 0 & \mathbb{1} \end{pmatrix}$ is contained in Γ_2, any Siegel modular form f admits a Fourier expansion which reads

$$f = \sum_T a(T) \exp(2\pi i \operatorname{Tr}(T\tau)). \tag{A.3.8}$$

Here the summation is over all half integer matrices $T \in \frac{1}{2}\mathbb{Z}^{2\times 2}$ which have integer diagonal elements. Next we introduce the Siegel operator Φ, which is a map $M_w(\mathfrak{S}_2) \longrightarrow M_w(\mathfrak{S}_1)$ and is defined by

$$\Phi f = \lim_{t\to\infty} f \begin{pmatrix} \tau & 0 \\ 0 & it \end{pmatrix}, \quad \tau \in \mathbb{H},\, t \in \mathbb{R}. \tag{A.3.9}$$

The elements of $\ker \Phi$ are called cusp forms. For $w \geq 4$ we define the Eisenstein series by

$$E_w(\tau) = \sum_{C,D} \det(C\tau + D)^{-w}. \tag{A.3.10}$$

The summation is over all inequivalent bottom rows $\begin{pmatrix} C & D \end{pmatrix}$ of elements of Γ_2. A classical theorem by Igusa states that the space of Siegel modular forms of genus two has a representation as

$$M = \mathbb{C}[E_4, E_6, \Phi_{10}, \Phi_{12}, \Phi_{35}]/\big\{\Phi_{35}^2 = R\big\}, \tag{A.3.11}$$

Here E_4 and E_6 denote the Eisenstein series of degree four and six, while the cusp forms are given as follows

$$\Phi_{10} = -\frac{43867}{2^{12}\cdot 3^5\cdot 5^2\cdot 7\cdot 53}\big(E_4E_6 - E_{10}\big) \tag{A.3.12}$$

$$\Phi_{12} = -\frac{131\cdot 593}{2^{13}\cdot 3^7\cdot 5^3\cdot 7^2\cdot 337}\big(3^2\cdot 7^2E_4^3 + 2\cdot 5^3E_6^2 - 691E_{12}\big) \tag{A.3.13}$$

R being a polynomial in $E_4, E_6, \Phi_{10}, \Phi_{12}$ [204].

Fourier expansion of Eisenstein series of genus two

In this subsection we want to discuss how to compute the Fourier coefficients of Eisenstein series. We start by introducing some terminology.

- Let d be a square-free integer and consider the field extension $K = \mathbb{Q}[\sqrt{d}]$ of the rational numbers. The discriminant of K is given as

$$\Delta_K = \begin{cases} d & \text{if } d \equiv 1 \pmod 4 \\ 4d & \text{if } d \equiv 2,3 \pmod 4 \end{cases}. \tag{A.3.14}$$

- The Möbius function $\mu : \mathbb{N} \longrightarrow \{-1, 0, 1\}$ is defined as follows

$$\mu(n) = \begin{cases} 1 \text{ if } n \text{ is a square-free, positive integer with an even number of prime factors} \\ -1 \text{ if } n \text{ is a square-free, positive integer with an odd number of prime factors} \\ 0 \text{ if } n \text{ has a squared prime factor} \end{cases} \tag{A.3.15}$$

- The divisor function $\sigma_k(n)$ with $x \in \mathbb{C}$ is defined as

$$\sigma_k(n) = \sum_{d|n} d^k \,. \tag{A.3.16}$$

- A Dirichlet character is a function $\chi : \mathbb{Z} \longrightarrow \mathbb{C}$ with the following properties
  1. There is a $k \in \mathbb{Z}$, such that $\chi(n) = \chi(n+k)$ for all n
  2. $\chi(n) \begin{cases} = 0 \text{ if} \gcd(n,k) > 1 \\ \neq 0 \text{ if} \gcd(n,k) = 1 \end{cases}$
  3. $\chi(mn) = \chi(m)\chi(n)$

  In particular, a Dirichlet character χ is a group homomorphism $\left(\mathbb{Z}/(k\mathbb{Z})\right)^* \longrightarrow \mathbb{C}^*$. Vice versa, any character of the unit group of $\mathbb{Z}/(k\mathbb{Z})$ extends to a Dirichlet character by setting $\chi(n) = 0$ for $n \notin \left(\mathbb{Z}/(k\mathbb{Z})\right)^*$

- A Dirichlet L-function associated to a Dirichlet character is given by

$$L(s, \chi) = \sum_{n=1}^{\infty} \frac{\chi(n)}{n^s}, \quad \mathrm{Re}(s) > 1 \,. \tag{A.3.17}$$

- Given a prime p, the Kroneckersymbol $\left(\frac{a}{p}\right)$ is for $a \in \mathbb{Z}$ defined as

$$\left(\frac{a}{p}\right) = \begin{cases} 1, \text{ if } a \text{ is a quadratic rest modulo } n \\ -1, \text{ if } a \text{ is not a quadratic rest modulo } n \\ 0, \text{ if } a \equiv 0 \bmod n \end{cases} \tag{A.3.18}$$

  For general $n \in \mathbb{N}$ with prime factorization $n = p_1^{\nu_1} \dots p_k^{\nu_k}$ one puts $\left(\frac{a}{n}\right) = \left(\frac{a}{p_1}\right)^{\nu_1} \dots \left(\frac{a}{p_k}\right)^{\nu_k}$. Note that $\left(\frac{\cdot}{n}\right)$ is a Dirichlet character modulo n.

Theorem. (e.g. [209]) *Let E_w be an Eisenstein series of weight w, $T = \begin{pmatrix} a & b/2 \\ b/2 & c \end{pmatrix} \in \frac{1}{2}\mathbb{Z}^{2\times 2}$ be positive semi-definite. Denote $D = b^2 - 4ac \leq 0$ and let D_0 be the discriminant of $\mathbb{Q}(\sqrt{D})$. Then the Fourier coefficient $a(T)$ is one, if $a = b = c = 0$ and*

$$\frac{-2w}{B_w} \sum_{d|gcd(a,b,c)} d^{w-1} \alpha(D/d^2) \tag{A.3.19}$$

otherwise. Here B_k denotes the kth Bernoulli number and α is defined by $\alpha(0) = 1$ and

$$\alpha(D) = \frac{1}{\zeta(3-2w)} C(w-1, D). \tag{A.3.20}$$

Here the Cohen function C is defined by

$$C(s-1,D) = L_{D_0}(2-s)\sum_{d|f}\mu(d)\Big(\frac{D_0}{d}\Big)d^{s-2}\sigma_{2s-3}(f/d), \qquad D = D_0 f^2. \tag{A.3.21}$$

In this expression, ζ denotes the Dedekind zeta-function and L_{D_0} is the Dirichlet L-series associated to the character $\big(\frac{\cdot}{D_0}\big)$.

Explicit Fourier expansions for Siegel modular forms of genus two

In the following we give the explicit Fourier expansions of the generators of the ring of Siegel modular forms at genus two where we use the notation $q_1 = e^{2\pi i\tau_{11}},\ q_2 = e^{2\pi i\tau_{22}},\ r = e^{2\pi i\tau_{12}}$.

$$\begin{aligned}
E_4(q_1,q_2,r) &= 1 + 240q_1 + 240q_2 + 2160q_1^2 + 30240q_1q_2 + 2160q_2^2 + 240\frac{q_1q_2}{r^2} + 13440\frac{q_1q_2}{r} \\
&\quad +13440q_1q_2r + 240q_1q_2r^2 + 6720q_1^3 + 181440q_1^2 + 181440q_1q_2^2 + 6720q_2^3 \\
&\quad +30240\frac{q_1^2q_2}{r^2} + 30240\frac{q_1q_2^2}{r^2} + 138240\frac{q_1^2q_2}{r} + 138240\frac{q_1q_2^2}{r} + 138240q_1^2q_2r \\
&\quad +138240q_1q_2^2r + 30240q_1^2q_2r^2 + 30240q_1q_2^2r^2 + \dots, \qquad (A.3.22) \\
E_6(q_1,q_2,r) &= 1 - 504q_1 - 504q_2 - 16632q_1^2 + 166320q_1q_2 - 16632q_2^2 - 504\frac{q_1q_2}{r^2} + 44352\frac{q_1q_2}{r} \\
&\quad +44352q_1q_2r - 504q_1q_2r^2 - 122976q_1^3 + 3792096q_1^2q_2 + 3792096q_1q_2^2 - 122976q_2^3 \\
&\quad +166320\frac{q_1^2q_2}{r^2} + 166320\frac{q_1q_2^2}{r^2} + 2128896\frac{q_1^2q_2}{r} + 2128896\frac{q_1q_2^2}{r} + 2128896q_1^2q_2r \\
&\quad +2128896q_1q_2^2r + 166320q_1^2q_2r^2 + 166320q_1q_2^2r^2 + \dots, \qquad (A.3.23) \\
\chi_{10}(q_1,q_2,r) &= \frac{1}{2}q_1q_2 - 9q_1^2q_2 - 9q_1q_2^2 + \frac{q_1^2q_2}{2r^2} + \frac{q_1q_2^2}{2r^2} - \frac{q_1q_2}{4r} + \frac{4q_1^2q_2}{r} + \frac{4q_1q_2^2}{r} - \frac{1}{4}q_1q_2r \\
&\quad +4q_1^2q_2r + 4q_1q_2^2r + \frac{1}{2}q_1^2q_2r^2 + \frac{1}{2}q_1q_2^2r^2 + \dots, \qquad (A.3.24) \\
\chi_{12}(q_1,q_2,r) &= \frac{5}{6}q_1q_2 - 11q_1^2q_2 - 11q_1q_2^2 + \frac{5}{6}\frac{q_1^2q_2}{r^2} + \frac{5}{6}\frac{q_1q_2^2}{r^2} + \frac{q_1q_2}{12r} - \frac{22}{3}\frac{q_1^2q_2}{r} - \frac{22}{3}\frac{q_1q_2^2}{r} \qquad (A.3.25) \\
&\quad +\frac{1}{12}q_1q_2r - \frac{22}{3}q_1^2q_2r - \frac{22}{3}q_1q_2^2r + \frac{5}{6}q_1^2q_2r^2 + \frac{5}{6}q_1q_2^2r^2 + \dots, \qquad (A.3.26) \\
x_1(q_1,q_2,r) &= 9 + 10368q_1 + 10368q_2 + 7651584q_1^2 + 16505856q_1q_2 + 7651584q_2^2 + 3456\frac{q_1^2}{r^2} \\
&\quad +10368\frac{q_1q_2}{r^2} + 3456\frac{q_2^2}{r^2} - 216\frac{q_1}{r} - 238680\frac{q_1^2}{r} - 216\frac{q_2}{r} - 508032\frac{q_1q_2}{r} - 238680\frac{q_2^2}{r} \\
&\quad -216r - 238680q_1r - 174078936q_1^2r - 238680q_2r - 382465152q_1q_2r \\
&\quad -174078936q_2^2r + 3456r^2 + 4188672q_1r^2 + 3277494144q_1^2r^2 + 4188672q_2r^2 \\
&\quad +7253463168q_1q_2r^2 + 3277494144q_2^2r^2 + \dots, \qquad (A.3.27) \\
x_2(q_1,q_2,r) &= -27 - 34992q_1 - 34992q_2 - 25824096q_1^2 - 22931424q_1q_2 - 25824096q_2^2 \\
&\quad -21384\frac{q_1^2}{r^2} - 34992\frac{q_1q_2}{r^2} - 21384\frac{q_2^2}{r^2} + 972\frac{q_1}{r} + 910764\frac{q_1^2}{r} + 972\frac{q_2}{r} + 653184\frac{q_1q_2}{r} \\
&\quad +910764\frac{q_2^2}{r} + 972r + 910764q_1r + 635595660q_1^2r + 910764q_2r + 838781568q_1q_2r \\
&\quad +635595660q_2^2r - 21384r^2 - 20015424q_1r^2 - 14164643016q_1^2r^2 - 20015424q_2r^2 \\
&\quad -23598639792q_1q_2r^2 - 14164643016q_2^2r^2 + \dots, \qquad (A.3.28) \\
x_3(q_1,q_2,r) &= -\frac{753}{2}q_1q_2 + \frac{243}{4}\frac{q_1q_2}{r} + \frac{525123}{4}q_1q_2r - 3411720q_1q_2r^2 + \dots. \qquad (A.3.29)
\end{aligned}$$

A.4. The BPS invariants for the half K3 and the diagonal classes of $\mathbb{P} \times \mathbb{P}^1$

Here we list the BPS invariants for the half K3 and the diagonal $\mathbb{P} \times \mathbb{P}^1$.

A.4.1. The diagonal $\mathbb{P} \times \mathbb{P}^1$ model

$2j_L \backslash 2j_R$	0	1
0		2

d=1

$2j_L \backslash 2j_R$	0	1	2	3
0				1

d=2

$2j_L \backslash 2j_R$	0	1	2	3	4	5
0						2

d=3

$2j_L \backslash 2j_R$	0	1	2	3	4	5	6	7	8
0						1		3	
1									1

$d = 4$

$2j_L \backslash 2j_R$	0	1	2	3	4	5	6	7	8	9	10	11
0						2		2		6		
1									2		2	
2												2

$d = 5$

$2j_L \backslash 2j_R$	0	1	2	3	4	5	6	7	8	9	10	11	12	13	14	15
0				1		3		5		7		10				
1							1		4		5		7		1	
2										1		4		5		
3													1		3	
4																1

$d = 6$

$2j_L \backslash 2j_R$	0	1	2	3	4	5	6	7	8	9	10	11	12	13	14	15	16	17	18	19
0		2		2		8		10		18		16		22		2		2		
1					2		4		10		14		20		18		4			
2								2		4		12		14		18		2		
3											2		4		10		10		2	
4														2		4		8		
5																	2		2	
6																				2

$d = 7$

Table A.1.: The GV invariants $n^d_{j_L,j_R}$ for $d = 1, 2, \cdots, 7$ for the local $\mathbb{P}^1 \times \mathbb{P}^1$ model

A.4.2. The massless half K3

$2j_L \backslash 2j_R$	0
0	1

d=0

$2j_L \backslash 2j_R$	0	1
0	8	
1		1

d=1

$2j_L \backslash 2j_R$	0	1	2
0	45		
1		9	
2			1

d=2

$2j_L \backslash 2j_R$	0	1	2	3
0	201		1	
1		54		
2	1		9	
3				1

d=3

$2j_L \backslash 2j_R$	0	1	2	3	4
0	781		9		
1		255		1	
2	9		55		
3		1		9	
4					1

d=4

$2j_L \backslash 2j_R$	0	1	2	3	4	5
0	2727		55			
1		1036		10		
2	55		264		1	
3		10		55		
4			1		9	
5						1

d=5

$2j_L \backslash 2j_R$	0	1	2	3	4	5	6
0	8785		264		1		
1		3764		64			
2	264		1091		10		
3		64		265		1	
4	1		10		55		
5				1		9	
6							1

d=6

Table A.2.: The refined Betti numbers $n^d_{j_L,j_R}$ for $d = 0, 1, \cdots, 6$ for the half K3 surface

$2j_L \backslash 2j_R$	0
0	1

d=0

$2j_L \backslash 2j_R$	0	1
0	248	
1		1

d=1

$2j_L \backslash 2j_R$	0	1	2
0	4125		
1		249	
2			1

d=2

$2j_L \backslash 2j_R$	0	1	2	3
0	35001		1	
1		4374		
2	1		249	
3				1

d=3

$2j_L \backslash 2j_R$	0	1	2	3	4
0	217501		249		
1		39375		1	
2	249		4375		
3		1		249	
4					1

d=4

$2j_L \backslash 2j_R$	0	1	2	3	4	5
0	1097127		4375			
1		256876		250		
2	4375		39624		1	
3		250		4375		
4			1		249	
5						1

$d = 5$

$2j_L \backslash 2j_R$	0	1	2	3	4	5	6
0	4791745		39624		1		
1		1354004		4624			
2	39624		261251		250		
3		4624		39625		1	
4	1		250		4375		
5				1		249	
6							1

$d = 6$

Table A.3.: The GV invariants n_{j_L,j_R}^{p+df} for $d = 0, 1, \cdots, 6$ for the local half K3 model

$2j_L \backslash 2j_R$	0	1	2	3
0		3876		
1			248	
2				1

n_b=2, d=2

$2j_L \backslash 2j_R$	0	1	2	3	4	5
0		186126		249		
1	4124		38877		1	
2		249		4373		
3			1		249	
4						1

n_b=2, d=3

$2j_L \backslash 2j_R$	0	1	2	3	4	5	6	7
0		3884370		39374		1		
1	225003		1287378		4623			
2		43499		260503		250		
3	249		4623		39623		1	
4		1		250		4375		
5					1		249	
6								1

$n_b = 2, d = 4$

$2j_L \backslash 2j_R$	0	1	2	3	4	5	6	7	8	9
0		52369748		1357878		4375				
1	5171499		22839873		300624		250			
2		1587254		6304873		44248		1		
3	39624		304749		1397006		4625			
4		4624		44248		261498		250		
5	1		250		4625		39625		1	
6				1		250		4375		
7							1		249	
8										1

$n_b = 2, d = 5$

Table A.4.: The GV invariants $n_{j_L,j_R}^{n_b p+df}$ for $n_b = 2$ and $d = 2, 3, 4, 5$ for the local half K3 model

$2j_L \backslash 2j_R$	0	1	2	3	4	5	6
0	30628		151374		248		
1		4124		34504		1	
2	1		248		4124		
3				1		248	
4							1

$n_b = 3, d = 3$

$2j_L \backslash 2j_R$	0	1	2	3	4	5	6	7	8	9
0	3694119		11393622		252004		249			
1		1434130		4880618		43498		1		
2	39125		295005		1286881		4623			
3		4622		43747		256377		250		
4	1		250		4623		39374		1	
5				1		250		4374		
6							1		249	
7										1

$n_b = 3, d = 4$

$2j_L \backslash 2j_R$	0	1	2	3	4	5	6	7	8	9	10
0		3480992		7726504		212879		248			
1	185878		1209127		3632614		38876		1		
2		38876		251755		1030753		4373			
3	248		4373		39125		217003		249		
4		1		249		4373		35000		1	
5					1		249		4125		
6								1		248	
7											1

$n_b = 4, d = 4$

Table A.5.: The GV invariants $n_{j_L,j_R}^{n_b p+df}$ for $(n_b, d) = (3,3), (3,4), (4,4)$ for the local half K3 model

A.4.3. The massive half K3

$2j_L \backslash 2j_R$	0	1
0		1

$\beta = (2p + 2f, \mathcal{O}_{2,2160}),$
$(2p + 3f, \mathcal{O}_{4,17280}),$
$(2p + 4f, \mathcal{O}_{6,60480}),$
$(2p + 5f, \mathcal{O}_{8,138240})$

$2j_L \backslash 2j_R$	0	1	2
0		7	
1			1

$\beta = (2p + 2f, \mathcal{O}_{1,240}),$
$(2p + 3f, \mathcal{O}_{3,6720}),$
$(2p + 4f, \mathcal{O}_{5,30240}),$
$(2p + 5f, \mathcal{O}_{7,69120}),$
$(2p + 5f, \mathcal{O}_{7,13440})$

$2j_L \backslash 2j_R$	0	1	2	3
0		36		
1			8	
2				1

$\beta = (2p + 2f, \mathcal{O}_{0,1}),$
$(2p + 4f, \mathcal{O}_{4,240})$

$2j_L \backslash 2j_R$	0	1	2	3
0		38		
1	1		9	
2				1

$\beta = (2p + 3f, \mathcal{O}_{2,2160}),$
$(2p + 4f, \mathcal{O}_{4,17280}),$
$(2p + 5f, \mathcal{O}_{6,60480})$

$2j_L \backslash 2j_R$	0	1	2	3	4
0		163		1	
1	8		52		
2		1		9	
3					1

$\beta = (2p + 3f, \mathcal{O}_{1,240}),$
$(2p + 4f, \mathcal{O}_{3,6720}),$
$(2p + 5f, \mathcal{O}_{5,30240})$

$2j_L \backslash 2j_R$	0	1	2	3	4	5
0		606		9		
1	44		237		1	
2		9		53		
3			1		9	
4						1

$\beta = (2p + 3f, \mathcal{O}_{0,1}),\ (2p + 5f, \mathcal{O}_{4,240})$

$2j_L \backslash 2j_R$	0	1	2	3	4	5
0		619		9		
1	47		240		1	
2		10		55		
3			1		9	
4						1

$\beta = (2p + 4f, \mathcal{O}_{2,2160}),\ (2p + 5f, \mathcal{O}_{4,17280})$

Table A.6.: The GV invariants $n^{\beta}_{j_L,j_R}$ for the classes $\beta = (n_b p + df, \mathcal{O}_{p,k})$ with $n_b = 2$ and $d \leq 5$ for the massive local half K3 model

$2j_L \backslash 2j_R$	0	1	2	3	4	5	6
0		2116		54			
1	215		952		10		
2		62		261		1	
3	1		10		55		
4				1		9	
5							1

$\beta = (2p + 4f, \mathcal{O}_{1,240}),\ (2p + 5f, \mathcal{O}_{3,6720})$

$2j_L \backslash 2j_R$	0	1	2	3	4	5	6	7
0		6690		254		1		
1	843		3378		63			
2		299		1063		10		
3	9		63		263		1	
4		1		10		55		
5					1		9	
6								1

$\beta = (2p + 4f, \mathcal{O}_{0,1})$

$2j_L \backslash 2j_R$	0	1	2	3	4	5	6	7
0		6717		256		1		
1	859		3395		64			
2		304		1068		10		
3	9		65		265		1	
4		1		10		55		
5					1		9	
6								1

$\beta = (2p + 5f, \mathcal{O}_{2,2160})$

$2j_L \backslash 2j_R$	0	1	2	3	4	5	6	7	8
0		19999		1043		9			
1	3067		11132		318		1		
2		1267		3897		65			
3	55		326		1096		10		
4		10		65		265		1	
5			1		10		55		
6						1		9	
7									1

$\beta = (2p + 5f, \mathcal{O}_{1,240})$

$2j_L \backslash 2j_R$	0	1	2	3	4	5	6	7	8	9
0		56468		3798		55				
1	10059		34113		1344		10			
2		4694		13033		328		1		
3	264		1389		4046		65			
4		64		328		1098		10		
5	1		10		65		265		1	
6				1		10		55		
7							1		9	
8										1

$\beta = (2p + 5f, \mathcal{O}_{0,1})$

Table A.7.: The GV invariants $n^{\beta}_{j_L,j_R}$ continued from table A.6

$2j_L \backslash 2j_R$	0	1	2
0			1

$\beta = (3p + 3f, \mathcal{O}_{4,17280})$
$(3p + 4f, \mathcal{O}_{7,69120})$
$(3p + 5f, \mathcal{O}_{10,241920})$

$2j_L \backslash 2j_R$	0	1	2	3
0	1		6	
1				1

$\beta = (3p + 3f, \mathcal{O}_{3,6720})$
$(3p + 4f, \mathcal{O}_{6,60480})$
$(3p + 5f, \mathcal{O}_{9,181440})$

$2j_L \backslash 2j_R$	0	1	2	3	4
0	7		30		
1		1		8	
2					1

$\beta = (3p + 3f, \mathcal{O}_{2,2160})$
$(3p + 4f, \mathcal{O}_{5,30240})$
$(3p + 5f, \mathcal{O}_{8,2160})$
$(3p + 5f, \mathcal{O}_{8,138240})$

$2j_L \backslash 2j_R$	0	1	2	3	4	5
0	36		119		1	
1		8		43		
2			1		8	
3						1

$\beta = (3p + 3f, \mathcal{O}_{1,240}),\ (3p + 4f, \mathcal{O}_{4,240}),$
$(3p + 5f, \mathcal{O}_{7,13440})$

$2j_L \backslash 2j_R$	0	1	2	3	4	5
0	37		129		1	
1		10		46		
2			1		9	
3						1

$\beta = (3p + 4f, \mathcal{O}_{4,17280}),\ (3p + 5f, \mathcal{O}_{7,69120})$

$2j_L \backslash 2j_R$	0	1	2	3	4	5	6
0	148		414		8		
1		44		184		1	
2	1		8		44		
3				1		8	
4							1

$\beta = (3p + 3f, \mathcal{O}_{0,1})$

$2j_L \backslash 2j_R$	0	1	2	3	4	5	6
0	156		473		9		
1		58		205		1	
2	1		10		52		
3				1		9	
4							1

$\beta = (3p + 4f, \mathcal{O}_{3,6720}),\ (3p + 5f, \mathcal{O}_{6,60480})$

Table A.8.: The GV invariants $n^{\beta}_{j_L,j_R}$ for some classes $\beta = (3p + df, \mathcal{O}_{p,k})$ with $d \leq 5$ for the massive local half K3 model

$2j_L \backslash 2j_R$	0	1	2	3
0				1

$\beta = (4p + 4f, \mathcal{O}_{7,69120}),$
$(4p + 5f, \mathcal{O}_{11,138240})$

$2j_L \backslash 2j_R$	0	1	2	3	4
0		1		5	
1					1

$\beta = (4p + 4f, \mathcal{O}_{6,60480}),$
$(4p + 5f, \mathcal{O}_{10,241920})$

$2j_L \backslash 2j_R$	0	1	2	3	4	5
0		7		23		
1			1		7	
2						1

$\beta = (4p + 4f, \mathcal{O}_{5,30240}),$
$(4p + 5f, \mathcal{O}_{9,181440})$

$2j_L \backslash 2j_R$	0	1	2	3	4	5	6
0		35		84		1	
1			8		35		
2				1		7	
3							1

$\beta = (4p + 4f, \mathcal{O}_{4,240})$

$2j_L \backslash 2j_R$	0	1	2	3	4	5	6
0		36		92		1	
1	1		9		37		
2				1		8	
3							1

$\beta = (4p + 4f, \mathcal{O}_{4,17280}),\ (4p + 5f, \mathcal{O}_{8,138240})$

$2j_L \backslash 2j_R$	0	1	2	3	4	5	6
0		37		102			
1	1		9		38		
2				1		9	
3							1

$\beta = (4p + 5f, \mathcal{O}_{8,2160})$

$2j_L \backslash 2j_R$	0	1	2	3	4	5	6	7
0		148		318		8		
1	7		50		154		1	
2		1		9		43		
3					1		8	
4								1

$\beta = (4p + 4f, \mathcal{O}_{3,6720}),\ (4p + 5f, \mathcal{O}_{7,13440})$

Table A.9.: The GV invariants $n^{\beta}_{j_L,j_R}$ for some classes $\beta = (4p + df, \mathcal{O}_{p,k})$ with $d = 4, 5$ for the massive local half K3 model

A.5. Data for $\mathbb{C}^3/\mathbb{Z}_5$

In the following we give the data for the ambiguities (compare (3.3.7)) of the propagator

$$A_1 = \frac{25}{17z_1}, \quad A_2 = \frac{11}{34z_2} \tag{A.5.1}$$

and

$$\begin{aligned} f_1^{11} &= -\frac{z_1}{325125}\Big(5098564 - 48684632z_1 + 147468484z_1^2 - 148117920z_1^3 + 43560000z_1^4 \\ &\quad +143757828z_2 - 1288023405z_1z_2 + 3234739300z_1^2z_2 - 1216323000z_1^3z_2 \\ &\quad -1089000000z_1^4z_2 + 166430700z_2^2 - 1438762500z_1z_2^2 + 114435000z_1^2z_2^2 \\ &\quad +17964984375z_1^3z_2^2 - 8206312500z_1^4z_2^2 + 49207500z_2^3 - 492075000z_1z_2^3 \\ &\quad -668250000z_1^2z_2^3 + 12344062500z_1^3z_2^3 + 29615625000z_1^4z_2^3\Big), \end{aligned} \tag{A.5.2}$$

$$\begin{aligned} f_1^{12} &= \frac{z_2}{650250}\Big(40041114 - 269282402z_1 + 445550264z_1^2 - 47203920z_1^3 + 43560000z_1^4 \\ &\quad +1123339428z_2 - 7901896905z_1z_2 + 13695488050z_1^2z_2 - 275823000z_1^3z_2 \\ &\quad -408375000z_1^4z_2 + 1151127450z_2^2 - 7474072500z_1z_2^2 - 14617665000z_1^2z_2^2 \\ &\quad +106153359375z_1^3z_2^2 - 14084437500z_1^4z_2^2 + 295245000z_2^3 - 2132325000z_1z_2^3 \\ &\quad -9021375000z_1^2z_2^3 + 55965937500z_1^3z_2^3 + 215240625000z_1^4z_2^3\Big), \end{aligned} \tag{A.5.3}$$

$$\begin{aligned} f_1^{22} &= -\frac{z_2^2}{1300500z_1}\Big(314459289 - 1437562352z_1 + 1651528144z_1^2 - 739920z_1^3 + 43560000z_1^4 \\ &\quad +8777675403z_2 - 42708178530z_1z_2 + 49819854300z_1^2z_2 + 7041927000z_1^3z_2 \\ &\quad +272250000z_1^4z_2 + 7822024200z_2^2 - 31605795000z_1z_2^2 - 168647265000z_1^2z_2^2 \\ &\quad +537219000000z_1^3z_2^2 - 19962562500z_1^4z_2^2 + 1771470000z_2^3 - 7873200000z_1z_2^3 \\ &\quad -70530750000z_1^2z_2^3 + 196830000000z_1^3z_2^3 + 1445006250000z_1^4z_2^3\Big), \end{aligned} \tag{A.5.4}$$

$$\begin{aligned} f_2^{11} &= -\frac{z_1^2}{325125z_2}\Big(16679528 - 178136464z_1 + 629919368z_1^2 - 758763840z_1^3 + 87120000z_1^4 \\ &\quad +82872351z_2 - 1062687185z_1z_2 + 4567463100z_1^2z_2 - 4937743500z_1^3z_2 \\ &\quad -3539250000z_1^4z_2 + 37859400z_2^2 - 450225000z_1z_2^2 + 897945000z_1^2z_2^2 \\ &\quad +9559968750z_1^3z_2^2 - 38687625000z_1^4z_2^2 + 16402500z_2^3 - 209587500z_1z_2^3 \\ &\quad +182250000z_1^2z_2^3 + 3130312500z_1^3z_2^3 + 3965625000z_1^4z_2^3\Big), \end{aligned} \tag{A.5.5}$$

$$\begin{aligned} f_2^{12} &= -\frac{z_1}{650250}\Big(14621188 - 160069244z_1 + 584181928z_1^2 - 733155840z_1^3 + 87120000z_1^4 \\ &\quad +439406451z_2 - 4634816685z_1z_2 + 15858861850z_1^2z_2 - 17162181000z_1^3z_2 \\ &\quad -2178000000z_1^4z_2 + 321744150z_2^2 - 3079113750z_1z_2^2 + 2111557500z_1^2z_2^2 \\ &\quad +47114062500z_1^3z_2^2 - 106131375000z_1^4z_2^2 + 98415000z_2^3 - 984150000z_1z_2^3 \\ &\quad -1336500000z_1^2z_2^3 + 21608437500z_1^3z_2^3 + 27168750000z_1^4z_2^3\Big), \end{aligned} \tag{A.5.6}$$

$$
\begin{aligned}
f_2^{22} &= -\frac{z_2}{1300500}\Big(104928138 - 770834984z_1 + 1603156688z_1^2 - 816447840z_1^3 + 87120000z_1^4 \\
&\quad +2925891801z_2 - 22389837435z_1z_2 + 48892420600z_1^2z_2 - 23840556000z_1^3z_2 \\
&\quad -816750000z_1^4z_2 + 2607341400z_2^2 - 17612640000z_1z_2^2 - 24031080000z_1^2z_2^2 \\
&\quad +270524250000z_1^3z_2^2 - 173575125000z_1^4z_2^2 + 590490000z_2^3 - 4264650000z_1z_2^3 \\
&\quad -18042750000z_1^2z_2^3 + 136485000000z_1^3z_2^3 + 398418750000z_1^4z_2^3\Big), \qquad \text{(A.5.7)}
\end{aligned}
$$

$$
\begin{aligned}
\tilde{f}_{11}^1 &= \frac{1}{1275z_1\Delta}\Big(-8049 + 48172z_1 - 60604z_1^2 - 13200z_1^3 - 221373z_2 + 1396485z_1z_2 \\
&\quad -1988525z_1^2z_2 - 206250z_1^3z_2 - 109350z_2^2 + 668250z_1z_2^2 + 1518750z_1^2z_2^2 - 9562500z_1^3z_2^2\Big), \qquad \text{(A.5.8)}
\end{aligned}
$$

$$
\begin{aligned}
\tilde{f}_{11}^2 &= \frac{1}{2550z_1^2\Delta}\Big(53199z_2 - 173272z_1z_2 + 112124z_1^2z_2 + 13200z_1^3z_2 + 1460673z_2^2 \\
&\quad -5230035z_1z_2^2 + 3864525z_1^2z_2^2 + 412500z_1^3z_2^2 + 656100z_2^3 - 2187000z_1z_2^3 \\
&\quad -13162500z_1^2z_2^3 + 20250000z_1^3z_2^3\Big), \qquad \text{(A.5.9)}
\end{aligned}
$$

$$
\begin{aligned}
\tilde{f}_{12}^1 &= \frac{1}{1275z_2\Delta}\Big(-2258 + 16414z_1 - 22928z_1^2 - 26400z_1^3 - 62316z_2 + 517995z_1z_2 \\
&\quad -1098800z_1^2z_2 - 36450z_2^2 + 324000z_1z_2^2 - 3796875z_1^3z_2^2\Big), \qquad \text{(A.5.10)}
\end{aligned}
$$

$$
\begin{aligned}
\tilde{f}_{12}^2 &= \frac{1}{2550z_1\Delta}\Big(17733 - 106024z_1 + 133768z_1^2 + 26400z_1^3 + 486891z_2 - 3065220z_1z_2 \\
&\quad +4369550z_1^2z_2 + 412500z_1^3z_2 + 218700z_2^2 - 1336500z_1z_2^2 - 3037500z_1^2z_2^2 \\
&\quad +20250000z_1^3z_2^2\Big), \qquad \text{(A.5.11)}
\end{aligned}
$$

$$
\begin{aligned}
\tilde{f}_{22}^1 &= \frac{1}{1275z_2^2\Delta}\Big(4244z_1 - 37252z_1^2 + 94304z_1^3 - 52800z_1^4 - 14697z_1z_2 + 152665z_1^2z_2 \\
&\quad -472350z_1^3z_2 + 825000z_1^4z_2 - 12150z_1z_2^2 + 141750z_1^2z_2^2 - 262500z_1^3z_2^2 - 843750z_1^4z_2^2\Big), \qquad \text{(A.5.12)}
\end{aligned}
$$

$$
\begin{aligned}
\tilde{f}_{22}^2 &= \frac{1}{2550z_2\Delta}\Big(2936 - 20188z_1 + 20576z_1^2 + 52800z_1^3 + 70497z_2 - 584865z_1z_2 \\
&\quad +1195100z_1^2z_2 + 72900z_2^2 - 648000z_1z_2^2\Big). \qquad \text{(A.5.13)}
\end{aligned}
$$

Any other combination of indices follows by symmetry.

A.5.1. The Gopakumar Vafa invariants

Here we list the refined Gopakumar Vafa invariants that can be read off from the prepotential (3.4.2) and the refined free energies at genus one (5.5.22).

	d_1	0	1	2	3	4	5	6	7	8
d_2										
0			3	-6	27	-192	1695	-17064	188454	-2228160
1		-2	4	-10	64	-572	6076	-71740	909760	-12146622
2		0	3	-12	91	-980	12259	-166720	2394779	-35737460
3		0	5	-12	108	-1332	18912	-289440	4632120	-76306398
4		0	7	-24	150	-1808	26983	-443394	7665776	-136440800
5		0	9	-56	294	-2982	42005	-689520	12254816	-227540162
6		0	11	-140	675	-5992	76608	-1192644	20764870	-386343036
7		0	13	-324	1738	-13550	158814	-2322056	38750866	-703362386
8		0	15	-686	4732	-33552	359898	-4954570	79050699	-1387505216

	d_1	0	1	2	3	4	5	6	7	8
d_2										
0			-4	35	-386	5161	-74368	1117672	-17319898	274571953
1		1	-4	45	-750	13174	-235148	4227874	-76326692	1381543835
2		0	-4	46	-900	19554	-420472	8861756	-183661746	3754800426
3		0	-20	46	-944	23394	-578872	13923300	-325336476	7413730499
4		0	-56	164	-1370	29417	-750734	19452681	-494871808	12281325148
5		0	-120	643	-3602	51118	-1121972	28252291	-735181136	19077844392
6		0	-220	2522	-11456	121392	-2132580	47798426	-1186598986	30575571450
7		0	-364	8526	-41314	340762	-4920912	95935665	-2184901598	53716745464
8		0	-560	24835	-154752	1078545	-12985696	220762885	-4561068642	105019097003

	d_1	0	1	2	3	4	5	6	7	8
d_2										
0			0	0	-10	231	-4452	80948	-1438086	25301295
1		0	0	0	-18	576	-13968	305244	-6329628	127275876
2		0	0	0	-24	896	-25636	650852	-15418734	349139480
3		0	0	0	-28	1152	-37032	1056780	-27964428	701652588
4		0	0	0	-30	1407	-48966	1515448	-43561508	1185905652
5		0	0	9	-66	2061	-68908	2174157	-65084016	1863846681
6		0	0	68	-280	4500	-119124	3489856	-102704154	2969225052
7		0	0	300	-1410	13413	-261576	6617379	-181806634	5100476481
8		0	0	988	-6760	48183	-695664	14702120	-365286402	9681953781

Table A.12.: GV invariants at genus 0 (top), (1,0) (middle), (0,1) (bottom).

A.6. Conventions of $\mathcal{N}=1$ actions and dimensionful constants

For reference in the main text, let us briefly introduce our conventions for the four-dimensional $\mathcal{N}=1$ effective action used in this work. The action takes the general form

$$S^{(4)}_{\mathcal{N}=1} = \frac{1}{\kappa_4^2}\int_{\mathbb{R}^{(3,1)}}\Big(-\frac{1}{2}R*1 - K_{M\bar{N}}\nabla M^M\wedge *\nabla\bar{M}^{\bar{N}} - \frac{1}{2}\mathrm{Re}f_{AB}F^A\wedge *F^B - \frac{1}{2}\mathrm{Im}f_{AB}F^A\wedge F^B - *V\Big)\,. \tag{A.6.1}$$

Here we introduced the four-dimensional graviational constant, the four-dimensional Ricci-scalar R, a number of chiral superfields with scalar components M^N that are the coordinates of the Kähler manifold of scalar fields with Kähler metric $K_{M\bar{N}} = \frac{\partial^2 K}{\partial M^M \partial \bar{M}^{\bar{N}}}$ and a number of vectormultiplets with field strengths F^A with gauge kinetic function f_{AB} of the chiral multiplets M^M. By $*$ we denote the four-dimensional Hodge star operator and V is the scalar potential that consists of the F-term and D-term scalar potential, $V = V_F + V_D$ for

$$V_F = e^K\big(K^{M\bar{N}}D_M W D_{\bar{N}}\bar{W} - 3|W|^2\big), \quad V_D = \frac{1}{2}\mathrm{Re}f^{-1\,AB}D_A D_B. \tag{A.6.2}$$

We introduced the superpotential W that is a holomorphic function of the chiral superfields M^M as well as the $\mathcal{N}=1$ covariant derivative $D_M = \partial_M + K_M$

In the course of deriving this action from String/M-/F-theory it is furthermore useful to introduce our conventions for the String, ten- and eleven-dimensional Planck scale as well as their relation to the D7-brane tension and the four- and three-dimensional Planck scale. These conventions were originally used in [150]

$$\kappa_{11}^{-2} = \kappa_{10}^{-2} = \kappa_4^{-2} = \kappa_3^{-2} = 2\pi = \mu_7 = T_7\,. \tag{A.6.3}$$

A.7. Linear multiplets and gauge couplings

Let us begin with the dualization of the chiral multiplets with complex scalars T_α into linear multiplets. More precisely, if $\mathrm{Im}T_\alpha$ has a shift symmetry it can be dualized into a two-form $\mathcal{C}_2^\alpha$, which together with $\mathrm{Re}T_\alpha$ forms the bosonic components of a linear multiplet [169]. To actually perform the dualization we collect all terms involving $\mathrm{Im}T_\alpha$. First we turn to the kinetic terms for the T_α. These are determined by the four-dimensional Kähler potential [146]

$$K = -\log(\tau-\bar{\tau}) - 2\log(\mathcal{V}(T+\bar{T}))\,, \tag{A.7.1}$$

where $\mathcal{V}$ is the volume of the Calabi-Yau threefold Z_3, which considered as a function of T_α is independent of $\tau,\bar{\tau}$. The metric for all complex scalars $M_I = (\tau, T_\alpha)$ is given by $K_{I\bar{\jmath}} = \frac{\partial^2}{\partial M_I \partial \bar{M}_{\bar{\jmath}}}K$. We note that the structure of K at this order implies that there are no kinetic mixing terms between T_α and τ.

Next we note that in (9.1.7) the imaginary part $\mathrm{Im}T_\alpha$ also appears in front of the theta-angle term $\mathrm{Tr}(F\wedge F)$ in the non-Abelian gauge theory. In this case we perform a partial integration and write

$$S^{(4)}_{\mathrm{gauge,im}} \;=\; -\frac{2\pi}{8}\int_{\mathcal{M}_4}\delta_S^\alpha\,\mathrm{Im}T_\alpha\;\mathrm{Tr}(F\wedge F) = \frac{2\pi}{8}\int_{\mathcal{M}_4}\delta_S^\alpha\, d\mathrm{Im}T_\alpha\wedge\omega_{\mathrm{CS}}\;, \tag{A.7.2}$$

which holds up to a total derivative, and we have defined

$$\omega_{\rm CS} = A \wedge dA + \tfrac{2}{3} A \wedge A \wedge A \ . \tag{A.7.3}$$

One can now eliminate $\mathcal{G}_\alpha = d{\rm Im}T_\alpha$ in favor of its dual $d\mathcal{C}_2^\alpha$. We formally achieve this by adding the Lagrange multiplier

$$S^{(4)}_{\rm Lag} = 2\pi \int_{\mathcal{M}_4} \mathcal{G}_\alpha \wedge d\mathcal{C}_2^\alpha . \tag{A.7.4}$$

and eliminate $\mathcal{G}_\alpha$ by its equations of motion. First we evaluate the equations of motion yielding

$$\mathcal{G}_\beta = -\tfrac{1}{2} K^{T_\gamma \bar{T}_\beta} * \mathcal{H}_3^\alpha \ , \qquad \mathcal{H}_3^\alpha = d\mathcal{C}_2^\alpha + \tfrac{1}{8}\delta_S^\alpha \omega_{\rm CS} \ , \tag{A.7.5}$$

where we have introduced the modified field strength $\mathcal{H}_3^\alpha$. Then we rewrite the relevant effective action including (9.1.2), (A.7.2) and (A.7.4) in terms of $\mathcal{G}_\alpha = d{\rm Im}T_\alpha$ and eliminate $\mathcal{G}_\alpha$ by using (A.7.5). Inserting this into the above action we obtain

$$\begin{aligned} S^{(4)}_{\mathcal{C}_2,F} \ &= \ 2\pi \int_{\mathcal{M}_4} \tilde{K}_{\alpha\beta}\, \mathcal{H}_3^\alpha \wedge * \mathcal{H}_3^\beta + \tfrac{1}{4} \tilde{K}^{\alpha\beta} d{\rm Re}T_\alpha \wedge * d{\rm Re}T_\beta - \tilde{K}_{\tau\bar{\tau}} d\tau \wedge * d\bar{\tau} \\ &\quad - \tfrac{1}{2}{\rm Im} f^{\rm flux}_{\mathcal{A}\mathcal{B}} F^{\mathcal{A}} \wedge F^{\mathcal{B}} - \tfrac{1}{2}{\rm Re} f_{\mathcal{A}\mathcal{B}} F^{\mathcal{A}} \wedge * F^{\mathcal{B}} \ . \end{aligned} \tag{A.7.6}$$

In order to bring the kinetic term for $\mathcal{C}_2^\alpha$ in the canonical form we have in addition used the Legendre-transformed dual Kähler potential of (A.7.1) given by [146]

$$\tilde{K}(\tau|L) = K + L^\alpha \, {\rm Re}T_\alpha = \log(\tfrac{1}{6} L^\alpha L^\beta L^\gamma \mathcal{K}_{\alpha\beta\gamma}) - \log(\tau - \bar{\tau}) \tag{A.7.7}$$

for the Legendre-transformed dual variables

$$L^\alpha = -\frac{\partial K}{\partial {\rm Re}T_\alpha} = \frac{v^\alpha}{\mathcal{V}} \, , \quad {\rm Re}T_\alpha = \frac{\partial \tilde{K}}{\partial L^\alpha} \tag{A.7.8}$$

that was defined in [146] to dualize the *real part* ${\rm Re}T_\alpha$ of the Kähler moduli to the scalar component of different linear multiplets.[1] Essentially we exploited here the basic relation $K_{T_\alpha \bar{T}_\beta} = -\frac{1}{4}\tilde{K}^{\alpha\beta}$, which is an immediate consequence of the general relations of Legendre transformations (A.7.8).

We conclude the discussion of the four-dimensional effective action by noting that $\mathcal{C}_2^\alpha$ has to also transform under a non-Abelian gauge transformations $A \to A + d\Lambda$ of the vector fields as $\mathcal{C}_2^\alpha \to \mathcal{C}_2^\alpha - \frac{1}{8}\delta_S^\alpha {\rm Tr}(\Lambda\, F)$ to ensure invariance of $\mathcal{H}_3^\alpha$ introduced in (A.7.5). Furthermore, the field strength $\mathcal{H}_2^\alpha$ obeys the Bianchi identity $d\mathcal{H}_3^\alpha = \frac{1}{8}\delta_S^\alpha \, {\rm Tr}(F \wedge F)$.

[1] This is not to be mixed up with the dualization of the imaginary part ${\rm Im}T_\alpha$ performed in this section. In particular, the two-forms D_2^α [146] forming the linear multiplet together with the L^α are different from the two-forms $\mathcal{C}_\alpha^2$ defined in (A.7.4).

A.8. Details of TN_k

In this appendix we review some details of the geometry of multi-center Taub-NUT space, TN_k. We start with the discussion of one monopole, TN_1. The metric is given as

$$ds^2_{TN} = \frac{1}{V}(dt + U)^2 + V d\vec{r}^2\,, \tag{A.8.1}$$

where t denotes a periodic coordinate on an S^1 and $\vec{r}=(x,y,z)$ three-dimensional Cartesian coordinates on $\mathbb{R}^3$. The circle is non-trivially fibered over $\mathbb{R}^3$. The function V and the S^1-connection U are related by

$$*_3 dU = \pm dV_1\,, \tag{A.8.2}$$

where $*_3$ denotes the Hodge star operator on the base $\mathbb{R}^3$ with standard orientation. The $\pm$-sign will lead to a self-dual respectively anti-selfdual two-form Ω as introduced below in (A.8.6). Note that the closedness of dU requires $V = 1 + V_1$ to be harmonic[2]. (A.8.2) is solved by

$$V_1 = \frac{r_{\rm A}}{4\pi|\vec{r}|}, \qquad U = \pm\frac{r_{\rm A}}{4\pi}\big(-1+\frac{z}{|\vec{r}|}\big)\frac{xdy - ydx}{x^2+y^2} = \pm\frac{r_{\rm A}}{4\pi}(-1+\frac{z}{|\vec{r}|})d\varphi, \tag{A.8.3}$$

where we have also introduced cylindrical coordinates[3] with $|\vec{r}| = \sqrt{\rho^2+z^2}$ for $\rho \in \mathbb{R}_+$, $\varphi \in [0,2\pi]$, $z \in \mathbb{R}_+$. r_A can be thought of as the charge of the monopole, but more importantly in our context is its interpretation as the circumference of the S^1-fiber at infinity, as discussed below. We note that the term $\mp d\varphi$ in U is an integration constant, that is not fixed by the condition $*_3 dU = \pm dV_1$ but by the condition of smoothness of U, i.e. the absence of a Dirac string. Indeed, the one-form U in (A.8.3) is only a local one-form representing the global connection of the Dirac monopole in a coordinate patch. To see this note the presence of the Dirac string, that is the locus where the local expression U is not well-defined. In cylindrical coordinates since $d\varphi$ is not well-defined at $\rho = 0$, in order to have a well-defined one-form containing $d\varphi$ its pre-factor has to vanish on the locus $\rho = 0$. However the pre-factor of $d\varphi$ in the one-form U in (A.8.3) vanishes only on the positive z-axis for the choice of integration constant -1 and U is ill-defined on the negative z-axis. This is precisely the Dirac string. Thus, U is only a local one-form well-defined only on the positive z-axis and one has to introduce at least one further patch and with another local one-form that is required to be well-defined on the negative z-axis. Thus, one introduces the two patches $\mathcal{U}_\pm$ and the corresponding connections denoted $U^\pm$ reading

$$\begin{aligned}
\mathcal{U}_+ &= \{(r,\varphi,z)\,|\,0 \le z\} : \quad U^+ = \pm\frac{r_{\rm A}}{4\pi}(-1+\frac{z}{\sqrt{\rho^2+z^2}})d\varphi\,,\\
\mathcal{U}_- &= \{(r,\varphi,z)\,|\,z \le 0\} : \quad U^- = \pm\frac{r_{\rm A}}{4\pi}(1+\frac{z}{\sqrt{\rho^2+z^2}})d\varphi,
\end{aligned} \tag{A.8.4}$$

that differ only by the integration constant in the $d\varphi$-component. They are related by the gauge transformation $U^+ = U^- \mp \frac{r_A}{2\pi}d\varphi$. In particular we note that $U^\pm$ vanishes precisely on the positive (negative) z-axis and thus can be glued together to form a smooth global gauge connection.

[2] Actually we consider fundamental solutions V with $\Delta V_1 = \delta^3(\vec{r})$ in the distributional sense.

[3] We note the spherical symmetry of the one-monopole configuration with $U = \pm\frac{r_{\rm A}}{4\pi}(-1+\cos\theta)d\varphi$ in spherical coordinates. We use cylinder coordinates to prepare for the discussion of appendix A.9.

Consequently, in order for the metric to be gauge invariant, i.e. the term $dt + U$ to be globally defined, the coordinate t has to compensate this gauge transformation and cannot be globally defined either. Thus we have to introduce two coordinates $t^{\pm}$ on $\mathcal{U}_{\pm}$ that are related by the gauge transformation

$$t^{+} = t^{-} \pm \frac{r_{\mathrm{A}}}{2\pi}\varphi \quad \Rightarrow \quad t \sim t + r_{\mathrm{A}}, \tag{A.8.5}$$

where the sign $\pm$ again refers to the choice in (A.8.2) and we inferred the periodicity of t as φ is identified modulo 2π [170]. Thus we see that the parameter r_{A} sets the circumference of the S^1 at infinity, $|\vec{r}| \to \infty$, as the potential $V \to 1$ in the metric (A.8.1). It is important to emphasize that only with this circumference we have a globally well-defined S^1- fiber radius.

Next we comment on the smoothness of TN_1, where we assume $*_3 dU = +dV_1$ for this paragraph to avoid confusion. In fact the singularity of V at the origin is just a coordinate singularity. In spherical coordinates one can expand the metric (A.8.1) around the origin using $V \sim V_1$ and the coordinate transformation $q^2 = |\vec{r}|$, $t^{\pm} = -\frac{r_A}{4\pi}(\psi \pm \varphi)$ to identify it near the origin as the flat metric on $\mathbb{R}^4$ iff ψ has period 4π. This metric is obviously smooth. We note that in the case of multiple monopoles TN_k discussed next, the space is still smooth for generic positions of the k monopoles, however, develops a deficit angle $2\pi/k$, i.e. locally becomes $\mathbb{R}^4/\mathbb{Z}_k$, for k coincident monopoles.

We conclude the analysis of the TN_1 geometry by analyzing its (co)homology. Depending on the sign in (A.8.2) TN_1 admits a selfdual (sign $+1$) respectively anti-selfdual (sign -1) two-form that is locally given by

$$\Omega = d\eta = \frac{1}{r_{\mathrm{A}}} d\Big(\frac{V_1}{V}\big(dt + U\big) - U\Big). \tag{A.8.6}$$

As the one-form U is not globally defined as pointed out in (A.8.4), the one-form η in turn is not a global form and thus Ω is not a globally exact form. On the two patches $\mathcal{U}_{\pm}$ the two local one-forms denoted $\eta^{\pm}$ are given by inserting $U^{\pm}$ defined in (A.8.4) into (A.8.6) yielding

$$\eta^{\pm} = \frac{1}{r_A}\left(\frac{V_1}{V}(dt + U) - U^{\pm}\right), \tag{A.8.7}$$

where we used that the term $dt + U$ is a global one-form by virtue of (A.8.5). It further holds the normalization[4]

$$\int \Omega \wedge \Omega = \pm 1. \tag{A.8.8}$$

[4]The sign of the Ω^2 can be obtained for any (anti-)selfdual Ω since $\Omega \wedge \Omega = \pm\Omega \wedge *\Omega$, but $\int \Omega \wedge *\Omega$ positive (negative). We can also switch between a self-dual and anti- selfdual form by changing the orientation on $\mathbb{R}^3$.

Furthermore we note the limit[5]

$$\Omega \wedge \Omega \to \pm \frac{1}{2\pi} \delta(\rho)\delta(z) d\tilde{t} \wedge d\rho \wedge d\varphi \wedge dz, \quad \text{for} \quad r_{\mathrm{A}} \to 0\,, \tag{A.8.10}$$

where we have introduced a new coordinate $\tilde{t}$ by $\tilde{t} = t/r_{\mathrm{A}}$. That identifies $\Omega \wedge \Omega$ as the dual of the origin in $\mathbb{R}^3$ for $r_{\mathrm{A}} \to 0$.

The results of the one-monopole geometry carry easily over to the multi-center case, denoted TN_k. For this one makes the multi-center ansatz

$$V = 1 + \sum_{I=1}^{k} V_I, \quad U = \sum_{I=1}^{k} U_I, \quad V_I = \frac{r_A}{4\pi|\vec{r} - \vec{r}_I|}, \quad *_3 dU_I = dV_I\,, \tag{A.8.11}$$

where $\vec{r}_I$ denote the positions of the k monopoles. The connection U is defined as the sum of gauge connections U_I constructed for each monopole I along the lines of (A.8.4). To write down an expression for the connection U in local coordinates is a bit subtle due to the dependence of the integration constant in $dV_I = *_{\mathbb{R}^3} dU_I$ on the choice of coordinate patches covering TN_k. As in (A.8.4) we have use two patches around each of the k monopoles with corresponding local one-forms $U_I^{\pm}$ in order to avoid a corresponding Dirac string. Placing the I-th monopole at the origin, we identify $U_I^{\pm} = U^{\pm}$ as defined in (A.8.4). Then, in writing down $U = \sum_I U_I$ at a given point on TN_k we have to decide for each connection U_I separately to either use the local one-form U_I^+ with integration constant $-1 \cdot d\varphi$ or U_I^- with $1 \cdot d\varphi$. Thus, adding up the respective integration constants of the U_I the integration constant in the local expression for U can take any value between $-k \cdot d\varphi$ and $k \cdot d\varphi$ depending on the point on TN_k. [6]

In contrast, the combination $dt + U$ is again unique since it is globally well defined by virtue of the condition (A.8.5) around each individual monopole. This then implies that in order to get a smooth solution all monopoles have to have the same charge r_{A}.

The multi-center solution TN_k admits k two-forms locally defined by

$$\Omega_I = d\eta_I = \frac{1}{r_{\mathrm{A}}} d\Big(\frac{V_I}{V}(dt + U) - U_I\Big)\,, \tag{A.8.12}$$

where the two different signs in $*_3 dU_I = \pm dV_I$ yield (anti-)selfduality. They obey the relation

$$\int_{\mathbb{R}^3 \times S^1} \Omega_I \wedge \Omega_J = \pm \delta_{IJ}. \tag{A.8.13}$$

[5] To prove that we use the following mathematical statement. Let $(f_j)_{j\in\mathbb{N}}$ be a sequence of positive functions defined on $\mathbb{R}^n$, s.t. $\int_{\mathbb{R}^n} f_j(x)dx = 1 \;\forall\; j$. Furthermore f_j converges uniformly to zero on any set $0 < a < |x| < 1/a$, for any $a > 0$, then $f_j \to \delta$ in the distributional sense. This can be seen by recalling that uniform convergence means convergence in the maximum norm and it is easy to see that

$$\max_{|\vec{r}|\in[a,\infty]} \frac{\frac{r_{\mathrm{A}}}{2\pi} r}{(|\vec{r}| + \frac{r_{\mathrm{A}}}{4\pi})^3} = \frac{\frac{r_{\mathrm{A}}}{2\pi} a}{(a + \frac{r_{\mathrm{A}}}{4\pi})^3} \overset{r_{\mathrm{A}}\to 0}{\longrightarrow} 0, \tag{A.8.9}$$

which establishes the desired result.

[6] To illustrate this further, let us define a patching of TN_k by drawing k two-dimensional planes in $\mathbb{R}^3$ through each of the k monopoles so that no other monopole is contained in the same plane. For each monopole this defines a partial order by what we call "above" and "below" the corresponding plane in $\mathbb{R}^3$ and we accordingly assign $U_I^{\pm} \cong U^{\pm}$. Then for every point in TN_k we know whether it lies above or below the I-th plane and can thus write down the local expression for U by adding up the integration constants ∓ 1 of the individual $U_I^{\pm}$.

Indeed, we can choose coordinates such that the I-th monopole is centered at the origin and that the two-plane $z = 0$ does not contain a different, K-th monopole, $K \neq I$.[7] This allows us to identify V_I and U_I with the one-monopole connection of TN_1 in (A.8.3). Then we introduce spherical coordinates and the coordinate patches of (A.8.4) and identify $U_I^\pm \equiv U^\pm$. Since the coordinate patches $\mathcal{U}_\pm$ are just the upper and lower halfspaces of $\mathbb{R}^3$, $z \leq 0$ respectively $z \geq 0$, they share, though with opposite orientation, the common boundary H given by

$$H = \{(r, \varphi, z = 0)\}\,. \tag{A.8.14}$$

By virtue of Stokes' theorem we may pull the integral of any exact form to this boundary H. Then we evaluate (A.8.13) taking into account the opposite orientation of H,

$$\begin{aligned} \int \Omega_I \wedge \Omega_J = \int_{S_t^1 \times H} (\eta_I^+ - \eta_I^-) \wedge \Omega_J &= \pm \int_{S_t^1 \times H} \frac{1}{2\pi} d\varphi \wedge \Omega_J \\ &= \pm \int_{S_t^1} \int_0^\infty \frac{1}{r_{\mathrm{A}}} d\frac{V_J}{V} \wedge dt = \pm \left.\frac{V_J}{V}\right|_{\rho=0}^{\infty} = \pm\delta_{IJ}\,, \end{aligned} \tag{A.8.15}$$

where we first used (A.8.7) with (A.8.4) and then integrated dt over S_t^1. In the last step we exploited that V_J/V vanishes at $\rho = \infty$, as $V \to 1$ while $V_1 \to 0$, and vanishes at $\rho = 0$ as well except when $V_J = V_I$ yielding $V_I/V = 1$, since the pole $V_I \to \infty$ cancels precisely the pole $V \to \infty$.

We note that the area of the two-cycles S_i spanning $H_2(TN_k, \mathbb{Z})$ introduced in (9.2.6) reads

$$\int_{S_i} \mathrm{vol}_{S_i} = \int_{S^1} \int_{\vec{r}_i}^{\vec{r}_{i+1}} V^{\frac{1}{2}} V^{-\frac{1}{2}} = r_{\mathrm{A}} |\vec{r}_i - \vec{r}_{i+1}|. \tag{A.8.16}$$

The forms $\hat{\omega}_i = \Omega_i$ - Ω_{i+1}, $i = 1, \ldots, k-1$, spanning its Poincare dual fulfill the following conditions

$$\int \hat{\omega}_i \wedge \hat{\omega}_j = \pm C_{ij}, \quad \int_{S_i} \omega_j = \pm C_{ij}\,, \tag{A.8.17}$$

again depending on (anti-)selfduality of Ω_I. The first statement is clear due to (A.8.13). For the second one we calculate

$$\int_{S_i} \omega_j = \int_{\partial S_i} \eta_j - \eta_{j+1} = \pm \left(\left.\frac{V_j}{V}\right|_{\vec{r}_i}^{\vec{r}_{i+1}} - \left.\frac{V_{j+1}}{V}\right|_{\vec{r}_i}^{\vec{r}_{i+1}} \right). \tag{A.8.18}$$

A.9. Details of TN_k^∞

The metric of infinitely many Kaluza-Klein monopoles placed with equal spacing r_{B} along a straight line in $\mathbb{R}^3$ is again of the from (A.8.1). Moreover due to the cylinder symmetry of the setup it is convenient to introduce cylindrical coordinates $\rho = \sqrt{x^2 + y^2}$, $\varphi = \arctan(y/x)$ and z being a coordinate on the axis along which the monopoles are aligned. After forming the quotient $z \sim z + r_{\mathrm{B}}$ we denote this space by TN_1^∞. The potential V reads

$$V = 1 + \frac{r_{\mathrm{A}}}{4\pi} \left(\sum_{\ell \in \mathbb{Z}} \frac{1}{\sqrt{\rho^2 + (z + \ell r_{\mathrm{B}})^2}} - \sum_{\ell \in \mathbb{Z}^*} \frac{1}{r_{\mathrm{B}} |\ell|} \right). \tag{A.9.1}$$

[7] We demand that the plane $z = 0$ contains no other monopole although both Ω_I and η_I are well-defined at $\vec{r} = \vec{r}_K$.

We note that V is now a harmonic function[8] on $\mathbb{R}^2 \times S^1$ due to the periodicity along the z-axis. Thus we can view the geometry of TN_1^∞ as a single Kaluza-Klein monopole on $\mathbb{R}^2 \times S^1$, treated as an image charge problem on $\mathbb{R}^3$. The last term in (A.9.1) is a regulator that assures the convergence of the sum. Note that the precise form of the regulator can be modified by any finite constant. The corresponding connection $U = \sum_I U_I$ with $*_3 dU_I = dV_I$ is given on the patch $z \in [0, r_B[$ as

$$U = \frac{r_\mathrm{A}}{4\pi}\left(-1 + \sum_{\ell\in\mathbb{Z}} \frac{z - \ell r_\mathrm{B}}{\sqrt{\rho^2 + (z-\ell r_\mathrm{B})^2}}\right) d\varphi\,, \tag{A.9.2}$$

where $-1 \cdot d\varphi$ is a choice of integration constant so that U is regular on $[0, r_B[$. In fact, treating TN_1^∞ as an image charge problem there is a Dirac string for every monopole at $\vec{r}_I = (0, 0, \ell r_B)$ as in appendix A.8. Again $d\varphi$ is ill-defined for $\rho = 0$ and so is U unless the coefficient of $d\varphi$ vanishes. Evaluating U in (A.9.2) at $\rho = 0$ we have chosen our regularization such that for $z \in [0, r_B[$,

$$\sum_\ell \frac{z - \ell r_\mathrm{B}}{\sqrt{\rho^2 + (z-\ell r_\mathrm{B})^2}}\bigg|_{\rho=0} = \sum_\ell \mathrm{sign}(z - \ell r_B) = 1 \tag{A.9.3}$$

and $U = 0$, i.e. well-defined. However, when considering for instance $z \in [r_B, 2r_B[$ we evaluate, in the same regularization $\sum_\ell \mathrm{sign}(z - \ell r_B) = 3$ and the one-form U in (A.9.2) is ill-defined. Thus, we introduce patches $\mathcal{U}_n$, n integer, that cover the z-axis in increments of r_B and local one-forms U^n,

$$\mathcal{U}_n = \{(\rho,\varphi,z)\,|\,nr_B \le z < (n{+}1)r_B\}\,:\quad U^n = \frac{r_\mathrm{A}}{4\pi}\left(-1 - 2n + \sum_{\ell\in\mathbb{Z}} \frac{z - \ell r_\mathrm{B}}{\sqrt{\rho^2 + (z-\ell r_\mathrm{B})^2}}\right) d\varphi\,. \tag{A.9.4}$$

The U^n are well-defined on $\mathcal{U}_n$ and related by the gauge transformation $U^{n+1} = U^n - \frac{r_A}{2\pi} d\varphi$. In other words, when crossing the lines $z = nr_B$ from below (above) we have to change the integration constant in the local one-form by $-2d\varphi$ ($+2d\varphi$). It is important to note, that U in (A.9.2) descends to a one-form which is well-defined along the whole S^1 of the compactified z-direction, $z \sim z + r_B$.

In order to get a better understanding of V and U we perform a Poisson resummation of these two quantities. Recall that a Poisson resummation relates a function f of period one and its Fourier-transform $\hat{f}(k) = \int_{-\infty}^{\infty} f(x) e^{-2\pi i k x} dx$ via [158]

$$\sum_{k\in\mathbb{Z}} \hat{f}(k) e^{2\pi i k x} = \sum_{k\in\mathbb{Z}} f(x + k). \tag{A.9.5}$$

The Fourier-transform of $f(z) = \frac{1}{\sqrt{\rho^2+z^2}}$ is $\hat{f}(k) = 2K_0(2\pi\rho k)$, which is the zeroth modified Bessel function of second kind and shows the following asymptotic behavior near zero,

$$K_0(x) = -\log\frac{x}{2} - \gamma, \quad x \to 0, \qquad \gamma = \lim_{N\to\infty} \sum_{k=1}^{N} \frac{1}{k} - \log N\,, \tag{A.9.6}$$

[8] Again we have $\Delta_3 V = \delta^3(\vec{r})$ in the distributional sense.

where γ is the Euler-Mascheroni constant. We now plug $f(z) = \frac{r_A}{4\pi r_B}\frac{1}{\sqrt{\hat\rho^2+\hat z^2}}$ with $\hat\rho = \frac{\rho}{r_B}$ and $\hat z = \frac{z}{r_B}$ as well as $\hat f(k) = \frac{r_A}{2\pi}K_0(2\pi\hat\rho|k|)$ into (A.9.5) and obtain

$$\begin{aligned} V &= 1+\frac{r_A}{4\pi r_B}\Big(\sum_{\ell\in\mathbb{Z}}\frac{1}{\sqrt{\hat\rho^2+(\hat z+\ell)^2}}-\sum_{\ell\in\mathbb{Z}^*}\frac{1}{|\ell|}\Big) \\ &= 1+\frac{r_A}{2\pi r_B}\Big(\sum_{\ell\in\mathbb{Z}^*}K_0(2\pi\hat\rho|\ell|)e^{2\pi i\ell\hat z}+K_0(0)-\sum_{\ell>0}\frac{1}{\ell}\Big). \end{aligned} \tag{A.9.7}$$

The right hand side contains two divergent terms, $K_0(0)$ and $\sum_{\ell>0}\frac{1}{\ell}$. We therefore have to take a suitable limit to get a finite result by considering and calculating, using (A.9.6),

$$\frac{r_A}{2\pi r_B}\lim_{N\to\infty}\Big(K_0(\frac{2\pi\hat\rho}{N})-\sum_{\ell=1}^{N}\frac{1}{\ell}\Big)=\frac{r_A}{2\pi r_B}\lim_{N\to\infty}\Big(-\log\frac{\pi\hat\rho}{N}-\gamma-\sum_{\ell=1}^{N}\frac{1}{\ell}\Big)=-\frac{r_A}{2\pi r_B}\log(\frac{\hat\rho}{\Lambda}), \tag{A.9.8}$$

where Λ comprises all constants including an eventually shift in the regulator term. For the concrete regulator in (9.2.11) we have $\Lambda = 1/(\pi e^{2\gamma})$. Finally we obtain

$$V = 1+\frac{r_A}{4\pi r_B}\Big(\sum_{\ell\in\mathbb{Z}}\frac{1}{\sqrt{\hat\rho^2+(\hat z+\ell)^2}}-\sum_{\ell\in\mathbb{Z}^*}\frac{1}{|\ell|}\Big)=1-\frac{r_A}{2\pi r_B}\Big(\log\frac{\hat\rho}{\Lambda}-2\sum_{\ell>0}K_0(2\pi\hat\rho\ell)\cos(2\pi\ell\hat z)\Big). \tag{A.9.9}$$

Similarly one can also perform a Poisson resummation for the connection U, which is given by

$$U=\frac{r_A}{4\pi}\Big(-1+\sum_{\ell\in\mathbb{Z}}\frac{(\hat z-\ell)}{\sqrt{\hat\rho^2+(\hat z-\ell)^2}}\Big)d\varphi\,, \tag{A.9.10}$$

for $0\le\hat z<1$. Using that the Fourier transform of $f(\hat z)=\frac{\hat z}{\sqrt{\hat\rho^2+\hat z^2}}$ reads $\hat f(k) = 2i\hat\rho\,\mathrm{sign}(k)K_1(2\pi\hat\rho|k|)$ we can perform a Poisson resummation for the connection as well, finding naively

$$U=\frac{r_A}{4\pi}\Big(-1+2i\hat\rho\sum_{\ell\in\mathbb{Z}}\mathrm{sign}(\ell)K_1(2\pi\hat\rho|\ell|)e^{2\pi i\ell\hat z}\Big)d\varphi\,. \tag{A.9.11}$$

Note that the contribution $\ell=0$ is again ill defined. We recall that

$$K_1(x)\sim\frac{1}{x},\qquad x\ll 1. \tag{A.9.12}$$

This enables us to regularize the $\ell=0$ contribution, i.e. sign(ℓ), as

$$\lim_{\ell\to0}\frac{1}{2}\Big(i\hat\rho\frac{1}{2\pi\hat\rho\ell}(1+2\pi i\ell\hat z)-i\hat\rho\frac{1}{2\pi\hat\rho\ell}(1-2\pi i\ell\hat z)\Big)=-\hat z\,. \tag{A.9.13}$$

We finally obtain

$$U=-\frac{r_A}{4\pi}\Big(1+2\hat z+4\hat\rho\sum_{\ell>0}K_1(2\pi\hat\rho\ell)\sin(2\pi\ell\hat z)\Big)d\varphi\,. \tag{A.9.14}$$

Note that this is cohomologically equivalent by adding a term proportional to $d(\hat z\varphi)$ and

$d\varphi$ yielding

$$U = \frac{r_{\rm A}}{2\pi}\varphi d\hat{z} + \frac{r_{\rm A}}{2\pi}\Big(- 2\hat{\rho}\sum_{\ell>0} K_1(2\pi\hat{\rho}\ell)\sin(2\pi\ell\hat{z})\Big)d\varphi\,. \tag{A.9.15}$$

As in the non-periodic case, one can easily generalize to the multi-center case TN_k^∞. We restrict ourselves to the case that all monopoles are located at $\big(\hat{\rho}=0,\hat{z}=\hat{z}_I\big)_{I=1,\ldots,k}$, i.e. we consider k periodic chains of monopoles that are shifted among each other. The corresponding re-summed potentials and connections are given for $I=1,\ldots,k$ and $\hat{z}\in[\hat{z}_I,\hat{z}_I+1[$ by

$$V_I = -\frac{r_{\rm A}}{2\pi r_{\rm B}}\Big(\log\frac{\hat{\rho}}{\Lambda} - 2\sum_{\ell>0} K_0\big(2\pi\hat{\rho}\ell\big)\cos(2\pi\ell(\hat{z}-\hat{z}_I))\Big)\,, \tag{A.9.16}$$

$$U_I = -\frac{r_{\rm A}}{4\pi}\Big(1+2(\hat{z}-\hat{z}_I) + 4\hat{\rho}\sum_{\ell>0} K_1(2\pi\hat{\rho}\ell)\sin(2\pi\ell(\hat{z}-\hat{z}_I)\Big)d\varphi\,, \tag{A.9.17}$$

that obey $*_3 dU_I = -dV_I$. Generalizing the patches of (A.9.4) to k monopoles as

$$\mathcal{U}_n(I) = \{(\hat{\rho},\varphi,\hat{z})\,|\,n+\hat{z}_I\le\hat{z}<\hat{z}_I+n+1\}\,, \tag{A.9.18}$$

we can construct local one-forms U_I^n for other values of $\hat{z}$ by changing the integration constant by ± 2. In direct analogy with (A.9.4) they read on $\mathcal{U}_n(I)$ as

$$U_I^n = -\frac{r_A}{4\pi}(1+2n+2(\hat{z}-\hat{z}_I) + 4\hat{\rho}\sum_{\ell>0} K_1(2\pi\hat{\rho}\ell)\sin(2\pi\ell(\hat{z}-\hat{z}_I))\Big)d\varphi\,, \tag{A.9.19}$$

Analogously to (A.8.12) the space TN_k^∞ also exhibits k anti-self-dual two-forms given by

$$\Omega_I^\infty = d\eta_I = \frac{1}{r_{\rm A}}d\Big(\frac{V_I}{V}(dt+U) - U_I\Big)\,. \tag{A.9.20}$$

The expression for the local one-forms η_I depends on the coordinate patches $\mathcal{U}_n(I)$, i.e. the value of $\hat{z}$, through the dependence of the U_I^n in (A.9.19) on the coordinate patch. The local one-forms are denoted η_I^n. The combination $(dt+U)$ for $U=\sum_I U_I$ is again globally defined by appropriately defining local coordinates t.

We would like to check that the relation

$$\int \Omega_I^\infty\wedge\Omega_J^\infty = -\delta_{IJ} \tag{A.9.21}$$

still holds in the periodic case. First we center the I-th monopole at the origin $(\hat{\rho},\varphi,\hat{z})=0$. Then we use as in the one monopole case (A.8.15) the exactness of Ω_I^∞ on the patches $\mathcal{U}_n(I)$ of (A.9.18). Since we eventually work on the quotient $\hat{z}\sim\hat{z}+1$ we integrate over the interval $\hat{z}\in[0,1]$, but have to keep in mind that the integration constant in U_I jumps by $-2d\varphi$ when $\hat{z}\to 1$ from below. As mentioned earlier the boundaries of $\hat{z}\in[0,1]$ representing S^1 are simply

$$H = \{(\hat{\rho},\varphi,z=0)\}\,, \tag{A.9.22}$$

with opposite orientation, respectively. We readily perform the pullback of the integral by

Stokes theorem as

$$\begin{aligned}\int \Omega_I \wedge \Omega_J &= \int_{S^1_t \times H} (\eta^1_I - \eta^0_I) \wedge \Omega_J = \int_{S^1_t \times H} \frac{1}{2\pi} d\varphi \wedge \Omega_J \\ &= \int_{S^1_t} \int_0^\infty \frac{1}{r_{\mathrm{A}}} d\frac{V_J}{V} \wedge dt = \left.\frac{V_J}{V}\right|_{\hat\rho=0}^{\infty} = -\delta_{IJ}\,. \end{aligned} \tag{A.9.23}$$

Here we used the local expression (A.9.19) and (A.9.20) to evaluate $\eta^1_I - \eta^0_I \sim 2d\varphi$ in the second equality and exploited the behavior of V_J/V at $\hat\rho = 0, \infty$ as for TN_1 to obtain the last equality.

We conclude by representing any metric of the form (A.8.1) in terms of Vierbeins e_i [170]

$$e^0 = \frac{1}{\sqrt{V}}\big(dt + U\big), \quad e^i = \sqrt{V} dx^i, \quad i = 1,2,3. \tag{A.9.24}$$

Vierbeins make it particularly easy to evaluate the Hodge star $*_4$ on Taub-NUT with any number of monopoles by specifying the orientation by the volume form as $e^0 \wedge e^1 \wedge e^2 \wedge e^3$. Then it is straightforward to check for instance the (anti-)selfduality of Ω_I respectively Ω^∞_I noting that

$$\Omega_I = (1 \pm *_4)\Big(\frac{V_I}{V} dU - dU_I\Big)\,. \tag{A.9.25}$$

Bibliography

[1] M. -X. Huang, A. Klemm and M. Poretschkin, "Refined stable pair invariants for E-, M- and $[p, q]$-strings," JHEP **1311** (2013) 112 [arXiv:1308.0619 [hep-th]].

[2] T. W. Grimm, D. Klevers and M. Poretschkin, "Fluxes and Warping for Gauge Couplings in F-theory," JHEP **1301** (2013) 023 [arXiv:1202.0285 [hep-th]].

[3] P. A. R. Ade *et al.* [Planck Collaboration], "Planck 2013 results. I. Overview of products and scientific results," arXiv:1303.5062 [astro-ph.CO].

[4] CMS and LHCb Collaborations [CMS and LHCb Collaboration], "Combination of results on the rare decays $B^0_{(s)} \to \mu^+\mu^-$ from the CMS and LHCb experiments," CMS-PAS-BPH-13-007.

[5] S. Chatrchyan *et al.* [CMS Collaboration], "Combined results of searches for the standard model Higgs boson in pp collisions at $\sqrt{s} = 7$ TeV," Phys. Lett. B **710** (2012) 26 [arXiv:1202.1488 [hep-ex]].

[6] G. Aad *et al.* [ATLAS Collaboration], "Observation of a new particle in the search for the Standard Model Higgs boson with the ATLAS detector at the LHC," Phys. Lett. B **716** (2012) 1 [arXiv:1207.7214 [hep-ex]].

[7] F. J. Dyson, "Divergence of Perturbation Theory in Quantum Electrodynamics," Phys. Rev., Vol. 85, 4, 1952.

[8] J. Polchinski, "String theory. Vol. 1: An introduction to the bosonic string," Cambridge, UK: Univ. Pr. (1998) 402 p

[9] J. Polchinski, "String theory. Vol. 2: Superstring theory and beyond," Cambridge, UK: Univ. Pr. (1998) 531 p

[10] L. E. Ibanez and A. M. Uranga, "String theory and particle physics: An introduction to string phenomenology," Cambridge, UK: Univ. Pr. (2012) 673 p

[11] C. Vafa, "Evidence for F theory," Nucl. Phys. B **469** (1996) 403 [hep-th/9602022].

[12] E. Witten, "On the Structure of the Topological Phase of Two-dimensional Gravity," Nucl. Phys. B **340** (1990) 281.

[13] E. Witten, "Topological Sigma Models," Commun. Math. Phys. **118** (1988) 411.

[14] P. Candelas, X. C. De La Ossa, P. S. Green and L. Parkes, "A Pair of Calabi-Yau manifolds as an exactly soluble superconformal theory," Nucl. Phys. B **359** (1991) 21.

[15] E. Witten, "Mirror manifolds and topological field theory," In *Yau, S.T. (ed.): Mirror symmetry I* 121-160 [hep-th/9112056].

[16] M. Kontsevich, "Homological algebra of mirror symmetry," Proceedings of the International Congress of Mathematicians (Zürich, 1994), Birkhäuser, Boston, 1995, pp. 120-139.

[17] A. Klemm, "On the geometry behind N=2 supersymmetric effective actions in four-dimensions," In *Trieste 1996, High energy physics and cosmology* 120-242 [hep-th/9705131].

[18] M. Gromov, "Pseudoholomorphic curves in symplectic manifolds," Invent. Math. **82** (1985) 307-347.

[19] N. Seiberg and E. Witten, "Electric - magnetic duality, monopole condensation, and confinement in N=2 supersymmetric Yang-Mills theory," Nucl. Phys. B **426**, 19 (1994) [Erratum-ibid. B **430**, 485 (1994)] [hep-th/9407087], "Monopoles, duality and chiral symmetry breaking in N=2 supersymmetric QCD," Nucl. Phys. B **431**, 484 (1994) [hep-th/9408099].

[20] P. C. Argyres, M. R. Plesser, N. Seiberg and E. Witten, "New N=2 superconformal field theories in four-dimensions," Nucl. Phys. B **461** (1996) 71 [hep-th/9511154].

[21] A. Strominger and C. Vafa, "Microscopic origin of the Bekenstein-Hawking entropy," Phys. Lett. B **379** (1996) 99 [hep-th/9601029].

[22] R. Gopakumar and C. Vafa, "M theory and topological strings. 1.," hep-th/9809187.

[23] R. Gopakumar, C. Vafa, "M theory and topological strings 2," hep-th/9812127.

[24] S. H. Katz, A. Klemm and C. Vafa, "M theory, topological strings and spinning black holes," Adv. Theor. Math. Phys. **3**, 1445 (1999) [hep-th/9910181].

[25] H. Ooguri, A. Strominger and C. Vafa, "Black hole attractors and the topological string," Phys. Rev. D **70** (2004) 106007 [hep-th/0405146].

[26] N. A. Nekrasov, "Seiberg-Witten prepotential from instanton counting," Adv. Theor. Math. Phys. **7**, 831 (2004) [hep-th/0206161].

[27] J. Choi, S. Katz and A. Klemm, "The refined BPS index from stable pair invariants," arXiv:1210.4403 [hep-th].

[28] N. Nekrasov and A. Okounkov, "The M-theory index," in preparation.

[29] M. x. Huang and A. Klemm, "Direct integration for general Omega backgrounds," arXiv:1009.1126 [hep-th].

[30] M. -x. Huang, A. -K. Kashani-Poor, A. Klemm, "The Omega deformed B-model for rigid N=2 theories," [arXiv:1109.5728 [hep-th]].

[31] J. A. Minahan, D. Nemeschansky, C. Vafa and N. P. Warner, "E strings and N=4 topological Yang-Mills theories," Nucl. Phys. B **527**, 581 (1998) [hep-th/9802168].

[32] A. Klemm, P. Mayr and C. Vafa, "BPS states of exceptional noncritical strings," In "La Londe les Maures 1996, Advanced quantum field theory" 177-194 [hep-th/9607139].

[33] M. Aganagic, V. Bouchard and A. Klemm, "Topological Strings and (Almost) Modular Forms," Commun. Math. Phys. **277** (2008) 771 [hep-th/0607100].

[34] S. Hosono, M. H. Saito and A. Takahashi, "Holomorphic anomaly equation and BPS state counting of rational elliptic surface," Adv. Theor. Math. Phys. **3**, 177 (1999) [hep-th/9901151].

[35] M. Demazure, "Surfaces de del Pezzo - I-V," in Séminaire sur les Singularités des Surfaces, Lecture Notes in Mathematics Volume 777 (1980) (Numdam).

[36] D. R. Morrison and C. Vafa, "Compactifications of F theory on Calabi-Yau threefolds. 2.," Nucl. Phys. B **476** (1996) 437 [hep-th/9603161].

[37] E. Witten, "Phase transitions in M theory and F theory," Nucl. Phys. B **471** (1996) 195 [hep-th/9603150].

[38] J. A. Minahan, D. Nemeschansky and N. P. Warner, "Partition functions for BPS states of the noncritical E(8) string," Adv. Theor. Math. Phys. **1**, 167 (1998) [hep-th/9707149].

[39] O. J. Ganor and A. Hanany, "Small E(8) instantons and tensionless noncritical strings," Nucl. Phys. B **474**, 122 (1996) [hep-th/9602120].

[40] E. Witten, "Some comments on string dynamics," In *Los Angeles 1995, Future perspectives in string theory* 501-523 [hep-th/9507121].

[41] E. Witten, "Small instantons in string theory," Nucl. Phys. B **460** (1996) 541 [hep-th/9511030].

[42] M. R. Douglas, S. H. Katz and C. Vafa, "Small instantons, Del Pezzo surfaces and type I-prime theory," Nucl. Phys. B **497**, 155 (1997) [hep-th/9609071].

[43] A. Johansen, "A Comment on BPS states in F theory in eight-dimensions," Phys. Lett. B **395**, 36 (1997) [hep-th/9608186].

[44] M. R. Gaberdiel and B. Zwiebach, "Exceptional groups from open strings," Nucl. Phys. B **518**, 151 (1998) [hep-th/9709013].

[45] M. R. Gaberdiel, T. Hauer and B. Zwiebach, "Open string-string junction transitions," Nucl. Phys. B **525**, 117 (1998) [hep-th/9801205].

[46] O. DeWolfe, T. Hauer, A. Iqbal and B. Zwiebach, "Uncovering the symmetries on [p,q] seven-branes: Beyond the Kodaira classification," Adv. Theor. Math. Phys. **3**, 1785 (1999) [hep-th/9812028].

[47] F. Denef, "Les Houches Lectures on Constructing String Vacua," `arXiv:0803.1194 [hep-th]`.

[48] M. R. Douglas and S. Kachru, "Flux compactification," *Rev. Mod. Phys.* **79** 733 (2007), `arXiv:hep-th/0610102`.

[49] R. Donagi and M. Wijnholt, "Model Building with F-Theory," `arXiv:0802.2969 [hep-th]`.

[50] C. Beasley, J. J. Heckman, and C. Vafa, "GUTs and Exceptional Branes in F-theory - I," *JHEP* **0901** (2009) 058, arXiv:0802.3391 [hep-th].

[51] A. P. Braun, A. Collinucci and R. Valandro, "G-flux in F-theory and algebraic cycles," *Nucl. Phys.* **B856** (2012) 129, arXiv:1107.5337 [hep-th].

[52] J. Marsano and S. Schafer-Nameki, "Yukawas, G-flux, and Spectral Covers from Resolved Calabi-Yau's," *JHEP* **1111** (2011) 098, arXiv:1108.1794 [hep-th].

[53] S. Krause, C. Mayrhofer and T. Weigand, "G_4 flux, chiral matter and singularity resolution in F-theory compactifications," *Nucl. Phys.* **B858** (2012) 1, arXiv:1109.3454 [hep-th].

[54] T. W. Grimm and H. Hayashi, "F-theory fluxes, Chirality and Chern-Simons theories," arXiv:1111.1232 [hep-th].

[55] M. Cvetic, T. W. Grimm and D. Klevers, "Anomaly Cancellation And Abelian Gauge Symmetries In F-theory," JHEP **1302** (2013) 101 [arXiv:1210.6034 [hep-th]].

[56] R. Donagi and M. Wijnholt, "Breaking GUT Groups in F-Theory," arXiv:0808.2223 [hep-th].

[57] R. Blumenhagen, "Gauge Coupling Unification in F-Theory Grand Unified Theories," Phys. Rev. Lett. **102** (2009) 071601 arXiv:0812.0248 [hep-th].

[58] R. Davies, "Dirac gauginos and unification in F-theory," JHEP **1210** (2012) 010 [arXiv:1205.1942 [hep-th]].

[59] T. Eguchi and K. Sakai, "Seiberg-Witten curve for the E string theory," JHEP **0205**, 058 (2002) [hep-th/0203025].

[60] S. Cecotti and C. Vafa, "Topological antitopological fusion," In *Trieste 1991, Proceedings, High energy physics and cosmology, vol. 2* 682-784

[61] A. Klemm, "Topological string theory on Calabi-Yau threefolds," PoS RTN **2005** (2005) 002.

[62] J. A. Minahan, D. Nemeschansky and N. P. Warner, "Investigating the BPS spectrum of noncritical E(n) strings," Nucl. Phys. B **508**, 64 (1997) [hep-th/9705237].

[63] T. Eguchi and K. Sakai, "Seiberg-Witten curve for E string theory revisited," Adv. Theor. Math. Phys. **7** (2004) 419 [hep-th/0211213].

[64] K. Hori, S. Katz, A. Klemm, R. Pandharipande, R. Thomas, C. Vafa, R. Vakil and E. Zaslow, "Mirror symmetry," (Clay mathematics monographs. 1)

[65] O. J. Ganor, "A Test of the chiral E(8) current algebra on a 6-D noncritical string," Nucl. Phys. B **479**, 197 (1996) [hep-th/9607020].

[66] S. H. Katz, A. Klemm and C. Vafa, "Geometric engineering of quantum field theories," Nucl. Phys. B **497**, 173 (1997) [hep-th/9609239].

[67] N. Drukker, M. Marino and P. Putrov, "From weak to strong coupling in ABJM theory," Commun. Math. Phys. **306**, 511 (2011) [arXiv:1007.3837 [hep-th]].

[68] O. Aharony, O. Bergman, D. L. Jafferis and J. Maldacena, "N=6 superconformal Chern-Simons-matter theories, M2-branes and their gravity duals," JHEP **0810**, 091 (2008) [arXiv:0806.1218 [hep-th]].

[69] I. Dolgachev, "Classical Algebraic Geometry: a modern view," Cambridge Univ. Press, Cambridge (2012).

[70] C. Faber and R. Pandharipande, "Hodge integrals and Gromov-Witten theory" Invent. Math. **139** (2000) 173-199 [arXiv:math/9810173 [math.AG]].

[71] R. Pandharipande and R. P. Thomas, "Curve counting via stable pairs in the derived category," Invent. Math. **178** (2009) 407 [arXiv:0707.2348 [math.AG]].

[72] R. Pandharipande and R. P. Thomas, "The 3-fold vertex via stable pairs," arXiv:0709.3823 [math.AG].

[73] R. Pandharipande and R. P. Thomas, "Stable pairs and BPS invariants," arXiv:0711.3899 [math.AG].

[74] R. Friedman, J. Morgan and E. Witten, "Vector bundles and F theory," Commun. Math. Phys. **187**, 679 (1997) [hep-th/9701162].

[75] F. Benini, S. Benvenuti and Y. Tachikawa, "Webs of five-branes and N=2 superconformal field theories," JHEP **0909**, 052 (2009) [arXiv:0906.0359 [hep-th]].

[76] B. Haghighat, A. Iqbal, C. Kozcaz, G. Lockhart and C. Vafa, "M-Strings," arXiv:1305.6322 [hep-th].

[77] P. C. Argyres, M. R. Plesser and A. D. Shapere, "The Coulomb phase of N=2 supersymmetric QCD," Phys. Rev. Lett. **75**, 1699 (1995) [hep-th/9505100].

[78] M. Aganagic, M. C. N. Cheng, R. Dijkgraaf, D. Krefl, C. Vafa, "Quantum Geometry of Refined Topological Strings," [arXiv:1105.0630 [hep-th]].

[79] M. Aganagic, A. Klemm, M. Marino and C. Vafa, "The Topological vertex," Commun. Math. Phys. **254**, 425 (2005) [hep-th/0305132].

[80] M. Aganagic and K. Schaeffer, "Refined Black Hole Ensembles and Topological Strings," arXiv:1210.1865 [hep-th].

[81] M. Aganagic and S. Shakirov, "Refined Chern-Simons Theory and Topological String," arXiv:1210.2733 [hep-th].

[82] M. Alim and E. Scheidegger, "Topological Strings on Elliptic Fibrations," arXiv:1205.1784 [hep-th].

[83] D. R. Morrison and C. Vafa, "Compactifications of F theory on Calabi-Yau threefolds. 1," Nucl. Phys. B **473** (1996) 74 [hep-th/9602114].

[84] V. Batyrev, "Dual Polyhedra and Mirror Symmetry for Calabi-Yau Hypersurfaces in Toric Varieties", arXiv:alg-geom/9310003.

[85] K. Behrend, "Donaldson-Thomas type invariants via microlocal geometry." Annals of Mathematics, 170, 1307–1338, (2009).

[86] M. Bershadsky, S. Cecotti, H. Ooguri and C. Vafa, "Kodaira-Spencer theory of gravity and exact results for quantum string amplitudes," Commun. Math. Phys. **165**, 311 (1994) [arXiv:hep-th/9309140].

[87] Y. Tachikawa, "N=2 supersymmetric dynamics for dummies," arXiv:1312.2684 [hep-th].

[88] L. Alvarez-Gaume and S. F. Hassan, "Introduction to S duality in N=2 supersymmetric gauge theories: A Pedagogical review of the work of Seiberg and Witten," Fortsch. Phys. **45** (1997) 159 [hep-th/9701069].

[89] A. Klemm, W. Lerche and S. Theisen, 'Nonperturbative effective actions of N=2 supersymmetric gauge theories," Int. J. Mod. Phys. A **11**, 1929 (1996) [hep-th/9505150]. arXiv:1306.3987 [hep-th].

[90] P. Horava and E. Witten, "Eleven-dimensional supergravity on a manifold with boundary," Nucl. Phys. B **475**, 94 (1996) [hep-th/9603142],
P. Horava and E. Witten, "Heterotic and type I string dynamics from eleven-dimensions," Nucl. Phys. B **460**, 506 (1996) [hep-th/9510209].

[91] M. A. Vasiliev, "Higher spin superalgebras in any dimension and their representations," JHEP **0412**, 046 (2004) [hep-th/0404124], "Higher spin gauge theories in various dimensions," Fortsch. Phys. **52**, 702 (2004) [hep-th/0401177].

[92] J. Maldacena and A. Zhiboedov, "Constraining conformal field theories with a slightly broken higher spin symmetry," Class. Quant. Grav. **30**, 104003 (2013) [arXiv:1204.3882 [hep-th]], "Constraining Conformal Field Theories with A Higher Spin Symmetry," J. Phys. A **46**, 214011 (2013) [arXiv:1112.1016 [hep-th]].

[93] D. Cox, "The Homogeneous Coordinate Ring of a Toric Variety, Revised Version," arXiv:alg-geom/9210008.

[94] R. Dijkgraaf, "Mirror symmetry and elliptic curves," in The Moduli Space of Curves, Progr. Math. **129** (Birkhäuser, 1995), 149–162.

[95] T. W. Grimm, T. -W. Ha, A. Klemm and D. Klevers, "The D5-brane effective action and superpotential in N=1 compactifications," Nucl. Phys. B **816**, 139 (2009) [arXiv:0811.2996 [hep-th]].

[96] A. Néron, "Propriètés arithmétiques de certaines familles de courbes algébriques," Proc. Int. Congress, Amsterdam, III (1954), 481-488.

[97] A. Néron, "Les propriètés du rang des courbes algébriques dans les corps de degré de transcendance fini," Centre National de la Recherche Scientifique, (1950), 65-69, for an explicite realization, see C.F. Schwartz, An elliptic surface of Mordell-Weyl rank 8 over the rational numbers," Journal de théorie des nombres de Bordeaux (1994).

[98] Ju.I.Manin, "The Tate height of points on an Abelian variety; its variants and applications," AMS Translations (series 2) 59 (1966), 82-110.

[99] W. Fulton, "Introduction to toric varieties," Annals of Math Studies 131, Princeton University Press (1993).

[100] L. Göttsche, "The Betti numbers of the Hilbert scheme of points on a smooth projective surface", Math. Ann. 286 (1990) 193-297.

[101] T. M. Chiang, A. Klemm, S. -T. Yau and E. Zaslow, "Local mirror symmetry: Calculations and interpretations," Adv. Theor. Math. Phys. **3** (1999) 495 [hep-th/9903053].

[102] A. Klemm and E. Zaslow, "Local mirror symmetry at higher genus," hep-th/9906046.

[103] S. Hosono, "Counting BPS states via holomorphic anomaly equations," Submitted to: Fields Inst.Commun. [hep-th/0206206].

[104] M. x. Huang and A. Klemm, "Holomorphic anomaly in gauge theories and matrix models," JHEP **0709**, 054 (2007) [arXiv:hep-th/0605195].

[105] A. Klemm, M. Poretschkin and T. Schimannek "Direct Integration for Genus Two Curves," *work in progress* .

[106] M. -x. Huang, A. Klemm and S. Quackenbush, "Topological string theory on compact Calabi-Yau: Modularity and boundary conditions," Lect. Notes Phys. **757**, 45 (2009) [hep-th/0612125].

[107] A. Iqbal and C. Kozcaz, "Refined Topological Strings and Toric Calabi-Yau Threefolds," arXiv:1210.3016 [hep-th].

[108] A. Iqbal, C. Kozcaz and C. Vafa, "The refined topological vertex," JHEP **0910**, 069 (2009) [arXiv:hep-th/0701156].

[109] M. Kaneko and D. B. Zagier, "A generalized Jacobi theta function and quasi-modular forms," in The Moduli Space of Curves, Progr. Math. **129** (Birkhäuser, 1995), 165–172.

[110] A. Klemm, J. Manschot and T. Wotschke, "Quantum geometry of elliptic Calabi-Yau manifolds," arXiv:1205.1795 [hep-th].

[111] B. Haghighat, A. Klemm and M. Rauch, "Integrability of the holomorphic anomaly equations," JHEP **0810** (2008) 097 [arXiv:0809.1674 [hep-th]].

[112] D. Krefl, J. Walcher, "Extended Holomorphic Anomaly in Gauge Theory," Lett. Math. Phys. **95**, 67-88 (2011). [arXiv:1007.0263 [hep-th]].

[113] D. Krefl, J. Walcher, "Shift versus Extension in Refined Partition Functions," [arXiv:1010.2635 [hep-th]].

[114] F. Klein, "Vorlesungen über die Theorie der elliptischen Modulfunktionen, Teubner, Leipzig, (1890) .

[115] Tadao Oda, "Convex Bodies and Algebraic Geometry: An Introduction to the Theory of Toric Varieties," Springer Berlin (1988).

[116] K. Sakai, "Topological string amplitudes for the local half K3 surface," arXiv:1111.3967 [hep-th].

[117] C. Vafa and E. Witten, "A Strong coupling test of S duality," Nucl. Phys. B **431**, 3 (1994) [hep-th/9408074].

[118] I. Connell, "Elliptic Curve Handbook," http://biblioteca.ucm.es/mat/doc8354.pdf

[119] J.J. Duistermaat, "Discrete Integrable Systems," Springer Monographs in Mathematics, 2010.

[120] R. Donagi, S. Katz and M. Wijnholt, "Weak Coupling, Degeneration and Log Calabi-Yau Spaces," arXiv:1212.0553 [hep-th].

[121] P. Slowody, "Simple singularities and simple algebraic groups," Lecture Notes in Mathematics 815, Springer Heidelberg (1980).

[122] C. Vafa and E. Witten, "A Strong coupling test of S duality," Nucl. Phys. B **431**, 3 (1994) [hep-th/9408074].

[123] V. Bouchard, A. Klemm, M. Marino and S. Pasquetti, "Remodeling the B-model," Commun. Math. Phys. **287**, 117 (2009) [arXiv:0709.1453 [hep-th]].

[124] P. Di Francesco, P. Mathieu and D. Senechal, "Conformal field theory," New York, USA: Springer (1997) 890 p

[125] W. Lerche and S. Stieberger, "Prepotential, mirror map and F theory on K3," Adv. Theor. Math. Phys. **2** (1998) 1105 [Erratum-ibid. **3** (1999) 1199] [hep-th/9804176].

[126] W. Lerche, S. Stieberger and N. P. Warner, "Quartic gauge couplings from K3 geometry," Adv. Theor. Math. Phys. **3**, 1575 (1999) [hep-th/9811228].

[127] K. Dasgupta and S. Mukhi, "BPS nature of three string junctions," Phys. Lett. B **423** (1998) 261 [hep-th/9711094].

[128] A. Mikhailov, N. Nekrasov and S. Sethi, "Geometric realizations of BPS states in N=2 theories," Nucl. Phys. B **531**, 345 (1998) [hep-th/9803142].

[129] N. Nekrasov, A. Rosly and S. Shatashvili, "Darboux coordinates, Yang-Yang functional, and gauge theory," Nucl. Phys. Proc. Suppl. **216** (2011) 69 [arXiv:1103.3919 [hep-th]].

[130] J. Louis and K. Foerger, "Holomorphic couplings in string theory," Nucl. Phys. Proc. Suppl. **55B** (1997) 33 [hep-th/9611184].

[131] M. Alim, M. Hecht, H. Jockers, P. Mayr, A. Mertens and M. Soroush, "Type II/F-theory Superpotentials with Several Deformations and N=1 Mirror Symmetry," JHEP **1106** (2011) 103 [arXiv:1010.0977 [hep-th]].

[132] M. Alim, M. Hecht, H. Jockers, P. Mayr, A. Mertens and M. Soroush, "Hints for Off-Shell Mirror Symmetry in type II/F-theory Compactifications," Nucl. Phys. B **841** (2010) 303 [arXiv:0909.1842 [hep-th]].

[133] T. W. Grimm, T. -W. Ha, A. Klemm and D. Klevers, "Computing Brane and Flux Superpotentials in F-theory Compactifications," JHEP **1004** (2010) 015 [arXiv:0909.2025 [hep-th]].

[134] T. W. Grimm, T. -W. Ha, A. Klemm and D. Klevers, "Five-Brane Superpotentials and Heterotic / F-theory Duality," Nucl. Phys. B **838** (2010) 458 [arXiv:0912.3250 [hep-th]].

[135] T. W. Grimm, A. Klemm and D. Klevers, "Five-Brane Superpotentials, Blow-Up Geometries and SU(3) Structure Manifolds," JHEP **1105** (2011) 113 [arXiv:1011.6375 [hep-th]]. C. Vafa, "Evidence for F theory," *Nucl.Phys.* **B469** (1996) 403–418, `arXiv:hep-th/9602022 [hep-th]`.

[136] K. Dasgupta, G. Rajesh and S. Sethi, "M theory, orientifolds and G - flux," *JHEP* **9908** (1999) 023, `hep-th/9908088 [hep-th]`.

[137] K. Kodaira, "On compact analytic surfaces II-III," Ann. of Math., 77, 563 (1963), ibid. 78 (1963)

[138] T. W. Grimm, "The N=1 effective action of F-theory compactifications," *Nucl. Phys.* **B845** (2011) 48, `[arXiv:1008.4133 [hep-th]]`.

[139] B. Andreas, "N=1 Heterotic / F theory duality," Fortsch. Phys. **47** (1999) 587 [hep-th/9808159].

[140] K. Becker and M. Becker, "M-Theory on Eight-Manifolds," *Nucl. Phys.* **B477** (1996) 155–167, `arXiv:hep-th/9605053`.

[141] H. Jockers and J. Louis, "The effective action of D7-branes in N = 1 Calabi-Yau orientifolds," *Nucl. Phys.* **B705** (2005) 167–211, `arXiv:hep-th/0409098`.

[142] M. B. Schulz, "Calabi-Yau duals of torus orientifolds," JHEP **0605**, 023 (2006) [hep-th/0412270].

[143] G. W. Gibbons and S. W. Hawking, "Gravitational Multi - Instantons," *Phys.Lett.* **B78** (1978) 430.

[144] H. Ooguri and C. Vafa, "Summing up D instantons," *Phys.Rev.Lett.* **77** (1996) 3296–3298, `arXiv:hep-th/9608079 [hep-th]`.

[145] D. Gaiotto, G. W. Moore and A. Neitzke, "Four-dimensional wall-crossing via three-dimensional field theory," Commun. Math. Phys. **299** (2010) 163 `arXiv:0807.4723 [hep-th]`.

[146] T. W. Grimm and J. Louis, "The effective action of N = 1 Calabi-Yau orientifolds," *Nucl. Phys.* **B699** (2004) 387–426, `arXiv:hep-th/0403067`.

[147] T. W. Grimm and D. V. Lopes, "The N=1 effective actions of D-branes in Type IIA and IIB orientifolds," *Nucl. Phys.* **B855**, (2012) 639, `arXiv:1104.2328 [hep-th]`.

[148] M. Kerstan and T. Weigand, "The Effective action of D6-branes in N=1 type IIA orientifolds," *JHEP* **1106** (2011) 105, `arXiv:1104.2329 [hep-th]`.

[149] T. W. Grimm and T. Weigand, "On Abelian Gauge Symmetries and Proton Decay in Global F-theory GUTs," *Phys.Rev.* **D82** (2010) 086009, `arXiv:1006.0226 [hep-th]`.

[150] T. W. Grimm, M. Kerstan, E. Palti and T. Weigand, "Massive Abelian Gauge Symmetries and Fluxes in F-theory," *JHEP* **1112** (2011) 004, `arXiv:1107.3842 [hep-th]`.

[151] F. Bonetti and T. W. Grimm, "Six-dimensional (1,0) effective action of F-theory via M-theory on Calabi-Yau threefolds," `arXiv:1112.1082 [hep-th]`.

[152] P. Townsend, "The eleven-dimensional supermembrane revisited," *Phys.Lett.* **B350** (1995) 184–187, arXiv:hep-th/9501068 [hep-th].

[153] P. Ruback, "The motion of Kaluze-Klein monopoles," *Commun.Math.Phys.* **107** (1986) 93–102.

[154] A. Sen, "A Note on enhanced gauge symmetries in M and string theory," *JHEP* **9709** (1997) 001, arXiv:hep-th/9707123 [hep-th].

[155] M. Bianchi, F. Fucito, G. Rossi, and M. Martellini, "Explicit construction of Yang-Mills instantons on ALE spaces," *Nucl.Phys.* **B473** (1996) 367–404, arXiv:hep-th/9601162 [hep-th].

[156] M. Blau and M. O'Loughlin, "Aspects of U duality in matrix theory," *Nucl.Phys.* **B525** (1998) 182–214, arXiv:hep-th/9712047 [hep-th].

[157] E. Eyras and Y. Lozano, "Exotic branes and nonperturbative seven-branes," *Nucl.Phys.* **B573** (2000) 735–767, arXiv:hep-th/9908094 [hep-th].

[158] L. Grafakos, *Classical Fourier Analysis*. Springer Verlag, 2008.

[159] J. H. Schwarz, "An SL(2,Z) multiplet of type IIB superstrings," Phys. Lett. B **360** (1995) 13 [Erratum-ibid. B **364** (1995) 252] [hep-th/9508143].

[160] T. Weigand, "Lectures on F-theory compactifications and model building," Class. Quant. Grav. **27** (2010) 214004 [arXiv:1009.3497 [hep-th]].

[161] M. Esole and S. -T. Yau, "Small resolutions of SU(5)-models in F-theory," arXiv:1107.0733 [hep-th].

[162] P. S. Aspinwall, "M theory versus F theory pictures of the Heterotic string," *Adv.Theor.Math.Phys.* **1** (1998) 127–147, arXiv:hep-th/9707014 [hep-th].

[163] P. S. Aspinwall and D. R. Morrison, "Point - like instantons on K3 orbifolds," Nucl. Phys. B **503** (1997) 533 [hep-th/9705104].

[164] T. Banks, M. R. Douglas and N. Seiberg, "Probing F theory with branes," Phys. Lett. B **387** (1996) 278 [hep-th/9605199].

[165] A. Sen, "F theory and orientifolds," *Nucl.Phys.* **B475** (1996) 562–578, arXiv:hep-th/9605150 [hep-th].

[166] A. Sen, "BPS states on a three-brane probe," Phys. Rev. D **55** (1997) 2501 [hep-th/9608005].

[167] A. Sen, "Orientifold limit of F theory vacua," *Phys.Rev.* **D55** (1997) 7345–7349, arXiv:hep-th/9702165 [hep-th].

[168] T. W. Grimm and R. Savelli, "Gravitational Instantons and Fluxes from M/F-theory on Calabi-Yau fourfolds," *Phys.Rev.* **D85** (2012) 026003, arXiv:1109.3191 [hep-th].

[169] G. Girardi and R. Grimm, "The Superspace geometry of gravitational Chern-Simons forms and their couplings to linear multiplets: A Review," *Annals Phys.* **272** (1999) 49–129, arXiv:hep-th/9801201 [hep-th].

[170] C. W. Misner, "The Flatter regions of Newman, Unti and Tamburino's generalized Schwarzschild space," *J.Math.Phys.* **4** (1963) 924–938.

[171] E. Witten, "Quantum background independence in string theory," hep-th/9306122.

[172] S. Yamaguchi and S. -T. Yau, "Topological string partition functions as polynomials," JHEP **0407** (2004) 047 [hep-th/0406078].

[173] M. Alim and J. D. Lange, "Polynomial Structure of the (Open) Topological String Partition Function," JHEP **0710** (2007) 045 [arXiv:0708.2886 [hep-th]].

[174] M. Aganagic, A. Klemm, M. Marino and C. Vafa, "Matrix model as a mirror of Chern-Simons theory," JHEP **0402** (2004) 010 [hep-th/0211098].

[175] P. Candelas, X. De La Ossa, A. Font, S. H. Katz and D. R. Morrison, "Mirror symmetry for two parameter models. 1.," Nucl. Phys. B **416** (1994) 481 [hep-th/9308083].

[176] M. Alim, "Mirror symmetry, toric branes and topological string amplitudes as polynomials,"

[177] S. Hosono, M.-H. Saito and J. Stienstra, "On Mirror Symmetry Conjecture for Schoen's Calabi-Yau 3-folds," in The Proceedings of Taniguchi Symposium, "Integrable Systems and Algebraic Geometry," Kobe/Kyoto(1997), pp.194-235 (alg-geom/9709027).

[178] J. J. Heckman, Y. Tachikawa, C. Vafa and B. Wecht, "N = 1 SCFTs from Brane Monodromy," JHEP **1011** (2010) 132 [arXiv:1009.0017 [hep-th]].

[179] M. Vonk, "A Mini-course on topological strings," hep-th/0504147.

[180] M. Alim, "Lectures on Mirror Symmetry and Topological String Theory," arXiv:1207.0496 [hep-th].

[181] S. Hosono, A. Klemm and S. Theisen, "Lectures on mirror symmetry," In *Helsinki 1993, Proceedings, Integrable models and strings* 235-280, and Harvard U. Cambridge - HUTMP-94-01 (94/02,rec.Mar.) 45 p. Muenchen U. - LWU-TPW-94-02 (94/02,rec.Mar.) 45 p [hep-th/9403096].

[182] S. Hosono, A. Klemm, S. Theisen and S. T. Yau, "Mirror symmetry, mirror map and applications to Calabi-Yau hypersurfaces," Commun. Math. Phys. **167** (1995) 301 [hep-th/9308122].

[183] K. Hori and C. Vafa, "Mirror symmetry," hep-th/0002222.

[184] P. Candelas and X. de la Ossa, "Moduli Space of Calabi-Yau Manifolds," Nucl. Phys. B **355** (1991) 455.

[185] P. Candelas, "Complex manifolds and Deformations of Complex Structures," Springer-Verlag, Berlin (1985).

[186] H. Ooguri, "Lectures on topological string theory," Lect. Notes Phys. **851** (2012) 233.

[187] V. V. Batyrev and D. van Straten, "Generalized hypergeometric functions and rational curves on Calabi-Yau complete intersections in toric varieties," Commun. Math. Phys. **168** (1995) 493 [alg-geom/9307010].

[188] D. A. Cox and S. Katz, "Mirror symmetry and algebraic geometry," (Mathematical surveys and monographs. 68)

[189] I. Antoniadis and S. Hohenegger, "Topological amplitudes and physical couplings in string theory," Nucl. Phys. Proc. Suppl. **171** (2007) 176 [hep-th/0701290 [HEP-TH]].

[190] I. Antoniadis, E. Gava, K. S. Narain and T. R. Taylor, "Topological amplitudes in string theory," Nucl. Phys. B **413** (1994) 162 [hep-th/9307158].

[191] N. P. Warner, "N=2 supersymmetric integrable models and topological field theories," In *Trieste 1992, Proceedings, High energy physics and cosmology* 143-179 and South. Calif. Univ. Los Angeles - USC-93-001 (93/01,rec.Feb.) 37 p. (304362) [hep-th/9301088].

[192] D. R. Morrison, "Where is the large radius limit?," In *Berkeley 1993, Proceedings, Strings '93* 311-315, and Inst. Adv. Stud. Princeton - IASSNS-HEP-93-068 (93/10,rec.Nov.) 5 p. (319974) [hep-th/9311049].

[193] M. Bershadsky, S. Cecotti, H. Ooguri and C. Vafa, "Holomorphic anomalies in topological field theories," Nucl. Phys. B **405** (1993) 279 [hep-th/9302103].

[194] M. Billo, F. Denef, P. Fre, I. Pesando, W. Troost, A. Van Proeyen and D. Zanon, "Special geometry of Calabi-Yau compactifications near a rigid limit," Fortsch. Phys. **47** (1999) 133 [hep-th/9801140].

[195] D. Z. Freedman and A. Van Proeyen, "Supergravity," Cambridge, UK: Cambridge Univ. Pr. (2012) 607 p.

[196] D. Ghoshal and C. Vafa, "C = 1 string as the topological theory of the conifold," Nucl. Phys. B **453** (1995) 121 [hep-th/9506122].

[197] M. Aganagic and K. Schaeffer, "Orientifolds and the Refined Topological String," JHEP **1209** (2012) 084 [arXiv:1202.4456 [hep-th]].

[198] M. Marino, "Topological strings, matrix models and nonperturbative effects", http://home.mathematik.uni-freiburg.de/mathphys/konf/Warwick_TQFT/marino.pdf

[199] B. Haghighat, "On Topological String Theory with Calabi-Yau Backgrounds", Dissertation, Universtität Bonn, 2009.

[200] U. H. Danielsson, M. E. Olsson and M. Vonk, "Matrix models, 4D black holes and topological strings on non-compact Calabi-Yau manifolds," JHEP **0411** (2004) 007 [hep-th/0410141].

[201] J. H. Bruinier, G. v. d. Geer, G. Harder and D. Zagier, "The 1-2-3 of Modular Forms," Springer, 2008.

[202] J. I. Igusa, "On Siegel Modular Forms of Genus Two," American Journal of Mathematics, Vol. 84, No. 1, 1962.

[203] J. I. Igusa, "On Siegel Modular Forms of Genus Two II," American Journal of Mathematics, Vol. 86, No. 1, 1964.

[204] J. I. Igusa, "Modular Forms and Projective Invariants," American Journal of Mathematics, Vol. 89, No. 3, 1967.

[205] M. Streng, "Computing Igusa Class Polynomials," [arXiv:0903.4766v3 [math.NT]].

[206] S. Mukhopadhyay and K. Ray, "Fractional branes on a noncompact orbifold," JHEP **0107** (2001) 007 [hep-th/0102146].

[207] X. De la Ossa, B. Florea and H. Skarke, "D-branes on noncompact Calabi-Yau manifolds: K theory and monodromy," Nucl. Phys. B **644** (2002) 170 [hep-th/0104254].

[208] S. Hosono, "Central charges, symplectic forms, and hypergeometric series in local mirror symmetry," hep-th/0404043.

[209] M. Eichler and D. Zagier, "The Theory of Jacobi Forms," Progress in Mathematics, Vol. 55, Birkhäuser, 1985.

[210] M. Aganagic, A. Klemm and C. Vafa, "Disk instantons, mirror symmetry and the duality web," Z. Naturforsch. A **57** (2002) 1 [hep-th/0105045].

[211] M. Alim, E. Scheidegger, S. -T. Yau and J. Zhou, "Special Polynomial Rings, Quasi Modular Forms and Duality of Topological Strings," arXiv:1306.0002 [hep-th].

[212] M. Marino, "Chern-Simons Theory, Matrix Models, and Topological Strings," Clarendon Press, Oxford, 2005.

[213] R. Dijkgraaf, H. L. Verlinde and E. P. Verlinde, "Notes on topological string theory and 2-D quantum gravity," PUPT-1217.

[214] D. Gaiotto, A. Strominger and X. Yin, "New connections between 4-D and 5-D black holes," JHEP **0602** (2006) 024 [hep-th/0503217].

[215] A. Brandhuber and S. Stieberger, "Periods, coupling constants and modular functions in N=2 SU(2) SYM with massive matter," Int. J. Mod. Phys. A **13** (1998) 1329 [hep-th/9609130].

[216] S. Hellerman, D. Orlando and S. Reffert, "String theory of the Omega deformation," JHEP **1201** (2012) 148 [arXiv:1106.0279 [hep-th]].

[217] I. Antoniadis, I. Florakis, S. Hohenegger, K. S. Narain and A. Zein Assi, "Worldsheet Realization of the Refined Topological String," Nucl. Phys. B **875** (2013) 101 [arXiv:1302.6993 [hep-th]].

[218] T. J. Hollowood, A. Iqbal and C. Vafa, "Matrix models, geometric engineering and elliptic genera," JHEP **0803** (2008) 069 [hep-th/0310272].